

Metabolic and Proteomic Characterization of Primary
Hepatocytes in Different *in vitro* Cultivation Conditions

Dissertation

zur Erlangung des Grades
des Doktors der Naturwissenschaften
der Naturwissenschaftlich-Technischen Fakultät
der Universität des Saarlandes

von
Saskia Sperber
Saarbrücken

2016

Tag des Kolloquiums: 09.12.2016

Dekan: Prof. Dr. Guido Kickelbick

Berichterstatter: Prof. Dr. Elmar Heinzle
Prof. Dr. Christoph Wittmann

Vorsitz: Prof. Dr. Uli Müller

Akademischer Mitarbeiter: Dr. Björn Becker

In der Krise beweist sich der Charakter.

Helmut Schmidt

*I don't pretend we have all the answers.
But the questions are certainly worth thinking about.*

Arthur C. Clarke

Abstract

In this study primary hepatocytes were characterized on a metabolic and proteomic level in different cultivation setups, namely collagen sandwich (SW) and monolayer (ML) culture. The impact of insulin and glucose on the central carbon metabolism and hepatic function was addressed as well, also integrating species differences between murine and human hepatocytes. Overall, the central carbon metabolism was very robust in regard of the used cultivation condition. Hepatic function and the handling of stress as induced by ammonia, however, were clearly affected, with a rapid loss of hepatic function in the ML culture. Proteome analysis revealed a development away from freshly isolated hepatocytes in both setups, which was stronger in the ML culture. Differential handling of oxidative stress marked the strongest difference between the used cultivation setups. If exposed to insulin, human and murine hepatocytes reacted by an increased uptake of amino acids and glucose. ^{13}C tracer experiments revealed a differential metabolic usage of carbon sources by both species, depending on the available amount of glucose. Hepatic function was differentially regulated by insulin, but also by glucose and the cultivation condition. Thereby, certain species-specific differences were detected, especially cytochrome P450 activity and insulin clearance. The susceptibility of primary hepatocytes to various factors has to be kept in mind when planning experiments and when comparing different studies.

Zusammenfassung

In dieser Arbeit wurden primäre Hepatozyten in Collagen Monolayer- (ML) und Sandwich-Kulturen (SW) proteomisch und metabolisch charakterisiert. Der Einfluss von Insulin und Glukose auf den Zentralstoffwechsel und die Funktionalität der Hepatozyten wurde ebenfalls untersucht, wobei auch Speziesunterschiede zwischen humanen und murinen Hepatozyten adressiert werden konnten. Der Zentralstoffwechsel erwies sich als sehr robust gegenüber den unterschiedlichen Kultivierungsformen, die Funktionalität der Zellen und ihr Umgang mit Stress, z.B. durch Ammonium, wurden jedoch stark beeinträchtigt. In der ML-Kultur kam es zu einem beträchtlichen Funktionsverlust der Hepatozyten. Die Proteomanalyse zeigte, dass sich die Zellen in beiden Kulturen von frisch isolierten Hepatozyten weg entwickelten, was stärker in der ML-Kultur war. Der größte Unterschied zwischen den Kultivierungsformen zeigte sich im Umgang mit oxidativem Stress. Insulin führte zu einer vermehrten Aufnahme von Aminosäuren und Glukose. Eine unterschiedliche Verwendung von Kohlenstoffquellen in Abhängigkeit von der Glukosekonzentration konnte durch ^{13}C -Markierungsexperimente gezeigt werden. Die hepatische Funktionalität wurde durch alle Faktoren beeinflusst, wobei diese sich in den beiden Spezies unterschiedlich auswirkten. Diese Empfindlichkeit von Hepatozyten gegenüber den verschiedenen Aspekten der Kultivierungsbedingungen muss beim Planen von Experimenten und beim Vergleichen von Studienergebnissen stets bedacht werden.

Extended Abstract

The liver is a highly complex organ essential to physiological body function. It is not only the major producer of plasma proteins as albumin but also responsible for detoxification of endogenous substances, such as ammonia, and xenobiotic substances, such as drugs or chemicals. One of the most important functions of liver is the maintenance of homeostasis for many metabolites and iron. Of these metabolites glucose is the most important. The liver thereby provides glucose for glucose-dependent tissues such as the brain during fasting and eliminates excessive glucose from the circulation after a meal. Hepatocytes, the parenchymal cells of the liver, are metabolically well equipped and adapted to these tasks and are mostly responsible for physiological liver function. Metabolic processes and other hepatic functions are regulated by numerous factors, such as hormones, substrate availability, pO_2 or innervation. The regulation of glucose metabolism by the hormones insulin and glucagon is the most prominent example, but also the availability of glucose itself is an important factor. In an *in vitro* cultivation setup the maintenance of liver function of hepatocytes to a level as close as possible to the *in vivo* situation is the ultimate goal. However, traditional cultivation systems, such as monolayer (ML) cultures, are known for a rapid loss of hepatic function. In the more complex collagen sandwich (SW) culture this loss of function and also the loss of morphological integrity can be delayed.

The metabolic and proteomic changes induced in primary mouse hepatocytes (PMH) by these two cultivation setups were addressed in the first part of the thesis presented here. In addition also the impact on hepatic function and the handling of certain stress factors, in this case ammonia, was analyzed. In these experiments two phases of cultivation were in focus, namely the first 24 h while the cells were still close to freshly isolated hepatocytes and adapting to the respective cultivation condition, and a time frame over five days, since hepatocytes in ML culture tend to lose their hepatic phenotype already. During the first 24 h hints for a stress response in the form of acetate and lactate production could be found in the ML culture. This could indicate that adaption of the cells to a rather artificial environment as the ML culture might induce a stressed phenotype. During the long-term cultivation over five days glucose metabolism seemed to be most susceptible to the cultivation condition, however, this time in the collagen SW culture. This indicates that also in the preferred cultivation setup the hepatocytes develop away from the original phenotype. Except for these findings the here analyzed part of the metabolome reflecting the central carbon metabolism remained surprisingly unchanged. Hepatic function, including the production of albumin and urea and

the detoxification of certain substrates by cytochrome P450s (CYP) was in accordance to the literature decreased over time in the ML culture. The handling of ammonia stress was also significantly affected by the cultivation condition, with the capacity of the urea cycle seeming to reach a maximum in the ML culture. Instead the cells dealt with this stress by reducing the amount of glutamine uptake and at the highest concentration even produced glutamine. In the SW culture such a maximum was not reached and the urea synthesis rate was increased in a dose-dependent manner. Overall, this might indicate that for essential metabolic functions as provided by the central carbon metabolism, especially in regard of glucose homeostasis, a great robustness exists, whereas other functions are more susceptible to changed conditions.

On the proteomic level no differences between PMH in collagen SW and ML culture have been detected after 24 h. If the intracellular proteome was compared at day 5 of cultivation between SW and ML culture, certain differences could be detected. The above described changes in albumin and urea production could also be confirmed at the proteomic level, with a significant higher amount in the SW culture. However, even in the SW culture these proteins were down-regulated to a certain degree compared to day 1 of cultivation. The most prominent effects were found for dealing of the cells with oxidative stress. In the ML culture proteins involved in oxidative stress defense were constantly down-regulated, whereas in the SW proteins related to oxidative stress were up-regulated. PMH in collagen SW and ML culture seem to be encountered with oxidative stress. However, in the SW culture the defense system is significantly up-regulated to deal with this, whereas in the ML culture a down-regulation of these important enzymes takes place. Regarding the multiple effects of ROS and oxidative stress on cells, one can assume that the down-regulation of these enzymes might also play a role in the loss of hepatic function observed in ML cultivation. Overall, proteome analysis revealed a development away from freshly isolated hepatocytes in both culture conditions, which was, however, stronger in the ML culture.

In the second part of the thesis here presented the influence of insulin and glucose on the central carbon metabolism and hepatic function was addressed. Thereby, also species differences between murine and human hepatocytes were analyzed. If exposed to insulin, human and murine hepatocytes generally reacted by increased uptake of amino acids. This was especially prominent for amino acids used as carbon sources, such as alanine and glutamine. However, insulin treatment also lead to an increase in albumin and urea production in both cell types under both cultivation conditions indicating that the amino acids taken up were also used for protein formation and also metabolized to a certain extent. Surprisingly,

the present amount of extracellular glucose had only a minor impact on amino acid consumption. The independence of amino acid consumption of glucose concentration might imply that energy metabolism for their own cellular demand is mostly independent from glucose, especially since at the same time increased insulin also leads to an increase in glucose consumption or a decreased glucose production respectively. This seems to be especially true for human hepatocytes, since even the production of lactate is completely detached from glucose consumption. Further species-specific differences in carbon usage were detected by ^{13}C tracer experiments. Depending on the amount of available glucose, PMH also used glucose to cover their own cellular demands, whereas in primary human hepatocytes (PHH) excessive glucose was almost entirely used for glycogen synthesis. These adaptations also reflect certain physiological differences between mice and humans *in vivo*, such as general higher metabolic activity in mice or their significantly lower overall glycogen stores, to name a few. Certain species specific differences were also detected for hepatic function, especially in regard of cytochrome P450 activity and insulin clearance. However, especially for CYP activity it cannot be excluded that in mice the used substrate to determine activity is metabolized by the same isoform as in humans. In addition, for these two parameters not only insulin played a role in regulation, but also glucose concentration and the cultivation condition.

The susceptibility of primary hepatocytes to various factors, which are constantly used in different setups in the scientific community, is highly interesting. However, it is also something which has to be kept in mind when planning future experiments and when comparing different studies from literature. Species differences and loss of function of primary hepatocytes are also serious problems in regard of *in vivo* and *in vitro* testing, if the study results are used to extrapolate to humans *in vivo*. Especially, if metabolism or CYP activity is concerned, rodents do not seem to be the ideal organism, although e.g. there are countless rodent diabetic models available. However, these differences in metabolism might also explain, why there is no single rodent model available showing the complete phenotype of type II diabetes. In regard of the cultivation setup to choose for hepatocyte cultivation, the “fit for purpose”-principle should be applied. For certain questions, as long-term testing or transport studies, a more *in vivo* like setup is desirable. However, it also has to be kept in mind that certain assays or experiments are not feasible with these 3D-cultivation setups, and on the other hand they might in this certain aspect not necessarily represent a superior culture system.

Table of Content

<u>1. INTRODUCTION</u>	1
1.1 THE LIVER: A HIGHLY COMPLEX ORGAN AND ITS VARIOUS TASKS	1
1.2 <i>IN VITRO</i> CULTIVATION SYSTEMS FOR STUDYING THE LIVER	4
1.3 METABOLISM IN THE LIVER: ADJUSTED TO SPECIAL NEEDS.	13
1.4 INSULIN: A SMALL MOLECULE WITH HUGE IMPACT	19
1.5 'OMICS STUDIES	23
1.6 AIM AND OUTLINE OF THE THESIS	33
<u>2. MATERIAL AND METHODS</u>	35
2.1 CHEMICALS	35
2.2 CELL CULTURE	36
2.3 MICROSCOPY	37
2.4 CHARACTERIZATION OF EXTRACELLULAR METABOLOME	37
2.5 DETERMINATION OF HEPATIC FUNCTION	38
2.6 PROTEOME ANALYSIS	39
<u>3. METABOLIC CHARACTERIZATION OF POLARIZED AND NON-POLARIZED PRIMARY MOUSE HEPATOCYTES</u>	45
3.1 INTRODUCTION	45
3.2 RESULTS	46
3.3 DISCUSSION	53
<u>4. PROTEOMIC CHARACTERIZATION OF PRIMARY MOUSE HEPATOCYTES IN COLLAGEN MONOLAYER AND SANDWICH CULTURE</u>	57
4.1 INTRODUCTION	57
4.2 RESULTS	58
4.3 DISCUSSION	66
<u>5. INFLUENCE OF INSULIN AND GLUCOSE ON CENTRAL CARBON METABOLISM OF PRIMARY MOUSE AND HUMAN HEPATOCYTES</u>	71
5.1 INTRODUCTION	71
5.2 RESULTS	72
5.3 DISCUSSION	102
<u>6. THE INFLUENCE OF GLUCOSE AND INSULIN ON HEPATIC FUNCTION</u>	113

6.1 INTRODUCTION	113
6.2 RESULTS	114
6.3 DISCUSSION	122
7. DISCUSSION AND OUTLOOK	127
8. ABBREVIATIONS	134
9. REFERENCES	139
10. SUPPLEMENTARY MATERIAL	166
DANKSAGUNG	201
CURRICULUM VITAE	203
PUBLICATIONS	204

1. Introduction

1.1 The liver: A highly complex organ and its various tasks

The liver is a reddish brown organ consisting of four differently sized lobes. It is the largest gland in the body, which accounts for about 2-5% of body weight, and is located in the right upper quadrant of the abdominal cavity (Si-Tayeb et al. 2010). The liver is supplied with blood by two major blood vessels, namely the hepatic artery, which carries blood from the aorta, and the portal vein, which brings nutrient-rich blood from the digestive system (Kietzmann et al. 2006). Together with a bile duct, the portal vein and the hepatic artery form the portal triad, which is the corner point of the basic architectural unit of the liver, the liver lobule. The lobule is more or less hexagonal with each of the corners marked by the presence of a portal triad. From the portal triad on the blood vessels subdivide into capillaries, named sinusoids, along the liver lobule until the central efferent vein is reached. The cellular structures from the portal triad to the central vein of the liver lobule form the functional units of the liver, the liver acinus (Figure 1-1) (Usynin and Panin 2008). A single layer of hepatocytes is arranged as irregularly folded sheets surrounding the sinusoids (Jungermann and Kietzmann 1996, Klover and Mooney 2004). They are separated from the flowing blood only by a

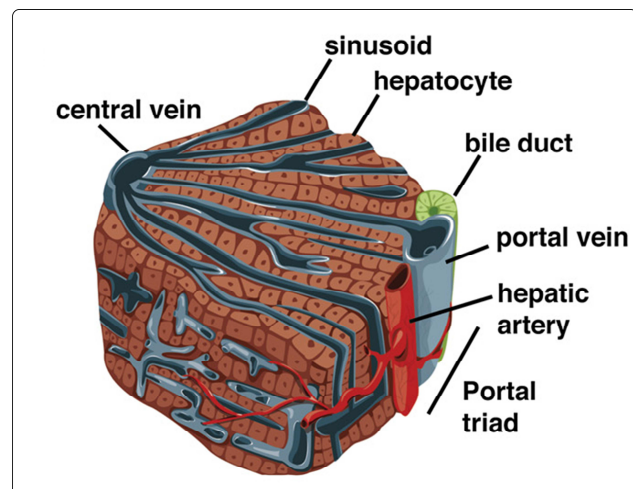


Figure 1-1 Schematic cross section of a liver lobule from the portal triad to the central vein (Si-Tayeb *et al.*, 2010).

single layer of endothelial cells interspersed with Kupffer cells (KC). Hepatic endothelial cells are specially adapted to liver tasks, since they form *fenestrae* of about 100-200 nm and have no basement membrane (Iredale and Arthur 1994, Si-Tayeb et al. 2010). Hepatocytes are separated from the sinusoids by the Space of Disse, where one can find hepatic stellate cells (HSC) and a specialized basement membrane like matrix, consisting mainly of collagen type IV, laminin and proteoglycans (Iredale and Arthur 1994). Hepatocytes, thereby, have no direct contact with blood, but are in contact with plasma components, which can penetrate into the Space of Disse through the *fenestrae* or *via* transcytosis through the sinusoidal epithelial cells (Usynin and Panin 2008). Hepatocytes are organized as specially polarized epithelia, where the basolateral surfaces face the sinusoids and are bound by extracellular

matrix (ECM), whereas the apical surfaces form bile canaliculi which are sealed by tight junctions between the hepatocytes (Ezzell et al. 1993, Berthiaume et al. 1996, Si-Tayeb et al. 2010). Basolateral and apical poles, thereby, have discrete functions and are equipped with suitable transporters. For example, plasma proteins synthesized in hepatocytes are transported across the basolateral surface and enter circulation, whereas bile salts and bilirubin are excreted over the apical membrane into the bile canaliculi (Ezzell et al. 1993). The small bile canaliculi combine and form the larger bile ductules which finally lead into the bile duct, which is connected to the gut (Klover and Mooney 2004). Thereby, the bile flow is reverse to the blood flow, from the center of each lobule to the bile duct of the portal triad.

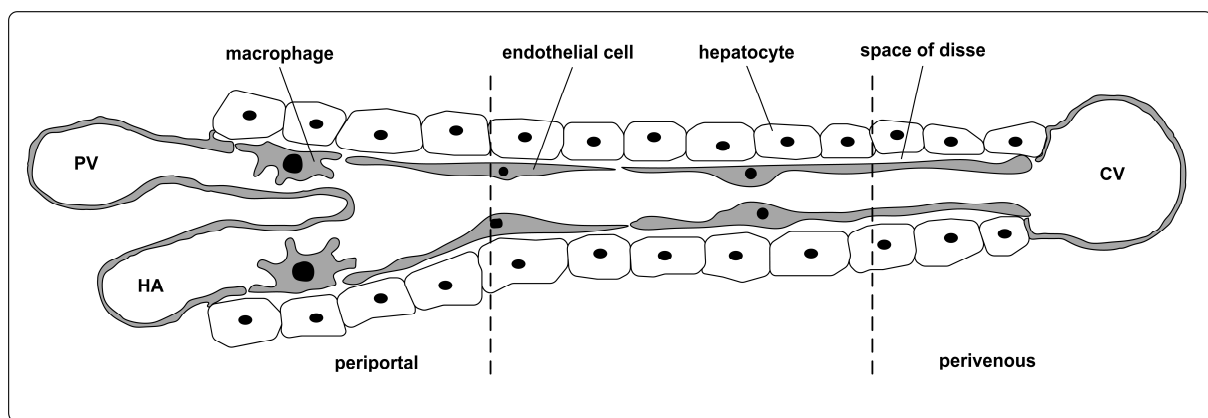


Figure 1-2 Scheme of the functional unit of the liver, the acinus. The blood flows from the portal vein (PV) and the hepatic artery (HA) through the sinusoid to the central vein (CV) (adapted from Usynin and Panin, 2008).

During the blood passage through the lobule different gradients develop along the acinus (Kietzmann et al. 1997), e.g. oxygen, different hormones (insulin, glucagon, catecholamines and glucocorticoids) and substrates (glucose, amino acids) (Nauck et al. 1981, Usynin and Panin 2008). These gradients, as well as different sympathetic and parasympathetic innervation, lead to a zonal restriction of gene expression, that is often related to the position of the portal triad (periportal) or the central vein (pericentral / perivenous) (Figure 1-2) (Si-Tayeb et al. 2010). This leads to a metabolic zonation along the acinus, meaning that different pathways are located in different areas of the liver acinus (Kietzmann et al. 2006). Well-known examples for this phenomenon are e.g. the zonation of glucose metabolism, ammonia detoxification or the zoned expression of cytochrome P450 (CYP) enzymes (Gebhardt 1992, Ananthanarayanan et al. 2011). The main part of glucose is taken up perivenously correlated with a high activity of glycogen synthesis. If the glycogen stores are filled, glucose is degraded *via* glycolysis to lactate. Periportally, glycolysis shows only minor activity. Here, glycogen stores are filled *via* gluconeogenesis from lactate (Jungermann and Kietzmann

1996). Not only metabolic pathways are zonated, but also the distribution of some non-parenchymal liver cells is depending on the position along the acinus (Usynin and Panin 2008).

The liver consists of various cell types. Apart from hepatocytes other resident liver cells are endothelial cells, cholangiocytes, KC, pit cells and HSC (Maher and Friedman 1993). Endothelial liver cells account for about 2.5% of the lobular parenchyma and form the sinusoids. As mentioned above, they are highly specialized, forming fenestrae between them, which permit free access for macromolecules but retain cellular components and large macromolecular aggregates. To further enhance this process they also lack a basement membrane. Endothelial cells also have an important role in signaling, since they secrete several cytokines and can even function as antigen presenting cells (Jungermann and Kietzmann 1996, Si-Tayeb et al. 2010). Cholangiocytes form the bile ducts and amount to 3% of liver cell population. They control not only the rate of bile flow, but also secrete water and bicarbonate, to control the pH of bile (Si-Tayeb et al. 2010). KC are resident liver macrophages. They are attached to the sinusoidal wall on the luminal surface, especially at branching points. KC are not only scavengers of foreign material, but also secrete a wide spectrum of regulators, for example cytokines, interleukins, prostaglandins and nitric oxide. There is also a metabolic cooperation between KC and hepatocytes in lipoprotein metabolism (Maher and Friedman 1993, Jungermann and Kietzmann 1996, Usynin and Panin 2008). Pit cells are resident liver killer cells. They are rather rare and show a high cytotoxic activity (Si-Tayeb et al. 2010). HSC are star-shaped cells located in the Space of Disse. They are also known as perisinusoidal cells, Ito cells or lipocytes. HSC are the major source of ECM in the liver. Under normal conditions vitamin A storage is a typical feature of these cells, but the retinoid droplets do contain triglycerides, phospholipids, cholesterol and free fatty acids as well. Due to changes in the surrounding ECM, exposure to lipid peroxides or products of damaged hepatocytes HSC become activated, what is still enhanced by infiltration of KC. During activation HSC lose their vitamin A stores and change into ECM producing, proliferating myofibroblasts. This process plays a major role in several liver diseases and liver injury, especially in liver fibrosis and steatosis (Moreira 2007). HSC closely interact with other liver cells and produce a wide range of factors, e.g. epidermal growth factor (EGF), hepatocyte growth factor (HGF), transforming growth factor alpha and beta (TGF) and prostaglandins. Because of this, HSC play a major role in coordination of liver regeneration and inflammation processes (Dooley et al. 2000, Friedman 2008). Hepatocytes, as parenchymal liver cells, account for about 60% of the liver cell number and 80% of volume

and are therefore the major cell type of the liver (Gille et al. 2010). In mammals hepatocytes are organized as a one cell thick cord of cubical cells with a diameter of 13-30 μm (Berthiaume et al. 1996). Hepatocyte metabolism integrates a vast array of differentially regulated biochemical pathways, which are responsible for the main part of physiological liver function. Hereby, one of the most important functions of the liver is the homeostasis of the blood glucose level. This is regulated through the special adaption of glucose metabolism in hepatocytes together with a complex interplay of insulin and glucagon and the ability of hepatocytes to react to those, which will be discussed in more detail in “Metabolism in the liver: Adjusted to special needs” and “Insulin: A small molecule with huge impact” (Lu et al. 2012). Another remarkable liver function, which is accomplished through clever adaption of hepatocyte metabolism, is the detoxification of ammonia *via* the urea cycle and glutamine and alanine synthesis to non-toxic nitrogen compounds (Kuepfer 2010). But not only ammonia is detoxified by the liver, but also a wide range of other endo- and xenobiotic compounds (Gille et al. 2010). CYPs and conjugating enzymes as glutathion-S-transferase, which are highly expressed in hepatocytes, are of utmost importance for this. Besides that, the liver is responsible for the homeostasis of many other metabolites and iron, the synthesis and secretion of plasma proteins, e.g. albumin and apolipoprotein, and of several hormones, e.g. insulin-like growth factor and thrombopoietin (Pan et al. 2009, Si-Tayeb et al. 2010). Additionally, also bile salts are formed by hepatocytes *via* CYP-mediated oxidation of cholesterol and finally transported into bile canaliculi.

All these tasks make the liver one of the most important organs for physiological body function. There are still many pending questions on physiological liver function as well as the many different disease states of the liver. These aspects alongside the continuously growing incidence rates of liver diseases in industrialized countries, as for example hepatic fibrosis and cirrhosis, and the fact that the liver is the major organ for drug metabolism, proof the high relevance and interest for further examination (Ong and Younossi 2007, Bhala et al. 2011).

1.2 *In vitro* cultivation systems for studying the liver

In vitro cultivation systems are gaining more and more importance in fundamental research, but also in pharmaceutical, cosmetic and chemical industry. Animal testing used to be the major focus of pre-clinical testing of pharmaceuticals and of testing for cosmetics and new chemical entities. However, out of ethical reasons, the high financial effort and time constraints related to animal testing and questionable transferability of results from animal to human, it has become the overall goal to reduce animal testing as much as possible (Krewski

et al. 2010, Holmes et al. 2010). Because of these factors, there are also regulatory efforts to minimize animal studies, as for example the complete ban of animal testing for cosmetic products throughout the EU, which has come into effect in 2013. This strongly increases the pressure to further improve existing *in vitro* test-systems, especially of liver, to obtain valuable data to answer pending questions regarding physiological function and toxicity.

1.2.1 The still pending question: Which cell type is most suitable?

To develop effective *in vitro* liver systems the choice of the used cell type is not trivial (Alépée et al. 2014). There are a lot of available alternatives, ranging from different cell lines, such as HepG2, HepaRG, HepLi5, Fa2N-4 or Huh-7, to primary hepatocytes from different origins, such as rodents or human patient material (Soldatow et al. 2013).

1.2.1.1 Hepatic cell lines

Cell lines are valuable tools, which are widely used for investigation of the liver. Their availability is usually unlimited due to immortalization (De Waziers et al. 1995). Thereby, the cells can be immortalized artificially, as it was done for HepLi5, or they can be cancer-derived, such as HepG2 (Maier et al. 2010, Pan et al. 2012). Because of their high availability, purchasing of cell lines often comes at comparably low costs. One of their greatest advantages is the stability of the phenotype and that most cell lines are well characterized due to their long-time use in *in vitro* cultivation systems.

The HepG2 cell line originates from a hepatocellular carcinoma of a 15 year old caucasian male (ATCC), and has widely been used for *in vitro* toxicology studies (Allen et al. 2001, Feierman et al. 2002, Hewitt and Hewitt 2004, Mueller et al. 2011a). They are less expensive than primary hepatocytes and provide reproducible results. The cells maintain some liver specific functions, e.g. albumin production, however, they show only low levels of CYP activity and lack many other key hepatic functions (Mueller et al. 2013a, Kostadinova et al. 2013). Because of the lack of hepatic functions, about 30% of toxic compounds tested with HepG2 cells were in-correctly classified as non-toxic (Takayama et al. 2013). Also the regulation of pathways leading to apoptosis seems to be differentially regulated in HepG2 cells compared to primary hepatocytes (Latta et al. 2000). Hep2/C3A is a clonal derivative of HepG2, which shows an improved differentiated hepatic phenotype (Mueller et al. 2013a). However, certain key functions of hepatocytes are still lacking, as the Hep2/C3A cells are still not able to detoxify ammonia (Pan et al. 2012). After differentiation, the newly established hepatoma-derived HepaRG cell line consists of hepatocyte-like cells and biliary cells in a

ratio of 1:1 (Mueller et al. 2014). Hepatocyte-like cells are morphologically comparable to normal hepatocytes (polarized, bile canaliculi) and show promising characteristics regarding hepatic function, such as high activity of enzymes involved in phase I and II metabolism and functionality of important membrane transporters (Aninat et al. 2006, Kanebratt and Andersson 2008). Drug metabolizing enzymes and transporters respond to inducers and inhibitors comparably to primary hepatocytes (Jossé et al. 2008, Turpeinen et al. 2009). HepaRG cells also lack the inter donor-variability and functional instability over cultivation time, which are usually observed for primary human hepatocytes (PHH) (Lambert et al. 2009). Mueller et al. could show, that the acetaminophen-induced toxicity in HepaRG cells, which is mainly caused by its metabolite NAPQI, is similar to PHH (Mueller et al. 2014). Gerets et al. investigated the sensitivity of different cellular systems to detect hepatotoxins (Gerets et al. 2012). They could show, that HepaRG cells, with a detection rate of 13%, are more sensitive than HepG2 cells, which only identified 6.3% of the toxins in a correct manner. However, both cells lines clearly were not comparable to freshly isolated PHH, which showed a detection rate of 31-44%, depending on the donor. An additional way of establishing hepatic cell lines is the immortalization of primary hepatocytes. The HepLi5 cell line, which was established and characterized by Pan et al., represents an example for this procedure (Pan et al. 2012). Immortalization of primary hepatocytes was achieved *via* transfection of Simian virus 40 large T antigen (SV40 LT). This resulted in a doubling time of about 8 h, but nevertheless the cells showed no tumorigenesis in mice even after 3 months. HepLi5 retained major characteristics of primary hepatocytes, such as albumin and urea production as well as the expression of glutamine synthetase and CYP enzymes. However, albumin and urea production remained significantly lower compared to primary hepatocytes. Stem cell-derived hepatocyte-like cells are a promising tool, which will gain more importance in the future. A comprehensive overview of the topic was given by Guguen-Guillouzo et al. (Guguen-Guillouzo et al. 2010). One generally differentiates between human embryonic stem cells (hESC), which are due to ethical concerns not commonly accepted, and induced pluripotent stem cells (iPSC) derived from somatic cells (Mandenius et al. 2011, Shtrichman et al. 2013). Thereby, the experimental protocol, namely the factors with which the cells are treated to differentiate, plays a most critical role. Takayama et al. showed, that in addition to treatment with optimized growth factors and cytokines the transient transduction of stem cells with FOXA2 and HNF1 α is important to induce hepatocyte differentiation (Takayama et al. 2013). 3D cultivation systems have an additional positive impact on differentiation (Takayama et al. 2013, Mueller et al. 2013a). Hepatocyte-like cells derived from iPSC show

many hepatocyte characteristics, such as glycogen storage, urea synthesis, drug metabolism capacity and the ability to take up low-density lipoprotein. One of the major advantages of hepatic cell lines derived from iPSC is the ability to use material from different donors, which can reflect the diverse genetic background of human population (Alépée et al. 2014). With this method even rare CYP polymorphisms could be analyzed and a further step towards personalized medicine could be taken (Takayama et al. 2013, Shtrichman et al. 2013). A crucial need is still to improve and standardize reprogramming protocols to gain higher efficacy.

Hepatic cell lines are valuable tools, but as described above, there are also certain drawbacks. Most of the cell-lines in use are tumor-derived going along with drastic metabolic rearrangements away from oxidative to anaerobic metabolism (Kim and Dang 2006, Pan et al. 2009). Pan et al. could also determine other up-regulated pathways in cell lines, such as cell cycle, DNA synthesis and RNA synthesis, due to immortalization (Pan et al. 2009). In addition to that, cell lines tend to lose hepatic functions in a more or less pronounced way and finally show a rather different phenotype compared to primary hepatocytes *in vivo*. Because of this, it is always necessary to validate findings from cell lines to the *in vivo* state, confirming that the cell line in use is physiologically relevant for a certain question.

1.2.1.2 Primary hepatocytes

Because of certain drawbacks of hepatic cell lines, primary hepatocytes, especially of human origin, still represent the gold standard (Mueller et al. 2014, Pfeiffer et al. 2015). The cells are usually isolated by collagenase perfusion as described by Seglen and Damm et al. (Seglen 1972, Damm et al. 2013). The most common sources for PHH are small liver resects from patients or rejected donor organs. Cultured primary hepatocytes are valuable tools to analyze mechanistic liver function, since freshly isolated cells retain many of their liver specific characteristics, especially the expression of CYP enzymes, and are therefore closer to the *in vivo* situation compared to cell lines (Rowe et al. 2010, Lu et al. 2012). Cultured primary hepatocytes are used in pharmaceutical industry to study drug metabolism, enzyme induction and hepatotoxicity, but they are also used for studies of molecular mechanisms involved in liver diseases and regeneration (Nüssler et al. 2006, Brulport et al. 2007, Höhme et al. 2007, Lilienblum et al. 2008, Schug et al. 2008). In the future, primary hepatocytes could also be used for bioartificial liver devices after end-stage liver disease and acute liver failure (Strain and Neuberger 2002, Carpentier et al. 2009). However, the high amount of cells needed and the limited availability, at least of human origin, might be a limiting factor. In addition to this,

PHH are usually derived from patient material, what gives them a difficult background. Also other factors, as lifestyle of the donor and genetic variability, especially regarding CYP polymorphisms, complicate *in vitro* studies. Thereby, genetic variability can be seen both ways, positive and negative. On the one hand the genetic background of different donors resembles variability in the human population (Alépée et al. 2014). On the other hand, this strongly hinders the detection and formulation of effects in a significant way (Mueller et al. 2011b). In comparison, primary mouse hepatocytes (PMH) show a strain dependent stable genetic background, as well as strictly regulated “lifestyle”, regarding diet and day- and night-cycles. Of course, there is no possibility to reflect the variation found in human population with hepatocytes of murine origin and there are certain inherited differences between primary human and mouse hepatocytes. Mice in general, show rather strong physiological differences compared to humans, since they are much smaller and have a much faster metabolism. Because of this differing metabolic demand, enzyme levels and activities and also the regulation of certain pathways are diverse in both species (MacDonald et al. 2011, Bunner et al. 2014, Kowalski and Bruce 2014). CYPs especially show various isoforms with different activities and substrate specificities in different species and therefore, the metabolism, as well as the toxicological response to certain xenobiotics, vary between species (Olson et al. 2000, Vassallo et al. 2004, Martignoni et al. 2006, Mattes et al. 2014). Because of this, results gained from animal testing *in vivo* or *in vitro* cannot simply be extrapolated to humans. Another problem regarding primary hepatocytes in general, and especially of rodent origin, is rapid dedifferentiation and loss of hepatic function in conventional 2D *in vitro* systems (Tuschl and Mueller 2006, Klingmüller et al. 2006, Rowe et al. 2010). This makes long-term analyses and toxicological testing impossible and there is only rudimentary understanding, why hepatocytes in cultivation start to dedifferentiate (Si-Tayeb et al. 2010). However, the differentiated hepatic phenotype can be elongated by media optimization or by using certain cultivation methods as described below.

1.2.2 How close do we have to get to *in vivo* conditions?

Conventional 2D monolayer (ML) cultures are the simplest experimental *in vitro* setup (see Figure 1-3 a). They have long been used and are therefore well established regarding available assays and method optimization. Cells adapt fast to 2D cultivation conditions and are easy to manipulate (Tuschl and Mueller 2006, Lu et al. 2012, Kostadinova et al. 2013). However, this setup is a highly artificial environment for hepatocytes. The cells are attached directly to cell culture plastic, or in the best case to a layer of ECM, whereas the other side of

the cells is in direct contact with cell culture medium. Only a small percentage of the cell surface is involved in cell-cell- and cell-ECM-contacts, which is the opposite *in vivo*, where hepatocytes never are in direct contact with blood (Bryant and Mostov 2008). Therefore, conventional 2D culture does not resemble the complex 3D environment *in vivo* (Mueller et al. 2014). Adult hepatocytes are difficult to maintain in ML cultures (Jasmund et al. 2007). They show a rapid loss of hepatic function, including loss of gluconeogenesis within 2 d, albumin and urea synthesis and CYP activity within 4 d and a general change of metabolism towards permanent cell lines (Lu et al. 2012). Going along with a loss of hepatic function come morphological changes towards a fibroblastic phenotype and a loss of polarity. The cells are flattened and spread out with increased nuclei volume and granulated cytoplasm (Iredale and Arthur 1994, Tuschl and Mueller 2006, Rowe et al. 2010). This process is called epithelial-mesenchymal-transition and was described in detail by Godoy et al. (Godoy et al. 2009, Godoy et al. 2010). To enhance hepatic phenotype and function, resembling the more complex three-dimensional *in vivo* situation, can help. The available possibilities range from rather simple setups, as collagen sandwich (SW) cultures over organoid-like spheroids to complex bioreactor systems.

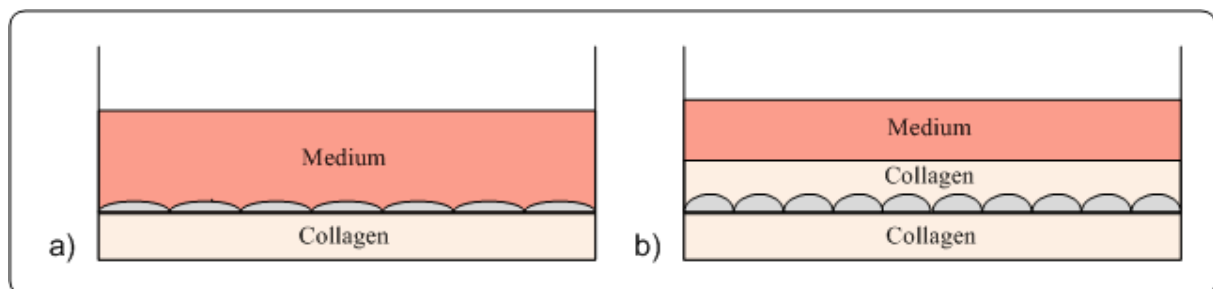


Figure 1-3 Schematic setup of collagen ML (a) and SW (b) culture. In the ML culture hepatocytes are spread out on a single layer of collagen with their surface directly in contact with the medium. In the SW culture hepatocytes are embedded within two layers of collagen, showing a much more cuboidal shape.

SW cultures represent the simplest “3D”-cultivation system (Figure 1-3 b). Hepatocytes are cultivated between two layers of ECM, most often collagen or Matrigel (Kiang et al. 2011, Reif et al. 2015). The extracellular matrix gives the cells structural support and the possibility of cell-matrix-binding *via* integrins and non-integrin-receptors. This enables a direct interaction with the actin based cytoskeleton (Iredale and Arthur 1994). The binding of hepatic receptors to ECM leads to the recruitment and activation of focal adhesion kinase. This results in activation of downstream signals, which are important for survival and differentiation of hepatocytes (Godoy et al. 2009). In addition to the important structural support, ECM serves as a reservoir for nutrients as well as growth factors and cytokines,

which can be even bound to ECM to elongate their half-life (Iredale and Arthur 1994). If hepatocytes are cultivated in the SW configuration, they re-establish their polarized phenotype, maintain the polarized distribution of transport proteins combined with functional excretion and the formation of a two-dimensional bile canalicular network (Berthiaume et al. 1996, Swift and Brouwer 2010). It was also shown in numerous studies, that hepatocytes in SW culture show a prolonged hepatic function, including CYP expression, albumin, as well as transferrin production (Ezzell et al. 1993, Peters et al. 2009, Kostadinova et al. 2013). Although this cultivation setup represents the current gold standard regarding polarization and functionality of hepatocytes and is applied in toxicity and drug-drug interaction studies as well as biliary transport studies, there are still certain drawbacks, which have to be mentioned (Kienhuis et al. 2007, Tuschl et al. 2009). Hepatocytes need distinctly longer to adapt to culture conditions compared to ML cultivation systems, which is important regarding experimental planning (Tuschl and Mueller 2006). Rowe et al. could show that even in the SW configuration hepatocytes show disturbances in steroid and vitamin metabolism already after 72 h of cultivation (Rowe et al. 2010). This somehow questions the stability of the hepatic phenotype over a longer cultivation period. In addition, the second layer of ECM might serve as a diffusion barrier for certain proteins, which might hinder kinetic studies (Berthiaume et al. 1996). However, it was shown that this is not the case for proteins of the size of albumin or fibrinogen (Peters et al. 2009). The reservoir function of the ECM can be a problem, if certain measurements are applied. Quantitative ^{13}C labeling studies, as well as assays in which quantitative analysis is based on the production of a chromatic or fluorescent substance, are strongly complicated due to reservoirs formed in the ECM phase. As mentioned above, the SW configuration is a rather simple setup, which is of course highly simplified compared to the complex liver architecture *in vivo*. Another way of achieving a three-dimensional environment is to make use of cellular adhesion. In the absence of an attachment surface the cells aggregate and self-assemble to form a multi-cellular spheroid

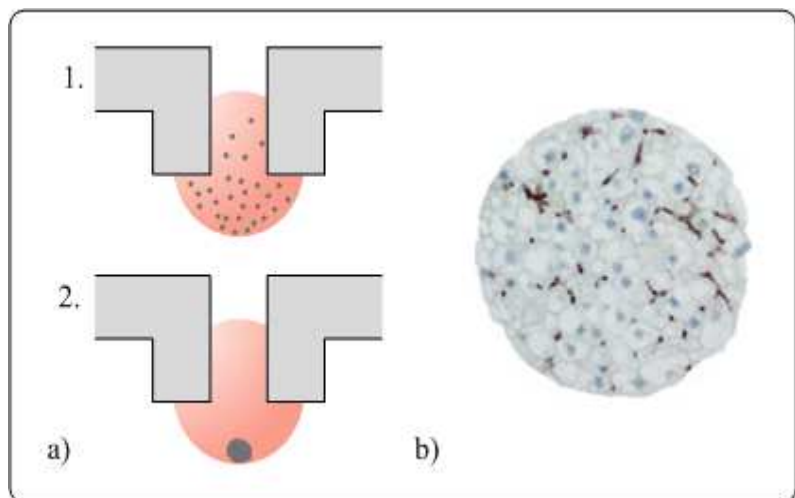


Figure 1-4 Formation of spheroids using the hanging drop technique (a) and a hepatic spheroid (b). Cells in the hanging drop of culture media settle under the pull of gravity to assemble as a miniature tissue. Spheroid formed of hepatic HepG2 cells (source: insphero.com).

(Figure 1-4 b). There are various techniques available to obtain spheroids, e.g. with a nanopillar plate, stirred bioreactor systems or rotating wall vessels, which have been reviewed in detail by Achilli et al. (Achilli et al. 2012, Takayama et al. 2013). The hanging drop technique, as an example, is depicted in (Figure 1-4 a). Improved hepatic function compared to conventional ML cultures, including phase I and II drug metabolizing enzymes, as well as long-time viability and the formation of liver structures, e.g. a complex bile canalicular network, has been shown not only for hepatocytes, but also for various cells lines and hepatocyte like cells derived from iPSC (Brown et al. 2003, Mueller et al. 2011a, Takayama et al. 2013, Mueller et al. 2014). However, due to the low cell number and the small sample volume, certain measurements are not easily applicable, depending on the sensitivity of the test method. It is not possible to increase spheroid size arbitrarily, since supply of the cells by diffusion is only guaranteed up to a diameter of 200-300 μm (Mueller et al. 2013a).

Mass transport through complex liver-like structures can be provided by perfusion systems as applied in microfluidic devices or bioreactor systems. Microfluidic devices can be multi-well or chip based and have the advantage of a small necessary cell number and a controlled medium flow and microenvironment (Alépée et al. 2014). In addition several perfusion chambers can be either connected in series, to create a certain gradient as for example along the liver acinus, or in parallel, which makes analysis of biological replicates possible. Different setups of the “Lab on a chip” and their applications especially in drug testing have been described and discussed by Wu et al. and van Midwoud et al. (Wu et al. 2010, van Midwoud et al. 2011).

Complex bioreactor systems have been originally developed as bioartificial livers (BALs) for patients waiting for a liver transplant after hepatic failure (Yu et al. 2009). BALs have been down-scaled to laboratory sizes for basic research. However, the cell number needed to guarantee *in vivo* like reorganization is still very high with $3\text{-}6 \times 10^7$ for HepG2 and 10^8 for PHH as described by Mueller et al. (Mueller et al. 2013b). This fact disqualifies bioreactors as a high throughput method and makes parallel approaches with cells from the same donor almost impossible. In a hollow fiber 3D bioreactor, as used by Zeilinger et al., hepatocytes aggregate around the fibers and form liver specific structures (Zeilinger et al. 2004). The hollow fibers themselves serve as a capillary network and allow the circulation of medium. This guarantees the supply with fresh medium, O_2 and CO_2 (Mueller et al. 2013a). Trostoes et al. cultivated primary rat hepatocyte (PRH) spheroids encapsulated with alginate and could show, that perfusion feeding had a positive effect on three independent liver specific functions

(urea synthesis, albumin production, phase I drug metabolism) (Tostões et al. 2011). Also improved maturation of hESCs towards the liver lineage could be shown in bioreactor systems compared to conventional 2D cultures (Sivertsson et al. 2012). However, not only the high amount of cellular mass needed is one reason why bioreactors are not regularly applicable, but also high costs related with the equipment and the high technical experience needed. Additionally, most bioreactors are closed systems, which makes only endpoint measurements possible. Due to the large perfusion volume, ^{13}C tracer experiment or other experiments with expensive substrates are also very costly.

Another way to further improve *in vitro* liver cultivation systems is to cultivate hepatocytes or hepatocyte-like cells together with other liver cells, as there are endothelial cells, macrophages or HSC. As described above, different liver cell types strongly influence each other by direct contact or the production of soluble factors, as for example cytokines, which is important for physiological liver function. Co-cultivation can be applied on the various levels of cultivation described above. Kim et al e.g., cultivated primary PRH as a ML and added a second layer of bovine endothelial cells (Kim et al. 2012). Hepatocytes could be cultivated for up to 28 d and hepatic function, namely the secretion of albumin and the expression of hepatocyte-specific genes was stable and higher in the co-cultivation system compared to the ML system. Krause et al. analyzed the effect of hepatic stellate cells on PRH cultivated as collagen ML culture (Krause et al. 2009). They could show that HSC lead to an enhanced hepatic phenotype, using the phosphoenolpyruvate carboxykinase activity in response to glucagon as a marker, even if no direct contact is established. However, this effect was much stronger, if direct contact was allowed. Co-cultivation of different liver cell types is a more physiological approach compared to conventional single cell type cultivation. At the same time, it represents also a further complication of the system, which might impact certain analytical aspects, e.g. metabolic flux analysis.

Although collagen SW cultures are more simplified than spheroids or bioreactor setups, they are complex enough for the short-term characterization done in this thesis. In contrast to spheroids, the SW culture is not limited regarding cell number, which was a necessity for proteomic characterization *via* 2D-gelelectrophoresis and difference gel electrophoresis (DIGE). In addition, the cultivation system is an open one, which makes easy visual and hands-on access to the cells possible, which is often difficult in complex closed bioreactor systems. It has been made clear, that the choice of cell type and the cultivation system are not trivial ones. Both decisions strongly depend on the purpose of the experiment and the data,

which is wished to be gained and the experimental design should fit the requirements (fit for purpose principle) (Alépée et al. 2014).

1.3 Metabolism in the liver: Adjusted to special needs.

1.3.1 The central carbon metabolism

The central carbon metabolism can be roughly subdivided into glycolysis/gluconeogenesis, pentose phosphate pathway (PPP), tricarboxylic acid (TCA) cycle and the fatty acid (FA) metabolism. The here described pathways are also depicted in Figure 1-5. Glycolysis converts glucose into two molecules of pyruvate thereby producing two molecules ATP and two molecules NADH. Glycolysis is strongly interconnected with other metabolic pathways. Pyruvate can be directly converted into acetyl-CoA by the pyruvate dehydrogenase complex, which can be further metabolized in the TCA cycle or it can be used for FA synthesis. Another connection exists *via* fructose 6-phosphate (F6P) and glyceraldehyde 3-phosphate to the PPP. Gluconeogenesis seems on first sight like an inversion of glycolysis. However, both pathways are regulated by differential irreversible steps. The first one of glycolysis is the phosphorylation of glucose catalyzed by hexokinase resulting in glucose 6-phosphate (G6P). This reaction has the advantage, that G6P can no longer leave the cytoplasm since it is not a substrate of glucose transporters. The second irreversible step in the pathway is catalyzed by phosphofructokinase-1 (PFK-1). The conversion of F6P into fructose 1,6-bisphosphate (F1,6BP) is mostly regulated by the ratio between ATP and AMP. Is the cellular energy state high, PFK-1 is inhibited. ATP thereby works as an allosteric inhibitor of PFK-1 leading to a reduced affinity of the enzyme towards its substrate. Pyruvate kinase catalyzes the last regulatory reaction of glycolysis, the conversion of phosphoenol pyruvate (PEP) into pyruvate. Here as well, ATP is an allosteric inhibitor. Alanine, in addition, works as a final product inhibitor, since it can be synthesized in one step from pyruvate. Gluconeogenesis usually does not use pyruvate as a direct substrate but lactate or oxaloacetate, an intermediate of the TCA cycle. Pyruvate can be directly converted into oxaloacetate catalyzed by pyruvate carboxylase. Through the reaction catalyzed by PEP carboxykinase oxaloacetate is decarboxylated and at the same time phosphorylated resulting in PEP. The next irreversible step of glycolysis is circumvented by the enzyme fructose 1,6-bisphosphatase (F1,6BPase). It dephosphorylates F1,6BP resulting in F6P. In most organs G6P is the endpoint of gluconeogenesis. In all other tissues except for liver no free glucose is produced, which could be transported over the cellular membrane.

As mentioned above, pyruvate, which is produced by glycolysis, can be further metabolized. Under anaerobic conditions it can be metabolized to lactate by the enzyme lactate dehydrogenase. Through this reaction NAD^+ , which was reduced to NADH during glycolysis, is recycled. Pyruvate can also be decarboxylated and transferred to coenzyme A by a multi enzyme complex called pyruvate dehydrogenase complex. The resulting acetyl-CoA can then be used as a precursor for the synthesis of fatty acids or can be further metabolized *via* the TCA cycle. The TCA cycle is a major intersection of carbon metabolism since not only acetyl-CoA, derived from carbohydrate and fatty acid metabolism, can enter the pathway, but also amino acids at different stages. At the same time its intermediates serve as precursors for numerous molecules such as nucleobases or porphyrines. The first step of the TCA cycle is the condensation reaction of acetyl-CoA and oxaloacetate to form citrate. This reaction is catalyzed by citrate synthase. In the first half of the TCA cycle the two carbon atoms derived from acetyl-CoA are further metabolized finally resulting in CO_2 . This is accomplished by the isomerization of citrate to isocitrate, which is then decarboxylated and oxidized to α -ketoglutarate. In this step NADH is produced. α -ketoglutarate is then further decarboxylated and under NADH production succinyl-CoA is formed. In the second half of the cycle oxaloacetate is recycled *via* several intermediates as there are succinate, fumarate and malate. Thereby another molecule of NADH and also one molecule of the related redox cofactor FADH_2 are formed as well as one molecule GTP. The intermediates of oxaloacetate recycling also serve as entry points for certain amino acids and as precursors for other reaction. Overall, the TCA cycle itself does not produce a lot of energy with only 1 GTP per entering acetyl-CoA, but it produces energy rich electrons in form of NADH and FADH_2 . These can be used for the formation of ATP when the electrons are transferred over several electron carriers to O_2 during oxidative phosphorylation. This process yields about 26 ATP per molecule glucose, which entered glycolysis.

The PPP has two major functions: Based on G6P it first produces NADPH and second C5-carbohydrates. NADPH is needed for reductive anabolic reactions, as the biosynthesis of fatty acids, cholesterol or nucleotides. The produced ribose 5-phosphate (R5P) (C5) is a precursors for the production of DNA, RNA, ATP and reduction equivalents as NADH or FADH_2 . As already mentioned above, the PPP is interconnected with glycolysis. Therefore, R5P, which is not needed for biosynthesis can enter glycolysis and be further metabolized in the TCA cycle. Because of this interconnectivity these pathways need to be regulated together to avoid a waste of resources and energy. The activity of the different pathways or to which level they are executed strongly depends on the cellular demand. As described above the energy level of

the cell is a major regulator of glycolysis. In concordance with this, NADP^+ , as a necessary reaction partner and indicator of the available amount of NADPH, regulates the rate-determining irreversible step of the pathway, the conversion of G6P to R5P. The complex interplay of these regulators enables the cell to react to its varying metabolic demands.

Fatty acids are well known for their role in energy storage in the form of triglycerides. However, they also have other important biological functions. As components of phospholipids and glycolipids they form cellular membranes, and fatty acid derivatives can also serve as important hormones or intracellular messengers. The synthesis and degradation of fatty acids work in an opposite manner, namely through the addition or removal of C_2 -units. Acetyl-CoA is the precursor for fatty acid synthesis. NADPH serves as reduction equivalent. Degradation of fatty acids is in contrast to the synthesis an oxidative process called β -oxidation resulting in acetyl-CoA which can then be further metabolized by the above described pathways.

1.3.2 Adaption and regulation in liver

To understand the differences in the regulation and utilization of metabolic pathways in the liver one has to understand its differential function. The liver is the major site for the synthesis, metabolism, storage and redistribution of carbohydrates, proteins and lipids (Bechmann et al. 2012). Its role as metabolic hub and modulator of plasma concentrations of different metabolites and proteins, make certain adaptations necessary, which are depicted in Figure 1-5. The liver metabolically connects various tissues, especially skeletal muscle and adipose tissue (Rui 2014). Its special role in glucose homeostasis first of all makes it a necessity that liver itself is not solely dependent on glucose as a carbon source for its own energy metabolism. Since it is not only responsible to remove excessive glucose from the blood but also has to guarantee glucose supply for other tissues during fasting, a possibility to store and to produce glucose from other sources has to be given. The possibility to store glucose is given in hepatocytes in the form of glycogen. The first step of hepatic glucose utilization is determined by Glut2 (glucose transporter 2), the major hepatic glucose transporter. In contrast to other glucose transporters Glut2 mediated transport is not insulin sensitive and the transporter only saturates above plasma glucose concentrations of 30 mM (Bechmann et al. 2012, Mueckler and Thorens 2013). The actual synthesis of glycogen starts from G6P, which is isomerized to glucose 1-phosphate (G1P) by the enzyme phosphoglucomutase. G1P is then activated by being transferred to UTP resulting in UDP-glucose, which acts as glucosyl-group donor for glycogen synthesis.

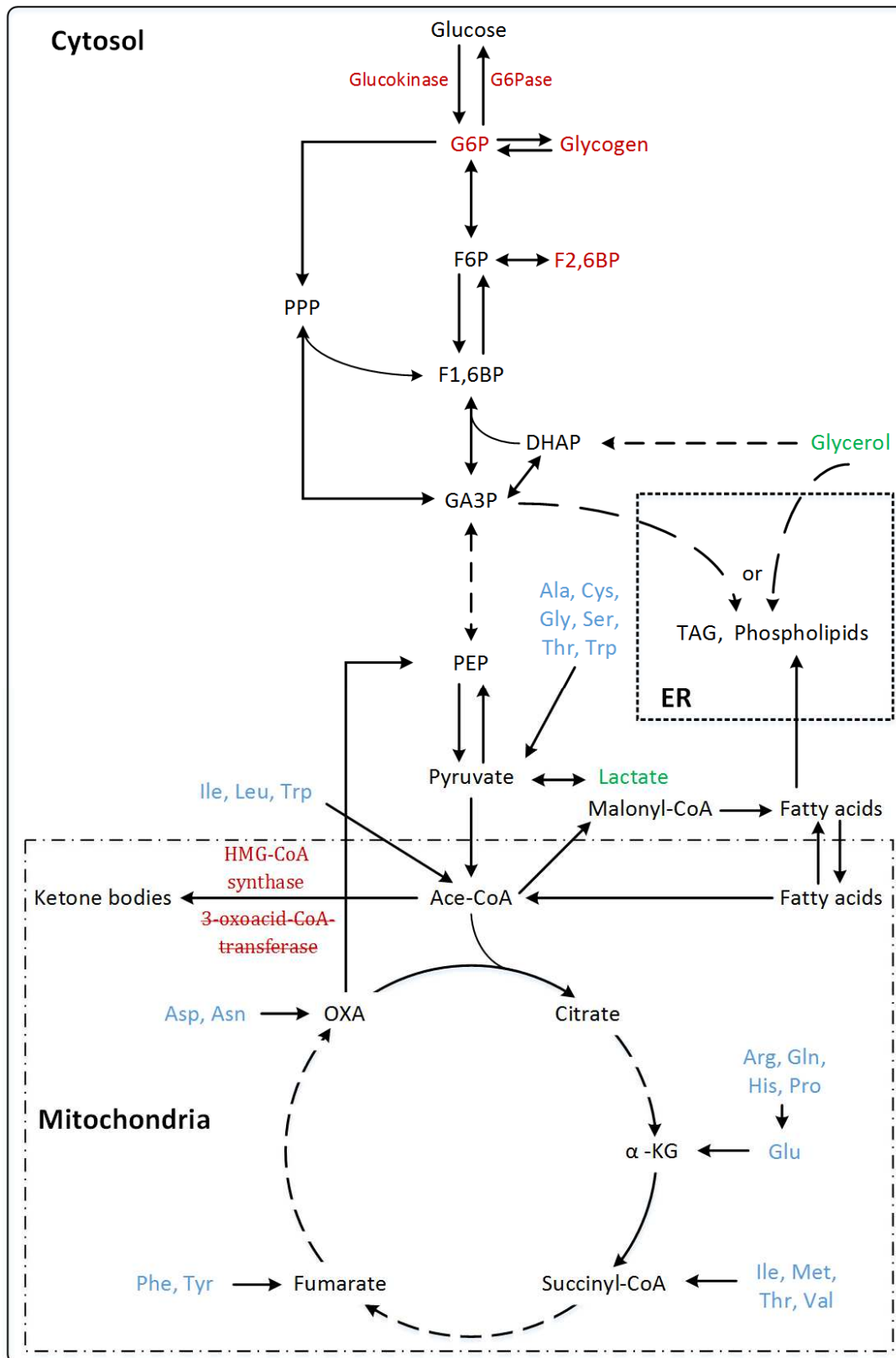


Figure 1-5 The central carbon metabolism and its special adaptations in liver. Detailed explanations are given in the text. Double headed arrows: Reversible reactions; Dashed arrows: Several reaction are condensed; Blue: Amino acids entering metabolism for degradation; Green: Gluconeogenic precursors; Red: Special adaptations in liver; Crossed out: In all other tissues but not in liver. Abbreviation: Amino acids are abbreviated by their three letter code; α -KG α -ketoglutarate; Ace acetyl; CoA coenzyme A; DHAP dihydroxyacetone phosphate; ER Endoplasmatic Reticulum; F16BP fructose-1,6-bisphosphate; F26P fructose-2,6-bisphosphate; F6P fructose-6-phosphate; G6P glucose-6-phosphate; G6Pase glucose-6-phosphatase; GA3P glyceraldehyde 3-phosphate; OXA oxaloacetate; PEP phosphoenolpyruvate; PPP pentose phosphate pathway; TAG triglyceride.

The degradation of glycogen during fasting is catalyzed by glycogen phosphorylase and moves more or less contrary to the synthesis resulting in G1P. Of course these reactions need to be strictly regulated. This is achieved by the opposing regulation of the two rate-limiting enzymes: glycogen synthase and glycogen phosphatase. Both enzymes are regulated by phosphorylation, however in an opposing manner. The phosphorylase is more active when phosphorylated, the synthase is more active when dephosphorylated (Hers et al. 1970). These enzymes are complexly regulated, amongst others by cyclic AMP (cAMP) and G6P. cAMP, an intracellular messenger, is increased due to glucagon signaling (Exton et al. 1971). This increase leads to the activation of protein kinase A (PKA), which then phosphorylates and therefore activates glycogen phosphatase (Rui 2014). The enzyme thereby also serves as a glucose sensor. G6P, on the other hand, acts as an allosteric activator of glycogen synthase, which can activate glycogen synthase even when it is highly phosphorylated (Srivastava and Pandey 1998, Bechmann et al. 2012). Glycogen synthase is also a target of insulin mediated signaling.

The first step of glycolysis is usually accomplished by hexokinase, which is only found in low amounts in liver. Instead, in liver glucokinase (GK) carries out this task (Katz and McGarry 1984). In contrast to hexokinase, GK has a low affinity for glucose and is not feedback-inhibited by its product G6P. Its activity increases sigmoidal with increasing glycemia (Wilson 2003). Since glucose is transported into hepatocytes by facilitated diffusion GK keeps intracellular glucose levels low and determines glucose clearance (Pilkis and Granner 1992). During fasting GK is bound to the glucokinase regulatory protein in the nucleus, which keeps it in an inactive state. Glucose itself leads to the dissociation of the complex and to its translocation to cytoplasm (Bechmann et al. 2012). The transcriptional control of GK is highly complex and influenced by many transcription factors, e.g. the sterol regulatory element binding protein-1c (SREBP-1c), which mediates insulin dependent transcription (Kim et al. 2004).

Gluconeogenesis is a pathway not only active in liver, but it has some specialties compared to other cell types. The most remarkable of these is that the last enzyme glucose-6-phosphatase (G6Pase), which catalyzes the production of free glucose from G6P, is only expressed in hepatocytes (Jitrapakdee 2012). G6P is transported into the endoplasmic reticulum (ER), where it is dephosphorylated by G6Pase, which is the rate limiting step in gluconeogenesis (Rui 2014). Because of this, hepatocytes are the only cell type which is able to produce free glucose, which can be transported over the cellular membrane.

Another special regulator of glucose metabolism in liver is fructose-2,6-bisphosphate (F2,6BP). This metabolite is produced and degraded from and to F6P by the bifunctional enzyme 6-phosphofructo-2-kinase/fructose-2,6-bisphosphatase (6PFK2/FBP2). When levels of F2,6BP are high, the activity of glycolysis is increased, whereas gluconeogenic activity is decreased. This is achieved by allosteric regulation of two major regulation enzymes of both metabolic pathways. These enzymes are 6-phosphofructo-1-kinase, which is allosterically activated and fructose-1,6-bisphosphatase, which is inhibited by F26BP (Wu et al. 2006). Both enzymes are directly connected to the precursor of F2,6BP, fructose 1-phosphate (F1P). The amount of F1P is tightly connected to the amount of available glucose. F2,6BP thereby serves as a sensitive glucose sensor for the liver. The expression of 6PFK2/FBP2 is hormonally regulated by insulin and glucocorticoids (Okar et al. 2004).

Not only glucose serves as a valuable energy source for extrahepatic tissues during fasting but also ketone bodies as acetoacetate and β -hydroxybutyrate. All enzymes involved in their production are also present in extrahepatic tissues. However, the enzyme catalyzing the rate-limiting step of ketogenesis, namely HMG-CoA synthase, is only found in liver in large quantities. The rate limiting step for ketone body utilization, 3-oxoacid-CoA-transferase, however, can be found in all tissues but liver (McGarry and Foster 1980) (Figure 1-5).

Liver metabolism comprises an immense spectrum of interrelated anabolic and catabolic functions which are performed simultaneously without wasting energy. To cope with this challenge, liver parenchyma shows a considerable heterogeneity known as metabolic zonation (Gebhardt and Matz-Soja 2014). Liver zonation is thereby established by displaying different morphological features, such as different number of mitochondria, or by differential enzyme expression. The most prominent zoned pathways of liver are glucose metabolism with glycolysis being located in the pericentral and gluconeogenesis being most prominent in the periportal region of the lobule. Also amino acid degradation (periportal), as well as fatty acid degradation (periportal) and lipogenesis (pericentral) are zoned. However, also hepatic functions such as detoxification of xenobiotics or detoxification of ammonia are zoned along the sinusoids. Ammonia detoxification is strictly separated with urea synthesis taking place in the periportal region and glutamine synthesis only occurring in the two innermost pericentral cell layers. CYPs are mainly expressed in pericentral hepatocytes as well (Braeuning et al. 2006). How these processes are exactly regulated and zonation is maintained is still not completely understood. However, gradients formed along the sinusoids, such as pO_2 and various hormones and nutrients, together with β -catenin signaling seem to play a

major role. Recent insights on this topic are given in an excellent review by Gebhardt and Matz-Soja (Gebhardt and Matz-Soja 2014). Working with primary hepatocytes the aspect of liver zonation has to be kept in mind, since the isolated cells usually represent a mixture of periportal and pericentral hepatocytes also resulting in a mixture on a metabolic level.

The adaptations described here are only a few examples and are described only very superficially. Especially the regulation of all these processes is much more complex. However, these examples are well suited to show, how liver metabolism is adapted to its tasks in homeostasis with differential gene expression and differential metabolic regulation. Especially glucose metabolism, ammonia and xenobiotic detoxification will be in the focus of this thesis.

1.4 Insulin: A small molecule with huge impact

Insulin is a small peptide hormone with a molecular weight of about 5800 Da. It is produced by the β -cells of the islets of Langerhans in the pancreas. Insulin itself consists of an α - and a β -chain, which are covalently linked by two disulfide bonds (Figure 1-6). However, it is first synthesized as one polypeptide, from which a signaling sequence is cleaved off which results in the generation of proinsulin, which is then further cleaved by intracellular enzymes to become the final active form of the hormone. Until needed, insulin is stored within the β -cells. The release of the hormone is regulated by several factors. The nutritional component, mainly an elevated blood glucose level, but also other nutritional factors as amino acids

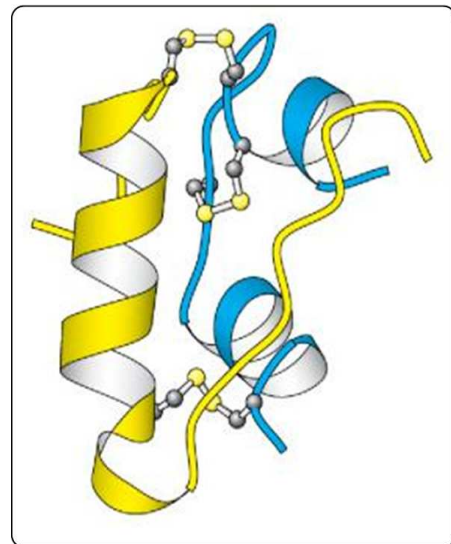


Figure 1-6 Structure of insulin. The final molecule consists of a α - (blue) and β -chain (yellow), which are covalently linked by two disulfide-bonds. Additionally, a third disulfide bond is found within the α -chain. (Adopted from Stryer Biochemie, 6. Auflage)

(arginine or leucine) or malonyl-CoA, an intermediate of fatty acid metabolism, play a major role in the regulation of insulin release (Sener et al. 1981, Corkey et al. 1989, Henningsson and Lundquist 1998, Yaney and Corkey 2003). Additionally, also hormonal signals, e.g. catecholamines, and neuronal signals are important for regulating the release (Malaisse et al. 1979, Cherrington 1999). The different factors, which lead to the release of insulin and the interplay of different organs are depicted in Figure 1-7 a. There are several insulin sensitive tissues, but the liver, skeletal muscle and adipose tissue are the major targets of insulin regarding glucose homeostasis. The blood from the pancreas is directly led into the portal

vein and therefore the pancreatic hormones first of all reach the liver sinusoids (Roden and Bernroider 2003). This underlines the special status the liver has in glucose regulation. But not only insulin gives an input to the liver. After a meal, the portal glucose concentration is elevated. Glucose itself can push its own uptake and metabolism and at the same time inhibit endogenous glucose production. This effect is known as glucose effectiveness (Tonelli et al. 2005). The impact of glucose effectiveness, which seems to be impaired during type II diabetes, is also depending on another factor: the free fatty acid (FFA) concentration. FFA and glycerol can be used as precursors for gluconeogenesis. Postprandial insulin secretion has an inhibitory effect on lipolysis and therefore the production of FFA in adipose tissue (Roden and Bernroider 2003, Kowalski and Bruce 2014). Glucose effectiveness is highest, if FFA blood levels are low. Additionally, also an altered neuronal input directly affects liver metabolism. The sympathetic and the parasympathic nervous system both directly innervate the liver. The sympathetic nervous system has a positive influence on hepatic glucose production, whereas the parasympathic system antagonizes glucose production and promotes the storage of fuels in the liver (Stanley et al. 2010, Rui 2014).

After reaching the hepatocytes, insulin binds to its receptor, which is expressed in almost all mammalian tissues with varying numbers, but highest in adipose and liver tissue. The insulin receptor consists of two α - and two β -subunits, which are covalently linked through disulfide bonds forming a $\alpha_2\beta_2$ -heterotetramer. Binding of insulin leads to autophosphorylation of the receptor and starts a signaling cascade. It leads to the inactivation of glycogen synthase kinase-3 (GSK-3). Active GSK-3 inhibits glycogen synthesis and at the same time, the transcription of phosphoenolpyruvate carboxykinase (PEPCK) and glucose-6 phosphatase (G6Pase) is downregulated, which leads to reduced gluconeogenesis (Saltiel and Kahn 2001, Klover and Mooney 2004). Apart from activation of glycogen synthesis and decreased gluconeogenesis, insulin also leads to an increased uptake of glucose by the cells. This is caused by the induced translocation of Glut4 (glucose transporter 4) to the plasma membrane and the decreased internalization of the transporter. Glut4 is the major glucose transporter on insulin-sensitive cells, but until stimulated by insulin, it is mostly located in the membranes of intracellular vesicles (Zierler 1999). Upon uptake glucose can follow three different paths. It can be stored, either as glycogen or in form of triglycerides or it can be metabolized *via* glycolysis. All three possibilities are positively influenced by insulin as depicted in Figure 1-7 b. On the other hand, the opposite pathways, as glycogenolysis, gluconeogenesis or lipolysis are inhibited by insulin.

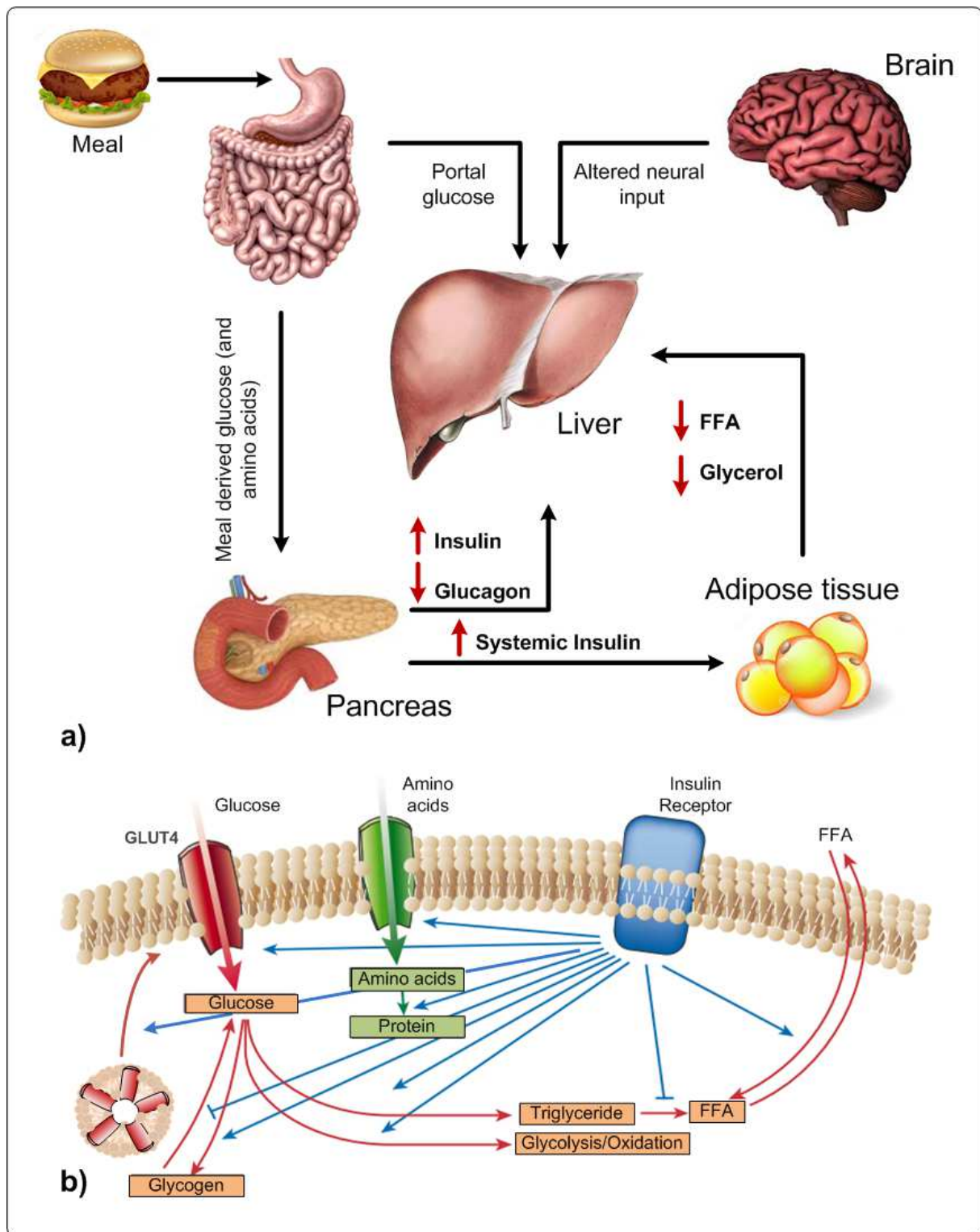


Figure 1-7 The cycle of glucose homeostasis after a meal and the various inputs on the liver from different organs; abbreviations: FFA – free fatty acids; ↑ increase; ↓ decrease; (a) and the direct effects of insulin on the liver (b) (adapted from Kowalski and Bruce 2014 and Saltiel and Kahn 2001).

Furthermore, insulin leads to an increased uptake of amino acids in hepatocytes, which is in accordance with an increased protein production. Although one might think, that insulin has only metabolic influence on different cells to guarantee glucose homeostasis, this is by far not true. The small peptide hormone has also drastic effects on gene transcription and mRNA

turnover, ion transport, protein degradation, and also on DNA synthesis, cell growth and differentiation and even on fertility (Draznin 1996, Duckworth et al. 1998a, Woodcroft and Novak 1999, Bunner et al. 2014). In accordance with this, Godoy et al. could show that *in vitro* insulin and dexamethasone antagonize epithelial to mesenchymal transition of hepatocytes and therefore dedifferentiation (Godoy et al. 2010). All these different effects of insulin cannot solely be explained by a simple ligand-receptor-interaction and it could be shown that there are different receptor signal transduction systems to initiate the different insulin effects (Duckworth et al. 1998a). It has also been long known, that other factors, as e.g. the internalization and intracellular processing of insulin by hepatocytes have a direct effect on increased amino acid consumption, whereas glucose metabolism is completely unaffected (Duckworth et al. 1988). However, the complete mode of action of insulin is still not fully understood.

To guarantee fast adaption to varying conditions, insulin has to be cleared from the blood rather fast. Postprandial insulin secretion in humans peaks after about 1 h and then goes back to basal levels (Kowalski and Bruce 2014). Thereby, the liver is the primary site of clearance and about 50% of secreted insulin are removed during its first pass (Jungermann and Kietzmann 1996). Impairment of insulin clearance is closely related to metabolic diseases as glucose intolerance, obesity or non-alcoholic fatty liver disease (Lee et al. 2013a).

The counter-regulatory player of insulin is glucagon. It is another peptide hormone produced by the α -cells of the pancreas. It is produced during fasting, if the blood glucose level falls too low. The complete pathway regulating glucagon secretion is, as for insulin, highly complex. It seems to involve paracrine and intrinsic regulation, comprising amongst other things stimulation by low glucose levels and inhibition by secreted insulin (Walker et al. 2011). Also amino acid and FFA levels are important regulators. In hepatocytes, binding of glucagon to its receptor leads to an activation of PKA and adenylate cyclase, which increases intracellular cAMP levels. This leads to activation of the glycogenolytic enzymes glycogen phosphorylase kinase (GPK) and glycogen phosphorylase and at the same time to transcription of gluconeogenic enzymes (Klover and Mooney 2004). Regarding their final outcome insulin and glucagon act more or less contrary, with insulin leading to increased glucose uptake and storage and glucagon leading to endogenous glucose production.

The complex interplay of hormones and metabolites in glucose homeostasis are disturbed in many metabolic diseases as obesity or non-alcoholic fatty liver disease (NAFLD) (Roden and Bernroider 2003). However, type II diabetes (TIID) is the most well-known and widespread

disease directly associated with insulin, with 171 million people affected in the year 2000 and with 552 million people estimated in 2030 (Friedrich 2012). The two forms of diabetes, type I and type II, can be distinguished by their completely different cause. Type I is characterized by an autoimmune destruction of insulin producing β -cells with a strong genetic component. T1DM, on the other hand, is characterized by a constantly increasing insulin resistance of tissues, mainly skeletal muscle, adipose tissue and liver, leading to inappropriate endogenous glucose production and diminished glucose utilization. This is followed by impaired β -cell function due to constant hyperglycemia (Cheatham and Kahn 1995, Friedrich 2012, Bunner et al. 2014). Thereby, T1DM is strongly influenced by the lifestyle of a person regarding diet, physical activity and stress, and is strongly related with obesity, with about 60-70% of T1DM patients being obese (Klover and Mooney 2004, Temelkova-Kurktschiev and Stefanov 2012). The epidemic dimension of the disease, especially in western countries, and the high economic burden related to it, with alone 218 billion \$ in the U.S. in 2007, underscores the urgency to completely understand metabolic glucose regulation and to find suitable *in vitro* systems to analyze the disease (Dall et al. 2010).

1.5 'omics studies

In the last decade systems biological approaches have gained more and more interest in life sciences. Systems biology seeks to achieve a global understanding of mechanisms on all organizational levels by which a system adapts to its environment (Wright et al. 2012). Thereby it has to be seen as clearly marked off from the traditional reductionist thinking of molecular biology in the last few decades. The paradigm of science in classical molecular biology was: 1 gene - 1 protein – 1 function. It postulated a direct link between gene and protein function and in conclusion the knowledge of all genes should be able to explain biological function (Hollywood et al. 2006, Bensimon et al. 2012). However, the more knowledge was gained, the clearer it became that biological systems are not that simple. Genotype and phenotype are not uniquely directed due to epigenetic marks, alternative splicing, non-coding RNAs, protein interaction networks and posttranslational modifications (Espina et al. 2008, Altelaar et al. 2013). Therefore, now a paradigm shift has taken place away from reductionist thinking to an integrative approach of interpretation of biological data. The driving forces of systems biology are omics techniques, including genomics, transcriptomics, proteomics, metabolomics and also fluxomics. By integrating the huge amounts of data created with the different omics techniques a holistic understanding of biological systems is now approached.

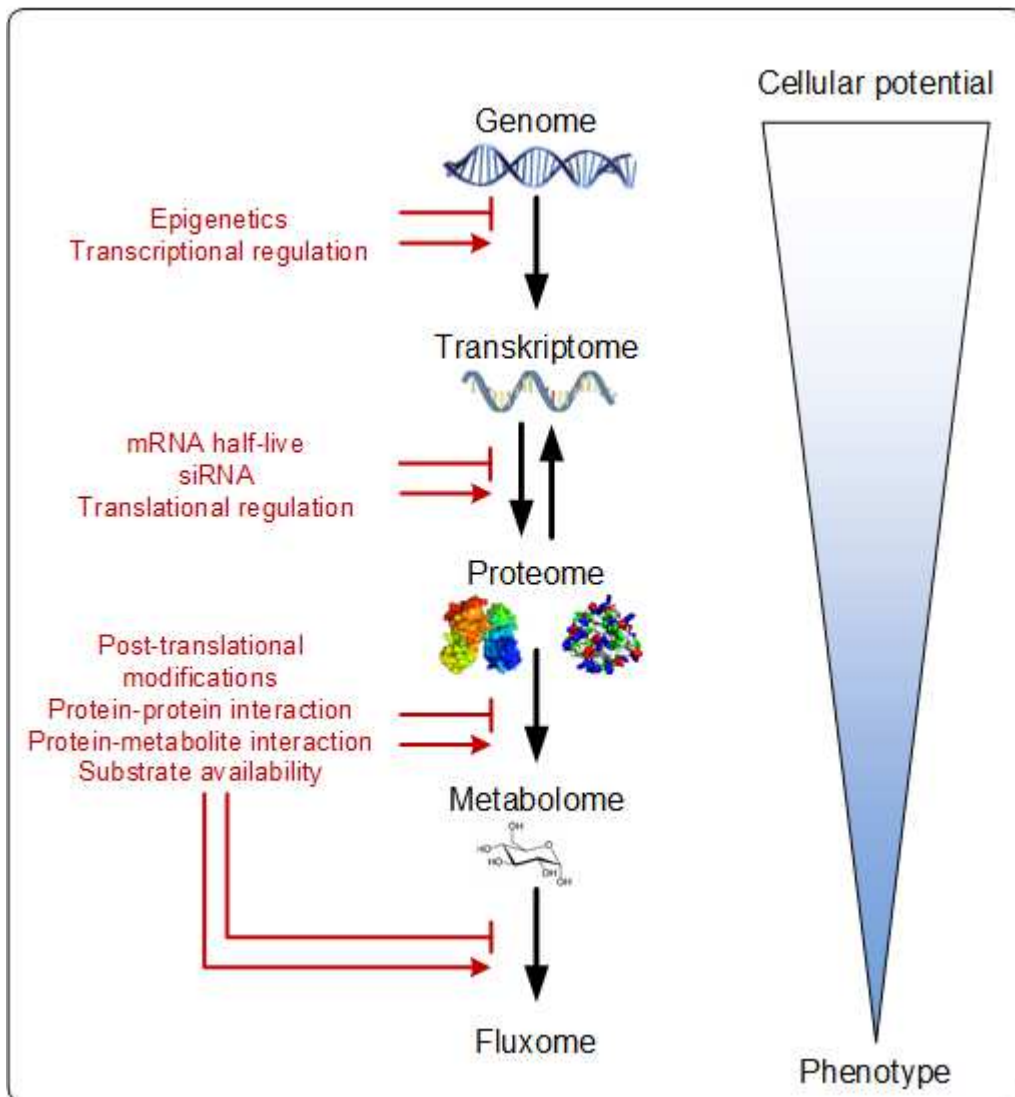


Figure 1-8 Different levels of cellular organization and exemplary regulatory influences. The genome thereby contains the full cellular potential, which is decreased alongside the organizational levels resulting in the actual phenotype.

1.5.1 Metabolomics: Gaining insight into cellular metabolism

The metabolome comprises all low-molecular weight molecules (< 3000 m/z), which are present in a system in a particular defined state (Hollywood et al. 2006). A system can thereby range from a single cell or a tissue to even a whole organism. Overall, the metabolome represents the endpoint of transcriptional, translational and environmental interactions, which includes regulation on all levels of organization (Rochfort 2005). Therefore, the metabolome closely reflects the actual phenotype (Figure 1-8). Compared to the transcriptome or the proteome, the metabolome is also the most rapid and sensitive representation of a systems phenotype, since it reflects changes in conditions already within seconds (Cox et al. 2014). The term metabolomics, analogous to other omics techniques, describes the measurement of

the metabolome and provides a snapshot of the actual metabolic state of the biological system (Friedrich 2012, Milburn and Lawton 2013). Although, certain metabolites have been related to certain disease conditions and analyzed for decades, e.g. glucose determination in urine in diabetes, the age of holistic metabolomics started about 20 years ago. In 1999 Nicholson et al. first used and defined the term metabolomics, which is often used synonymously with metabolomics (Nicholson et al. 1999, Ryan and Robards 2006). Since then metabolomics enjoys increasing popularity with more than 2400 publications in 2015.

1.5.1.1 Different metabolomics approaches

Metabolomic approaches in general can be roughly subdivided in targeted and un-targeted approaches. In metabolomic profiling, a targeted approach, a set of chosen metabolites, e.g. from a specific pathway or a chemical class, are quantitatively analyzed (Kasture et al. 2012). This was also the method of choice in this study, since the central carbon metabolism was of particular interest. The advantage of this approach is, that the most suitable analytical technique for the metabolites of interest can be chosen and that these can be quantified absolutely using calibration standards. On the other hand, considerable influences of the experimental conditions on other pathways can be missed. Untargeted approaches, or “classical” metabolomics, have the aim to give an unbiased holistic snapshot of the metabolome. Under certain perturbations, as disease or drug treatment, the term metabolic fingerprinting is also used. In this case, the snapshots from the set condition are compared to the control condition to identify possible target pathways (Ellis et al. 2007). Analogous to that, there is also metabolic footprinting, when only the extracellular metabolome is concerned. This method can be used in cell cultures and for the analysis of body fluids as blood or urine (Hollywood et al. 2006). The advantage of this un-targeted approach is clearly that it represents a hypothesis-free holistic analysis. However, quantification of all metabolites, or rather as many as possible, is a difficult undertaking. This is why metabolites mostly are only quantified in a semi-quantitative manner (Oldiges et al. 2007). A deeper insight on how metabolites are connected and how different substances are metabolized is gained, if a labeled substrate is used. ^{13}C labeling is the most common, but there are also approaches with ^{15}N or ^2H . Due to high mass accuracy of analytical methods mass differences of one neutron can be detected and conclusions on the activity of metabolic pathways can be gained. This is often supported by modeling metabolic networks (Kohlstedt et al. 2010, Nicolae et al. 2014, Dersch et al. 2016).

1.5.1.2 Analytical techniques in metabolomics

To analyze the metabolome it is most common to couple a method of separation, as gas chromatography (GC) or liquid chromatography (LC) with mass spectrometry (MS). But also nuclear magnetic resonance (NMR) spectroscopy is an often used technique (Lindon et al. 2006). NMR spectroscopy provides highly reproducible quantitative results as well as structural information on the analytes (Lindon et al. 2006, Athersuch 2016). In addition it is a non-destructive method, which covers a wide range of chemical classes (Rochfort 2005, Athersuch 2016). However, it is by far not as sensitive as MS-based methods and the obtained spectra are highly complex, which complicates data interpretation (Cox et al. 2014). The identification by MS is based on the characteristic ionization and fragmentation pattern of each metabolite. By measuring the mass to charge ratio (m/z) of these, MS allows the simultaneous detection of multiple analytes with high sensitivities (Boccard et al. 2009). MS thereby allows detection in the picomole to femtomol range (Lei et al. 2011). There are numerous different high-resolution mass spectrometers in use with orbitrap, time of flight (ToF)-MS, and Fourier transform ion cyclotron resonance (FT-ICR) –MS being the most common (Wang et al. 2015). Coupling of MS with a separation method as GC or LC in advance adds a further dimension to the data, namely the retention time based on the physico-chemical properties of the respective analyte. This increases the resolution and also gives valuable information for identifying the respective metabolites. The GC based methods use an inert gas, often helium, as mobile phase which carries the analytes through the column. In order to be transported in the carrier gas (mobile phase) the metabolites must be volatile. This can be achieved by heating or through additional derivatization, using e.g. silylating agents as BSTFA or MBDSTFA. By derivatization, active hydrogens present in functional groups are blocked by silylation (Monteiro et al. 2013). By this also polar and higher molecular weight compounds can be analyzed. Compared to LC-MS GC-MS highly profits from extensive databases of spectra, which help identifying metabolites (Griffiths et al. 2010). The high reproducibility of retention times further improves identification (Kopka 2006). Besides the additional derivatization step, which can lead to a loss of metabolites, the molecular ions of the analytes may be absent from the spectra, due to extensive fragmentation. Information on the molecular weight of the starting molecule might therefore be missing (Griffiths et al. 2010). Also incomplete derivatization or different forms of the same metabolite can occur. This also represents a problem regarding quantification. The basic principle of LC is the separation of metabolites on the basis of their interaction with a mobile and a stationary phase, with the mobile phase being liquid. With this method a wide range of molecules can be

analyzed and normally no derivatization is necessary. In addition, only very low sample volumes are needed for LC-MS analysis. Reversed phase (RP) chromatography is the most widely used technique, but also others as hydrophilic interaction chromatography (HILIC) are well used. More recent devices as ultra high performance liquid chromatography (UPLC) by using sub-2 μm particles are able to decrease the run time while at the same time leading to an increased resolution (Guillarme et al. 2010). The most prominent problem regarding LC-MS is the limited databases available. Compared to GC-MS this greatly hinders metabolite identification. The most commonly used ionization technique coupling LC and MS is electrospray ionization (ESI). Due to the high voltage applied to the liquid an ionized aerosol can be formed. This enables a direct connection between LC and MS. However, this can also lead to ion suppression effects further complicating quantification (Yanes et al. 2011, Monteiro et al. 2013). For targeted approaches also HPLC coupled with UV detection is used frequently (Mueller et al. 2011b, Wahrheit et al. 2013). UV detectors do not identify compounds directly as in MS, but identification is possible through retention time when adequate standards are used. Here also no derivatization is necessary unless it is needed for the detection.

1.5.1.3 Application of metabolomics in science

The applications of metabolomics approaches are numerous and include (1) basic research (as provided in this study, Wahrheit et al. 2014); (2) metabolic engineering and biotechnology, e.g. improvement of microbial strains for the industrial production of biologicals (Klein et al. 2015); (3) functional genomics and proteomics, identifying the function of unknown genes and proteins (Fiehn et al. 2000, Saghatelian and Cravatt 2005); (4) toxicology, in the risk assessment of drugs and chemicals (Wang et al. 2009, van Ravenzwaay et al. 2012, Mattes et al. 2013); (5) drug discovery and development (Birkenstock et al. 2012, O'Sullivan et al. 2013); (6) disease diagnosis by biomarker identification (Gowda et al. 2008); (7) with the ultimate goal of personalized medicine, e.g. to identify responders and non-responders to certain treatments (Weiss and Kim 2012, Raz et al. 2013).

In contrast to other omics techniques metabolomics has the advantage, that it determines a real biological endpoint. Metabolite levels reflect the activity of metabolic pathways, which directly reflect the actual phenotype without further regulatory interventions (Ryan and Robards 2006, Kamp et al. 2012). Due to the significant lower number of metabolites (~ 2500), compared to the number of genes (~ 40000), transcripts (~ 150000) and proteins (~ 1000000), metabolomics provides less complex and more precise quantitative data, which

makes it a more sensitive approach compared to other omics techniques to detect biological changes (Kasture et al. 2012, den Ouden et al. 2016). In addition, cellular pathways are highly conserved between different species and therefore a large part of metabolites are not species specific (Hollywood et al. 2006). Since metabolomics can also be used in a minimally invasive manner, using blood or urine as a matrix, it can easily be adapted from the lab to the clinics. Thereby, metabolomics highly profits from the robust and stable analytical platforms in use, which guarantee an excellent reproducibility. The low cost per single sample analysis as well as the ease of sample preparation and data acquisition further speak for metabolomics.

However, the analytical methods in use can still be improved regarding sensitivity and their dynamic range. The high physico-chemical diversity of metabolites is another problem, since so far there is not a single method available to determine all metabolites of a sample. This can be somehow circumvented by complementary approaches using different analytical platforms on one sample. Differentiating between stereoisomers of metabolites is also a problem, which needs to be addressed. There are already techniques available, however, these are so far highly specific for particular analytes (Athersuch 2016). The most urgent issue that needs to be addressed in the context of metabolomics is the missing standardization of methods in different labs. This makes data comparison almost impossible and establishing of comprehensive metabolome databases very challenging.

1.5.2 Proteomics: Identifying the working machinery of life

Proteomics is defined as the detailed analysis of proteins and their function in an organ, tissue or in a cell culture system. It thereby also includes the identification, modification, quantification and localization of these proteins (Yates et al. 2009, Uto et al. 2010). The proteome is highly dynamic and depends not only on cell type but also on differentiation state, cellular environment, extracellular signals and other factors (Mueller et al. 2013a). Analytical methods used for the analysis of the proteome can be roughly classified into gel-based and LC based approaches. Both methods, however, rely on MS for the identification of the respective proteins.

A well-known gel based separation method is the two-dimensional sodium dodecyl sulfate polyacrylamide gel electrophoresis (SDS-PAGE). It is a well-established method and was already introduced in the seventies (O'Farrell 1975). The first dimension of the separation is usually an isoelectric focusing (IEF). The separation is based on the amphoteric nature of proteins. At low pH basic groups become positively charged, at basic pH acidic groups

become negatively charged. Proteins will attain a zero net charge at their isoelectric point (pI) (Righetti and Bossi 1998). Today a good separation can be achieved using immobilized pH gradients (IPG). The second dimension is usually based on the molecular weight of the protein. They are coupled to the denaturizing and negatively charged agent SDS. Because of the negative charge all proteins migrate towards the anode when an electric field is applied. The separation is driven by the pore size of the polyacrylamide gel since larger proteins migrate slower than smaller ones (Garfin 2003). The proteins are then usually stained with Coomassie Blue, which has a dynamic range of 10^1 , cut out and digested with trypsin and then identified using MS. Silver nitrate is another commonly used staining method, which is more sensitive and has a higher dynamic range of up to 10^2 , but it is incompatible with MS-based identification (Lilley and Friedman 2004). Due to the low dynamic range of these staining methods and since every sample is run on a separate gel protein quantification with this setup is not reliable.

1.5.2.1 Gel-based proteomic approaches

A variant of conventional SDS-PAGE called DIGE highly improves protein quantification. This technique was introduced by Unlü et al. and is based on the labeling of two samples, which are to be compared, with fluorescent dyes (Unlü et al. 1997) (Figure 1-9). The used fluorescent dyes are N-hydroxy succinimidyl ester reagents for low-stoichiometric labeling of the ϵ -amine groups of lysine side-chains and fluorescing in the red (Cy3) and blue (Cy5) part of the spectrum (Lilley and Friedman 2004). The protein samples can therefore be run on the same gel, which facilitates quantitative comparison enormously. An internal standard, consisting of the same amount of protein from the samples, which are to be compared, is also labeled with a third dye (Cy2) and run on the same gel. This enables intra- and inter-gel comparability (Lilley and Friedman 2004). DIGE is capable of detecting about 2000 soluble proteins without need to limit investigation to proteins relative to a certain hypothesis and the used dyes have a dynamic range of five orders of magnitude with a detection limit of 150-500 pg (Prabakaran et al. 2007, Gozal et al. 2009). Up to now DIGE has been used in numerous studies with a multitude of cell types including human breast cancer cells, human liver, brain tissue of genetically modified mice and rat heart tissue (Gharbi et al. 2002, Skynner et al. 2002, Sakai et al. 2003, Prabakaran et al. 2007). Thereby DIGE can be applied for *in vitro* cultivation systems as well as for patient material from various diseases, ranging from schizophrenia to sleep apnea in children (Prabakaran et al. 2007, Gozal et al. 2009, Haas

et al. 2012). DIGE has the great advantage that no hypothesis has to be generated in advance of analysis, but that the proteome can be analyzed in an unprejudiced manner.

Valuable information about the physiological isoelectric point and the molecular weight of the respective proteins is obtained and can be very useful to confirm MS-based protein identification (Diamond et al. 2006). Through to the use of the more sensitive fluorescent dyes the dynamic range of conventional SDS-PAGE could be improved as well as the high inter-gel-variability by the use of an internal standard. However, reproducibility is still an issue of all gel-based approaches and spot-matching on different gels can still be tedious and error-prone work. The number

of samples, which can be compared with this approach is not necessarily limited to two samples, but the more samples are compared the more complex the setup becomes. Membrane-proteins, as well as proteins with a very high or a very low pI as well as low abundant proteins are also difficult to analyze with this method (Gonnet et al. 2003, Wright et al. 2012). In addition, DIGE and other gel-based approaches are far from high-throughput, since the whole procedure of sample preparation, protein separation and identification takes several days, and the data obtained has to be considered qualitative rather than quantitative. However, DIGE has undergone a rapid development and will have a major impact in fields as disease

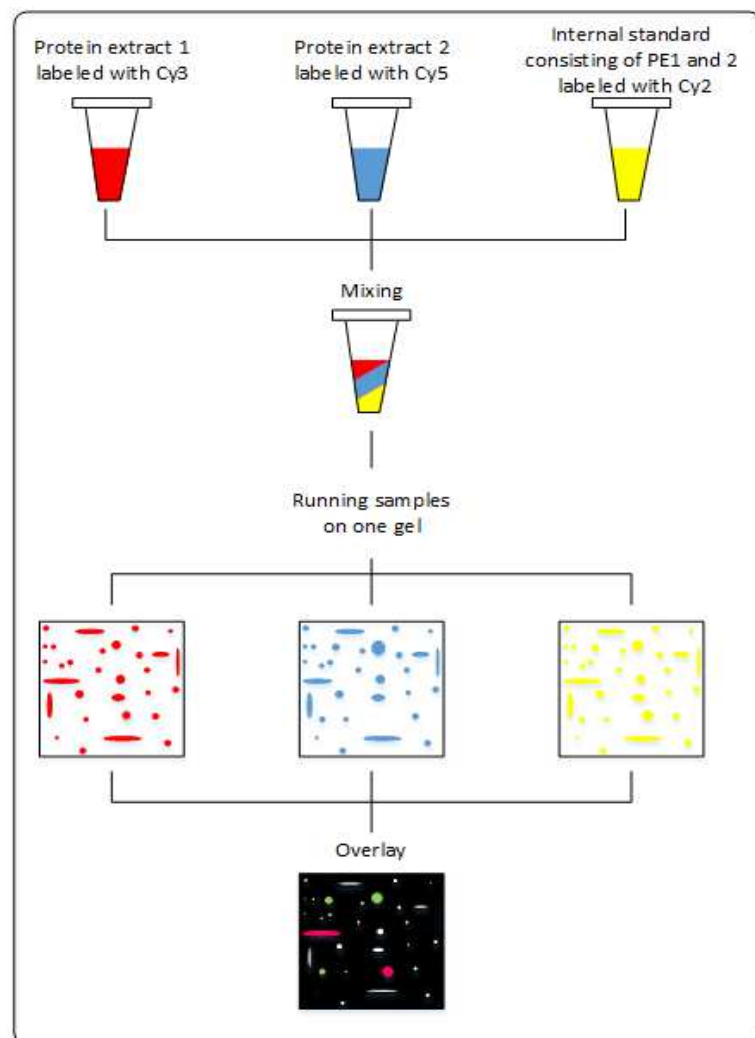


Figure 1-9 General principle of differential gel electrophoresis (DIGE). Each protein sample is labeled with a fluorescent dye (Cy3 and Cy5) and an internal standard (IS), consisting of the same amount of protein of both samples, is labeled with another dye (Cy2). All preparations are mixed and run on the same gel. Pictures with each respective fluorescent filter are obtained and an overlay of all three pictures is created. Proteins, which are only present in the protein extract 1 and the IS appear pink, proteins present in protein extract 2 and the IS appear green. Proteins, which are present in the same amounts in all three preparations, are white. The amount of protein is determined by peak intensity compared to the internal standard. Abbreviations: PE protein extract.

diagnosis in the future (Lilley and Friedman 2004).

1.5.2.2 Non-gel-based proteomic approaches

Non-gel-based approaches for proteome analysis mostly use different LC-MS methods for protein separation. One of the major differences compared to gel-based approaches is, that the proteins are in most cases turned into peptides by tryptic digestion before the separation takes place. However, also with LC-MS labeling of the samples in one or the other way is helpful for quantification. The labeling methods can thereby be differentiated as metabolic and chemical labeling and synthetic spiking. The most common metabolic labeling method is stable isotope labeling by amino acids in cell culture (SILAC). The isotopically labeled amino acids $^{15}\text{N}_4$ -arginine or $^{13}\text{C}_6$ -lysine are added to the cell culture medium and are incorporated by the cells into their proteins. This enables a direct comparison of the protein samples and, as for DIGE, a semi-quantitative comparison between two experimental conditions. An alternative to metabolic labeling is chemical labeling. Here, no high protein turn-over rate is necessary, since the labeling takes place after protein extraction from the cells. Two representatives of this approach are isotope-coded affinity tags (ICAT) and isobaric tags. The quantification principle is thereby analogue to the metabolic labeling approach. ICATs are often specified for labeling of the cysteine side chain, whereas isobaric tags label free amines in peptides (Patton et al. 2002, Yates et al. 2009). A general problem of chemical labeling is that the peptides are labeled relatively late in the workflow. Differences in the protein amount resulting from sample preparation can therefore not be detected. Another problem can be the labeling efficiency of the respective tag used. To circumvent the problem of labeling efficiency there is also the possibility to use an external peptide standard of a known concentration. This method is called synthetic spiking and the standard usually consists of synthetically produced signature peptides, with incorporated stable isotopes, corresponding to a specific protein identity (Gerber et al. 2003). Due to the known concentration of standard peptides, this method can be used for absolute quantification of the protein amount in a sample. There are also protein quantification approaches without using any kind of labeling. Thereby, signal intensity is used for quantification. The great advantage of label-free quantification is that the number of conditions, which can be compared is not limited (Bantscheff et al. 2012). However, reproducibility remains the point of question in this approach, since peptide intensities can vary from run to run, which makes direct comparison of different samples questionable. A problem, which is common to all the above-mentioned LC-based approaches is co-elution of identical peptides from different proteins. This occurs

when a bottom-up approach, also called shotgun-proteomics, in which the whole proteome is digested into peptides by trypsin before separation, is used. This can be reduced to a certain degree if e.g. the samples are somehow pre-fractionated.

1.5.2.3 MS-based detection of proteins

DIGE as well as the different LC-based methods available for proteome analysis both rely on MS or MS/MS based protein identification. Thereby, soft ionization methods are necessary to keep proteins and peptides intact (Yates et al. 2009). Most widely used are ESI-MS and matrix assisted laser desorption/ionization (MALDI) –ToF–MS (Fenn et al. 1989, Tanaka 2003). MALDI-ToF-MS is often used together with gel based approaches. The protein spots are picked from the gel, digested into peptides by trypsin and after purification and preparation of the samples mixed with a matrix. The matrix analyte mixture is then spotted on a designated metal plate. The matrix absorbs the energy of the laser and transfers it to the peptides. Laser heating causes desorption of the matrix, which finally leads to $[M+H]^+$ ions omitting into gas phase (Karas and Krüger 2003). There are different matrices available for MALDI, which have special characteristics for different analytes. α -Cyano-4-hydroxycinnamic acid (HCCA) is well suited for peptides with a mass lower than 2500 Da. Sinapinic acid (SA) on the other hand should be used for the analysis of peptides with a mass higher than 2500 Da. 2,5-Dihydroxybenzoic acid (DHB) or 3-hydroxypicolinic acid (3-HPA) are well suited for hydrophobic peptides and phosphorylated or glycosylated peptides (Gonnet et al. 2003). ESI is mostly coupled with LC since this technique enables a continuous measurement (Diamond et al. 2006). Ions are here directly produced from solution driven by high voltage applied between the emitter at the end of separation pipeline and the inlet of the MS (Yates et al. 2009). The assignment of the found peptides to their respective protein with both methods is based on database comparison. There are several databases, as e.g. UniProtKB/Swiss-Prot or PRIDE, publically available. The experimentally gained spectra can then be matched against these databases with professional search algorithms as e.g. MASCOT. This finally leads to the identification of the analyzed proteins.

None of the above described methods is optimal for a comprehensive analysis of proteome, since each of the methods has certain drawbacks and is not suitable for all proteins or all experimental setups. However, the strength in the different proteomic approaches lies in the combination of the different techniques, which offers a wider spectrum of information.

1.5.2.4 Application of proteomics in liver science

Large efforts are undertaken to understand liver function on a proteomic level. The most popular field of application is the detection of biomarkers for certain disease states and toxicity, e.g. Rodriguez-Suarez et al. used DIGE and MALDI-ToF/ToF to find protein signatures associated with NAFLD and NASH (Rodriguez-Suarez et al. 2012). Also in the field of cultivation optimization proteomics is used to analyze the factors leading to dedifferentiation of hepatocytes in culture (Heslop et al. 2016). Rowe et al. used proteomics to compare the profiles of freshly isolated hepatocytes, cultivated adult hepatocytes, freshly isolated fetal hepatocytes and HepG2 cells (Rowe et al. 2013). These profiles can then be used to characterize stem-cell derived hepatocyte models and to guarantee their state of differentiation. However, since the liver not only consists of hepatocytes the proteomic characterization of other liver cell types, as done by Azimifar et al., is of high importance as well and can give us new insights into their actual roles in liver (Azimifar et al. 2014). To achieve a holistic understanding of the hepatic proteome there are also major initiatives as The Chinese Human Liver Proteome Profiling Consortium or The Human Liver Proteome Project, which collect and analyze the proteomic liver profiles of human adult liver of multiple donors to characterize the hepatic proteome on a broad level and to build up reference databases (<https://www.hupo.org/human-liver-proteome-project/>).

Experiments like these especially in combination with other omics techniques can lead to an in-depth understanding of this highly complex biological system. This knowledge can be used to create improved cultivation systems urgently needed, to understand complex disease mechanisms and ultimately to treat these in a personalized fashion.

1.6 Aim and outline of the thesis

The aim of the presented thesis was to increase the knowledge of metabolic and proteomic behavior of primary hepatocytes in dependence of the cultivation technique used in a quantitative way. A lot is known about hepatic function, which is prolonged in SW cultivation. This includes the extended production of liver specific metabolites and proteins as urea and albumin as well as the constantly higher activity of CYP enzymes, which are of utmost importance for xenobiotic metabolism. Also the regained polarity of hepatocytes in SW culture and the long time maintenance of it is a well-known and well-described phenomenon. Although a lot is also known about differentiated gene expression in consequence of the cultivation condition, only little information is available about metabolic and proteomic changes, especially not in a quantitative manner.

First, a general metabolic characterization of PMH in collagen ML and SW culture was accomplished which is presented in **Chapter 3** of this thesis. Thereby the focus lay on the phase of repolarization directly after seeding of the cells and on dedifferentiation during a 5 d period of cultivation. In addition to the metabolic characterization, a throughout analysis of hepatic function was accomplished. In a systemic approach the collected metabolic data were completed with data gained from proteomic analysis (**Chapter 4**). For that purpose, the intracellular proteome of PMH in collagen ML and SW culture was compared after day 1 and day 5 of cultivation. To also characterize possible influences of the cultivation time itself, samples from day 1 and day 5 of the same cultivation condition were compared as well. Changes in protein expression were determined in a semi-quantitative manner with DIGE and in a second step identified with MALDI-ToF-MS. Due to the results gained by the general metabolic characterization of PMH in SW and ML culture, namely the susceptibility of glucose metabolism, the focus of **Chapter 5** is on the direct influence of glucose concentration itself and its major regulator, insulin. A low initial glucose concentration resembling fasting conditions (7 mM) and a high concentration resembling postprandial conditions (25 mM) were chosen for this approach. Additionally, five different insulin concentrations were tested. To further elucidate metabolic processes, ^{13}C labeling was applied with $[\text{U}^{13}\text{C}]$ -glucose and $[\text{U}^{13}\text{C}]$ -glutamine serving as substrates. In this study not only the metabolome of PMH in both culture conditions was characterized, but also that of PHH. This comparative approach was performed to determine, if metabolic species differences *in vivo* are also displayed in *in vitro* cultivation systems. The final chapter deals with the effects of glucose and insulin on the hepatic function of primary human and mouse hepatocytes (**Chapter 6**). Therefore, insulin degradation, CYP 3A activity and albumin and urea synthesis were analyzed.

2. Material and Methods

2.1 Chemicals

Dexamethasone, ammonium chloride, amodiaquine, phenacetin, bupropion hydrochloride, tolbutamide, calcein AM, human insulin, 4',6-diamidino-2-phenylindole (DAPI), bovine serum albumin (BSA), trichloroacetic acid (TCAA), tetrahydrofuran, N-laurylsarcosine, 3-[(3-cholamidopropyl)dimethylammonio]-1-propanesulfonate hydrate (CHAPS), sodium dodecyl sulfate (SDS), glycerol, ammonia bicarbonate, bromophenol blue, *N,N,N',N'*-tetramethylethylenediamine (TEMED), ammonium persulfate (APS), 4-chloro- α -cyanocinnamic acid (CCA), trifluoro acetic acid (TFA), *N,N*-dimethylformamide (DMF), L-lysine, indoleacetic acid (IAA), methoxyamine hydrochloride, acetonitrile and methanol were obtained from Sigma Aldrich (Steinheim, Germany). 5-chloromethylfluorescein diacetate (CMFDA) and insulin/transferrine/selenium (ITS) were purchased from Invitrogen (Molecular Probes, Gibco, Darmstadt, Germany) and lyophilized collagen from Roche (Penzberg, Germany). Rhodamine/phalloidin was obtained from Cytoskeleton Inc. (Denver, CO, USA) and propafenone from Abbott GmbH & Co. KG (Wiesbaden, Germany). S-mephenytoin and atorvastatin were purchased from Toronto Research Chemicals (Toronto, Canada). Labeled substrates ([U-¹³C]-glucose and [U-¹³C]-glutamine) were obtained from Cambridge Isotope Laboratories, Inc. (Andover, MA, USA). Tris(hydroxymethyl)aminomethane (TRIS), dithiothreitol (DTT) and urea were purchased from Carl Roth (Karlsruhe, Germany). Ethylene diamine tetraacetic acid (EDTA) was obtained from ICN Biomedicals GmbH (Eschwege, Germany) and thiourea from Merck (Darmstadt, Germany). Mineral oil, Bio-lyte 3-10 and 10x Tris/Glycine/SDS-buffer were bought from Bio-Rad Laboratories, Inc. (Hercules, CA, USA) and NaCl from VWR International GmbH (Bruchsal, Germany). LE Agarose was purchased from Biozym Scientific GmbH (Hessisch Oldendorf, Germany). Pyridine and acetic acid were obtained from Thermo Fisher Scientific (Waltham, MA, USA). *N,O*-Bis(trimethylsilyl)trifluoroacetamide (BSTFA) and *N*-(*tert*-butyldimethylsilyl)-*N*-methyl-trifluoroacetamide (MBDSTFA) were purchased from Macherey-Nagel (Düren, Germany).

2.2 Cell culture

2.2.1 Primary mouse hepatocytes

PMH were isolated from livers of male C57/BL6 mice using collagenase perfusion as described by Seglen et al and Zellmer et al. (Seglen 1972, Zellmer et al. 2010). After overnight shipping in suspension or directly after isolation, the transport medium was removed *via* centrifugation (Heraeus Laborfuge 400R Functionline, Thermo Scientific; 50 x g, 5 min, RT). If not mentioned otherwise, the cells were seeded at a density of $6 \cdot 10^5$ cells per well in 6 well plates precoated with 400 μ l collagen solution with a concentration of 1 mg/ml. The cultures were prepared as collagen SW and collagen ML cultures (Tuschl and Mueller 2006). Hepatocytes were cultivated in William's medium E (WME) (Pan Biotech GmbH, Aidenbach, Germany) containing 100 U/ml penicillin, 100 μ g/ml streptomycin, 0.00001% ITS and 100 nM dexamethasone at 37 °C in a humidified atmosphere containing 95% air and 5% CO₂ for up to 5 days.

2.2.2 Primary human hepatocytes

PHH were isolated from human liver resectates using a two-step collagenase perfusion technique as described by (Damm et al. 2013) at Charité Berlin. After an overnight transport in suspension the transport medium was removed *via* centrifugation (Heraeus Laborfuge 400R Functionline, Thermo Scientific; 70 x g, 5 min, RT) and the cells were resuspended in WME containing 10% FCS. After determination of the living cell number with trypan blue staining the cells were further purified with percoll (Easycoll Separation Solution, Biochrom, Berlin, Germany) gradient centrifugation if the determined viability was below 75%. The cells were seeded at a density of $1 \cdot 10^6$ cells per well in 6 well plates precoated with a collagen solution according to the procedure for PMH.

2.2.3 Determination of living cell number

2.2.3.1 Trypan blue staining

A 10 μ l aliquot of cells was mixed with the same volume of trypan blue (Invitrogen, Karlsruhe, Germany). 10 μ l were transferred into a Neubauer chamber and then counted under the microscope (IX70 microscope, Olympus, Hamburg, Germany). Cells appearing white were counted as living cells, whereas blue ones represented dead cells.

2.2.3.2 Calcein AM staining

Calcein AM was diluted with serum free WME to a final concentration of 4 µg/ml. Cells were stained and analyzed as described by Priesnitz et al. (Priesnitz et al. 2014).

2.3 Microscopy

For phase contrast and fluorescence recordings an IX70 microscope (Olympus, Hamburg, Germany) linked with a digital CC12 camera (Olympus, Hamburg, Germany) was used.

2.3.1 Fluorescence stainings

PMH were incubated with 5 µM CMFDA in WME for 30 min at 37 °C. After washing twice with phosphate-buffered saline (PBS; Invitrogen, Gibco, Darmstadt, Germany) the fluorescence intensities were documented immediately (Absorption: 492 nm; Emission: 517 nm). Following this, the cells were fixed and permeabilized as described by Dooley et al. (Dooley et al. 2003). A staining solution with DAPI (100 nM) (Absorption: 358 nm; Emission: 461 nm) and rhodamine/phalloidine (100 nM) (Absorption: 535 nm; Emission: 585 nm) in PBS was prepared. The cells were incubated with the staining solution for 1 h in the dark. After staining, the cells were washed twice for 15 min with PBS. Fluorescence was then documented immediately.

2.4 Characterization of extracellular metabolome

2.4.1 Quantification of extracellular metabolites

Amino acids were determined with an Agilent 1100 Series HPLC (Agilent Technologies, Waldbronn, Germany) equipped with a C18-column (Phenomenex, Aschaffenburg, Germany) following a protocol described by Strigun et al. (Strigun et al. 2011). Quantification of glucose and organic acids were carried out by HPLC (Kroma Systems, Kontron Instruments, Neufahrn, Germany) using an Aminex HPX-87H column as described by Strigun et al. (Strigun et al. 2011). Urea was determined with HPLC using the method described by Clark et al. (Clark et al. 2007).

2.4.2 Determination of ¹³C labeling in extracellular metabolites

[U¹³C]-glucose and [U¹³C]-glutamine were used as labeled substrates in separate experimental setups. Labeling was determined using a HP 6890 gas chromatograph (Hewlett Packard, Palo Alto, CA, USA) equipped with a HP-5 MS column (5% phenyl-methyl-siloxan-diphenylpolysiloxane; 30 m x 0.251 m x 0.25 µm; Agilent, Waldbronn, Germany)

and a quadrupole mass spectrometer (MS 5973, Agilent, Waldbronn, Germany). Labeled amino acids and lactate were separated and detected after the method described by Nicolae et al. (Nicolae et al. 2014).

For the detection of labeled glucose 25 μ l of sample were lyophilized over night. Samples were resuspended in 80 μ l methoxyamin solution (75 mM in pyridine) and incubated for 30 min at 80 °C. After cooling down at room temperature, 50 μ l BSTFA were added followed by 30 min incubation at 80 °C. Samples were centrifuged at maximum speed (Heraeus Biofuge Fresco; 12300 g, 5 min, 4 °C) and the supernatants transferred into glass vial inserts. The injected sample volume was 1 μ l. Separation of metabolites was carried out with a flow rate of 1.1 ml/min with helium as carrier gas. The temperature gradient started from 160 °C for 1 min and was then increased up to 320 °C with a rate of 20 °C/min. The inlet temperature was increased from 160 °C to 280 °C with a rate of 720 °C/min. The interface temperature was set to 320 °C and the quadrupole temperature to 150 °C. For the determination of labeling distribution in glucose, a fragment with the mass to charge ratio 319 (unlabeled) was chosen. This fragment only contains four carbon atoms of glucose. However, it is the fragment with the highest stability and intensity. Since only fully labeled or unlabeled substrates were used, it served to detect glucose production from other substrates.

Correction of labeling for the natural isotope abundance was accomplished as described by Yang et al. (Yang et al. 2009).

2.5 Determination of hepatic function

2.5.1 Albumin quantification

Albumin, as a serum protein specifically produced and secreted by hepatocytes, was quantified using a two-site enzyme linked immunoassay (ELISA) purchased from Genway (Immunoperoxidase Assay for determination of albumin in mouse samples, Genway, San Diego, CA, USA). For supernatants of PHH the according assay for human samples was chosen. ELISAs were used according to manufacturer's instructions.

2.5.2 Determination of aspartate aminotransferase activity

Aspartate aminotransferase (AST) activity can be used as a hepatocyte specific marker in liver cell cultures. The enzyme is released into the culture supernatant when membrane integrity is no longer given. Therefore, it can be used as a hepatocyte specific viability

marker. AST activity in the culture supernatants of PMH was determined using the Fluitest® GOT AST test kit from Analyticon Biotechnologies AG (Lichtenfels, Germany).

2.5.3 Cytochrome P450 activity

2.5.3.1 LC-MS/MS

The CYP assay solution contained phenacetine (50 μ M), bupropion (25 μ M), amodiaquine (5 μ M), tolbutamide (100 μ M), mephenytoin (100 μ M), and atorvastatine (35 μ M) in WME. With this assay solution it was possible to determine the activity of human CYP 1A2, CYP 3A4, CYP 2B6, CYP 2C8, CYP 2C9 and CYP 2C19. PMH were incubated for 2 h while samples (50 μ l) were taken every 30 min. 5 μ l of 250 mM formic acid were added directly into each sample and mixed thoroughly to stop metabolic activity. Samples were kept at -20 °C until shipping. The samples were analyzed by LC-MS/MS (by the group of Ute Hofmann (IKP Stuttgart, Germany)) according to the method described by Feidt et al. (Feidt et al. 2010).

2.5.3.2 Luminescence assay

To determine CYP3A activity in primary hepatocytes the P450-Glo™ CYP3A4 Assay (Luciferin-IPA) (Promega GmbH, Mannheim, Germany) was used. Cells were incubated with 3 μ M Luciferin-IPA in serum free WME for 1 h. Supernatants were collected and transferred into a 96 well plate (Cell Culture Microplate 96 Well Black, Greiner bio-one, Kremsmünster, Austria). Luciferin Detection Reagent was added followed by another 20 min of incubation. Luminescence was detected using a Glomax 96 Microplate Luminometer (Promega GmbH, Mannheim, Germany).

2.6 Proteome analysis

2.6.1 Protein extraction

Supernatants were collected and the ML and SW cultures of PMH were washed with PBS (4 °C) two times followed by addition of 600 μ l cold lysis buffer (50 mM Tris, pH 7.4; 150 mM NaCl; 0.1% N-laurylsarcosine; 1 mM EDTA; 0.4 mM Pefabloc® SC Plus (Roche Diagnostics GmbH, Mannheim, Germany)). Cells were incubated for 30 min at 4 °C. Collagen and cells were scraped of the dishes, transferred into Eppendorf reaction tubes and centrifuged at maximum speed (Heraeus Biofuge Fresco; 12300 x g, 10 min, 4 °C). TCAA was added to the supernatant to reach a final concentration of 7.5% to precipitate protein and the mixture was incubated for 2 h on ice followed by another centrifugation step at maximum

speed (Heraeus Biofuge Fresco; 12300 x g, 10 min, 4 °C). The pellet was washed with 2 ml tetrahydrofuran (4 °C) twice, centrifuged as mentioned above and resuspended in 125 µl rehydration buffer (7 M urea; 2 M thiourea; 4% CHAPS; 0.6% Bio-lyte 3-10 (Bio-Rad Laboratories, Inc., Hercules, CA, USA); 40 mM DTT) by sonication for 30 min.

2.6.2 Bradford Assay

The determination of the intracellular protein content was carried out using the method described by Bradford (Bradford 1976). BSA in a concentration range of 0-1 mg/ml served as calibrator. Samples were diluted accordingly with MilliQ water to be within calibration range. The Protein Assay Dye Reagent Concentrate (Bio-Rad Laboratories, Inc., Hercules, CA, USA) was also diluted 1:5 with MilliQ water. 10 µl of calibrator or sample were prepared in duplicates in a 96-well plate and 200 µl reagent added per well. The plate was shaken for 10 min then absorbance was determined at 595 nm with an iEMS absorbance Reader MF (Labsystems, Helsinki, Finland).

2.6.3 Protein purification

After determination of protein content using Bradford assay, intracellular protein extracts were cleaned from ionic detergents, salts, lipids and nucleic acids prior to 2D-gel electrophoresis using the ReadyPrep 2-D cleanup kit (Bio-Rad Laboratories, Inc., Hercules, CA, USA) according to manufacturer's instructions. 500 µg protein were transferred into an Eppendorf reaction tube and diluted with MilliQ water to a final volume of 150 µl. To precipitate protein, 300 µl of agent 1 were added and well mixed with the sample by vortexing. After 15 min incubation on ice, 300 µl of agent 2 were added. Samples were vortexed and then centrifuged at maximum speed (Heraeus Biofuge Fresco; 12300 x g, 10 min, 4 °C). Supernatants were completely discarded and pellets washed with 40 µl of wash reagent 1. Again supernatants were discarded and pellets vortexed for 20 sec with 25 µl MilliQ water. 1 ml of wash reagent 2 (pre-chilled at -20 °C) and 5 µl of wash 2 additive were added. The samples were incubated for 30 min on ice and thereby vortexed every 10 min for 30 sec. After centrifugation at maximum speed (Heraeus Biofuge Fresco; 12300 x g, 10 min, 4 °C), supernatants were again completely discarded and protein pellets resuspended in an appropriate amount of rehydration buffer (7 M urea; 2 M thiourea; 4% CHAPS; 0.6% Bio-lyte 3-10; 40 mM DTT).

2.6.4 2D-gel electrophoresis

IPG strips (pH 3-10, non-linear) (Bio-Rad Laboratories, Inc., Hercules, CA, USA) were thawed at room temperature 1 h before use. 100 µg protein were transferred into an Eppendorf reaction tube and diluted with rehydration buffer (7 M urea; 2 M thiourea; 4% CHAPS; 0.6% Bio-lyte 3-10; 40 mM DTT) to a final volume of 125 µl. The sample was pipetted at the edge of a lane avoiding air bubbles, with the IPG strips carefully gliding over the sample. Afterwards, the strips were overlaid with 1 ml mineral oil and left for 16 h at room temperature to passively rehydrate. After rehydration mineral oil was carefully dapped away with filter paper. Paper wicks were moisturized with MilliQ water and laid on the contacts of the focusing tray. The IPG strips were laid on top of the paper strips and overlaid with 1.5 ml mineral oil. IEF was carried out in a Protean IEF cell (Bio-Rad Laboratories, Inc., Hercules, CA, USA) according to the program described in Table 2-1 with a total of 46000 volthours.

Table 2-1 Program used for isoelectric focusing (25 h)

Stage	Voltage [V]	Duration [h]
S1	100	1
S2	200	1
S3	500	2
S4	700	1
S5	2500	6
S6	2500	14
S7	500	Unlimited

After, IEF strips were again freed from mineral oil with filter paper and equilibrated on a rocking table in equilibration buffer I (6 M urea; 2% SDS; 0.375 M TRIS; 30% glycerol; 1% DTT) for 15 min followed by 15 min incubation in equilibration buffer II (as buffer I, but 2.5% IAA instead of 1% DTT). For second dimension the IPG strip was placed on a 12.5% SDS-gel avoiding air bubbles and overlaid with agarose (1% low-melt agarose (w/v) and 0.4% bromphenol blue in 5x Tris/glycine/SDS-buffer). The gels were put in the Mini-

PROTEAN Tetra cell (Bio-Rad Laboratories, Inc., Hercules, CA, USA) and the chamber was filled with an appropriate amount of 1x Tris/Glycine/SDS-buffer. A constant current of 15 mA per gel was applied until the bromophenol blue tracking lane reached the end of the gel.

2.6.5 2D protein staining

For Coomassie blue staining, gels were rinsed 3 x 5 min with deionized water to wash away SDS. Gels were fixed in 50% methanol, 10% acetic acid for 15 min followed by washing in deionized water for another 15 minutes. Gels were stained with EZBlue™ staining reagent (Bio-Rad Laboratories, Inc., Hercules, CA, USA) for 1 h and washed with water to reduce background staining.

2.6.6 Difference gel electrophoresis (DIGE)

The Amersham™ CyDye™ DIGE Fluor (minimal dye) labeling kit (GE Healthcare, Little Chalfont, UK) was used to prepare protein samples according to manufacturer's instructions. CyDyes were solved in DMF to obtain a stock solution of 1 mM. Each condition (internal standard, untreated and treated) contained 15 µg of protein, which were diluted with lysis buffer (30 mM TRIS; 7 M urea; 2 M thiourea; 4% CHAPS) to a final volume of 7.5 µl. For each measurement 3 gels were prepared to allow statistical evaluation to guarantee significance of the results. 1 µl of CyDye was added to each preparation followed by 30 min incubation in the dark on ice. To stop the labeling reaction 1 µl of 10 mM lysine were added and mixed with the samples. For another 10 min the preparations were incubated in the dark on ice, followed by the addition of 9.5 µl sample buffer (8 M urea; 4% CHAPS; 2% Biolyte; 130 mM DTT). Again, the samples were incubated for 10 min on ice in the dark and then the three preparations for each gel (internal standard, untreated and treated) were pooled. In the end each sample contained 45 µg protein per gel. 2D gel electrophoresis was carried out according to paragraph 4.2 "2D-gel electrophoresis" using special low-fluorescence glass plates (NH Dyeagnostics, Halle, Germany) to prepare SDS-gels. Fixation of the gels was not necessary since the gels were directly documented within the glass plates using a Typhoon Trio Variable Mode Imager (GE Healthcare, Little Chalfont, UK). The obtained fluorescence images were analyzed with DeCyder 2D v 7.0 software according to developer's instructions. Statistical evaluation was accomplished by applying one-way analysis of variance (ANOVA) and Student's t-test. Only proteins with a threshold change of at least 1.5 or -1.5 and a

minimum significance level of $p=0.05$ were accepted as significantly changed in the treated group.

2.6.7 In-Gel digest

For the identification of proteins which show significantly changed expression in DIGE analysis, Coomassie stained spots were picked using a clean scalpel and transferred into a 0.5 ml Eppendorf tube. Gel pieces were washed with 100 μ l water and with 100 μ l 50% acetonitrile for 2 x 5 min at 37 °C in a Thermomixer Comfort (Eppendorf AG, Hamburg, Germany). Gel pieces were destained completely by washing with 100 μ l 50% acetonitrile several times. The destained gel-pieces were dehydrated with 100 μ l of 100% acetonitrile, 5 μ l of sequencing-grade modified trypsin (0.15 μ g/ μ l in 40 mM ammonia bicarbonate buffer; Promega Corp., Madison, USA) were added and incubated at room temperature until the trypsin solution was soaked completely into the gel. The gel pieces were covered with 40 mM ammonia bicarbonate buffer followed by incubation overnight at 37 °C for digestion. Trypsin proteolysis was stopped by adding 0.5 μ l of 10% TFA. For further peptide extraction, gel pieces were covered with 60% acetonitrile, 0.1% TFA and sonicated for 15 min. This step was repeated with 100% acetonitrile. All supernatants were pooled and the volume was reduced in a SpeedVac (Jouan RC 10.22). The peptide samples were concentrated and purified using ZipTip C18 (Merck, Billerica, USA) according to manufacturer's instructions and eluted in a matrix solution (5 mg/ml CCA in 70% acetonitrile, 0.1% TFA) prior to spotting onto a MALDI-target (384 well Opti-TOF, Applied Biosystems, Darmstadt, Germany).

2.6.8 Matrix-assisted laser desorption/ionization (MALDI) mass spectrometry (MS)

MS and MS/MS analysis was performed on an Applied Biosystems 4800 MALDI TOF/TOF Analyzer (Applied Biosystems). The analyzer was calibrated using the 4700 Proteomics Analyzer Calibration Mixture (Applied Biosystems). MS-data was generated in positive reflector-mode in a mass range of 700-4000 m/z with 50 shots per subspectrum accumulating 1000 shots in total. Common fragments of the calibrant and matrix were added to an exclusion list. Laser frequency was set to 200 Hz using a Nd:YAG laser operating at 355 nm and laser intensity was adjusted according to spectrum quality (usually 2700- 3000). For MS/MS analysis a total of 5 precursor ions per fraction were selected by the software (4000 series explorer software, version 3.5.1, Applied Biosystems) for MS/MS-analysis.

The threshold criteria for MS/MS were a minimum signal-to-noise ratio of 20 and a precursor mass tolerance between spots of 100 ppm. MS/MS data was produced with 100 shots per subspectrum with 2000 shots in total or after achieving stop criteria of a signal-to-noise ratio of 20 for at least 10 peaks in the MS/MS spectrum and accumulation of at least 12 subspectra. Peptides were fragmented by 1 kV collisions *via* collision-induced dissociation (CID).

Generated spectra were searched with MASCOT search algorithm (Perkins et al. 1999) (version 2.1.03) against the SwissProt database with mouse taxonomy using GPS explorer software v. 3.6 (Applied Biosystems). Search parameters were: maximum missed cleavages: 1; precursor mass tolerance: 100 ppm; MS/MS fragment tolerance: 0.3 Da; variable modifications allowed: oxidation of methionine and carbamidomethylation of cysteine.

3. Metabolic characterization of polarized and non-polarized primary mouse hepatocytes

3.1 Introduction

Non-alcoholic fatty liver disease (NAFLD), alcoholic liver disease and other liver related diseases, e.g. diabetes, are very common in western countries with increasing incidence (Stewart et al. 2001, Rombouts and Marra 2010). Especially NAFLD, strongly connected to carbon and fatty acid metabolism, is expected to become the most common cause of advanced liver disease in the 21st century (Davis and Roberts 2010). It is estimated that 20% of the general adult population in the USA has NAFLD. 2-3% of these have non-alcoholic steatohepatitis (NASH) and 20% of these patients develop liver cirrhosis with up to 40% requiring liver transplantation or dying of liver failure (Neuschwander-Tetri 2005, Kanuri and Bergheim 2013). A thorough understanding of the liver and its metabolism under normal and disease conditions would be most useful to improve the treatment of these diseases and to find better drug targets. An *in vitro* model, which resembles the *in vivo* situation as closely as possible is most desirable. Different hepatic cell lines, e.g. HepG2 or HepaRG cells, have been and are currently used as liver models. Since these cell lines are usually derived from cancer cells or liver progenitor cells, they do not show the full spectrum of hepatic functions (Koebe et al. 1994). For this reason primary hepatocytes are still the gold standard as *in vitro* liver model, although they also have their limitations. If primary hepatocytes are cultivated under standard conditions, namely on a collagen ML, they tend to dedifferentiate into a fibroblast-like morphology, lose hepatocyte functions and show a decrease in viability within one week of cultivation (Iredale and Arthur 1994, LeCluyse et al. 1994, Hengstler et al. 2009). There are several methods to optimize culture conditions in order to delay the dedifferentiation process of primary hepatocytes in culture. They range from relatively simple methods, such as the addition of a second layer of extracellular matrix (e.g. collagen SW cultivation) (Koebe et al. 1994) or media optimization (Mueller et al. 2012), to co-culture with other liver cell types (Peters et al. 2010) or complex bioreactor-systems (Mueller et al. 2011b).

Compared to other epithelial cells, hepatocytes show a complex form of polarity. Apical poles develop at cell-cell-contacts with other hepatocytes and form the bile canalicular network. A hepatocyte can therefore have several apical poles. The basolateral sites on the other hand face the sinusoids with the blood. Both poles are separated by tight junctions and have different secretory and absorbing functions (Decaens et al. 2008). During the isolation process of primary hepatocytes

via collagenase I perfusion, the hepatocytes lose polarity (LeCluyse et al. 1994, Vinken et al. 2006). However, in collagen sandwich culture, the primary hepatocytes show a more *in vivo* like polarized morphology and develop functional bile canaliculi at cell-cell-contacts (Godoy et al. 2009). As compared to monolayer cultures, primary hepatocytes maintained in collagen sandwich cultures show higher liver specific albumin and urea production in addition to higher expression and activity of CYPs (Dunn et al. 1991, Hamilton et al. 2001). However, cultivation of hepatocytes in collagen SW culture also has certain drawbacks compared to standard cultivation conditions. The extracellular matrix *in vivo* not only serves as structural support but also as a reservoir for cytokines, proteins in general and nutrients (Badylak 2002, Hynes 2009). In this respect sandwich culture mimics the *in vivo* situation more closely, but at the same time can complicate sampling and analysis. Harvesting of cells is more complex as well, since the upper collagen layer has to be dissolved, which might affect cell viability. Therefore, the cultivation system used must be chosen carefully depending on the question to be answered.

It is still an open question whether and to which extent central metabolism of hepatocytes differs between 2D and 3D sandwich cultures. In this study the influence of these two cultivation methods on the central carbon metabolism as well as on hepatocyte functionality was analyzed. On the one hand we focused on the short-term effect of repolarization after seeding in collagen sandwich culture and on the other hand on the long-term effect of dedifferentiation in collagen monolayer culture. Hepatic metabolism was examined by determining the consumption of substrates and the secretion of products. In addition, an analysis of hepatocyte function was carried out, including not only the secretion of liver specific serum-protein albumin and urea, but also the functionality of formed bile canaliculi, CYP activity and the ability to detoxify ammonia.

3.2 Results

3.2.1 Morphological characterization of polarized and non-polarized PMH

Hepatocellular polarity was confirmed by several visual markers as described by LeCluyse et al. (LeCluyse et al., 1994) (Figure 3-1). The typical hexagonal hepatocyte shape could be observed in both cultures, although the hepatocytes were much more spread out in the ML culture. The cell-cell-contacts are clearly visible between the cells cultivated in the SW culture. *In vivo*, actin accumulates at the cell-cell-contacts of hepatocytes, as could be observed for hepatocytes cultivated in SW cultures (Ezzell et al. 1993). Only few cells in ML culture showed this actin accumulation, instead actin was widespread all over the cells. Functionality of the bile canaliculi can be observed using CMFDA. The fluorescent dye 5-chloromethylfluorescein (CMF) is produced from the colorless substrate by intracellular enzymatic deacetylation. This dye is

specifically transported into the bile canaliculi by the bile salt pump *mrp2*, which is located at the apical pole of the cells (Cantz et al. 2000). In the SW culture, the dye accumulated specifically within the bile canaliculi as early as 24 h after seeding whereas in the ML culture most of the dye remained within the cells.

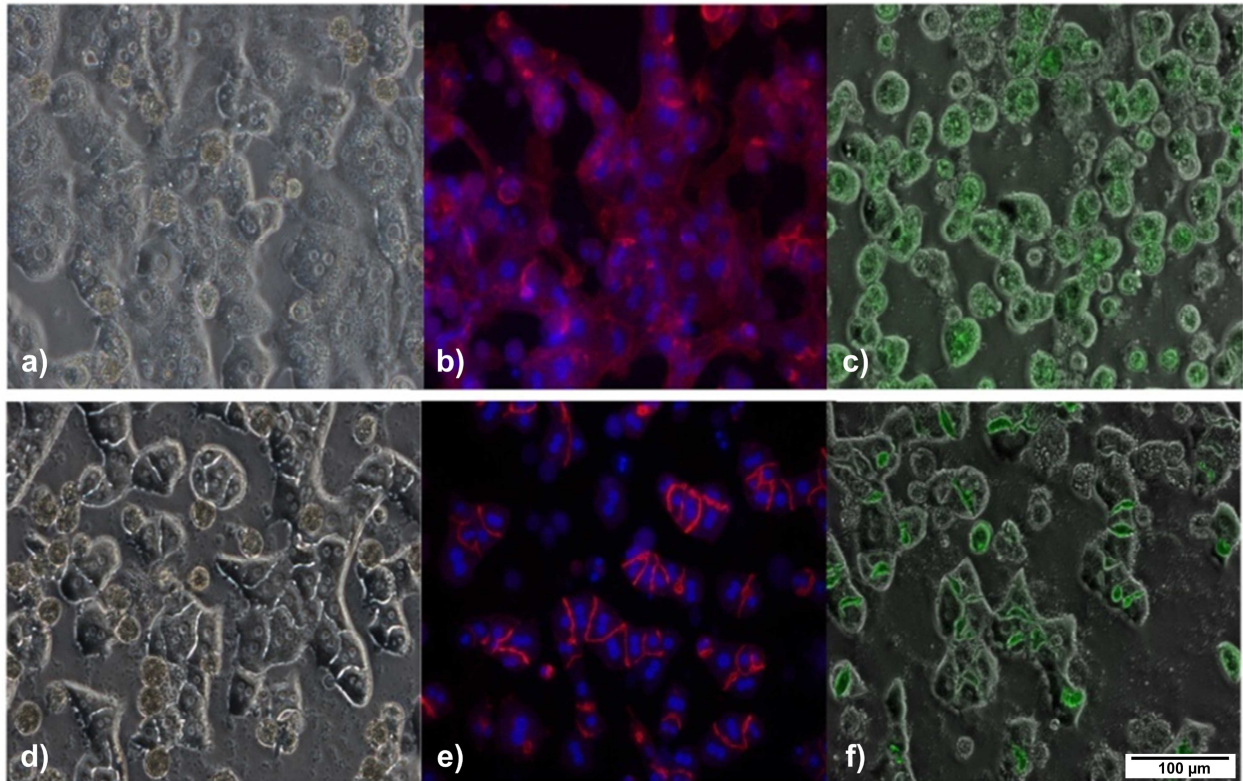


Figure 3-1 Primary mouse hepatocytes in collagen ML (upper row) and SW (lower row) culture. Phasecontrast (a and d), rhodamin/phalloidin and DAPI staining (b and e) and CMFDA staining (c and f) at day 3 of cultivation showing cell-cell contacts and polarity.

3.2.2 Metabolic characterization of primary mouse hepatocytes

3.2.2.1 Central carbon metabolism in repolarization phase

PMH were cultivated in SW and ML cultures. In the early phase of cultivation, namely the first 24 to 48 h, the cells redeveloped their polarized phenotype in the SW cultures. The extracellular metabolome, namely proteinogenic amino acids, organic acids and glucose, was determined in SW and ML cultures and uptake and secretion rates calculated (Figure 3-2). The metabolic profiles found for both culture conditions were comparable.

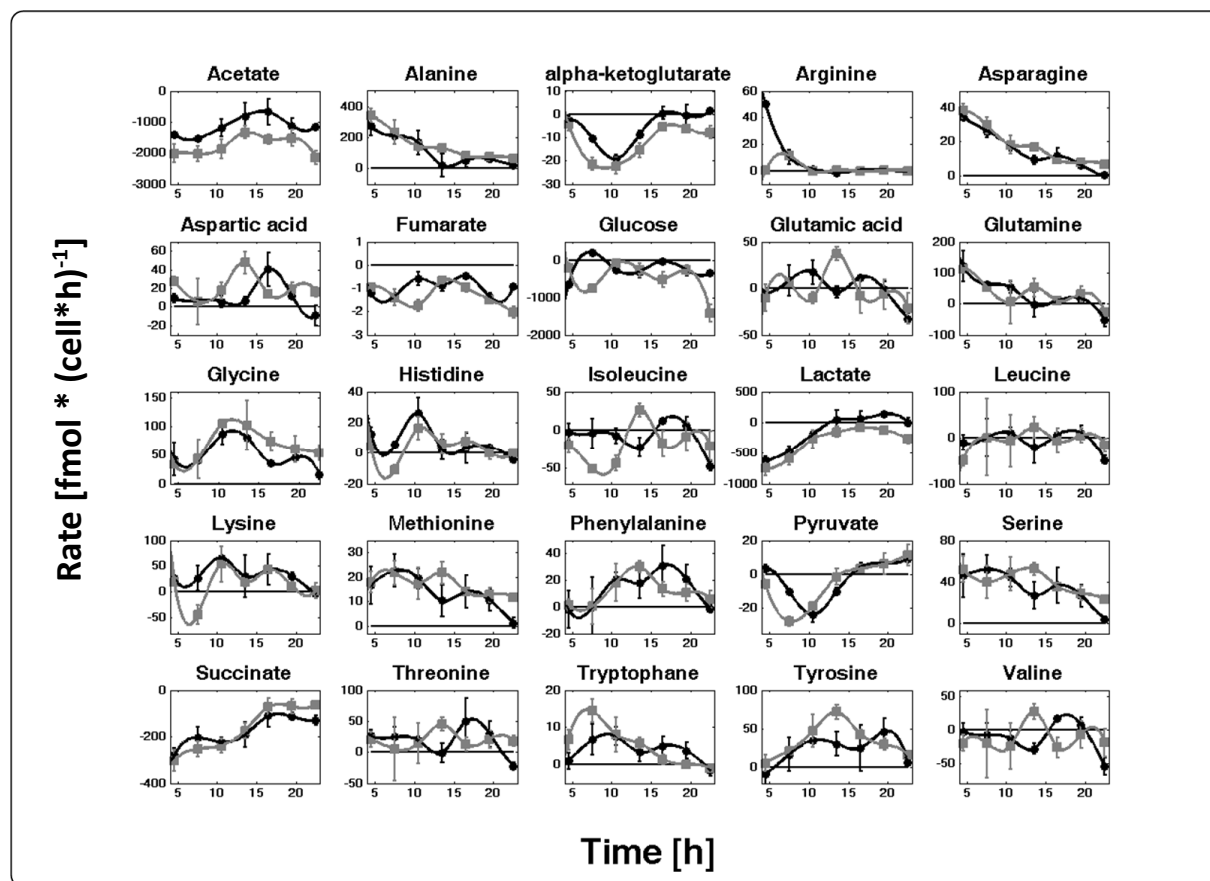


Figure 3-2 Secretion and uptake rates of metabolites in primary mouse hepatocytes maintained in collagen monolayer culture (grey) and collagen sandwich (black) for 24 hours of cultivation. Positive values indicate consumption and negative values indicate production. Error bars indicate standard deviations ($n = 3$). Living cell number was determined after 24 h using calcein AM staining.

Glutamine, alanine and pyruvate served as the major carbon sources for hepatocytes in both culture conditions. Thereby, pyruvate was almost completely used up within the first 3 h of cultivation with a rate of 167 ± 5 fmol/cell/h in ML and 165 ± 4 fmol/cell/h in SW cultures (data not shown). Glucose production was observed at the beginning for both culture conditions and at the end of cultivation in the ML culture. In between the net uptake rate was around zero. Lactate was constantly produced within the first 9 h. Afterwards, lactate excretion ceased. In SW culture, even a slight net uptake of lactate was observed. Acetate showed a continuously higher production in ML culture.

3.2.2.2 Central carbon metabolism during dedifferentiation

Primary hepatocytes, especially of rodent origin, cultivated on a collagen ML dedifferentiate within a few days of cultivation (Godoy et al. 2009, Hengstler et al. 2009). In SW culture, on the other hand, polarization and hepatic function can be maintained for several weeks (LeCluyse et al. 1994). In order to test for possible alterations in the central carbon metabolism during the process

of dedifferentiation, hepatocytes were cultivated over a period of 5 days in ML and SW culture. The extracellular metabolome was analyzed every 12 h. The consumption rates of proteinogenic amino acids, selected organic acids and glucose are depicted in Figure 3-3. As observed during repolarization (Figure 3-2) the metabolic profiles of both cultures are mostly very similar.

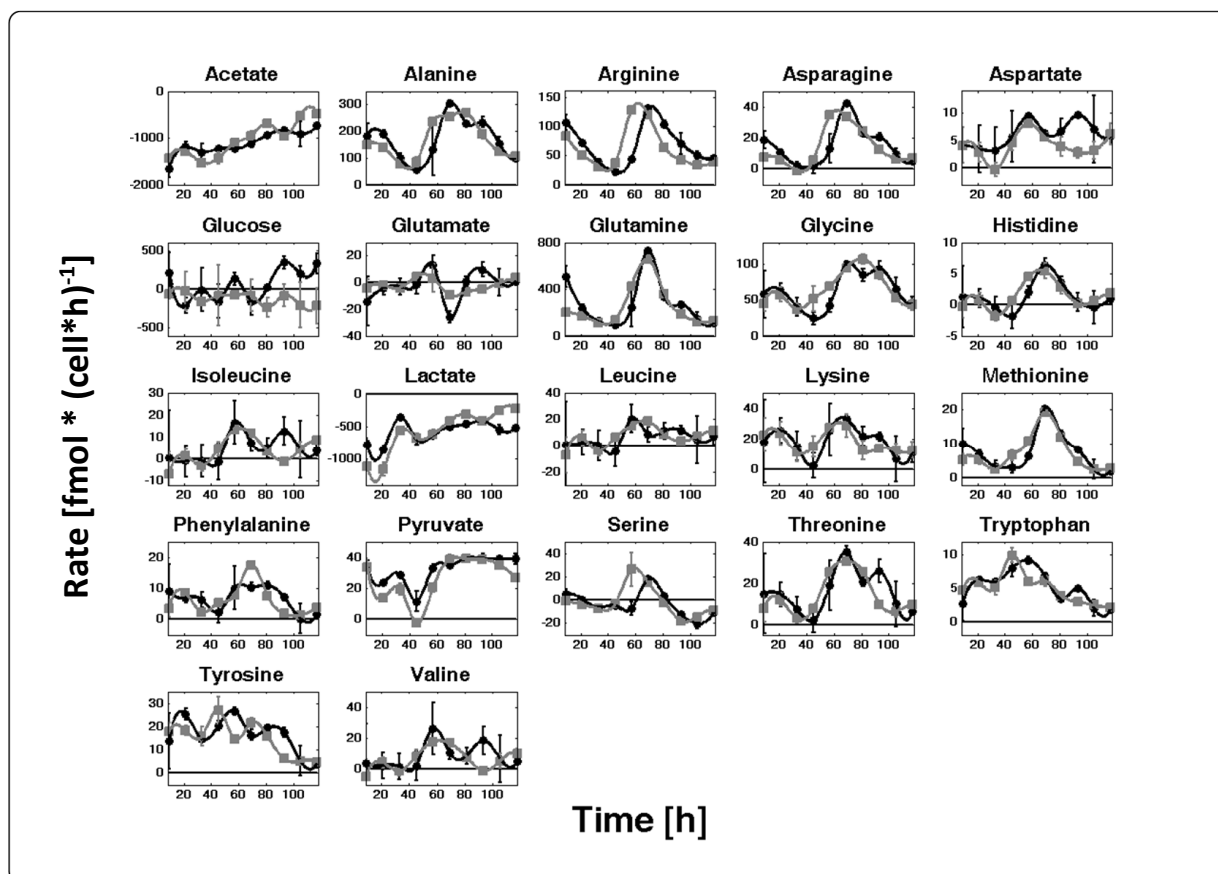


Figure 3-3 Secretion and uptake rates of metabolites in primary mouse hepatocytes maintained in collagen monolayer culture (grey) and collagen sandwich culture (black) for 5 days of cultivation. Samples were taken every 12 hours. Positive values indicate consumption and negative values indicate production. Error bars indicate standard deviations ($n = 3$). Living cell number was determined every 24 h using calcein AM staining.

The production rates of acetate and lactate decreased over time under both conditions. Most amino acid consumption rates were more or less identical at the beginning and at the end of cultivation, whereas between 48 and 84 h an elevated consumption could be observed for the majority of amino acids. This was most prominent for alanine, arginine, asparagine, glutamine and threonine. In the ML culture this is temporally shifted compared to the SW culture and is observed earlier than in the SW culture. A remarkable difference between the two culture conditions could be found for glucose. After three days of cultivation with a nearly constant rate around zero for both conditions the consumption rate of glucose in SW cultures showed a marked increase compared to ML cultures.

3.2.3 Albumin and urea production and AST activity

Within the first 24 h albumin was constantly produced by PMH under both culture conditions (Figure 3-4). Urea was produced in a large amount by cells in both culture conditions within the first 3 h of cultivation (not shown). Within the remaining 21 h, however, urea production decreased. AST is only released into the culture supernatant if the integrity of the cellular membrane is impaired. Therefore, it can be used as a viability marker. The highest AST release was found within the first 3 h of cultivation, namely 158 ± 7 nU/cell/h in ML and 104 ± 9 nU/cell/h in SW culture (data not shown). Afterwards, the activity reached a more or less constant level in both cultures. Hence, the hepatocytes released AST during the stressful first phase after seeding and showed a constant high viability during the remaining cultivation phase.

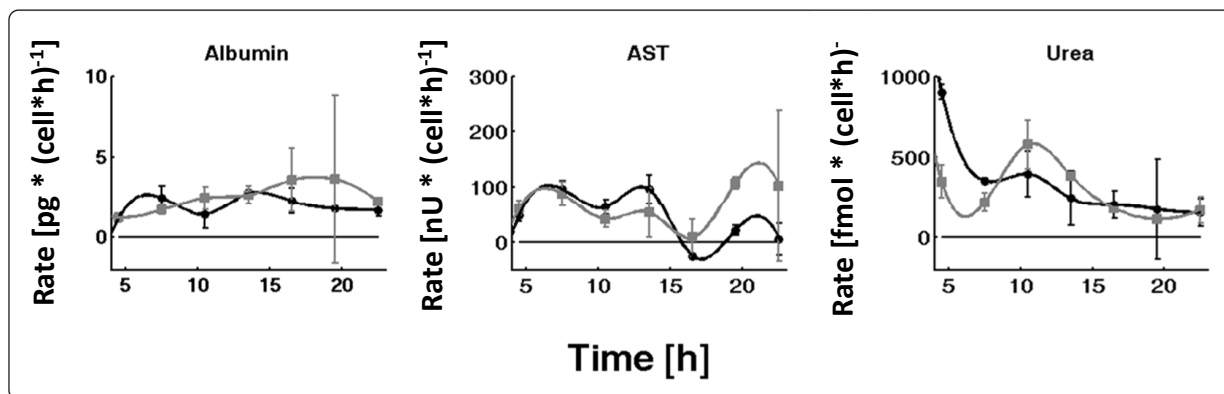


Figure 3-4 Liver specific production rates of albumin, AST and urea in primary mouse hepatocytes maintained in collagen monolayer culture (grey) and collagen sandwich (black) during the first 24 hours of cultivation. Positive values indicate production of a metabolite whereas negative values indicate degradation. Error bars indicate standard deviations ($n = 3$). Living cell number was determined after 24 h using calcein AM staining.

The liver specific albumin and urea production and AST activity was also monitored during long term cultivation of PMH for 5 days in both cultures as depicted in Figure 3-5. The albumin production rate slowly increased for 48 h in both culture conditions reaching the same values and then remained constant in the SW cultures. After 48 h, the production rate strongly decreased to almost zero at the end of cultivation in ML cultures. AST was released into the medium from dying cells during the first 48 h after seeding. Then AST activity reached a basal level and remained constant for the rest of cultivation. Urea production was significantly higher in the ML culture at the beginning of cultivation but decreased to a similar production rate as in the SW cultures.

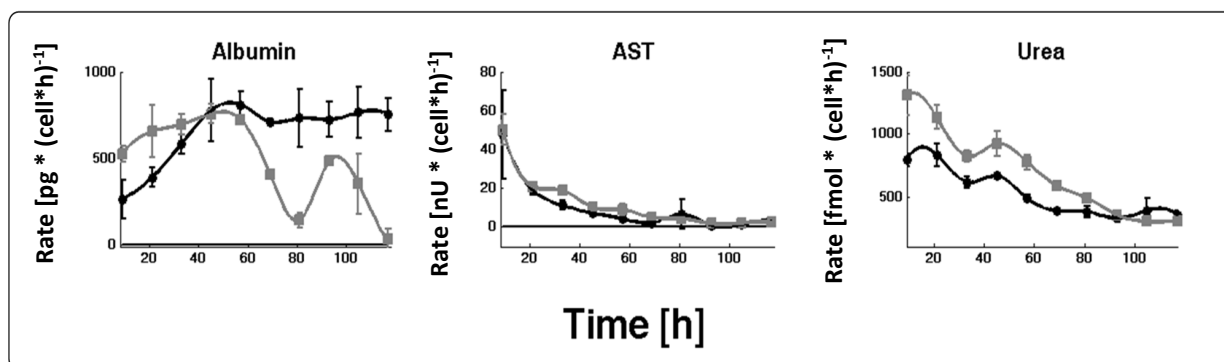


Figure 3-5 Liver specific production rates of albumin, AST and urea in primary mouse hepatocytes maintained in collagen monolayer culture (grey) and collagen sandwich (black) during 5 days of cultivation. Samples were taken every 12 hours. Positive values indicate production of a metabolite whereas negative values indicate consumption. Error bars indicate standard deviations ($n = 3$). Living cell number was determined every 24 h using calcein AM staining.

3.2.4 CYP activity

The drug metabolizing competence of PMH in SW cultures was compared to that in ML cultures as depicted in Figure 3-6. At day one of cultivation hepatocytes in both cultures showed comparable CYP activities for mouse homologues of human CYP 2C8, 2C9 and 2C19 while activities of CYP 1A2, 3A and 2B6 were significantly higher in ML compared to SW culture, by 40 - 50% roughly. After five days of cultivation CYP2B6 activity was strongly induced, about 7-fold in SW and about 3-fold in ML culture, resulting in a comparable activity. All other CYP activities showed a considerable decrease compared to day 1 in ML culture. For SW culture, the decrease was less pronounced. CYP 3A even showed a slight induction to 128% in SW culture, while in ML culture a reduction to 28% was observed.

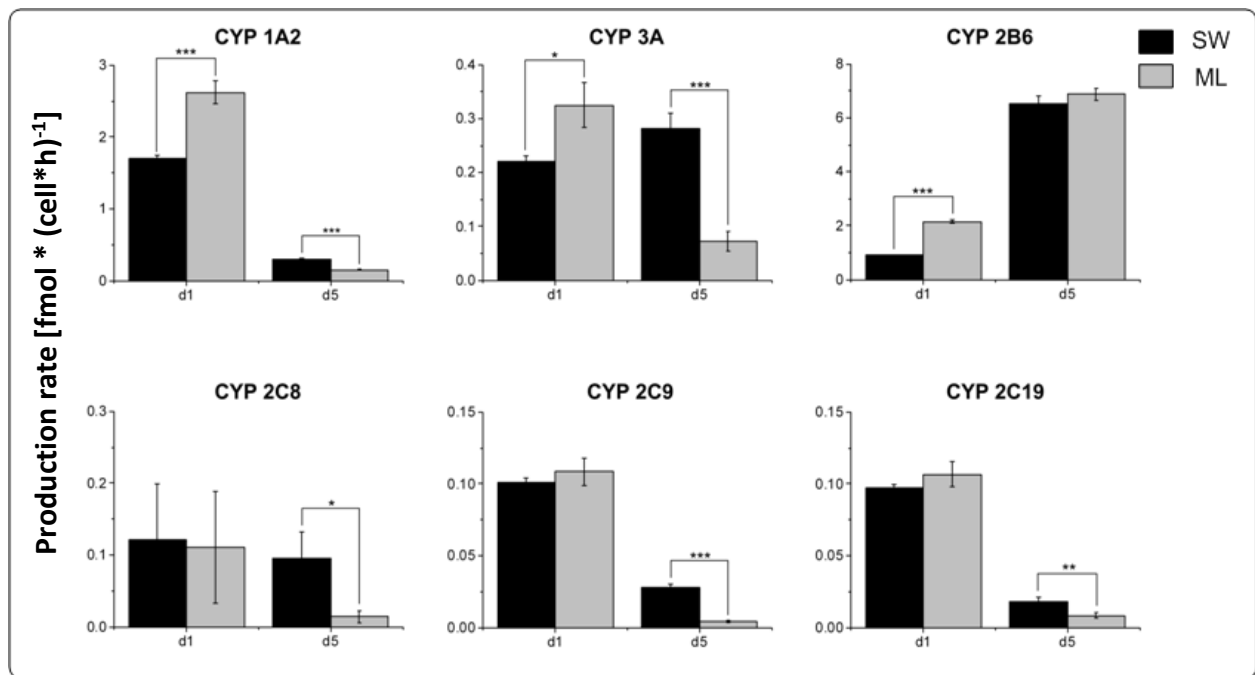


Figure 3-6 Cytochrome P450 activities in primary mouse hepatocytes in collagen sandwich (black) and collagen monolayer culture (grey) at day 1 (d1) and day 5 (d5) of cultivation. Hepatocytes were incubated with substrates specific for the CYPs and the formation of the corresponding products was quantified. Production rates of acetaminophen from phenacetin by the mouse homologue of human CYP 1A2 (a), of o-OH-atorvastatin from atorvastatin by the mouse homologue of human CYP 3A4 (b), of OH-bupropion from bupropion by the mouse homologue of human CYP 2B6 (c), of N-DE-amiodiaquine from amiodiaquine by the mouse homologue of human CYP 2C8 (d), of OH-tolbutamide from tolbutamide by the mouse homologue of human CYP 2C9 (e) and of 4'-OH-mephenytoin from S-mephenytoin by the mouse homologue of human CYP 2C19 (f) as indicators for the activity of the respective CYPs are shown. Error bars indicate standard deviations (n=3). *, ** and *** indicate significance at p=0.05, p=0.01 and p=0.001, respectively. Living cell number was determined after day 1 and 5 using calcein AM staining.

3.2.5 Ammonia detoxification

Hepatocytes have the ability to detoxify ammonia *via* the urea cycle and glutamine synthesis. To test the influence of the cultivation method on ammonia detoxification, cells in both cultures were incubated with different ammonia concentrations for 24 h after 5 days of cultivation. The production rate of urea as well as the consumption rate of glutamine are depicted in Figure 3-7. Urea production increased with increasing ammonia concentration under both conditions but the increase in SW culture was significantly higher. For 10 mM ammonia urea production in SW culture was about 2.5-fold of the control condition without ammonia, while for ML culture only a change to 1.5-fold was observed. Glutamine consumption was not altered in SW culture compared to control conditions. In ML culture the consumption rate of glutamine decreased significantly with increasing ammonia concentration with a shift to glutamine production at the highest ammonia concentration.

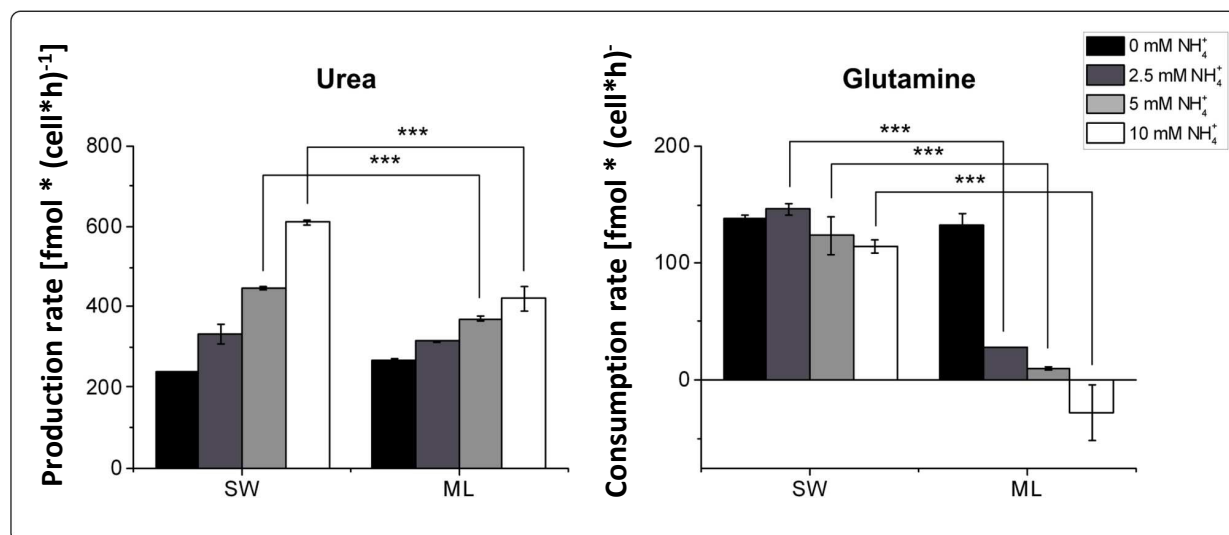


Figure 3-7 Urea production rates and glutamine consumption rates in primary mouse hepatocytes in collagen sandwich (SW) and monolayer (ML) culture challenged with different ammonia concentrations after 5 days of cultivation. Cells were incubated with increasing ammonia concentrations. Error bars indicate standard deviations ($n = 3$). *** indicate significance at $p=0.001$. Living cell number was determined after day 5 using calcein AM staining.

3.3 Discussion

During the cultivation PMH showed a cuboidal shape as typically observed for hepatocytes *in vivo*, which was maintained in the SW culture for the whole cultivation period. In the ML culture the hepatocytes were much more spread out and lost their typical morphology within 3 days of cultivation (Ezzell et al. 1993, Berthiaume et al. 1996). This epithelial-mesenchymal transition has been described previously for hepatocytes in ML culture (Bryant and Mostov 2008). PMH cultivated within SW culture showed clear cell-cell barriers and formed bile canaliculi within the first 24 h after seeding (about 94% of hepatocytes, which were in contact with other cells) whereas this took place only partly in the ML culture (about 13% of hepatocytes, which were in contact with other cells) (LeCluyse et al. 2000). Also the development of sealed bile canaliculi in SW culture could be confirmed by the specific transport of the fluorescent *mrp2* substrate CMF into the bile canaliculi.

We analyzed the extracellular metabolome of PMH during the process of repolarization to investigate if the alteration of cellular architecture is going along with changes in the central carbon metabolism. The first sampling timepoint (after 3 h) was not depicted since medium change resulted in a strong stress response of the cells. Thereby large amounts of glucose and amino acids were released by the hepatocytes in both culture conditions. To enhance resolution and comparability, rates are shown from the second sampling timepoint (6 h) on. The different experimental setups for the metabolic characterization during repolarization, namely sampling

every 3 h without medium change, and during long-time cultivation, complete medium change every 12 h, is also the reason why rates from both experiments cannot be directly compared, since rates obtained from the long-time cultivation are not corrected for this stress response. However, metabolic profiles of PMH cultivated in SW and ML culture were more or less comparable, except for glucose and acetate. Glucose homeostasis is one of livers major functions (König et al. 2012, Lu et al. 2012). Thereby blood glucose levels are kept constant in the narrow range of 5.5–6 mM, with a maximum of approximately 9 mM postprandially and a minimum of 3 mM in a prolonged state of fast, respectively (Nuttall et al. 2008). This is regulated by a complex interplay of insulin, glucagon and other factors, controlling glycogen synthesis and gluconeogenesis. The sudden change to glucose production in collagen ML at the end of the cultivation period is therefore especially remarkable. However, only the very last timepoint showed this change in glucose metabolism. At this point there already might be a shortage of some substrates, which could lead to this reaction. Acetate constantly showed a higher production rate in ML cultures. It is produced by degradation of acetyl-CoA and acetoacetate, which are produced during amino acid metabolism and ketogenesis. Ketogenesis hints at a stressed phenotype. Higher acetate production in ML culture indicates stress in this type of culture. The constantly higher production rate of lactate in ML culture as well points towards this direction. It can be concluded that hepatocytes in ML are slightly more susceptible to initial stress after seeding.

During the process of epithelial-mesenchymal transition we also determined the extracellular metabolome. As during repolarization no significant differences in the central carbon metabolism could be found except for glucose metabolism. After 96 h of cultivation PMH in SW culture started utilizing glucose to a certain extent whereas in ML culture hepatocytes increased glucose production. How this contrary behavior can be interpreted is still unclear. However, glucose metabolism seems to be the most sensitive to different cultivation conditions.

Albumin production decreased extensively after 3 days in ML culture whereas it remained constant in the SW culture for the remaining cultivation period. This finding is in accordance with other studies (Peters et al. 2010). Urea production, however, decreased constantly with time in both culture conditions.

The liver is the main organ of xenobiotic metabolism and detoxification (Hamilton et al. 2001) (Wen et al. 2013). Therefore, the activity of drug metabolizing enzymes (CYPs) and other detoxification reactions, as e.g. the urea cycle, are of utmost importance for understanding liver physiology and establishing a useful *in vitro* liver model. Additionally, hepatocytes are widely used as *in vitro* test systems during drug development (Messner et al. 2012, Martínez Sánchez et

al. 2012). An *in vivo* like CYP activity is therefore most desirable to predict drug metabolism and toxicity. A rapid loss of CYP activity in hepatocytes cultivated on a collagen monolayer has long been reported (Smet et al. 2000), whereas in collagen sandwich culture, CYP activity is maintained for a longer cultivation period (Kern et al. 1997). In our study, we tested the CYP activity of PMH in collagen sandwich and monolayer culture after 24 and 120 h of cultivation. At day 1, 3 of the 6 tested CYPs showed significantly higher activity in ML culture. However, after 5 days of cultivation activity dropped under both conditions for most CYPs. The drop was significantly stronger in ML culture. Especially CYP3A, which is responsible for the metabolism of a vast majority of xenobiotics (Zuber et al. 2002), shows a high activity in SW cultures after 5 days compared to ML cultures. This indicates that polarized hepatocytes in SW culture represent a superior *in vitro* system for toxicity testing after long-term cultivation, especially of CYP 3A.

Hepatocytes possess the ability to detoxify ammonia resulting from amino acid metabolism *via* the urea cycle and the synthesis of glutamine (Dunn et al. 1991). These two pathways are strictly zoned along the liver acinus. Urea cycle is active in the periportal region, whereas the detoxification *via* the synthesis of glutamine takes place in only 1-3 cell layers around the central vein (Ghafoory et al. 2013). After ammonia challenge, urea production was increased under both cultivation conditions in a dose dependent manner, which was significantly stronger in SW culture. Glutamine consumption, on the other hand, was completely unchanged in collagen SW culture. In ML culture, however, glutamine consumption was dose dependently reduced and glutamine even produced at the highest ammonia concentration. This is not observed under standard culture conditions. There are two possible explanations for this phenomenon. First of all, with an increasing ammonia challenge urea cycle reaches its maximum capacity. To avoid further ammonia stress, glutamine consumption is decreased accordingly. Synthesis of glutamine in addition allowed to fix NH_4^+ and reduce ammonia stress accordingly. On the other hand, it is known that cultivation conditions, e.g. hormone concentration, can increase the fraction of hepatocytes with periportal or perivenous phenotype in culture (Jungermann and Kietzmann 1996). The used cultivation conditions could have a similar effect, with hepatocytes in ML culture showing a more perivenous behavior. This could be confirmed by determining the fraction of glutamine synthase positive hepatocytes. However, not only ammonia detoxification is zoned along the liver acinus but also glucose metabolism or CYP expression. The activity of CYPs can in our case not serve as a representative marker, since primary hepatocytes lose CYP activity within the first days of cultivation (Figure 3-6). To confirm if collagen ML culture leads to a more perivenous phenotype, these other aspects of zonation need to be addressed as well.

In conclusion the cultivation condition determines cellular morphology and functional performance. Metabolically, however, neither the process of repolarization nor dedifferentiation of hepatocytes seem to have a major influence on the central carbon metabolism. Reorganization of cellular architecture and morphology are dramatic events and morphology has a significant influence on hepatic function, as could be seen for albumin production, CYP activity and the ability to detoxify ammonia. The central carbon metabolism, however, except for glucose metabolism, seems to be very robust and is not directly influenced by these events. Studies on other organisms as *E.coli*, *S. cerevisiae* or plants also showed that the central carbon metabolism, even after deletion of several genes, is robust enough to counterbalance even drastic disturbances (Blank et al. 2005, Spielbauer et al. 2006, Nakahigashi et al. 2009). Hiroaki Kitano defines robustness as a property that allows a system to maintain its functions despite external and internal perturbations and as an essential feature of complex evolving systems to adapt to environmental perturbations (Kitano 2004). It might therefore be understandable that although certain hepatocyte features are influenced by the cultivation system of choice, the central carbon metabolism is more or less unaffected. However, further studies with ^{13}C -labeling and also the inclusion of bile acid formation could give further insight into flux distribution so that an advanced understanding of how hepatocytes deal with disturbances concerning cellular polarity will be gained.

4. Proteomic characterization of primary mouse hepatocytes in collagen monolayer and sandwich culture

4.1 Introduction

Dedifferentiation of primary hepatocytes in *in vitro* cultures is a well-known problem hindering long-term studies, which are necessary for e.g. *in vitro* drug toxicity testing (Alépée et al. 2014). There are several approaches to abate this dedifferentiation process, ranging from media optimization over co-cultivation with other liver cells to cultivation of hepatocytes in scaffolds of ECM (Klingmüller et al. 2006, Peters et al. 2010, Kostadinova et al. 2013, Mueller et al. 2014). Cultivation of hepatocytes in a SW of the extracellular matrix protein collagen is one of these approaches. It is well described in the literature that the cultivation of primary hepatocytes in collagen SW culture leads to improved hepatic function over a period of several weeks. That includes prolonged albumin and urea production and the activity of CYP enzymes (Iredale and Arthur 1994, Chapter 3). Also morphologically, hepatocytes cultivated in the SW configuration regain a more *in vivo* like structure compared to hepatocytes cultivated in the standard ML condition. The cells maintain their typical cuboidal shape, actin is assembled close to cell-cell contacts and functional bile canaliculi are formed in between (Berthiaume et al. 1996, Rowe et al. 2010, Figure 3-1). It is also well known that the SW cultivation method leads to changes in gene expression (Dunn et al. 1992, Schug et al. 2008). However, proteome changes do not necessarily correlate with the transcriptomic changes (Slany et al. 2010, Altelaar et al. 2013). This can be due to differences in synthesis rates and half-lives of mRNA and proteins, phenotypic modifications of proteins, e.g. numerous post-translational modifications, interaction of proteins with other proteins or molecules as well as the subcellular distribution of the different components (Diamond et al. 2006). Because of this, the proteome is closer connected to the actual phenotype than the transcriptome.

Proteomics is defined as the study of the protein complement of cells, including identification and quantification of proteins (Yates et al. 2009). In this study we used 2D DIGE and matrix assisted laser desorption ionization time of flight mass spectrometry (MALDI ToF MS/MS) to analyze the intracellular proteome of primary mouse hepatocytes (PMH) cultivated in collagen SW and ML culture. In 2D gel electrophoresis proteins were separated in the first

dimension based on their isoelectric point (pI), whereas separation in the second dimension is based on the molecular weight of the protein. Subsequent, MALDI ToF MS/MS was used to identify the respective proteins based on the mass of their peptides. The technique of DIGE was established by the lab of Jon Minden (Unlü et al. 1997). The proteins of the samples are labeled with fluorescent dyes and an internal standard consisting of a mixture of all samples, also labeled with a fluorescent dye. Two samples and the internal standard were then run on the same gel, enabling a direct quantitative comparison of the protein samples. Our results show, that on a proteomic level, PMH in collagen SW culture are closer to the *in vivo* phenotype than in ML culture, but still show signs of dedifferentiation.

4.2 Results

PMH were cultivated in collagen SW and ML culture for 5 days. The intracellular proteome was extracted 24 h and 120 h after the start of the experiment. The exact experimental setup can be found in Figure 4-1.

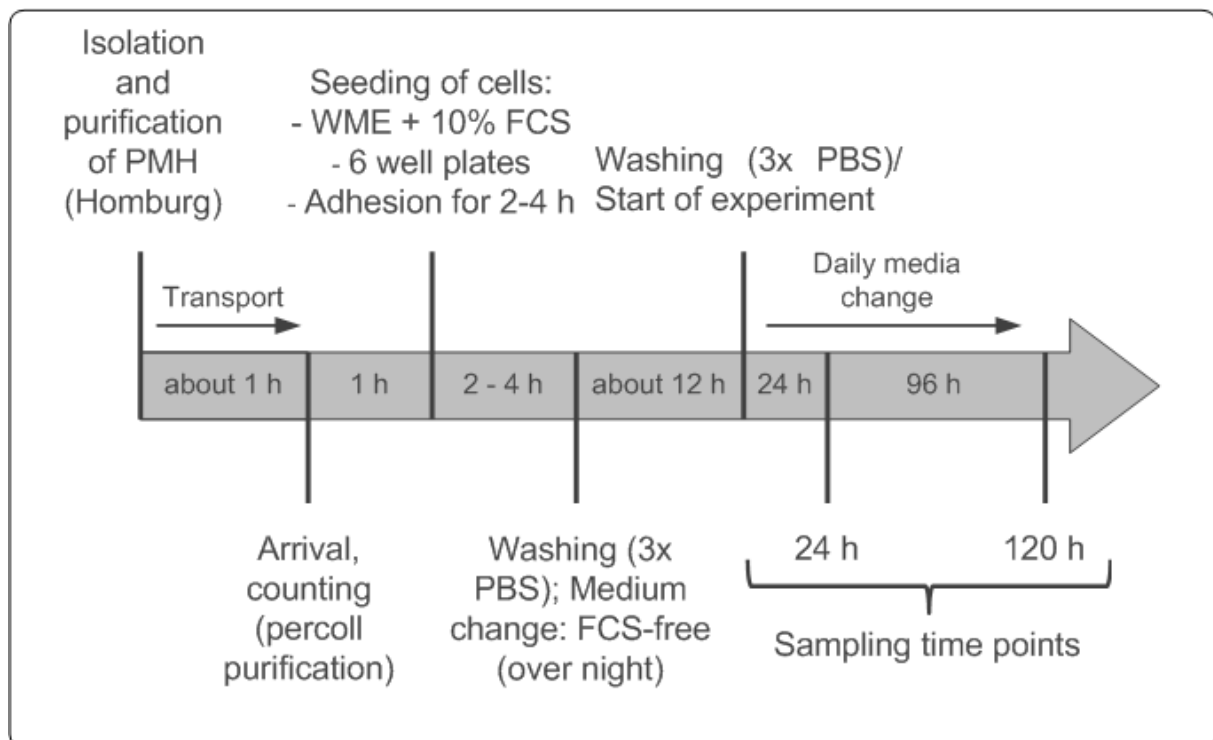


Figure 4-1 Experimental setup of the proteomic characterization of PMH in collagen SW and ML culture. The intracellular proteome was extracted 24 and 120 h after experimental start. Proteins were separated by 2D gelelectrophoresis and quantified using 2D DIGE.

The samples were purified and proteins further concentrated before starting 2D gel electrophoresis. 2D gel electrophoresis was accomplished in two variants: First as preparative

Coomassie- stained gels to separate proteins for further identification with MALDI-ToF-MS and second with fluorescent labeled proteins for quantification (2D DIGE).

DIGE enables a quantitative comparison between two different conditions at a time. In this experimental setup, all available conditions were compared to each other. The primary aim of this study was to characterize differing protein expression in collagen SW and ML culture. Therefore, the samples from ML d1 were compared to SW d1 and ML d5 to SW d5 for three individual mice. Representative gels are shown in Figure 4-2.

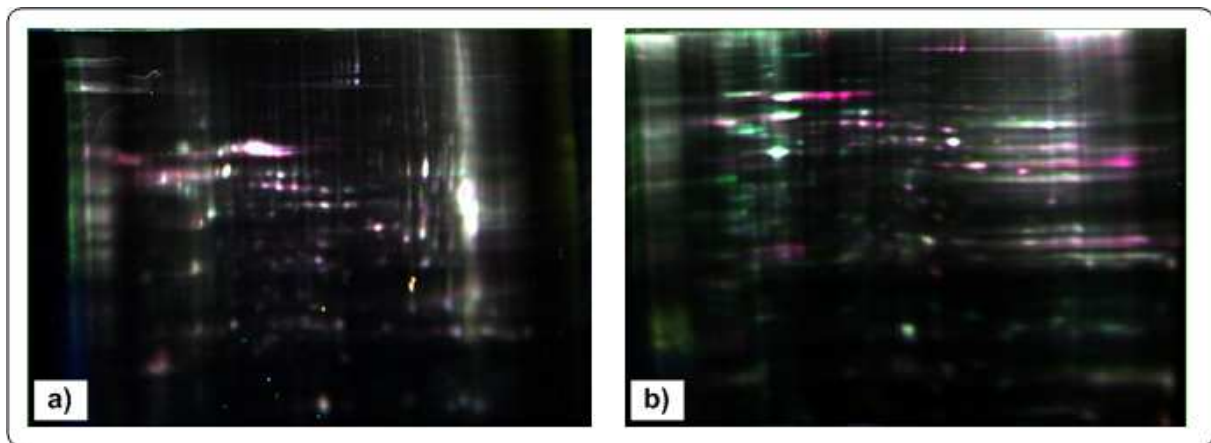


Figure 4-2 Overlay of representative DIGE gels to analyze differential protein abundance between PMH in collagen ML and SW culture. Comparison between samples at day 1 (a) and at day 5 (b). Spots that are only present in the ML culture: green; SW culture: red; both conditions: white. 1 gel per mouse was prepared (n=3).

When the intracellular proteomes of PMH in collagen SW and ML from day 1 of cultivation were compared to each other (Figure 4-2 a), it could directly be observed that only few spots were only present in one of the conditions and most spots were white. This indicates a good overlap of the proteomic profiles. After statistical evaluation it could be confirmed that there were no differentially expressed proteins 24 h after start of the experiment. After 5 days of cultivation (Figure 4-2 b), clear differences between the two culture types could be observed. Statistical evaluation of the DIGE-gels revealed 51 significantly altered spots.

In addition to the comparison of collagen SW and ML culture, it was analyzed, if incubation time influences protein expression in both cultivation conditions. This was achieved by comparing samples from ML d1 with ML d5 and SW d1 with SW d5 (Figure 4-3).

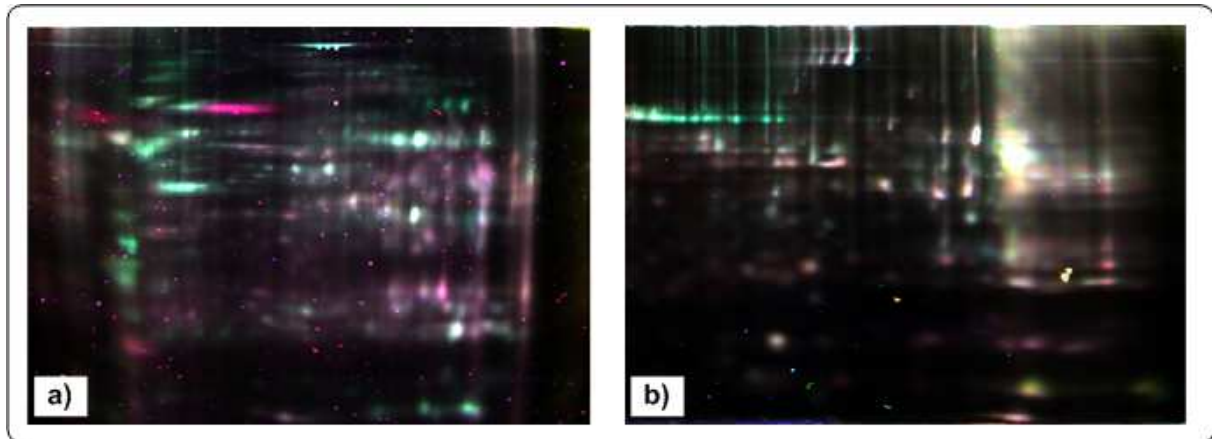


Figure 4-3 Overlay of representative DIGE gels to analyze differential protein abundance between PMH in collagen ML and SW culture due to cultivation time. Comparison between ML samples from day 1 and day 5 (a) as well as for SW (b). Spots that are only present at day 1: green; day 5: red; both conditions: white. 1 gel per mouse was prepared (n=3).

Both DIGE-gels revealed major differences in protein expression after optical examination. With one-way ANOVA and student's t-test ($p \leq 0.05$) it could be confirmed that the duration of incubation has a strong influence on the intracellular proteome. In collagen ML culture 75 significantly altered spots could be detected. In the SW culture still 32 were significantly changed.

The differentially expressed proteins, which were detected and quantified with DIGE, were then identified with MALDI-ToF-MS/MS. To achieve this, the intracellular proteins were first separated with 2D-gel electrophoresis (Figure 4-4). The according spots on the gels were digested by trypsin and then identified using MALDI-ToF-MS/MS and a Swissprot database search.

Using conventional 2D gel electrophoresis with colloidal Coomassie Blue (G250) staining of the protein spots, significantly less spots were detectable on the gels compared to the DIGE gels. This also implicated, that some spots, which were identified as differentially expressed under certain conditions, could not be found on those gels. The major reason for this is the higher sensitivity, which is reached by using fluorescent dyes, as in DIGE, compared to Coomassie Blue staining.

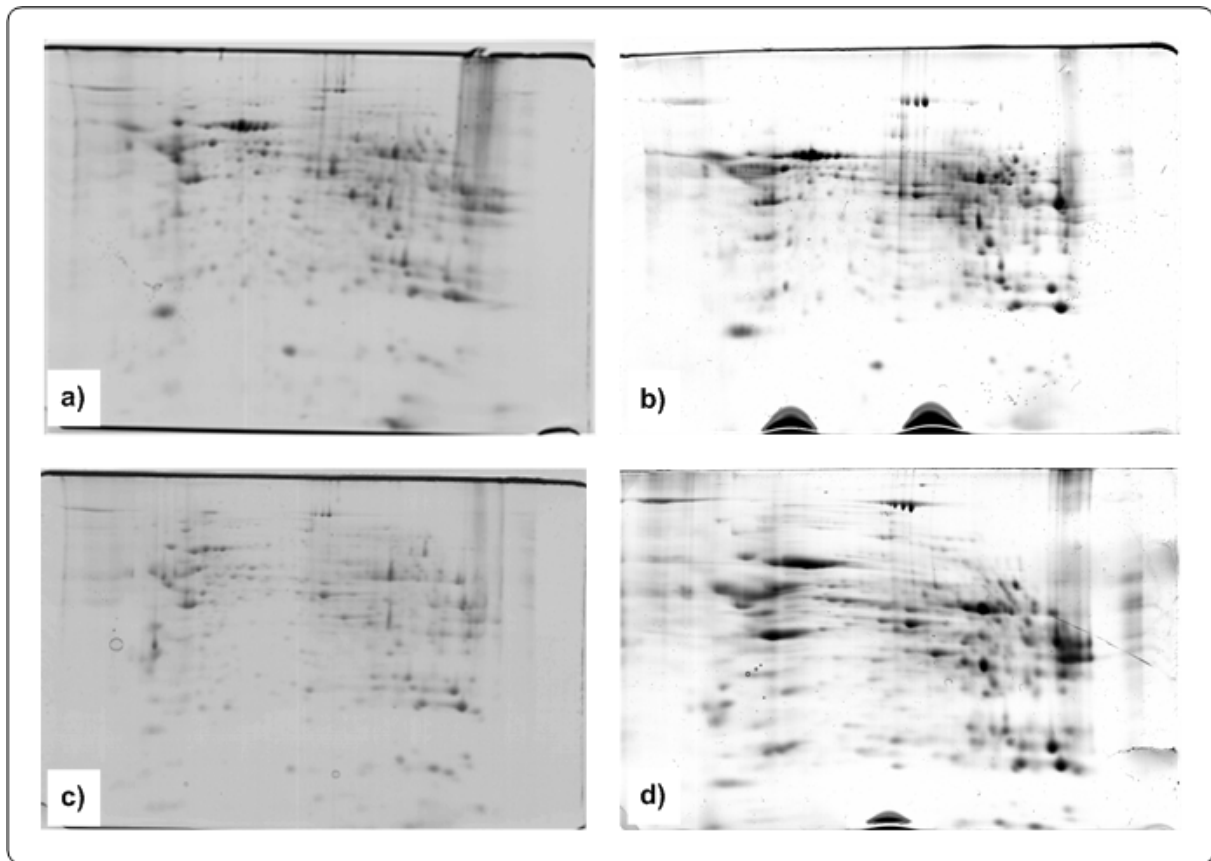


Figure 4-4 2D-gels to separate the intracellular proteins of PMH in collagen ML and SW culture for identification of spots with MALDI-ToF-MS. Isoelectric focusing was used in the first dimension, followed by SDS page in the second dimension. Intracellular proteome samples from collagen ML (a) and SW (b) culture at day 1 of cultivation and from collagen ML (c) and SW culture (d) at day 5 of cultivation. 1 gel per mouse was prepared (n=3).

Spot identification with MALDI ToF MS/MS showed, that for some proteins, e.g. albumin, more than one isoform could be found. In addition, only proteins are listed for which MALDI ToF MS/MS identification was clearly unequivocal. These two facts, in combination with the reduced sensitivity of Coomassie Blue staining compared to fluorescence staining, explain, why the number of identified differentially expressed proteins is significantly lower than the number of spots, which were originally identified as differentially expressed on DIGE gels.

In the following tables the significantly changed proteins, which were identified are listed. No difference was detected when PMH in collagen ML and SW culture were compared at day 1 of cultivation. The results of the comparison of the expressed proteins at day 5 are depicted in Table 4-1.

Table 4-1 Identified proteins, which were significantly different in PMH cultivated in collagen ML and SW culture after 5 d of incubation. The proteome of the ML culture served as control to which the proteome of the cells in SW culture was compared. Positive values indicate a higher abundance of the detected protein in the tested condition compared to the control, whereas negative values indicate a lower abundance. Shown are the means of the fold change from the different gels (n=3) and if more than 1 spot per protein was available (n=variable). Abbreviations: Std. dev. - Standard deviation.

Accession no.	Protein	Fold change	Std. dev.	Protein function
Q03265	ATP synthase	-2.02	0.07	ATP formation (proton gradient)
P11588	Major urinary protein	-1.95	0.13	Male pheromone
Q64374	Regucalcin	-1.88	0.34	Calcium-binding protein; oxidative stress defense
P60710	Actin	-1.53	0.01	Cytoskeleton
P11725	Ornithine carbamoyltransferase	1.71	0.01	Urea cycle
Q91Y97	Fructose-bisphosphate aldolase B	1.82	0.19	Glycolysis and gluconeogenesis
P08226	Apolipoprotein E	2.45	1.09	Binding, internalization, and catabolism of lipoprotein particles and oxidative stress
P07724	Serum albumin	2.52	0.39	Main plasma protein produced by liver; ligand for macromolecules and for antioxidant defense

From the 2D gels 24 spots per gel could be assigned to differentially expressed spots on the according DIGE gels. For albumin, ATP synthase and actin we found several isoforms. In total we could identify 8 differentially expressed proteins in PMH cultivated in ML compared to SW culture after 5 days of cultivation. The detected proteins covered different metabolic pathways such as the urea cycle, glycolysis and gluconeogenesis as well as the formation of ATP during oxidative phosphorylation. However, no proteins involved in TCA cycle were significantly changed in abundance (Supplementary Table 2). In addition to metabolic pathways, the cytoskeleton, Ca²⁺-signaling and pheromone production were concerned as

well. The amounts of major urinary protein, regucalcin and actin were clearly lower in the SW culture with the highest difference found for ATP synthase. Ornithine carbamoyltransferase, fructose-bisphosphate aldolase B, apolipoprotein E, on the other hand, showed a significantly higher abundance in the SW culture with the highest difference found for serum albumin, which was more than twice as abundant as in the ML culture.

The results found for the influence of cultivation time on the proteome of PMH in collagen ML culture are listed in Table 4-2. From the 2D-gels 34 spots per gel could be assigned to differentially expressed spots on the according DIGE gels. More than 1 spot was detected for albumin, ATP synthase and actin. In total we could identify 12 differentially expressed proteins in PMH cultivated in ML culture after 1 and 5 days of cultivation. In this case as well the detected proteins covered different metabolic pathways as the urea cycle, detoxification as well as the formation of ATP by oxidative phosphorylation. In addition to metabolic pathways, the cytoskeleton, serum protein production, iron storage, Golgi transport, oxidative stress and pheromone production were also affected.

Sarcosine dehydrogenase, argininosuccinate synthase, glutathion-S-transferase, carbamoyl-phosphate synthase, aldehyde dehydrogenase, selenium-binding protein and 75kD glucose regulated protein showed a significantly lower abundance after 5 days cultivation in ML culture with the highest difference found for serum albumin, which was reduced more than fivefold. Ferritin, ATP synthase and transitional ER ATPase were upregulated with increasing cultivation time. The highest increase was found for major urinary protein, a male pheromone binding protein, which showed a two times higher abundance compared to the culture 1 day after seeding.

Table 4-2 Identified proteins, which were significantly different in PMH cultivated in collagen ML culture after 1 and 5 d of incubation. The proteome of the ML culture at day 1 served as control to which the proteome of the cells of day 5 was compared. Positive values indicate a higher abundance of the detected protein in the tested condition compared to the control, whereas negative values indicate a lower abundance. Shown are the means of the fold change from the different gels (n=3) and if more than 1 spot per protein was available (n=variable). Abbreviations: Std. dev. Standard deviation.

Accession no.	Protein	Fold change	Std. dev.	Protein function
P07724	Serum albumin	-5.07	1.10	Main plasma protein produced by liver; ligand for macromolecules and for antioxidant defense
P38647	75kD glucose regulated protein	-1.97	0.02	Binds estrogens, fatty acids and metals/heat shock or stress proteins
P17563	Selenium-binding protein	-1.91	0.29	Involved in Golgi transport, sensing of reactive xenobiotics
P30416	Aldehyde dehydrogenase	-1.81	0.28	Detoxification of alcohol-derived acetaldehyde
Q8C196	Carbamoyl-phosphate synthase	-1.77	0.14	Urea cycle
P13745	Glutathione-S-transferase	-1.75	0.04	Conjugation of reduced glutathione
P16460	Argininosuccinate synthase	-1.67	0.13	Urea cycle
Q99LB7	Sarcosine dehydrogenase, mitochondrial	-1.63	0.13	Reduction of electron transfer proteins
Q3SXD2	Ferritin	1.54	0.01	Iron storage
Q03265	ATP synthase	1.56	0.06	ATP formation (proton gradient)
Q01853	Transitional ER ATPase	1.69	0.14	Role in fragmentation of Golgi stacks
P11588	Major urinary protein	2.3	0.02	Pheromone binding protein

Of the found proteins, albumin, ATP synthase and the major urinary protein were detected as changed in the comparison of ML and SW culture at day 5 of cultivation as well. Not exactly the same enzymes of the urea cycle were detected in both approaches, but the urea cycle was a common target.

The results found for the influence of cultivation time on the proteome of PMH in collagen SW culture are listed in Table 4-3. From the 2D gels 32 spots per gel could be assigned to differentially expressed spots on the according DIGE gels. More than 1 spot were detected for albumin, carbamoyl-phosphate synthase and ATP synthase. In total we could identify 8 differentially expressed proteins in PMH cultivated in SW culture after 1 and 5 days of cultivation. In this case as well the detected proteins covered different metabolic pathways as the urea cycle, glycolysis and gluconeogenesis as well as the formation of ATP during oxidative phosphorylation. In addition to metabolic pathways the serum protein production, Ca^{2+} -signaling, oxidative stress and protein rearrangement were also concerned. In contrary no proteins involved in lipid metabolism are significantly changed in abundance (Supplementary Table 2).

Glutathione S-transferase, ATP synthase, superoxid dismutase and fructose-bisphosphate aldolase showed a significantly higher abundance after 5 days cultivation in SW culture with the highest difference found for regucalcin, which showed a two times higher abundance after 5 days. Protein disulfide-isomerase and carbamoyl-phosphate synthase were downregulated with increasing cultivation time. The highest decrease was found for the serum albumin, which showed a three times lower abundance compared to the culture 1 day after seeding. ATP synthase, regucalcin, fructose-bisphosphate aldolase and serum albumin were also detected as differentially expressed in the comparison between SW and ML culture. However, although not the same enzymes could be found, urea cycle, which was differential in ML and SW culture after 5 days of cultivation, was also affected over time in the SW culture.

In both culture conditions it could be observed that after 5 days of cultivation ATP synthase, carbamoyl-phosphate synthase and serum albumin were differentially expressed with comparable magnitude.

Table 2-3 Identified proteins, which were significantly different in PMH cultivated in collagen SW culture after 1 and 5 d of incubation. The proteome of the SW culture at day 1 served as control to which the proteome of the cells of day 5 was compared. Positive values indicate a higher abundance of the detected protein in the tested condition compared to the control, whereas negative values indicate a lower abundance. Shown are the means of the fold change from the different gels (n=3) and if more than 1 spot per protein was available (n=variable). Abbreviations: Std. dev. Standard deviation.

Accession no.	Protein	Fold change	Std. dev.	Protein function
P07724	Serum albumin	-3.08	1.06	Main plasma protein produced by liver; ligand for macromolecules and for antioxidant defense
Q8C196	Carbamoyl-phosphate synthase	-2.00	0.22	Urea cycle
P09103	Protein disulfide-isomerase	-1.83	0.06	Rearrangement of -S-S- bonds in proteins
P13745	Glutathione S-transferase	1.71	0.12	Conjugation of reduced glutathione
Q03265	ATP synthase	1.71	0.24	ATP formation (proton gradient)
P08228	Superoxide dismutase	1.88	0.02	Destroys superoxide anion
P05064	Fructose-bisphosphate aldolase	1.90	0.18	Glycolysis and gluconeogenesis
Q64374	Regucalcin	2.00	0.04	Calcium-binding protein; oxidative stress defense

4.3 Discussion

In this study the intracellular proteome of PMH in collagen SW and ML culture was compared after 1 and 5 days of cultivation. In addition to this, the samples of each cultivation condition at day 1 and day 5 were compared to each other as well. This gave us not only the opportunity to analyze the effect of cultivation time on protein expression, but also guaranteed a correct interpretation of the results gained from the comparison of the ML and SW culture. The quantification of proteins using DIGE is not absolute, but only relative to a set control

condition. In the comparison of the proteome of the ML and the SW culture the ML culture, as the commonly used standard cultivation condition, was used as control. This gives us information on higher or lower protein abundance in the SW culture. A direct conclusion, if the protein has been e.g. up-regulated in the SW culture or down-regulated in the ML culture is not possible. This can only be said, if the samples are compared to the original condition at day 1 of cultivation.

In accordance with the findings in Chapter 3 the concentration of albumin in the SW culture was more than twice as high as in the ML culture after 5 days of cultivation (Table 4-1). However, also in the SW culture the intracellular amount of albumin was decreased after 5 days of cultivation compared to beginning of the cultivation (Table 4-3). It was however found in Chapter 3, that the albumin production rate remained constant throughout the whole cultivation time. This discrepancy could indicate, that the excretion of albumin represents the rate-limiting step and the intracellular formation of albumin is already affected before this can be detected on the basis of the excretion rate.

The concentration of ornithine carbamoyltransferase, which catalyzes the formation of L-citrulline from L-ornithine in the urea cycle, was about 70% higher in the SW culture (Table 4-1). In the ML comparison ornithine carbamoyltransferase was not found as differentially expressed. However, carbamoyl-phosphate synthase and argininosuccinate synthase, two other enzymes of the urea cycle, were down-regulated after 5 days of cultivation (Table 4-2). This indicates a strong negative effect on the urea cycle triggered by the cultivation in collagen ML. These findings reflect the significant down-regulation of urea production observed for PMH in other studies (Figure 3-5). However, also in PMH cultivated in collagen SW carbamoyl-phosphate synthase was down-regulated after 5 days of cultivation (Table 4-3). No effect on urea production was observed as described in Chapter 3. The formation of carbamoyl-phosphate and thereafter the formation of argininosuccinate represent the rate limiting steps of the urea cycle. However, this formation rate is mostly limited by substrate availability and not by enzyme activity (Shambaugh 1977). Since in both cultivation conditions the enzyme is down-regulated to about the same extent, other factors might play a role. These could involve post-translational modifications, leading in addition to a lower activity of the enzymes, or a lower formation rate of ammonia. An example could be the acetylation status. SIRT5, a protein induced by oxidative stress, is known to lead to the deacetylation of carbamoylphosphate synthase, which is then activated (Nakagawa et al. 2009, Bell and Guarente 2011). The expression of actin was also influenced by the cultivation

condition. The amount of the cytoskeletal protein was clearly lower in PMH cultivated in collagen SW (Table 4-1). Since actin could not be confirmed as differentially expressed in the comparison of SW and ML culture at day 1 and day 5, respectively, no clear conclusion could be drawn, if the protein was up-regulated in the ML culture or down-regulated in the SW culture. The possible reasons for this are discussed below in detail. However, Beigel et al. showed that actin was up-regulated in primary rat hepatocytes cultivated in ML culture already after 48 h of cultivation (Beigel et al. 2008). This supports an up-regulation of the protein in PMH in collagen ML culture as well. The reason for this might be found in the differential distribution of actin in the cell, which is described in Chapter 3 (Figure 3-1). In the SW culture actin was accumulated close to the cell-cell contacts, where bile canaliculi are formed (Figure 3-1, LeCluyse et al. 2000). In the ML culture actin stress fibers were found throughout the cytoplasm. Stress fiber formation may therefore go along with increased actin production. Besides typical hepatic functions and cellular morphology also carbon and energy metabolism were affected. Fructose-bisphosphate aldolase, the glycolytic enzyme which catalyzes the split of F1,6BP into glyceraldehyde 3-phosphate and dihydroxyacetone phosphate, was up-regulated over time to about two times its original amount in the collagen SW culture (Table 4-3). This enzyme does not catalyze an irreversible step in glycolysis and gluconeogenesis. This is why it cannot be said, if glycolysis or gluconeogenesis activity is increased in PMH in SW culture. However, it gives us a strong hint, that these pathways may be affected, which is also in accordance to our findings described in Chapter 3, where glucose utilization was changed in the SW culture over time. Thereby, enzymes catalyzing reversible steps of the respective pathways do not necessarily have to be altered regarding the total amount of protein, but can also be strongly regulated by post-translational modification. ATP synthase was up-regulated over time in SW and ML culture (Table 4-2, 4-3), but if the proteome was compared at day 5 of cultivation the amount in the SW was two times lower compared to the ML culture (Table 4-1). The most prominent effects were found with proteins dealing with oxidative stress. Reactive oxygen species (ROS) are constantly produced by aerobic metabolic processes such as respiration (Apel and Hirt 2004). ROS cause oxidative damage to proteins, DNA, and lipids. Therefore, cells have special defense systems, which prevent the formation of ROS or which repair the damage created by it (Halliwell 1991). However, our results indicate that, with the exception of superoxide dismutase, no proteins directly scavenging free radicals are changed in abundance (Supplementary Table 2). In the ML culture proteins involved in oxidative stress defense were down-regulated (Table 4-2), whereas in the SW culture proteins related to oxidative stress were up-regulated (Table 4-

3). PMH in collagen SW and ML culture seem to be confronted with oxidative stress. However, in the SW culture the defense system is significantly up-regulated to deal with this, whereas in the ML culture a down-regulation of these important enzymes takes place. Regarding the multiple effects of ROS and oxidative stress in cells, one can assume that the down-regulation of these enzymes might also play a role in the loss of hepatic function observed in ML cultivation. Surprisingly, no changes of enzymes involved in phase I and II metabolism of xenobiotics were detected (Supplementary Table 2). However, many of these proteins are only weakly expressed and information on low abundant proteins are often lost on protein gels (Beigel et al. 2008, Natarajan et al. 2009). Therefore, it is not surprising that non of these enzyme have been detected.

The gel-based approach to detect differences in protein abundance used in this experiment has certain drawbacks. The inter-gel variability is rather high, which leads to difficulties regarding reproducibility. Using two separate gels for quantification and identification makes it necessary to assign matching spots manually. This is tedious work and can be prone to errors. An automated spot-picker, as used by Gozal et al., could reduce the risk of wrong spot assignment (Gozal et al. 2009). In their approach, they loaded the DIGE-gel in addition to the fluorescent-labeled proteins with a higher amount of unlabeled protein, which could be used for tryptic digestion and identification using MALDI-ToF-MS/MS subsequent to DIGE-based quantification. This spares the necessity of a second gel-separation. Due to sample preparation to reduce the amount of the most abundant proteins, which is necessary to increase the resolution of protein separation, a loss of low-abundant proteins is possible. The proteins can for example be bound to albumin or other proteins. In general, every step of sample preparation can lead to a loss of protein. This may also lead to a reduced sensitivity of the approach. Further analysis with LC-MS/MS, which offers high resolution, needs less sample preparation and is the most commonly used technique in proteomics, might give further insight into differential protein expression in hepatocytes in collagen ML and SW culture (Yates et al. 2009, Bantscheff et al. 2012). However, the gel-based approach also has a major advantage since with this method the physiological molecular weight as well as information on the pI of the respective proteins is gained. This can be used for example to differentiate between different isoforms of proteins, which cannot be achieved with direct LC-MS approaches (Diamond et al. 2006). General top-down approaches with LC-MS in addition do have other problems. It requires back mapping of identified peptides to parent proteins, which can be difficult due to insufficient protein sequence coverage and sequence redundancy (a sequence can be present in multiple proteins) and it can also lead to a loss of labile post-

translational modifications (Diamond et al. 2006, Yates et al. 2009). As there is no perfect experimental approach for the analysis of the proteome, a combination of different analysis methods leads to the most promising and holistic results.

Overall, the most protein changes were induced by the cultivation in ML culture. Proteins involved in multiple pathways were concerned. The loss of hepatic function, which could be observed in Chapter 3, could be confirmed by this study. However, protein expression was also changed to a certain extent in PMH cultivated in collagen SW culture, although the changes were not as pronounced as in the ML culture. Still also in SW culture various pathways were affected. This is in accordance with the results gained by Farkas et al. with primary rat hepatocytes in collagen SW cultivation (Farkas et al. 2005). In this study it was shown, that also the secretome of primary hepatocytes is changed over time towards dedifferentiation. Other studies, which were also conducted with PRH found similar results for hepatocytes cultivated in ML over time and if the two cultivation methods were compared (Beigel et al. 2008, Rowe et al. 2010). In this studie oxidative stress, cytoskeletal remodeling and glucose metabolism were identified as major disturbed pathways. Overall, a more in-depth analysis of the detected pathways, e.g. using a targeted LC-MS/MS approach, could reveal if other enzymes of the detected pathways in both cultivation conditions are concerned, which could not be detected due to the above-mentioned reasons. In conclusion, it can be said, that on a proteomic level, PMH in collagen SW culture are closer to the original phenotype. However, although this cultivation condition better resembles the *in vivo* situation, a development away from the original phenotype could be observed.

5. Influence of insulin and glucose on central carbon metabolism of primary mouse and human hepatocytes

5.1 Introduction

Metabolomics approaches have been widely used in science and pharmaceutical industry to characterize cultivation systems, to improve production strains and to detect early markers of toxicity or disease (Peifer et al. 2012, Wahrheit et al. 2014, Klein et al. 2014, Mattes et al. 2014). The metabolome and fluxome are closest to the actual phenotype of a system, compared to the genome, transcriptome or proteome, and additionally are highly sensitive to environmental changes (Beger et al. 2010). An in-depth understanding of metabolic reactions can therefore lead to a substantial increase in knowledge about physiological processes. Through the general characterization of metabolic processes in mouse hepatocytes in collagen ML and SW culture, we could show that the direct metabolism of glucose is most susceptible to changes during long-time cultivation (Figure 3-3). The brain is strongly dependent on glucose as a carbon source and one of the liver's major tasks is to guarantee its supply. Therefore, glucose is taken up from the blood, if the concentration is high after a meal and stored as glycogen or triglycerides. If the blood glucose levels are low, e.g. during fasting, it is produced *via* glycogenolysis or gluconeogenesis and secreted into the blood. These processes are mostly regulated by the complex interplay of two major hormonal players, namely insulin and glucagon. Insulin, which is secreted by the β -cells of the pancreas if blood glucose levels are increased, leads to an increased uptake of glucose in insulin sensitive tissues. In hepatocytes glycogen synthesis is stimulated and at the same time glycogenolysis and gluconeogenesis are diminished. Glucagon generally leads to the exact opposite effects, through an increase in glucose production *via* the respective pathways (Zierler 1999). The regulation of glucose homeostasis is not a straightforward process, since also various other factors such as other hormones and metabolite levels play a significant role, and the whole process is still not completely understood (Draznin 1996). Additionally, insulin itself has also many other effects in insulin sensitive tissues, which cannot directly be related to glucose homeostasis (Takenaka et al. 1989, Saltiel and Kahn 2001). This complicates a thorough understanding. Another problem, which arises during the investigation of insulin and glucose effects is that at least *in vivo* these processes are

regulated differently in different species. This is also the case in rodents and humans. Still, primary hepatocytes from mice, rats and humans represent the major sources for *in vitro* studies in this field (Kowalski and Bruce 2014). This significantly complicates comparison of data from different studies and makes a generalization of data gained from different species almost impossible, although this can be regularly found in literature (König et al. 2012, König and Holzhütter 2012).

In this study the effects of glucose itself and insulin as its major regulator on the central carbon metabolism are in the focus. Therefore, a quantitative characterization of the response to insulin and glucose in primary hepatocytes from mice and humans was conducted to make a direct comparison possible. Additionally, hepatocytes from both origins were, as for the general metabolic characterization (Chapter 3), cultivated in SW and ML culture to determine if the cultivation condition influences the reaction of the cells to certain glucose or insulin concentrations.

5.2 Results

PMH and PHH were cultivated with different insulin and glucose concentrations for 24 h to investigate the influence of both on the central carbon metabolism. The standard glucose concentration in WME especially designed for cultivating hepatocytes is 2 g/l which makes 11.1 mM. We choose 7 mM as a concentration to represent fasting and 25 mM to represent postprandial conditions. The peripheral plasma insulin concentration in humans lies between 10^{-10} – 10^{-9} M (Cheatham and Kahn 1995) and is about three times higher in the portal vein (Roden and Bernroider 2003). The chosen insulin concentration ranges from 0.1 to 100 nM (0.1, 1, 10 and 100 nM) included the physiological range of insulin in the liver. Additionally, hepatocytes were not only cultivated in collagen ML but also collagen SW culture to examine if the cells react identically to insulin and glucose under both culture conditions.

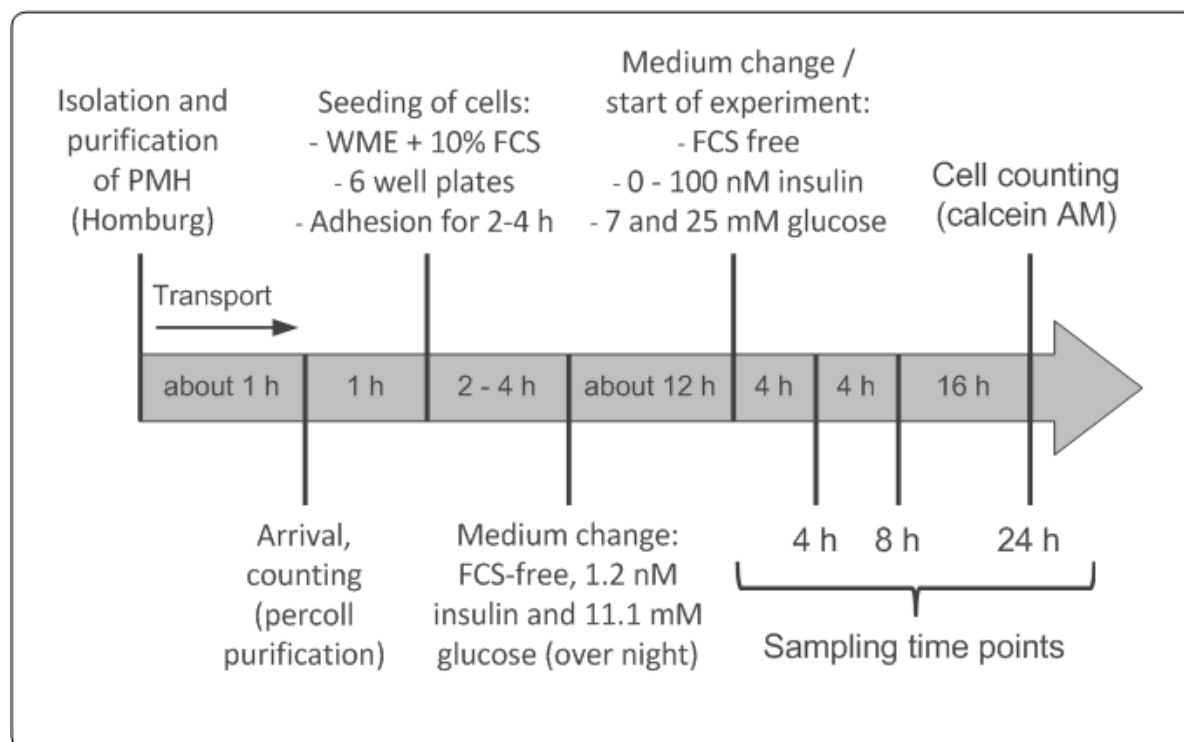


Figure 5-1 Experimental setup to examine the influence of insulin and glucose on the central carbon metabolism of PMH *in vitro*. PMH were isolated at Universitätsklinikum des Saarlandes by the group of Prof. Dr. F. Lammert (Homburg, Saar). The used insulin concentrations were 0, 0.1, 1, 10 and 100 nM. Glucose was used at a concentration of 7 or 25 mM. The cells were cultivated as collagen ML and SW.

5.2.1 Influence on the central carbon metabolism of mice

PMH were seeded in ML and SW and were allowed to adapt to culture conditions over night under standard cultivation conditions (1.2 nM insulin and 11.1 mM glucose) (Figure 5-1). The medium was then changed to experimental conditions and samples taken after 4, 8 and 24 h. The extracellular metabolome, namely proteinogenic amino acids, organic acids and glucose, was determined using HPLC and uptake and secretion rates were calculated.

In order to analyze if insulin has an influence on the hepatocyte metabolome and if so, which metabolites are most influenced, a principle component analysis (PCA) was performed. The PCA is a mathematical method which is used to structure, simplify and to illustrate complex data sets first formulated by Pearson (Pearson 1901, Bollard et al. 2005). The PCA concentrates strongly correlating variables in a data set into a new variable, called principal component, by linear combination of the original variables (van der Werf et al. 2005). To make sure, that the levels or variance were similar for all metabolites, range scaling was applied. Hereby, the measured intensities are divided by the range of those intensities, namely the standard deviation, over all the samples (Smilde et al. 2005).

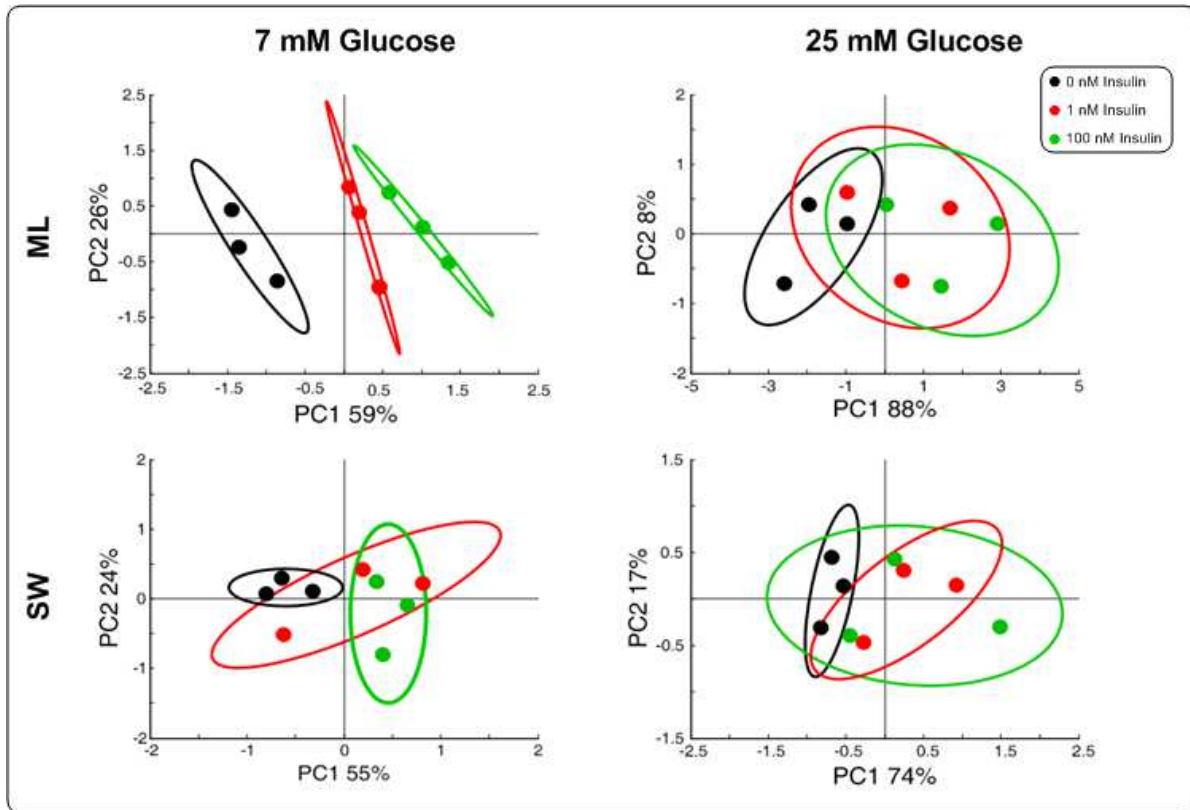


Figure 5-2 Principal component analysis of the uptake and secretion rates of metabolites of primary mouse hepatocytes in collagen sandwich and monolayer culture incubated with different insulin (0-100 nM) and glucose concentrations (7 and 25 mM). The results for the first 4 h of incubation treated with 0 (black), 1 (red) and 100 nM insulin (green) are shown for 3 mice (means of 3 technical replicates) (N=3; n=9) with a confidence interval of 95%. Values were normalized by range scaling.

In Figure 5-2 the PCAs for the metabolite uptake and secretion rates of PMH in SW and ML culture are depicted. On grounds of clarity and since only little variation between the technical replicates was found, the mean values of each mouse are shown. PMH in ML culture incubated with 7 mM glucose show a clear segregation between the different insulin concentrations used after 4 h of incubation. For all other conditions the segregation is not as explicit, but a trend towards segregation between 0 and 100 nM insulin is clearly recognizable, at least for the SW cultivation incubated with 7 mM glucose.

With PCA it is possible to calculate which metabolites have the most influence on segregation between two conditions. In Figure 5-3 (a) an example for this can be found for 7 mM glucose ML. The metabolites with the highest loading coefficients (positive or negative) also have the highest influence. In Figure 5-3 (b) the nine metabolites are listed which had taken together the highest coefficients in all four conditions depicted in Figure 5-3. Glucose metabolism thereby was by far the most influenced, but also other typical carbon

sources as glutamine and alanine were influenced by insulin. The metabolites with the highest coefficients were chosen for closer examination. The influence of insulin and glucose on typical hepatic functions including albumin and urea production will be discussed in detail in Chapter 6.

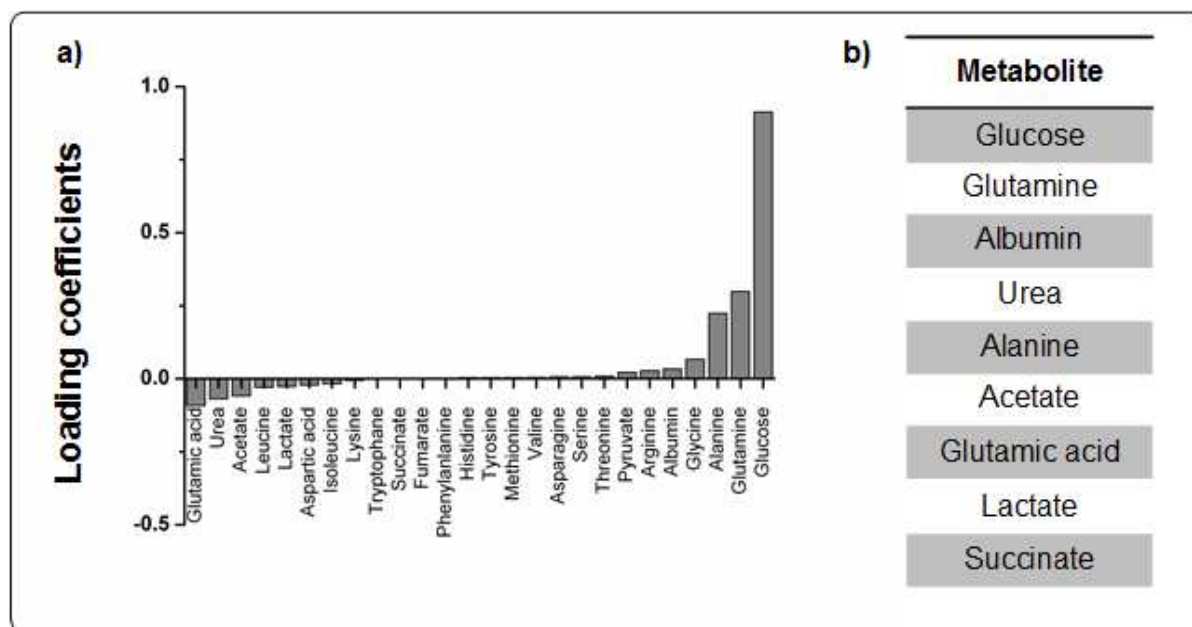


Figure 5-3 Metabolites with the greatest influence on segregation on the extracellular metabolome of primary mouse hepatocytes incubated with different insulin concentrations. (a) The loading coefficients of principle component 1 of PMH cultivated in collagen ML culture incubated with 7 mM glucose are depicted. (b) List of metabolites with the highest positive or negative loading coefficients in all four culture conditions (SW, ML, 7 and 25 mM glucose).

The uptake and secretion rates of glucose and selected organic acids, acetate, lactate and succinate, of PMH cultivated in ML culture over 24 h are depicted in Figure 5-4. Acetate was produced independently from the used glucose concentration and constantly during the cultivation period. After 8 h significant differences between 0, 10 and 100 nM insulin developed at 7 mM glucose, whereas changes were not significant in the cells treated with 25 mM glucose. Glucose uptake or production by the cells is largely dependent on the extracellular glucose concentration. If the extracellular glucose concentration is low and insulin is lacking, glucose is produced by PMH with a secretion rate of about 700 fmol/cell \cdot h $^{-1}$. If 25 mM extracellular glucose is administered, it is taken up by the cells with a rate of about 1000 fmol/cell \cdot h $^{-1}$. Additional to the sensitivity to extracellular glucose levels, this was also significantly influenced by the applied insulin concentration.

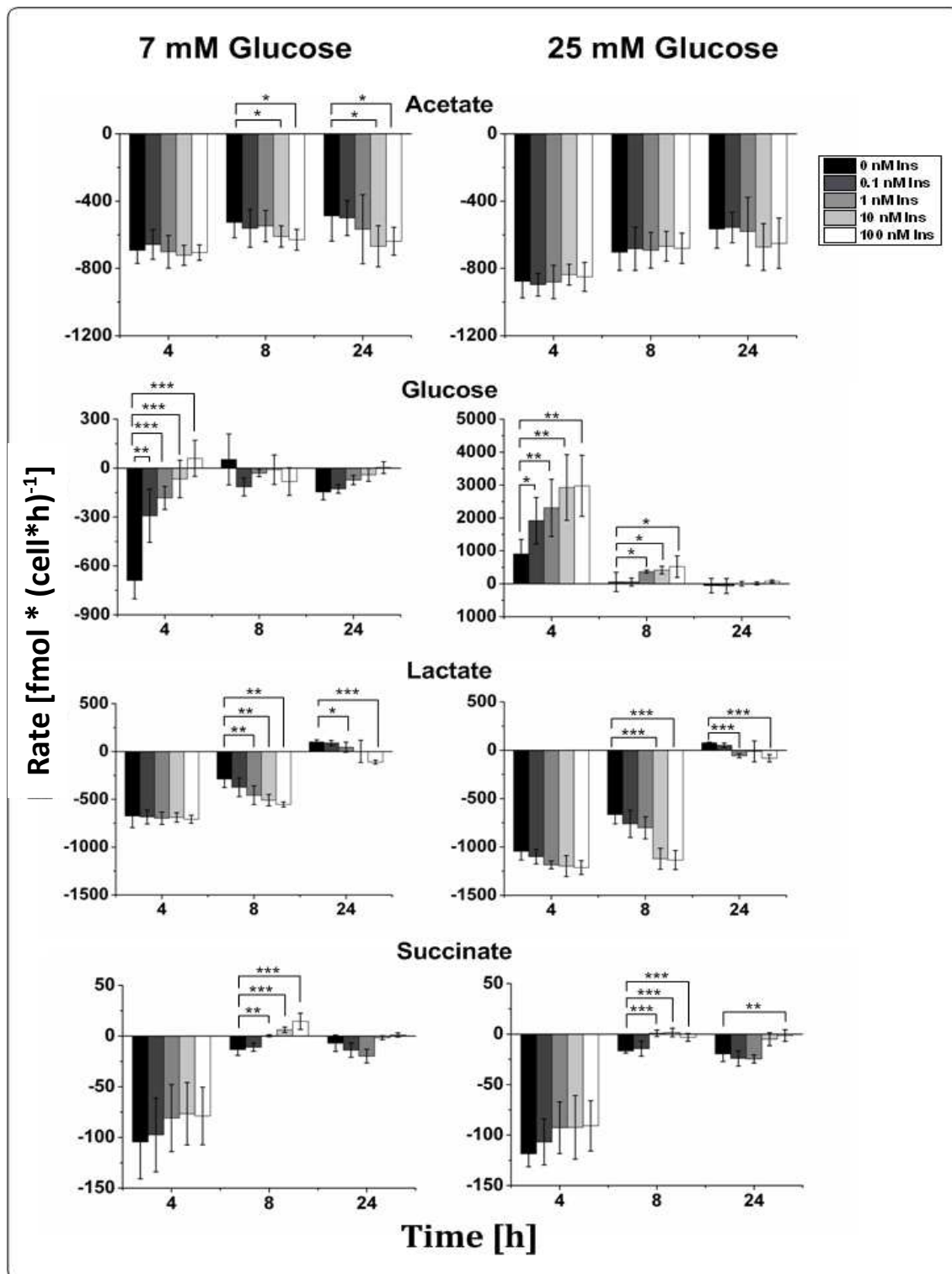


Figure 5-4 Conversion rates of glucose and selected organic acids of primary mouse hepatocytes cultivated in collagen monolayer culture under the influence of different insulin (0-100 nM) and glucose (7 and 25 mM) concentrations. Positive values indicate uptake, negative values production. Error bars indicate standard deviation (N=3; n=9). Statistical significance was determined with student's t-test. *, ** and *** indicate significance at $p=0.05$, $p=0.01$ and $p=0.001$, respectively. Living cell number was determined after 24 h of cultivation using calcein AM staining. Abbreviations: Ins Insulin.

In the first 4 h insulin decreased glucose production in the low glucose condition, until glucose was even consumed with the highest tested insulin concentration, and accordingly increased glucose uptake with high extracellular glucose levels. After 8 h glucose uptake or production was strongly diminished in both culture conditions, however the influence of insulin was still apparent, even if not significant.

Lactate is a final product of non-oxic fermentational glycolytic metabolism. Its production at high extracellular glucose levels was nearly doubled compared to that at a low glucose concentration. After 8 h of incubation lactate production was significantly enhanced in accordance with increasing insulin concentration. After 24 h lactate was no longer produced but taken up by the cells. However, increasing insulin concentration led to a further production. Succinate is an important intermediate of the TCA cycle and was strongly produced within the first 4 h of cultivation. The concentration of extracellular glucose had no influence on the production rate. After 8 h of cultivation, however, insulin significantly influenced succinate production in a concentration dependent manner, which even led to uptake of extracellular succinate.

In contrast to ML culture, hepatocytes cultivated in collagen SW culture produced acetate with a high rate of $1300 \text{ fmol/cell}\cdot\text{h}^{-1}$ within the first 4 h of cultivation as depicted in Figure 5-5. After that the production declined to $500 \text{ fmol/cell}\cdot\text{h}^{-1}$ and remained constant for the residual cultivation time. Thereby, production was completely unaffected by glucose or insulin. As in the ML culture, hepatocytes in the SW culture produced glucose if the extracellular glucose concentration resembled fasting conditions and took up glucose at postprandial conditions. In both conditions insulin had a significant dose-dependent effect, diminishing glucose production and enhancing glucose consumption. The highest production rate as well as the highest consumption rate were thereby slightly lower as in the ML culture. The amount of produced lactate was strongly dependent on the applied extracellular glucose concentration and about twice as high with the postprandial glucose level. After 8 h lactate production was significantly increased by insulin in a concentration dependent manner. In general lactate production was slightly lower in SW culture compared to ML culture. Succinate was produced at comparable rates in ML and SW culture. In collagen SW culture insulin had also the effect of significantly reducing succinate production. In contrast to insulin, the applied glucose concentration had no influence on the production of succinate.

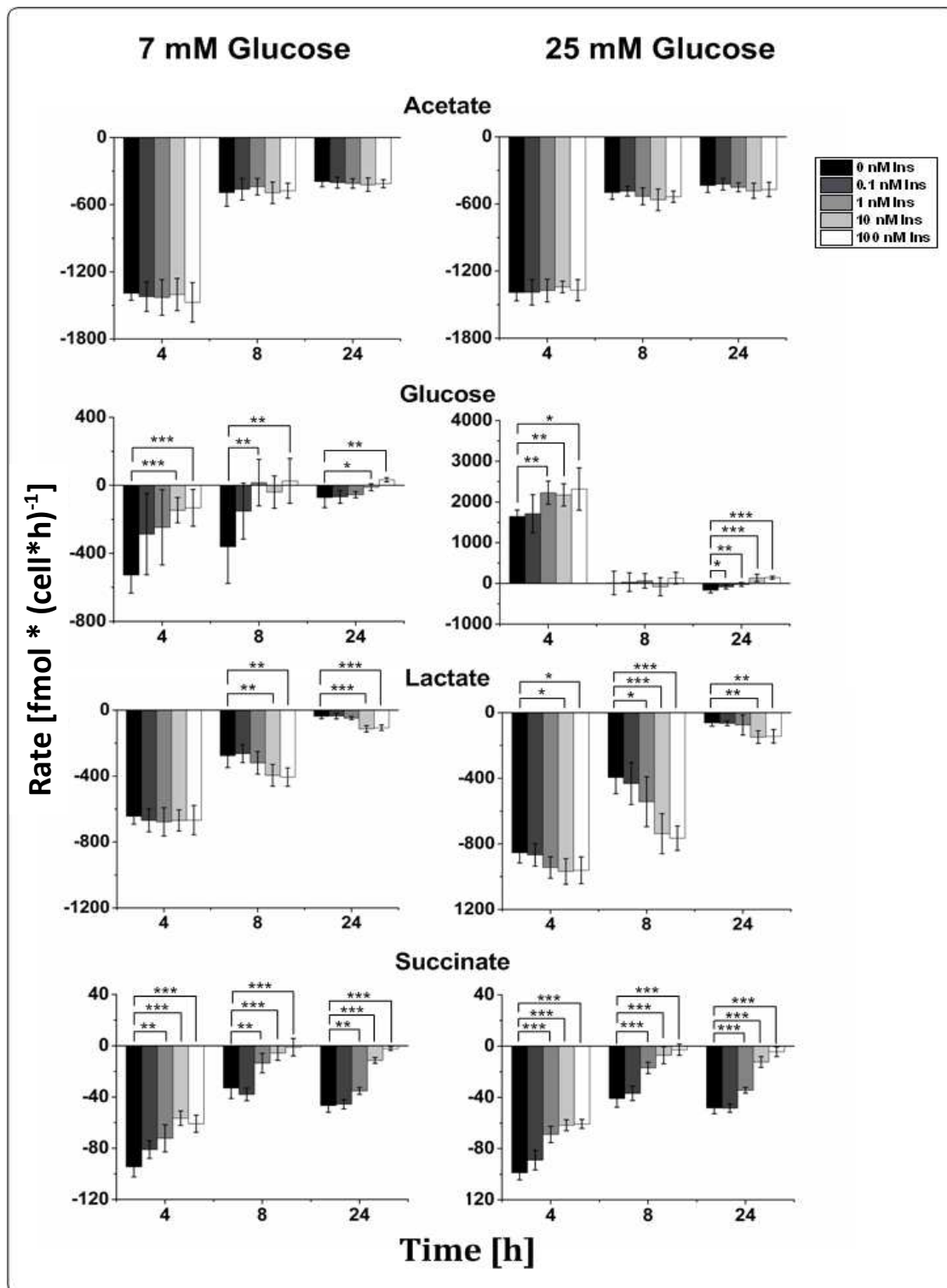


Figure 5-5 Conversion rates of glucose and selected organic acids of primary mouse hepatocytes cultivated in collagen sandwich culture under the influence of different insulin (0-100 nM) and glucose (7 and 25 mM) concentrations. Positive values indicate uptake, negative values production. Error bars indicate standard deviation (N=3; n=9). Statistical significance was determined with student's t-test. *, ** and *** indicate significance at $p=0.05$, $p=0.01$ and $p=0.001$, respectively. Living cell number was determined after 24 h of cultivation using calcein AM staining. Abbreviations: Ins Insulin.

Because of the results from the PCA (Figure 5-3) certain amino acid were chosen for presentation, namely alanine, glutamic acid, glutamine and glycine. The uptake and production rates for PMH in ML culture are depicted in Figure 5-6, whereas for SW culture they are presented in Figure 5-7. Glutamine and alanine were, apart from glucose, the major carbon sources in ML as well as in SW culture. PMH in ML showed high initial consumption of alanine with an uptake rate between 200 and 400 $\text{fmol} \cdot (\text{cell} \cdot \text{h})^{-1}$. If 7 mM glucose were applied, alanine consumption was significantly increased by insulin from the beginning of cultivation. The rate thereby constantly decreased from 4 to 24 h of incubation. If postprandial conditions were simulated, namely 25 mM glucose applied, alanine was strongly consumed, however hardly influenced by the used insulin concentrations. As for the fasting conditions, the uptake rate decreased over time as well, however after 8 h of incubation insulin showed a rate increasing effect. Even if this was not significant after 24 h, a trend to that effect could clearly be observed. The overall amount of consumed alanine was thereby completely independent of the extracellular glucose concentration. Glutamic acid was strongly produced in the beginning of cultivation in a glucose independent manner. Insulin, however, significantly increased the production rate in both cases. As well as for alanine, the rate decreased over time until glutamic acid even showed a net consumption at the end of cultivation. Glutamic acid can be directly converted into glutamine by glutamine synthetase and produced from glutamine by glutaminase. Both amino acids are therefore closely connected. Glutamine was strongly consumed independently of the extracellular glucose concentration. Insulin on the other hand increased the consumption in a concentration dependent manner. Although all three mice showed the same trend, due to varying absolute rates this was not as significant as for the other amino acids. During the cultivation the rates also decreased strongly. Glycine consumption was as well strongly increased by insulin, so that at 8 h the uptake rates were about thrice as high with the highest insulin concentration compared to standard conditions without insulin. From 8 h onwards the absolute consumption of glycine was not significantly influenced by the applied extracellular glucose concentration, although initially higher at 7 mM glucose.

PMH cultivated in collagen SW culture showed a more or less comparable amino acid profile (Figure 5-7). Insulin had a rate increasing effect, regardless of the consumption of alanine, glutamine and glycine or the production of glutamic acid.

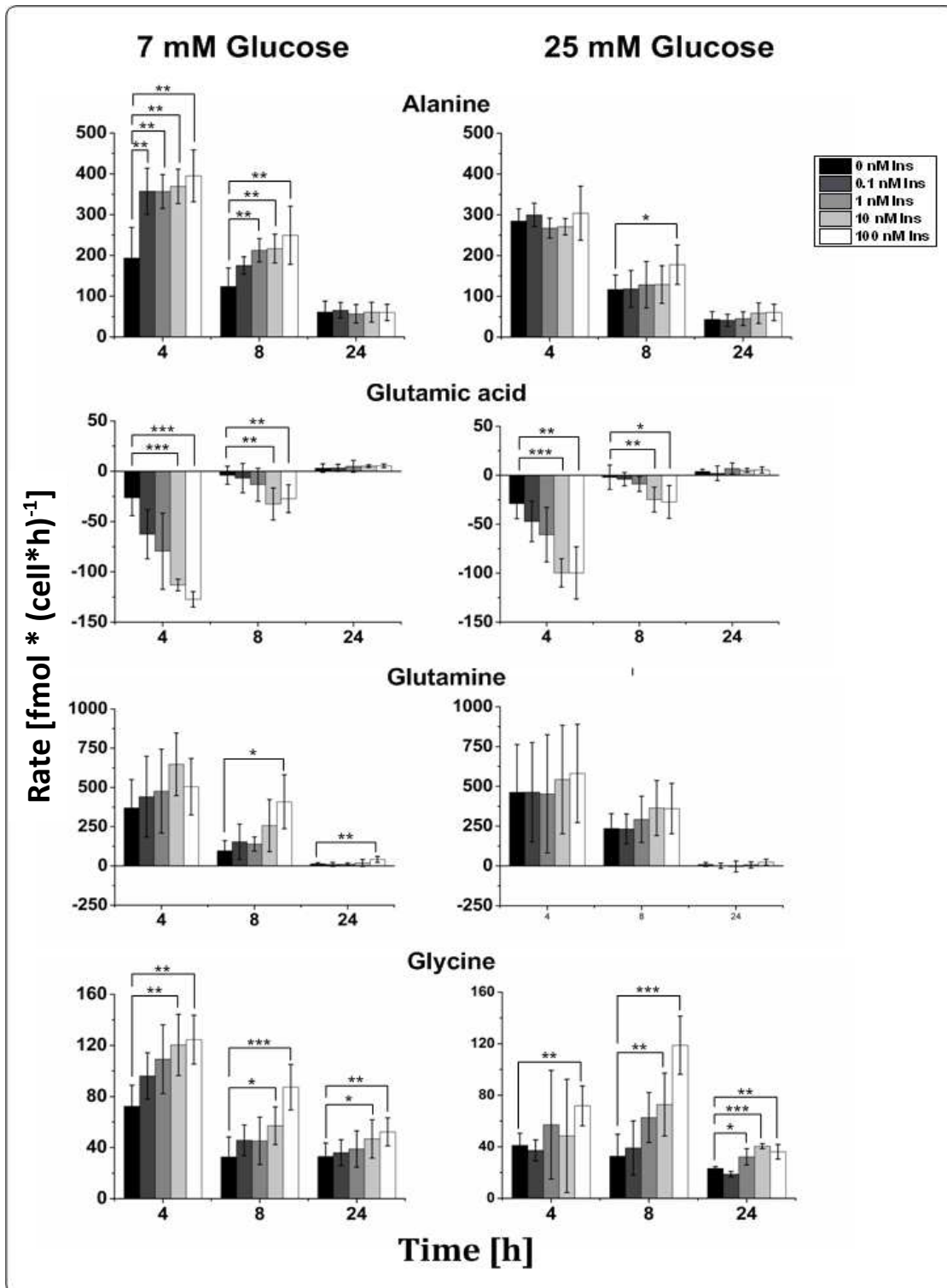


Figure 5-6 Conversion rates of selected amino acids (alanine, glutamic acid, glutamine and glycine) of primary mouse hepatocytes cultivated in collagen monolayer culture under the influence of different insulin (0-100 nM) and glucose (7 and 25 mM) concentrations. Positive values indicate uptake, negative values production. Error bars indicate standard deviation (N=3; n=9). Statistical significance was determined with student's t-test. *, ** and *** indicate significance at $p=0.05$, $p=0.01$ and $p=0.001$, respectively. Living cell number was determined after 24 h of cultivation using calcein AM staining. Abbreviations: Ins Insulin.

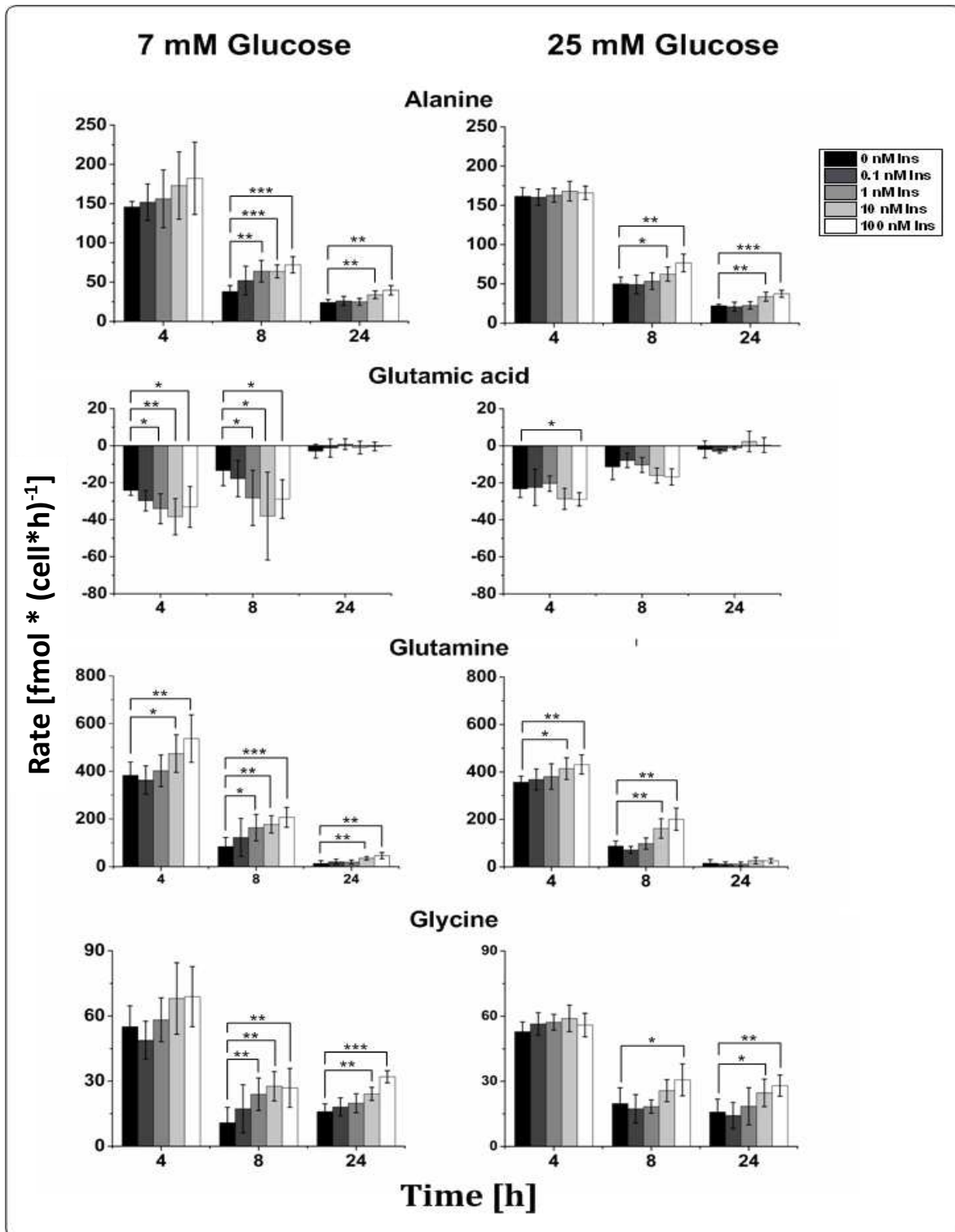


Figure 5-7 Conversion rates of selected amino acids (alanine, glutamic acid, glutamine and glycine) of primary mouse hepatocytes cultivated in collagen sandwich culture under the influence of different insulin (0-100 nM) and glucose (7 and 25 mM) concentrations. Positive values indicate uptake, negative values production. Error bars indicate standard deviation (n=9). Statistical significance was determined with student's t-test. *, ** and *** indicate significance at $p=0.05$, $p=0.01$ and $p=0.001$, respectively. Living cell number was determined after 24 h of cultivation using calcein AM staining. Abbreviations: Ins Insulin.

In general, the overall rates were independent of the glucose concentration chosen. Remarkably, the rates were only about half as high as for PMH in ML culture.

5.2.2 Influence on the central carbon metabolism of humans

PHH were seeded in collagen SW and ML culture after an overnight transport. To adapt to culture conditions and to give them the chance to replenish glycogen stores they were kept over night under standard cultivation conditions (1.2 nM insulin and 11.1 mM glucose). On the next morning they were treated completely identical to PMH with different insulin (0, 0.1, 1, 10 and 100 nM) and glucose concentrations (7 and 25 mM). Sampling took place at the same intervals as for PMH after 4, 8 and 24 h and the determination of the extracellular metabolome was done accordingly.

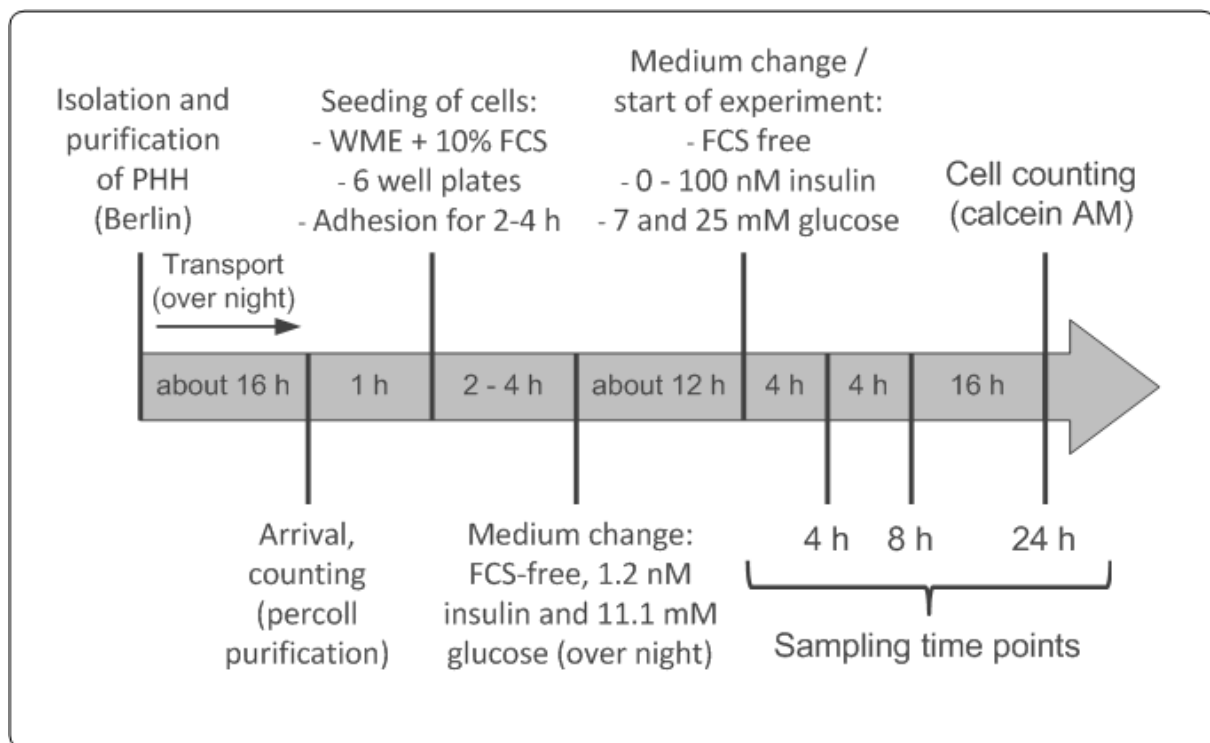


Figure 5-8 Experimental setup to examine the influence of insulin and glucose on the central carbon metabolism of PHH *in vitro*. PHH were isolated at Charité Berlin. The used insulin concentrations were 0, 0.1, 1, 10 and 100 nM. Glucose was used in a concentration of 7 or 25 mM. The cells were cultivated as collagen ML and SW.

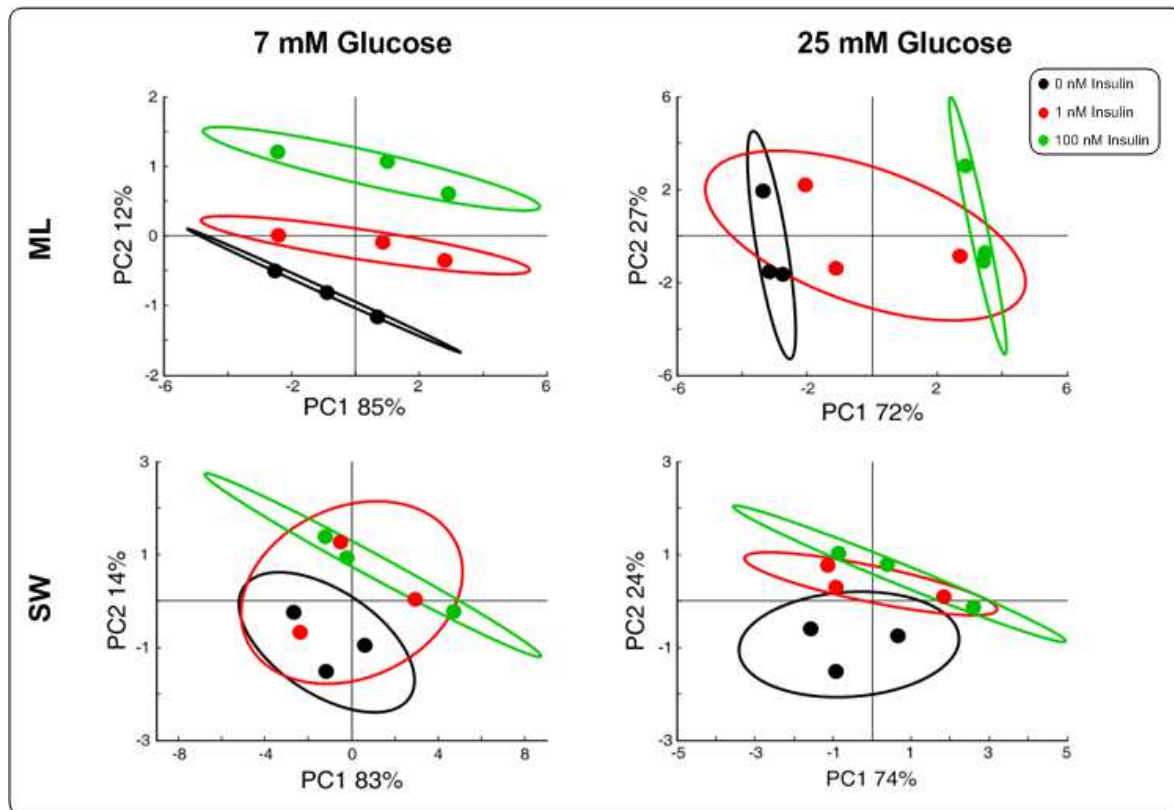


Figure 5-9 Principal component analysis of the uptake and secretion rates of metabolites of primary human hepatocytes in collagen sandwich and monolayer culture incubated with different insulin (0-100 nM) and glucose concentrations (7 and 25 mM). The results for the first 4 h of incubation treated with 0 (black), 1 (red) and 100 nM insulin (green) are shown for 3 donors (means of 3 technical replicates) (N=3; n=9) with a confidence interval of 95%. Values were normalized by range scaling.

In order to determine if insulin has a concentration dependent effect on the metabolome of PHH a PCA was accomplished with metabolome data. The results are depicted in Figure 5-9. On grounds of clarity and since only little variation between the technical replicates was found the mean values of each donor are shown. For all chosen conditions, except the collagen SW culture incubated with 7 mM glucose, a clear segregation between 0 and 100 nM insulin could be observed. The metabolome of PHH incubated with 1 nM insulin showed an intermediate state between the ones incubated with 0 and 100 nM insulin, which was not clearly distinguishable.

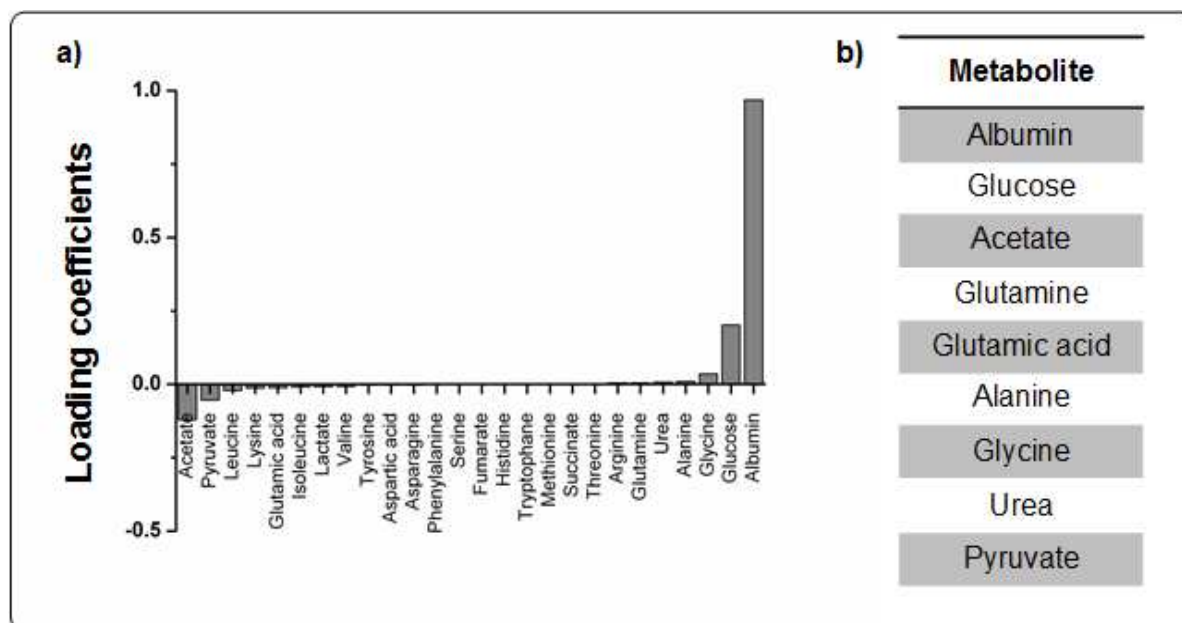


Figure 5-10 Metabolites with the greatest influence on segregation on the extracellular metabolome of primary human hepatocytes incubated with different insulin concentrations. (a) The loading coefficients of principle component 1 of PHH cultivated in collagen ML culture incubated with 7 mM glucose are depicted. (b) List of metabolites with the highest positive or negative loading coefficients in all four culture conditions (SW, ML, 7 and 25 mM).

According to the procedure applied to PMH, the loading coefficient of every analyzed metabolite was calculated. Metabolites with the highest positive or negative coefficients had the greatest influence on the segregation of the metabolic data. In Figure 5-10 (a) an example of the distribution of the loading coefficients of the first principal component of the different metabolites is shown for PHH cultivated in collagen ML culture with 7 mM glucose. Metabolites with the highest loading coefficients in all four used culture conditions, namely hepatocytes in ML culture incubated with 7 and 25 mM glucose, as well as SW culture with the same glucose concentrations are depicted in Figure 5-10 (b). Albumin had the highest loading coefficient in all culture conditions. Together with urea production it will be further discussed in Chapter 6 with other hepatic functions. Of all the available carbon sources, glucose had the highest coefficient in all culture conditions and therefore the greatest influence on the segregation in the PCA. As for PMH acetate, alanine, glutamic acid, glutamine, glycine and succinate were also the major factors which were influenced by insulin in PHH. Because of this overlap we focus on these metabolites and have a closer look at their metabolic profile over time.

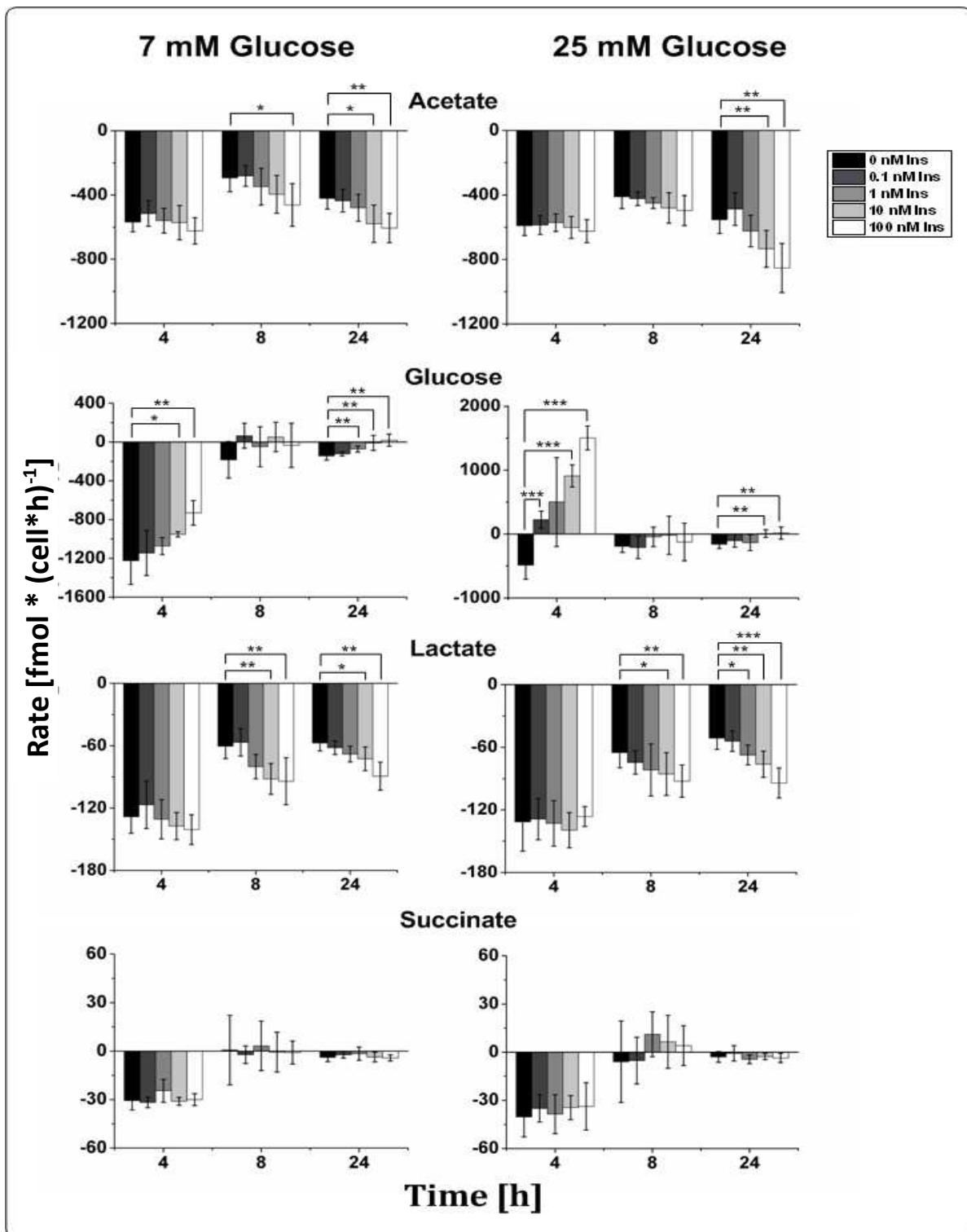


Figure 5-11 Conversion rates of glucose and selected organic acids of primary human hepatocytes cultivated in collagen monolayer culture under the influence of different insulin (0-100 nM) and glucose (7 and 25 mM) concentrations. Positive values indicate uptake, negative values production. Error bars indicate standard deviation (N=3; n=9). Statistical significance was determined with student's t-test. *, ** and *** indicate significance at $p=0.05$, $p=0.01$ and $p=0.001$, respectively. Living cell number was determined after 24 h of cultivation using calcein AM staining. Abbreviations: Ins Insulin.

Interestingly, lactate was not amongst the most influential metabolites in PHH. Since lactate production, however, is closely linked with glucose metabolism and can hint at glycolytic activity, lactate is included in the closer examination.

The consumption and production rates of glucose and selected organic acids of PHH cultivated in collagen ML culture are shown in Figure 5-11. Acetate was strongly produced independent of the glucose concentration with a more or less constant rate over time. Within the first 4 h of cultivation acetate production was also independent of the applied insulin concentrations. From 8 h on, however, the production of acetate was significantly increased with increasing insulin concentration. This effect was slightly stronger if 25 mM glucose were used. If the hepatocytes were exposed to fasting conditions, glucose was strongly produced with a maximum rate of about $1200 \text{ fmol} \cdot (\text{cell} \cdot \text{h})^{-1}$ within the first 4 h of cultivation if no insulin was added to the medium. Glucose production was decreased with increasing insulin concentration down to a rate of about $700 \text{ fmol} \cdot (\text{cell} \cdot \text{h})^{-1}$ with the highest used insulin concentration of 100 nM. Afterwards the production rate strongly decreased and oscillated around zero between 4 and 8 h of cultivation without a noticeable insulin influence. Within the last sampling period glucose was produced again in an insulin dependent manner, however with much lower rates compared to the initial production and was even consumed if the highest insulin concentration was applied. 25 mM extracellular glucose were used to simulate postprandial conditions. If no insulin was applied, which served as control, glucose was still produced even though the extracellular concentration already was high. If insulin was added to the medium, glucose was initially taken up by the cells in an insulin dependent manner with a maximum rate of $1500 \text{ fmol} \cdot (\text{cell} \cdot \text{h})^{-1}$ reached with the highest insulin concentration. As for fasting conditions the rate strongly ceased after the initial cultivation period with no noteworthy dependence on insulin. At the end of the cultivation period glucose was produced again with a very low rate at the three lowest insulin concentrations. With both glucose conditions lactate production was insulin independent during the first 4 h of cultivation. Then insulin significantly increased the production of lactate for the remaining cultivation period. Remarkable, however, was, that the extracellular glucose concentration had no influence on the amount of produced lactate. Succinate was produced by PHH in ML culture with a strongly decreasing rate after 4 h. Neither glucose nor insulin, however, showed a significant effect on the rates.

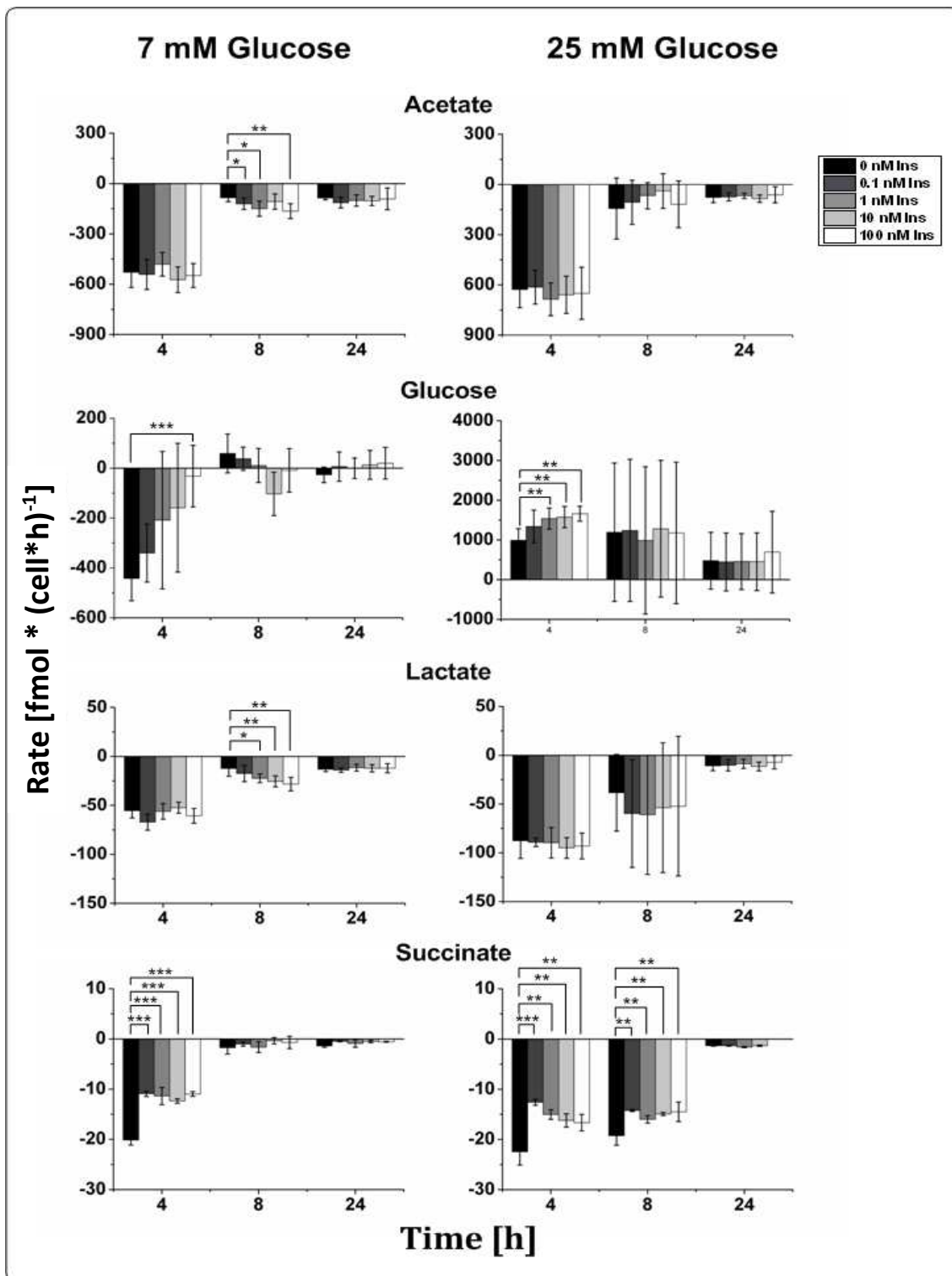


Figure 5-12 Conversion rates of glucose and selected organic acids of primary human hepatocytes cultivated in collagen sandwich culture under the influence of different insulin (0-100 nM) and glucose (7 and 25 mM) concentrations. Positive values indicate uptake, negative values production. Error bars indicate standard deviation (N=3; n=9). Statistical significance was determined with student's t-test. *, ** and *** indicate significance at $p=0.05$, $p=0.01$ and $p=0.001$, respectively. Living cell number was determined after 24 h of cultivation using calcein AM staining. Abbreviations: Ins Insulin.

The uptake and production rates of glucose and organic acids of PHH cultivated in collagen SW culture are depicted in Figure 5-12. Acetate was strongly produced within the first sampling period, whereas in contrast to the ML culture, the rate ceased afterwards. Only between 4 and 8 h of cultivation with 7 mM glucose, an insulin dependent increase of the production rate could be observed. Acetate production was additionally independent of the applied extracellular glucose concentration. As for the ML culture, glucose was strongly produced within the first 4 h if fasting conditions were applied. Insulin had a rate decreasing effect, which was only significant for the highest used insulin concentration, due to higher donor variation. For the remaining culture period rates were alike rates of the ML culture. 25 mM glucose led to a high uptake by PHH during the first sampling period, which was significantly increased by insulin. During the remaining cultivation period absolute rates of the different donors varied so much, that no statement could be made, except that the consumption rates in general seemed to decrease. Results for single donors are shown in Supplementary Figure 6. However, also here no clear trend could be observed except for the decreasing of the absolute rates. Interestingly, lactate production was about 40% higher in the SW culture if the extracellular glucose concentration was 25 mM. After 4 h an insulin dependent increase of the production rate could be observed, but only if the cells were incubated with 7 mM glucose. For the cells exposed to 25 mM glucose no such development could be observed due to high variation between the different donors. The rates in general decreased over time in both culture conditions in contrast to PHH cultivated in collagen ML culture. Succinate showed a significantly higher production rate with both glucose concentrations if no insulin was added to the culture medium. After 4 h or 8 h the rate however strongly decreased to remain around zero.

The uptake and production rates of the amino acids of PHH cultivated in collagen ML and SW culture determined as important features by PCA are depicted in Figure 5-13 (ML) and Figure 5-14 (SW). Although the consumption rates of amino acids in general were much lower in PHH compared to PMH, alanine and glutamine were the major carbon sources besides glucose. With both glucose concentrations, alanine was increasingly consumed in an insulin dependent manner during the first 4 h. After that the influence of insulin could only be observed during the last sampling period, although this was only significant for 25 mM glucose. The amount of extracellular glucose had no significant influence on the consumption rates. Glutamic acid was increasingly produced with higher insulin concentrations during the first 4 h of cultivation. After that the production rate strongly decreased and was not further influenced by insulin for the remaining cultivation period.

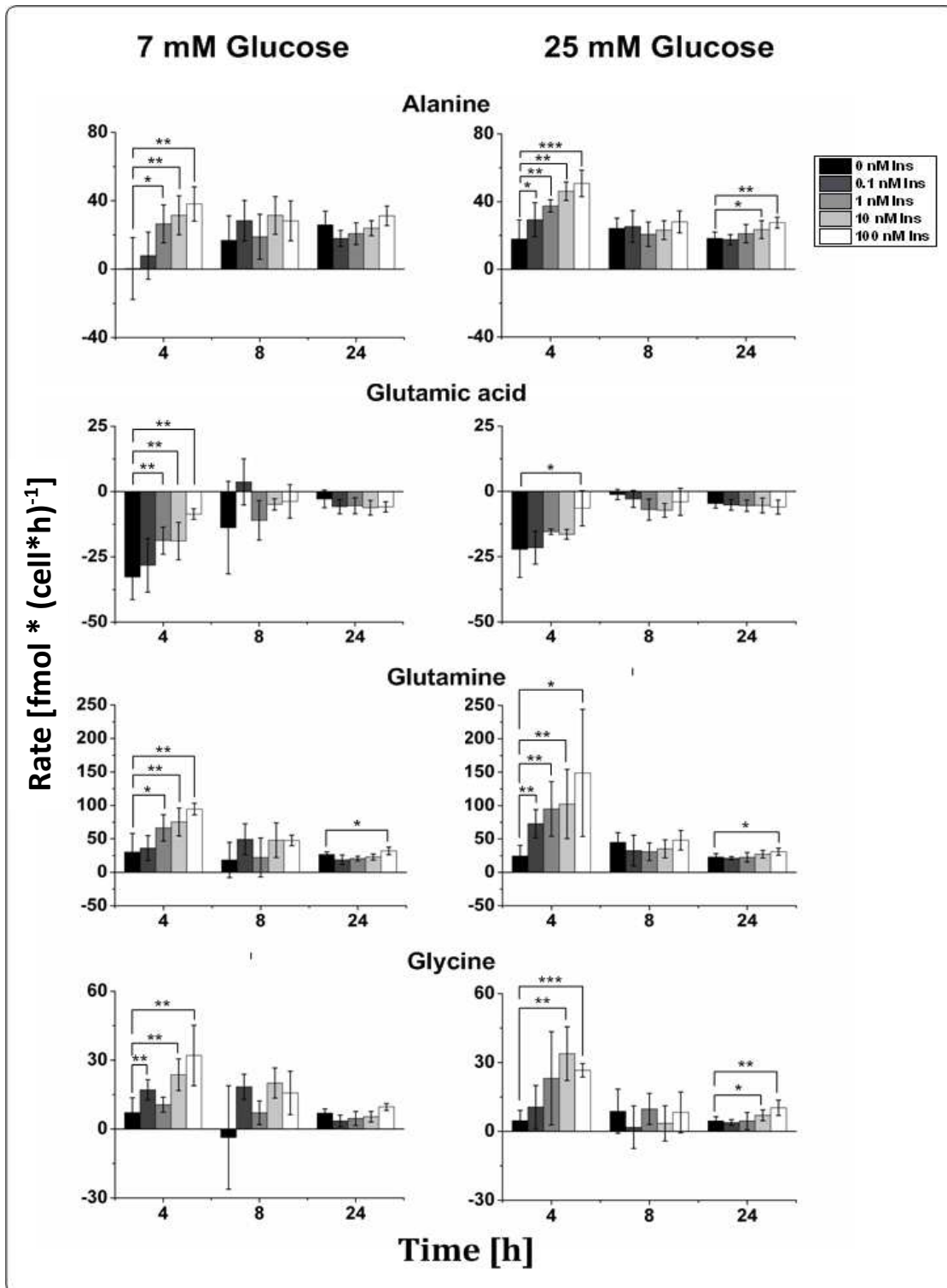


Figure 5-13 Conversion rates of selected amino acids (alanine, glutamic acid, glutamine and glycine) of primary human hepatocytes cultivated in collagen monolayer culture under the influence of different insulin (0-100 nM) and glucose (7 and 25 mM) concentrations. Positive values indicate uptake, negative values production. Error bars indicate standard deviation (N=3; n=9). Statistical significance was determined with student's t-test. *, ** and *** indicate significance at $p=0.05$, $p=0.01$ and $p=0.001$, respectively. Living cell number was determined after 24 h of cultivation using calcein AM staining. Abbreviations: Ins Insulin.

Glutamine was increasingly consumed by the cells in an insulin dependent manner particularly in the first 4 h, but clearly less in later phases. The rates slowly decreased over time and were not dependent on the glucose concentration administered. Glycine showed a comparable profile to glutamine. Primary human hepatocytes consumed glycine, which was increased if insulin was added to the medium. As for glutamine, the glycine uptake rate decreased slightly over time and the extracellular glucose concentration had no influence on the rates.

For alanine and glycine the metabolic profiles of primary human hepatocytes in collagen ML and SW culture resembled each other, even if the alanine consumption rates were slightly higher in the SW culture (Figure 5-14). Both amino acids were consumed and this consumption was increased by insulin. Even if this was not significant due to a high variability of absolute rates between the different donors, a trend could clearly be observed. The rates of single donors cultivated in ML culture for glycine are depicted in Supplementary Figure 8. The observed trend could be confirmed for Donor 1 and 2, whereas Donor 3 showed a somehow inconclusive picture at least if incubated with 25 mM glucose. The single donor results for PHH in SW culture are depicted in Supplementary Figure 10. Here, Donor 2 incubated with 25 mM glucose showed divergent results compared to all others. Glutamic acid showed a different behavior depending if 7 or 25 mM were applied in the culture. If fasting conditions were simulated, glutamic acid production was diminished by increasing insulin concentrations until the amino acid was even consumed. Within the first 4 h of cultivation glutamic acid production increased by added insulin if postprandial conditions were applied. During the last sample period this trend changed again. Glutamine was strongly consumed during the first 4 h of cultivation if the cells were incubated with 7 mM glucose with a rate up to $300 \text{ fmol} \cdot (\text{cell} \cdot \text{h})^{-1}$. Glutamine uptake was strongly increased by insulin. Afterwards the rate decreased to a minimum, with insulin having the exactly opposite effect. On the other hand, if the cells were incubated with 25 mM glucose, net glutamine uptake was almost zero at the beginning of cultivation. During the remaining cultivation time the standard deviation between different donors was so high, that no conclusion could be drawn. The rates for single donors cultivated in collagen ML culture are depicted in Supplementary Figure 7. As for glycine, a general increase of the glutamine consumption rate was observable, except for donor 3 cultivated with 25 mM glucose. Consumption rates of glutamine for single donors cultivated in SW culture are depicted in Figure 9. As for glycine, Donor 1 and 3 showed a very good overlap reflecting the increased uptake caused by insulin. The results for Donor 2 were inconclusive.

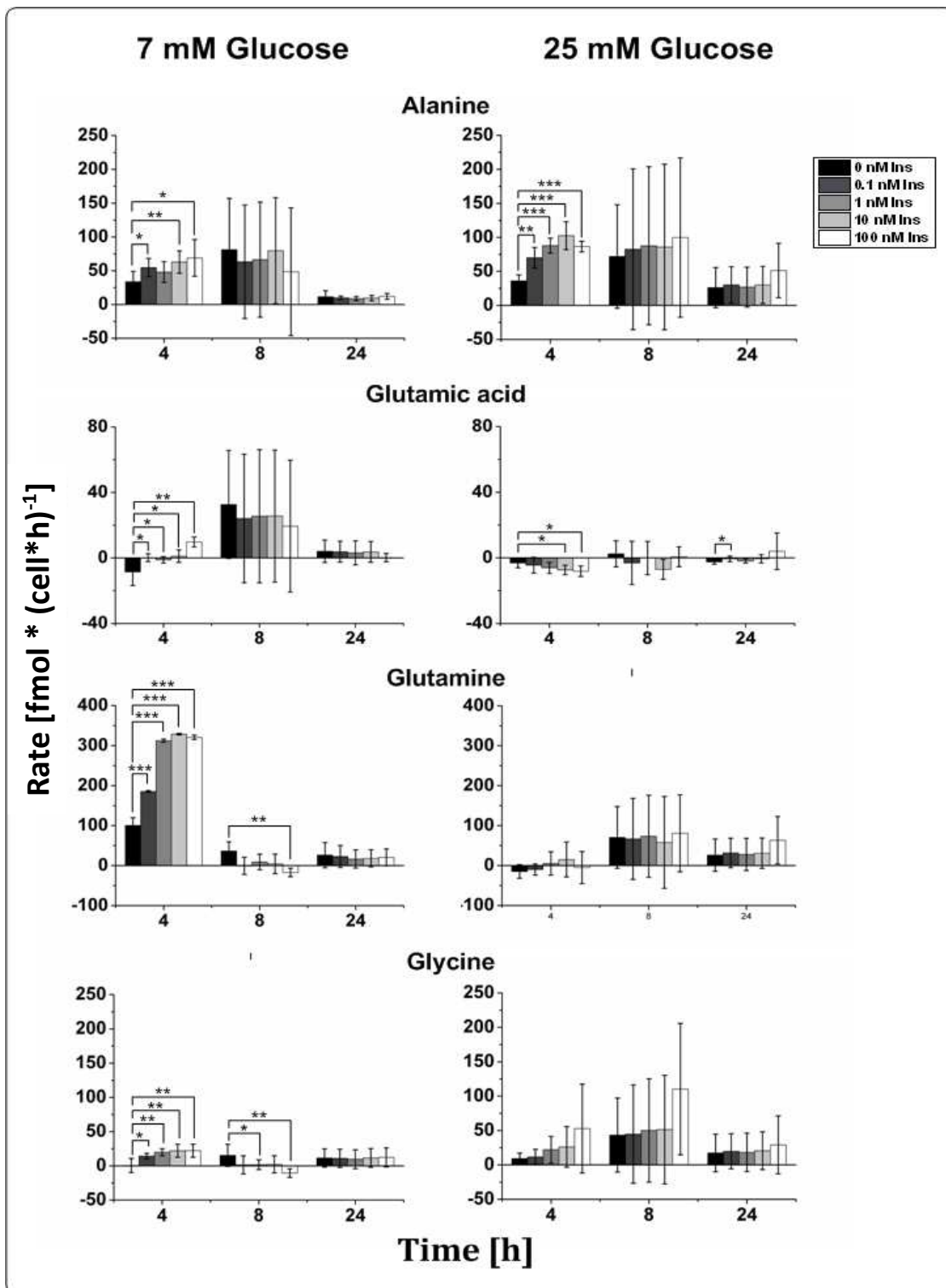


Figure 5-14 Conversion rates of selected amino acids (alanine, glutamic acid, glutamine and glycine) of primary human hepatocytes cultivated in collagen sandwich culture under the influence of different insulin (0-100 nM) and glucose (7 and 25 mM) concentrations. Positive values indicate uptake, negative values production. Error bars indicate standard deviation (N=3; n=9). Statistical significance was determined with student's t-test. *, ** and *** indicate significance at $p=0.05$, $p=0.01$ and $p=0.001$, respectively. Living cell number was determined after 24 h of cultivation using calcein AM staining. Abbreviations: Ins Insulin.

5.2.3 Carbon use of primary mouse and human hepatocytes

The metabolic profiles of PMH and PHH in collagen ML and SW culture were determined. Thereby, glucose consumption or production were strongly dependent on the administered insulin concentration as well as on the extracellular glucose concentration in the medium. If fasting conditions were applied, glucose was produced by both cell types in all culture conditions. Glucose was taken up, however, if postprandial conditions were simulated. The question arising from this was, where does the produced glucose come from? Does it derive from glycogenolysis or gluconeogenesis? On the other hand, what does happen to the high amounts of glucose taken up by the cells if 25 mM extracellular glucose were applied? Was it used to fill up glycogen stores or was it metabolized by the cells for their own metabolic needs? To answer these questions the cells were cultivated with U¹³C labeled glucose and glutamine. Glucose was chosen as a tracer to track possible metabolites resulting from glycolysis and TCA cycle. Glutamine was the major carbon source besides glucose almost in all culture conditions. As a potential carbon origin for gluconeogenesis, fully labeled glutamine was chosen as a tracer as well. Since the effects of increasing insulin on the metabolic rates were observed to be gradual and to keep the sample number at bay, only 0 and 100 nM insulin were tested, where the highest effects were expected.

Hepatocytes were seeded in collagen SW and ML culture as described above. After the cells were allowed to adapt to culture conditions and to refill glycogen stores, medium was changed to experimental conditions, namely to WME containing 7 or 25 mM fully labeled glucose or 2 mM U¹³C glutamine with either 0 or 100 nM insulin. Samples were taken at the same interval as described above and labeling of metabolites was determined using GC-MS.

5.2.3.1 Determination of background contamination from unlabeled glucose and glutamine

The collagen coating used not only serves as a mechanical support for the seeded hepatocytes but also is a reservoir for proteins and metabolites. Since the cells were seeded with medium which was not labeled, one has to expect that, although the cells were washed twice before adding the medium with labeled substrate, a certain amount of unlabeled glucose or glutamine will remain within the gel and falsify results. To quantify the background contamination, empty wells coated with collagen as ML or SW were treated in exactly the same way as during cultivation with cells. The results are depicted in Figure 5-15.

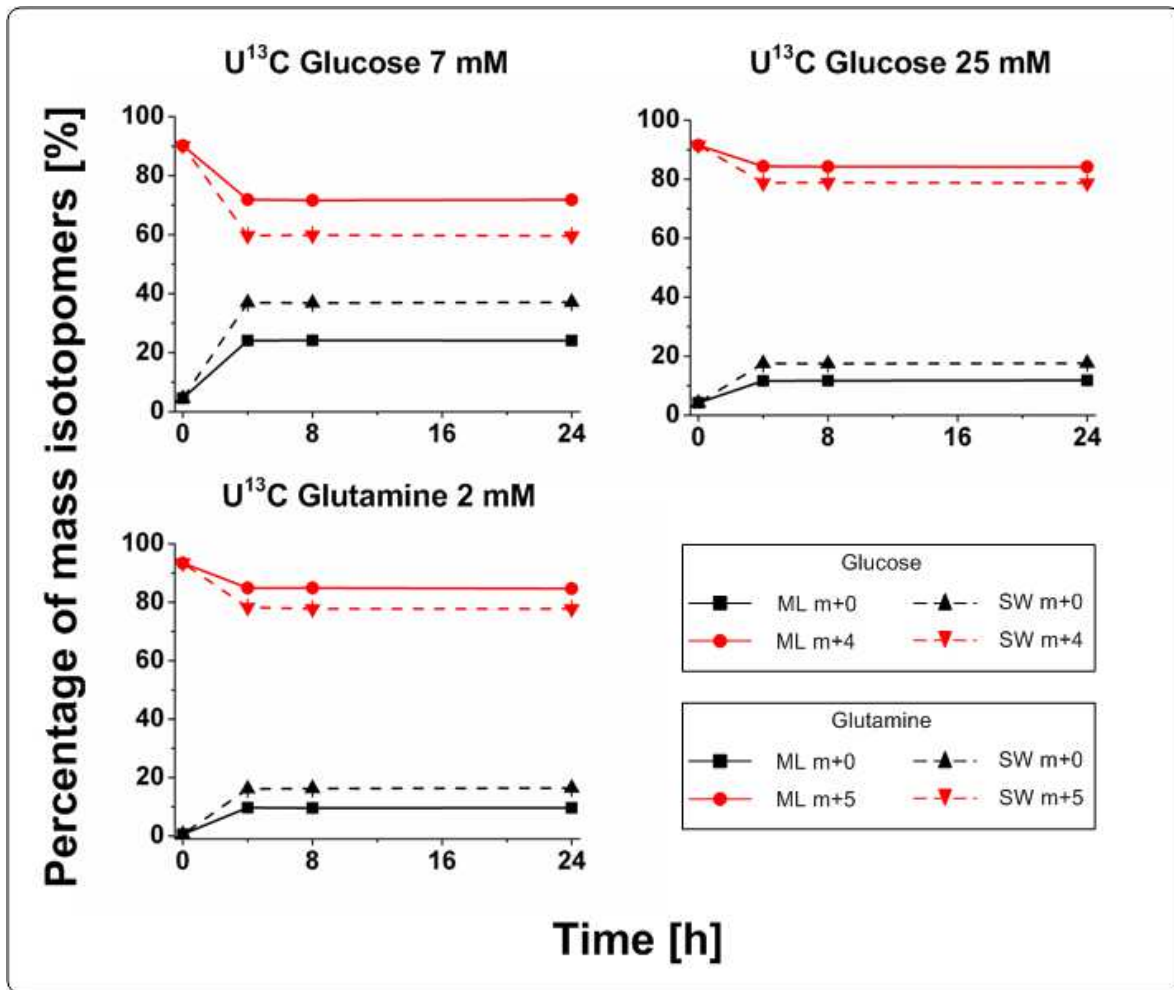


Figure 5-15 Background determination of substrate labeling. Shown are the percentages of fully ^{13}C labeled (red) and unlabeled (black) glucose and glutamine mass isotopomers in SW (dashed line) and ML (block line) culture with m+x pointing at the number of labeled carbons. Values were corrected for natural abundance of isotopes. Error bars indicate standard deviation (n=3).

For glucose instead of the fully labeled molecule (m+6) a fragment with four carbon atoms (m+4) was chosen due to higher stability. In addition, this fragment was also the most common and therefore easier to detect. The percentage of unlabeled substrate was strongly dependent on its concentration in the unlabeled medium and the concentration of the substrate under experimental conditions. The glucose concentration in standard WME, which was used for seeding and over-night cultivation of hepatocytes, was 11.1 mM. The concentration of glucose was then changed to 7 or 25 mM. If 7 mM were applied the falsification with unlabeled glucose was about twice as high as if 25 mM glucose was added. The concentration of glutamine was identical during seeding and in the experimental setup, namely 2 mM. Here a contamination of 10% unlabeled glutamine could be observed in ML culture. The percentage of unlabeled substrate in SW culture was about twice as high as in

the ML culture for all substrates. Within the first 4 h an equilibrium was established and the contamination with unlabeled substrate from the collagen reservoir was constant for the remaining cultivation period.

5.2.3.2 Metabolism of glucose by primary murine and human hepatocytes

The labeling results for glucose and lactate, if PHH were incubated with [U-¹³C]-glucose in ML culture, are depicted in Figure 5-16. Figure 5-17 shows the same for PMH.

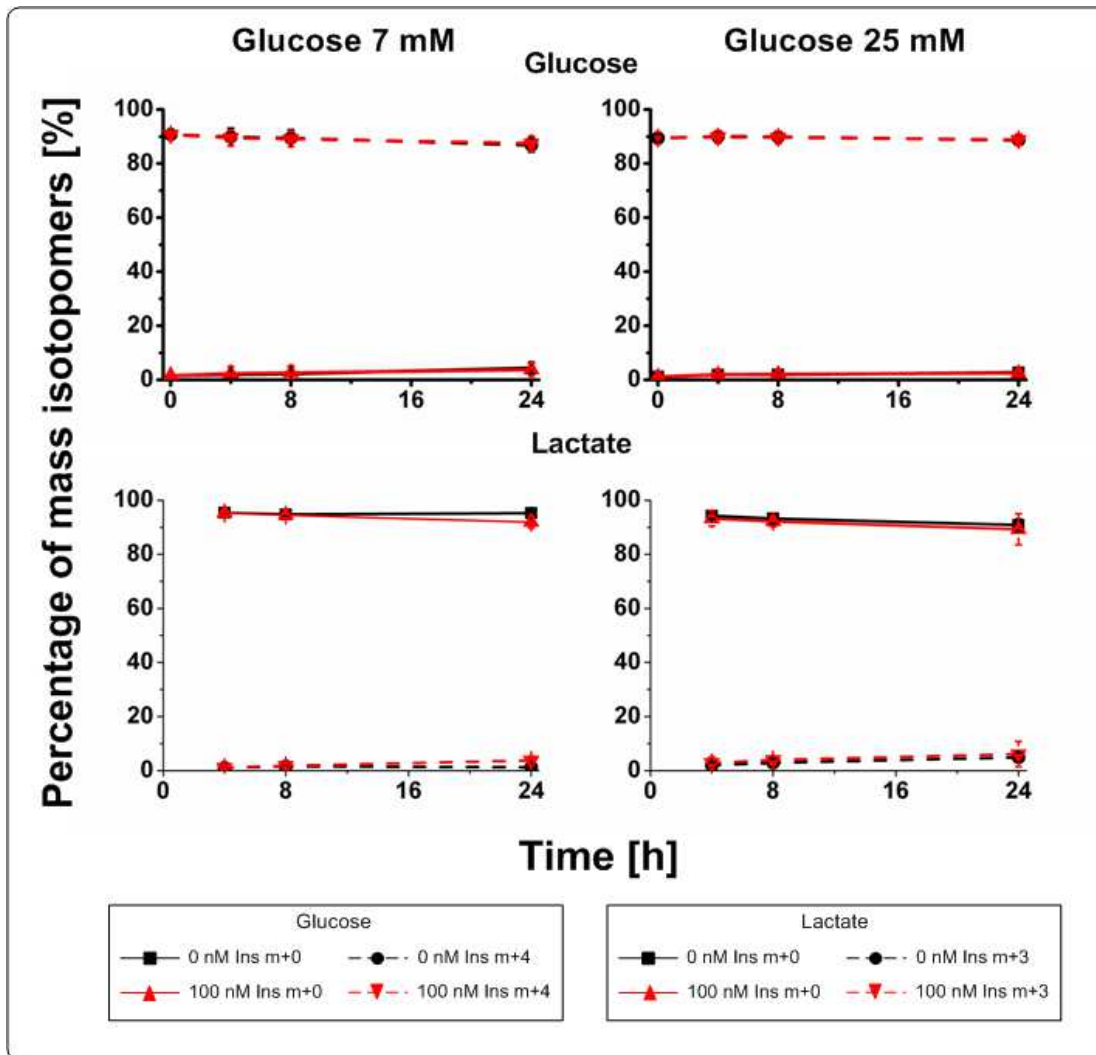


Figure 5-16 Percentages of unlabeled and fully labeled glucose and lactate of PHH cultivated in collagen ML culture with [U-¹³C₆] glucose. Shown are the percentages of fully labeled (dashed line) and unlabeled (block line) glucose and lactate mass isotopomers if 0 nM insulin (black) or 100 nM insulin (red) were used with m+x pointing to the number of labeled carbons. Error bars indicate standard deviation (N=2; n=6). Glucose values were corrected for background contamination. Abbreviations: Ins Insulin.

If PHH were exposed to fasting conditions a slight production of unlabeled glucose could be observed over time. This was not the case if the medium contained 25 mM glucose. Labeled lactate was only produced in negligible amounts.

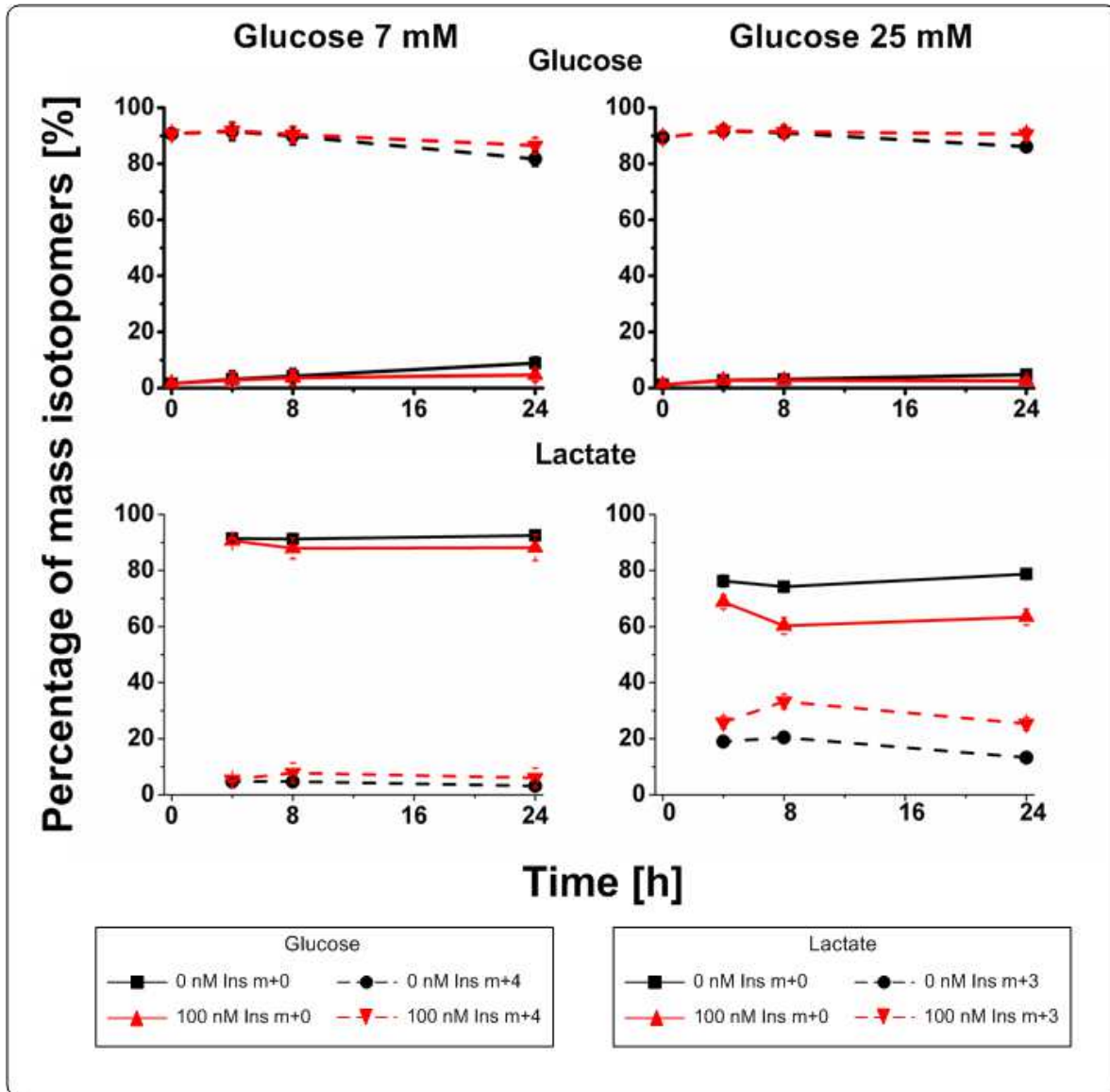


Figure 5-17 Percentages of unlabeled and fully labeled glucose and lactate of PMH cultivated in collagen ML culture with $[U-^{13}C_6]$ glucose. Shown are the percentages of fully labeled (dashed line) and unlabeled (block line) glucose and lactate mass isotopomers if 0 nM insulin (black) or 100 nM insulin (red) were used with m+x pointing to the number of labeled carbons. Error bars indicate standard deviation (N=2; n=6). Glucose values were corrected for background contamination. Abbreviations: Ins Insulin.

For human hepatocytes almost no difference could be found in glucose use if cells were incubated with or without insulin. Only a slightly higher production of lactate from glucose was observed if cells were incubated with 7 mM glucose. PMH on the other hand produced

more unlabeled glucose over time if incubated with 7 mM glucose. Production of glucose $m+0$ was considerably less when 100 nM insulin were applied. The same effect could be observed if the cells were incubated with 25 mM, where no more unlabeled glucose was produced if 100 nM insulin were added to the medium. No labeled lactate was produced by PMH if incubated under fasting conditions with no insulin administered. This can directly be read from Figure 5-17, since glucose was the only labeled substrate available. Figure 5-18 shows the fractions of selected amino acids (alanine, glutamine and glycine) which were produced from labeled glucose by PMH in collagen ML culture. Alanine was produced from glucose for the first 8 h of cultivation if the cells were incubated with 7 mM glucose and no insulin. If insulin was added to the medium the percentage of produced alanine more than doubled and was constant over the whole cultivation period. 25 mM glucose still enhanced this effect. Glycine with the mass $m+1$ was constantly produced by PMH over the whole cultivation time. Up to 60% of glycine were labeled after 24 h of cultivation under fasting conditions. If insulin was added, the production of labeled glycine was even enhanced up to 85%. If no insulin was added, postprandial conditions had the same effect on glycine production. With insulin the enhancing effect however was still stronger with about 95% of glycine produced from glucose. For glutamine the fraction of $m+4$ is depicted since in this fraction an enrichment took place. Fully labeled glutamine ($m+5$) was not formed from glucose. No glutamine was produced from glucose if no insulin was added to the medium independent of the applied glucose concentration. If insulin was added, however, a slight increase in glutamine originating from glucose could be found under fasting conditions. 25 mM glucose increased this percentage to about 10%. The labeling profiles of amino acids derived from PHH cultivated in ML with fully labeled glucose were determined as well. However, no labeling changes could be detected in any amino acid, even if insulin was added to the medium. PHH and PMH cultivated in collagen SW culture closely resembled the carbon usage profiles of the ML cultures.

The addition of insulin to the medium made for a slight increase in lactate production from glucose, although glucose showed a net production under fasting conditions, which is possible due to reversibility of glucose uptake from the medium and release from the cytosol (compare to Figure 5-4 and Figure 5-5). This effect was a lot stronger if the cells were incubated with 25 mM glucose. PMH produced about 20% of lactate from glucose within the first 8 h of cultivation, which was enhanced to 40% if insulin was added.

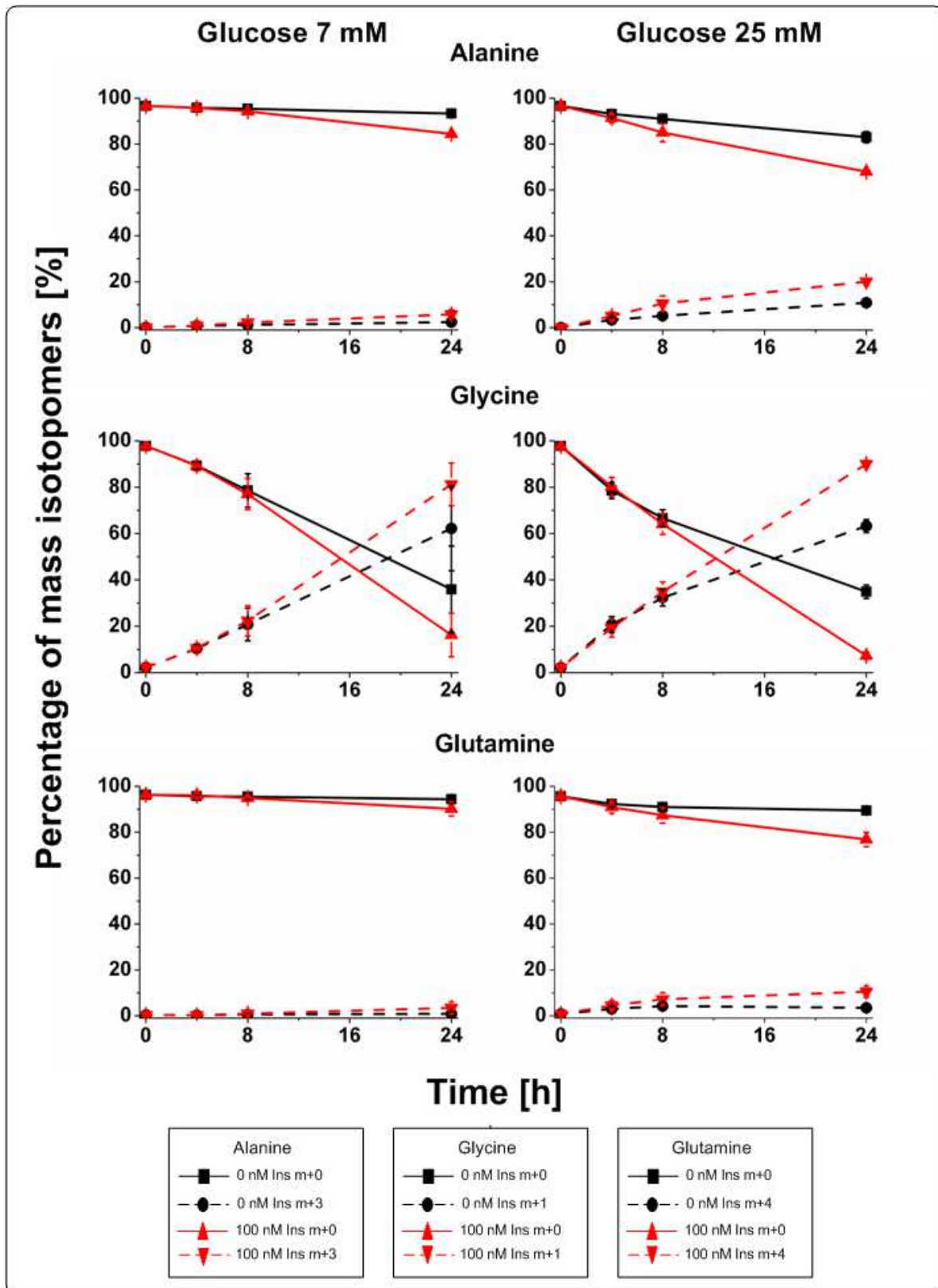


Figure 5-18 Percentages of unlabeled and labeled alanine, glycine and glutamine of PMH cultivated in collagen ML culture with [U-¹³C₆] glucose. Shown are the percentages of labeled (dashed line) and unlabeled (block line) alanine, glycine and glutamine mass isotopomers if 0 nM insulin (black) or 100 nM insulin (red) were used with m+x pointing to the number of labeled carbons. Error bars indicate standard deviation (N=2; n=6). Abbreviations: Ins Insulin.

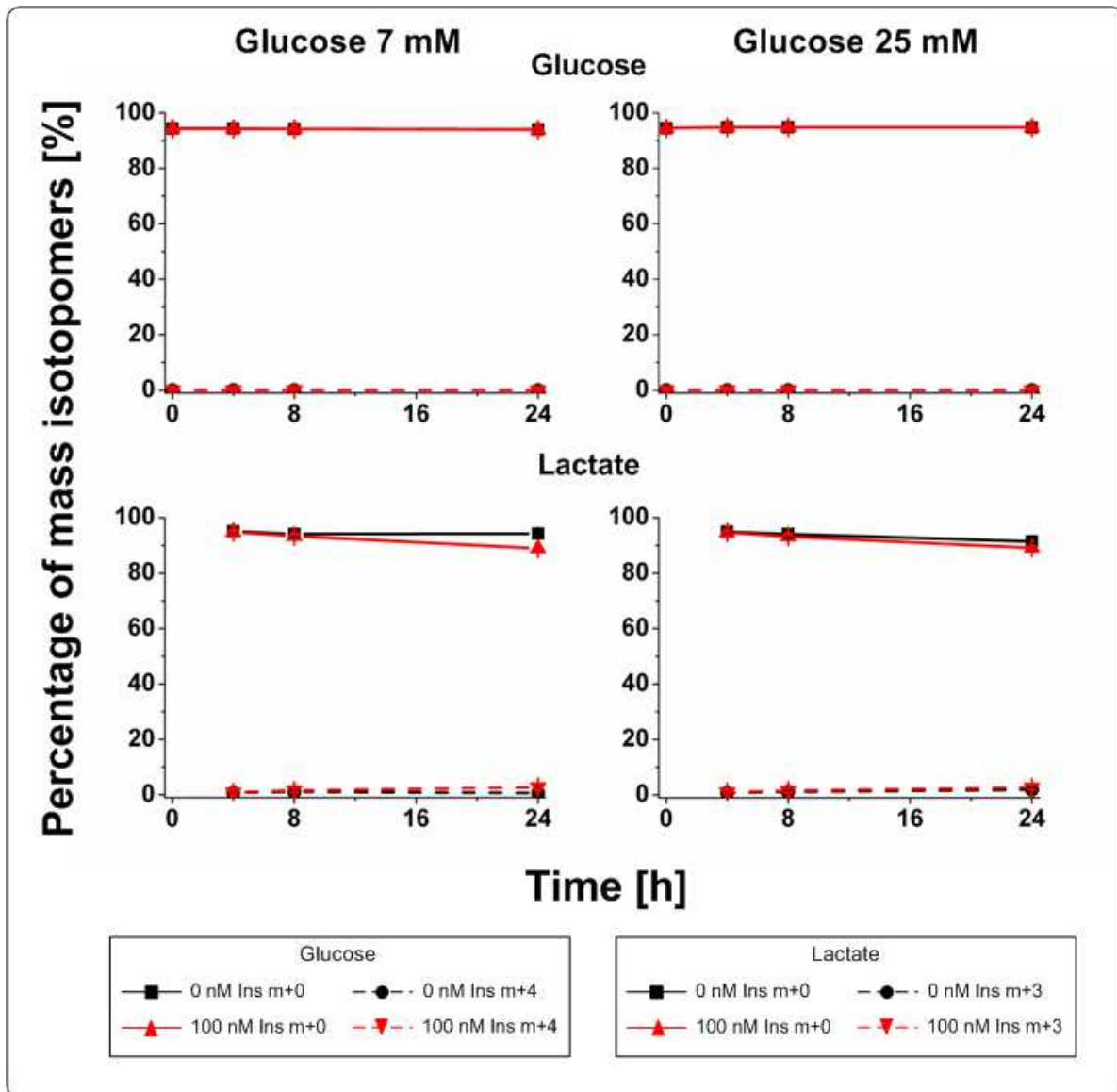


Figure 5-19 Percentages of unlabeled and fully labeled glucose and lactate of PHH cultivated in collagen ML culture with [U-¹³C₅] glutamine. Shown are the percentages of fully labeled (dashed line) and unlabeled (block line) glucose and lactate mass isotopomers if 0 nM insulin (black) or 100 nM insulin (red) were used with m+x pointing to the number of labeled carbons. Error bars indicate standard deviation (N=2; n=6). Abbreviations: Ins Insulin.

5.2.3.3 Metabolism of glutamine by primary murine and human hepatocytes

Primary human and mouse hepatocytes were not only cultivated with [U¹³C]-glucose but also with [U-¹³C₅]-glutamine. The amino acid represents the major carbon source besides glucose and therefore a potential source for gluconeogenesis. In Figure 5-19 the labeling patterns of glucose and lactate are depicted for PHH cultivated in collagen ML.

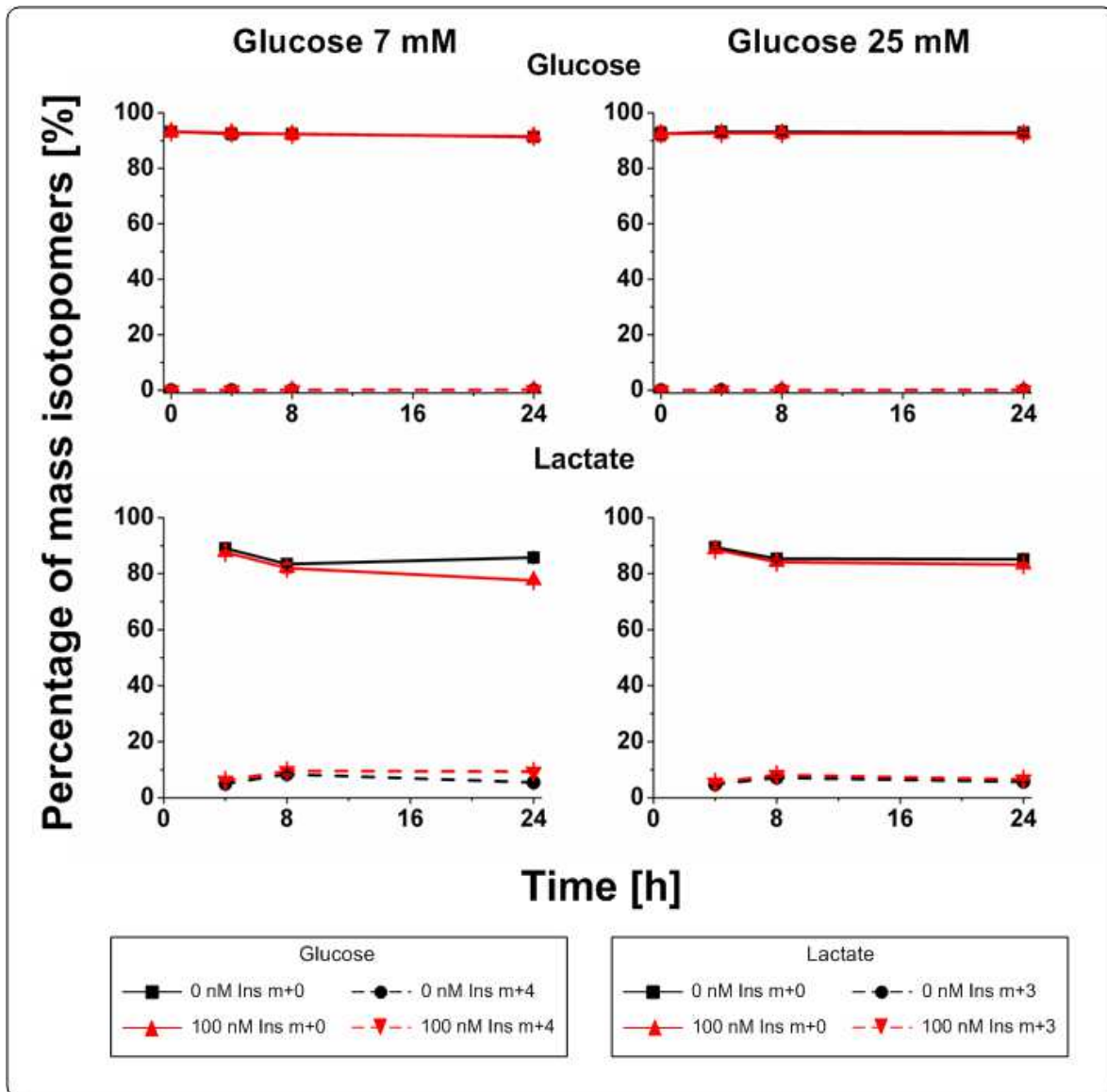


Figure 5-20 Percentages of unlabeled and fully labeled glucose and lactate of PMH cultivated in collagen ML culture with [U-¹³C₅] glutamine. Shown are the percentages of fully labeled (dashed line) and unlabeled (block line) glucose and lactate mass isotopomers if 0 nM insulin (black) or 100 nM insulin (red) were used with m+x pointing to the number of labeled carbons. Error bars indicate standard deviation (N=2; n=6). Abbreviations: Ins Insulin.

If glutamine was used as carbon source and gluconeogenesis was active, labeling should be found in glucose. However, this was not the case. No matter if the cells were incubated with 7 or 25 mM no labeling in glucose could be found. Insulin had an increasing effect on lactate production from glutamine, especially if the cells were incubated with 7 mM glucose.

PMH showed a similar pattern (Figure 5-20). No labeling of glucose could be detected independent of the used glucose concentration. Lactate production from glutamine was about two times higher in PMH if incubated with 7 mM glucose within the first 8 h of

cultivation. After that, lactate was only further produced if insulin was added to the media. Murine hepatocytes incubated with 25 mM glucose produced lactate originating from glutamine only within the first 8 h of incubation. Under postprandial conditions insulin showed no increasing effect.

Alanine was not only produced by PMH from glucose but also from glutamine (Figure 5-21). As for glucose alanine production from glutamine was increased if PMH were incubated under fasting conditions with 100 nM insulin. This was not the case if the cells were incubated with 25 mM glucose. The same could be observed for glycine which was as well produced from both carbon sources, but exclusively mass isotopomer m+1. If PMH were incubated with [U-¹³C] glutamine and 7 mM glucose, the effect of insulin on glycine production was stronger compared to postprandial conditions where the increasing effect was still there but not as pronounced. The percentage of labeled glutamine however constantly decreased over time independently of the extracellular glucose concentration. This was still enhanced if insulin was present in the medium. There was no difference in the carbon usage if the PMH were cultivated in collagen SW culture.

PHH were cultivated with fully labeled glutamine in collagen SW and ML culture as well. In both cultivation conditions alanine was not produced from glutamine independent of the used glucose or insulin concentration. Glycine with the mass m+1 was produced over time with a percentage of 10% after 24 h in SW and in ML culture (Supplementary Figure 12). However, in contrast to PMH neither insulin nor glucose had an influence on the produced amount.

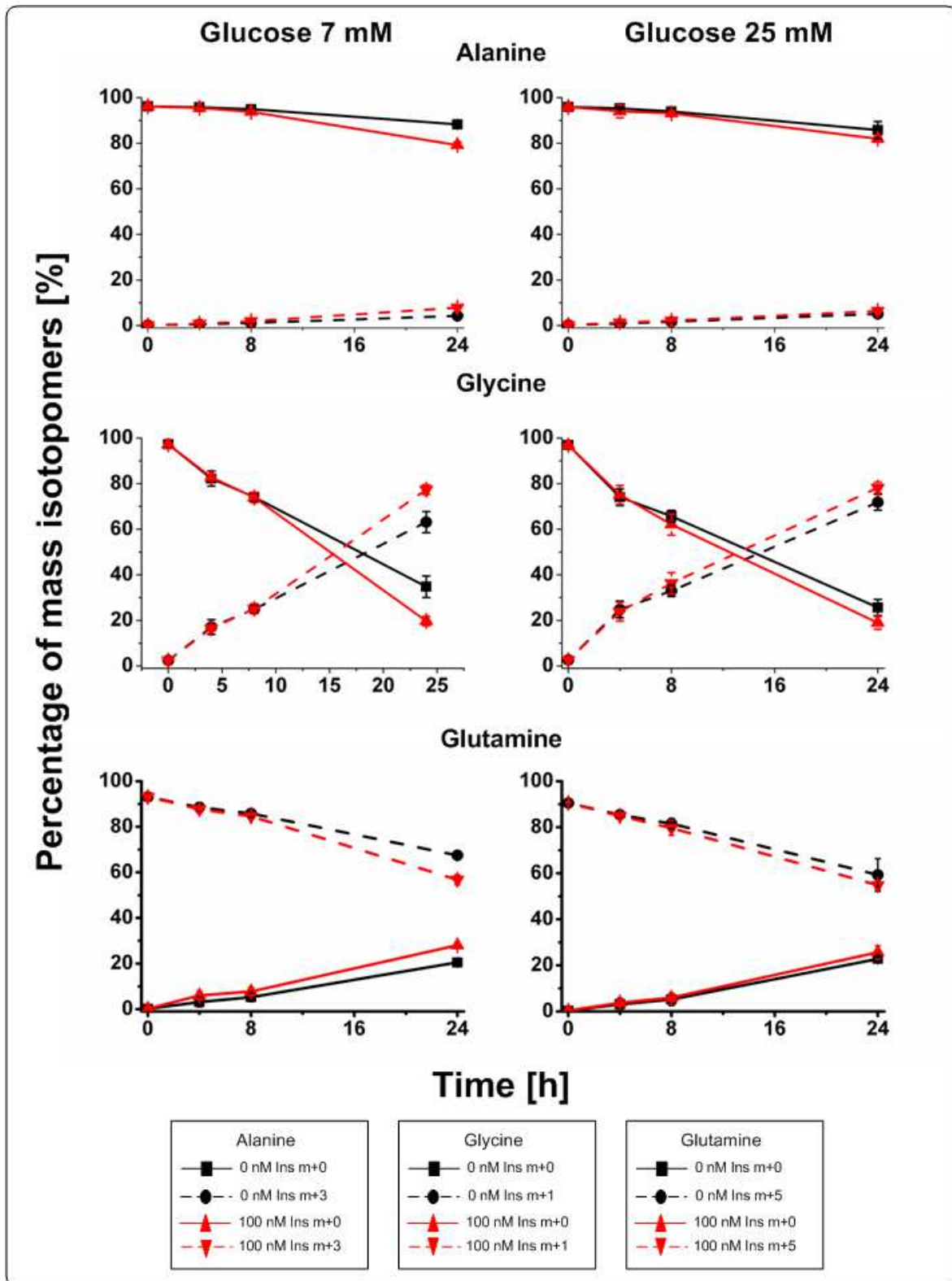


Figure 5-21 Percentages of unlabeled and labeled alanine, glycine and glutamine of PMH cultivated in collagen ML culture with [U-¹³C₅] glutamine. Shown are the percentages of labeled (dashed line) and unlabeled (block line) alanine, glycine and glutamine mass isotopomers if 0 nM insulin (black) or 100 nM insulin (red) were used with m+x pointing to the number of labeled carbons. Error bars indicate standard deviation (N=2; n=6). Values for glutamine were corrected for background contamination. Abbreviations: Ins Insulin.

5.3 Discussion

To characterize the metabolic influence of insulin and glucose on PMH and PHH, the cells were cultivated in collagen ML and SW culture with different insulin and glucose concentrations. The chosen glucose concentrations were 7 and 25 mM whereas the insulin concentrations were in the range of 0.1-100 nM. The blood glucose level normally lies within the narrow range of 4-6 mM in humans and 7-9 mM in mice and it is one of the liver's major tasks to keep the glucose concentration in this range after a meal or during fasting (Kowalski and Bruce 2014). However, the glucose concentrations applied *in vitro* in specialized hepatocyte media as WME (11 mM) or high glucose Dulbecco's modified Eagle Medium (25 mM) are much higher than typically found *in vivo* (Ananthanarayanan et al. 2011). Therefore, we chose 7 mM glucose as lower and 25 mM as higher glucose concentration compared to standard cultivation methods. Basal blood insulin levels in humans are around 0.11 nM, whereas in mice basal levels are significantly higher with 0.2-0.3 nM (Cherrington 1999, Kowalski and Bruce 2014). The experimental insulin concentrations cover the basal insulin levels found *in vivo* and higher concentrations to simulate postprandial conditions. The cells were cultivated only for 24 h to avoid metabolic changes induced by dedifferentiation. The extracellular metabolome was then determined using HPLC and GC-MS and uptake and production rates were calculated.

With the metabolic rates determined for glucose, organic acids, proteinogenic amino acids, urea and albumin a PCA was performed (Figure 5-2 and Figure 5-9). A clear separation between the metabolic sets for 0 and 100 nM insulin could be achieved for almost all culture conditions, whereas 1 nM insulin showed an intermediate state in all conditions. Insulin, therefore, has a significant influence on the metabolome of primary hepatocytes, which was then examined in more detail. The metabolites which were most involved in segregation of the metabolome profiles were more or less identical in humans and mice, namely glucose, acetate, glutamine, glutamic acid, alanine, albumin and urea (Figure 5-3, Figure 5-10). Additionally, pyruvate, lactate, succinate and glycine played a major role either in mice or humans. The metabolic profiles of these were closer examined except for albumin and urea, which will be discussed in detail in Chapter 6.

If fasting conditions were simulated, namely the incubation of hepatocytes with 7 mM glucose and no or low insulin levels, PHH and PMH showed a strong net production of glucose within the first 4 h of cultivation (Figure 5-4, 5-5, 5-11, 5-12). Increasing insulin concentration had a significant rate decreasing effect and even led to net glucose

consumption in PMH cultivated in ML culture. This finding is in accordance with the *in vivo* reaction of hepatocytes to increasing insulin plasma levels. Insulin thereby has an inhibitory effect on gluconeogenesis. At the same time it leads to translocation of the insulin dependent GLUT4 glucose transporters to the plasma membrane and increases glycogen synthesis (Saltiel and Kahn 2001, Lu et al. 2012). Glycogenolysis seems to be the origin of the produced glucose, since no labeling was found in glucose if the cells were incubated with [U¹³C]-glutamine (Figure 5-19, Figure 5-20). However, also alanine and lactate have to be considered as possible substrates for gluconeogenesis. In Chinese hamster ovary (CHO) cells a certain gluconeogenic activity could be proven by newly synthesized glycine from [U¹³C]-glutamine (Nicolae et al. 2015). Glutamine enters the TCA cycle *via* glutamate and is metabolized to oxaloacetate, which can enter gluconeogenesis. 3-phosphoglycerate, an intermediate of glycolysis and gluconeogenesis then serves as a precursor for serine and glycine production (Wang et al. 2013). A reason for this gluconeogenic activity might be seen in the generally stronger dependence of mice on gluconeogenesis compared to humans. Mice usually show a rapid depletion of liver glycogen stores, which are also lower compared to humans (100-200 compared to 250-300 μmol/g wet weight) (Kowalski and Bruce 2014). However, although gluconeogenesis is at least partly active in mice, glucose resulting from the pathway is not released into the culture medium to cope with the low extracellular glucose concentration. This can be taken as a sign that neither in mice nor humans the glycogen stores are completely emptied after the first 4 h of incubation. Although hepatocytes of both origins show a net production of glucose, lactate is still produced (Figure 5-4, 5-5, 11, 5-12). Thereby, the lactate production rates within the first 4 h of cultivation in PMH were about 4 times higher compared to PHH. Metabolization of glucose *via* glycolysis represents a minor source for lactate production, since almost no labeling could be found in lactate if the cells were incubated with fully labeled glucose (Figure 5-16, Figure 5-17). Only if 100 nM insulin were used, labeling could be detected at all. Alanine and pyruvate are other possible sources for lactate production. In PMH pyruvate can make up for about 10% of lactate production, whereas in PHH this share is much bigger with 50-100% (compare consumption rates of pyruvate depicted in Supplementary Table 3 to 10). In PMH amino acid metabolism therefore seems to play a more important role than in PHH. The influence of insulin on lactate production is delayed in time compared to the uptake or production of glucose, where insulin directly shows a decrease of glucose production. After 8 h increasing insulin concentration leads to a doubling of lactate production in PMH (Figure 5-4, Figure 5-5). In PHH lactate production was increased to 1.5 times the initial rate

in the ML culture and 3-fold in the SW culture (Figure 5-11, Figure 5-12). This increase might result partly from decreased net glucose production and from increased amino acid consumption, which will be discussed later in detail. The overall rates were significantly higher in hepatocytes from both origins, if the cells were incubated in ML culture. However, in PHH this effect was much more pronounced with rates three times as high compared to SW culture (Figure 5-11, Figure 5-12). If this was the case for all metabolites one could assume that the second layer of collagen is hindering or delaying insulin action. However, this was not the case. A possible explanation could be that the cultivation condition has an influence on glucose sensitivity of the hepatocytes.

To simulate postprandial condition, the hepatocytes were incubated with 25 mM glucose. Hepatocytes of both origins and in both culture conditions took up glucose in large amounts (Figure 5-4, 5-5, 5-11, 5-12). This was strongly enhanced with increasing insulin concentrations of up to 4 times the initial rate in the ML cultures, whereas in the SW cultures the rate increase was only about 50%. The uptake rate of glucose of PMH in ML culture was only about 60% of the uptake rate of PMH cultivated in the SW system if incubated without insulin. However, if insulin was added to the medium the enhancing effect of the hormone was significantly higher in the ML culture compared to the SW culture. This could also be observed for PHH, where in ML culture glucose was even produced if the cells were incubated without insulin. This also hints at a differentiated glucose sensitivity in the two culture conditions, as observed with 7 mM glucose. If glucose is taken up into the cells, it can mainly enter two pathways: glycogen synthesis or glycolysis (Klover and Mooney 2004). Regarding the use of the glucose taken up there are distinct differences between primary human and primary mouse hepatocytes. For PHH no labeling in any metabolite could be found, except for a small fraction in lactate (Figure 5-16). This indicates that almost the whole glucose taken up by the cells is used to fill glycogen stores. In PMH a small fraction of labeled glucose was found in intermediates or endproducts of glycolysis or TCA cycle as in lactate, alanine, glycine and glutamine (Figure 5-17, Figure 5-18). This is a sign that the respective pathways are active in hepatocytes of murine origin in both culture conditions and that glucose is used as a carbon source. The activity of these pathways is thereby also strongly dependent on the applied insulin concentration. The hormone significantly increased the fractions of labeled metabolites resulting from glucose metabolism in accordance with a strongly increased uptake of glucose. The overall amount of produced lactate was also about twice as high if postprandial conditions were applied in PMH compared to fasting conditions (Figure 5-4, Figure 5-5). This was not the case for

PHH. Insulin had no enhancing effect on glycolytic glucose use, which is evident from the lacking incorporation of labeling into intermediates of the central carbon metabolism.

It was remarkable that especially the uptake or secretion of glucose showed its highest rates during the first 4 h of cultivation (Figure 5-4, 5-5, 5-11, 5-12). Afterwards, the rates in all conditions strongly decreased and then settled down around zero. It seems that at extracellular glucose concentrations between 8.4 ± 1.1 and 17.8 ± 1.76 mM, hepatocytes no longer showed a net production or consumption of glucose. This effect has already been observed earlier (Figure 3-3). Thereby, the range found *in vitro* seemed to be slightly shifted to higher glucose levels and to be much wider compared to the close range found *in vivo*. In humans the blood glucose levels are between 3 and 9 mM including phases after a meal, but are usually kept within the narrow range of 5.5 to 6 mM (Nutall et al. 2008, König et al. 2012, Lu et al. 2012). As discussed before, this again might be a hint that hepatocytes *in vitro* show a decreased glucose sensitivity compared to *in vivo* conditions. A reason for this can be seen in the simplified cultivation setup, in which the complex environment, in which glucose regulation usually takes place, is not given. *In vivo* glucose homeostasis is not only dependent on blood glucose and insulin levels, but also signals from the sympathetic system as well as concentrations of other metabolites, e.g. free fatty acids, and hormones, such as glucagon or growth hormones, play a role in the regulation, as well as the formation of gradients along the acinus (Jungermann and Kietzmann 1996, Roden and Bernroider 2003). The accumulation of toxic waste products can be avoided and a metabolic steady state can be reached by continuous cultivation. Thereby the culture medium is constantly diluted by fresh medium and „spent“ medium is removed at the same rate (Europa et al. 2000). This can be further improved by perfused systems, which also allow the formation of nutritional and hormonal gradients as found *in vivo* (Bhatia and Ingber 2014). However, in an *in vitro* cultivation system simplification and focusing on certain aspects is always necessary and inevitable. This explains why not the complete spectrum of hepatic regulation and zonation can be analyzed by the setup used in this approach.

Succinate, an intermediate of the TCA cycle, was produced in all culture conditions by hepatocytes of both origins (Figure 5-4, 5-5, 5-11, 5-12). The secretion of this metabolite could hint at a stress response leading to an overflow of the TCA cycle. In all cases insulin had a decreasing effect on the secretion of succinate. It is widely discussed in the literature that the presence of insulin in the culture media is important for hepatic functionality and cultivation of cells in general (Chan et al. 2003, Johnson et al. 2006). Therefore, it can be

reasoned that insulin not only has direct metabolic consequences regarding glucose metabolism, but also acts as a reducer of cellular stress. Stress for the hepatocytes in this condition is created by the medium change at the beginning of the experiment, leading to a sudden concentration change and over-availability of extracellular metabolites. Wellen and Thompson have discussed how this can lead to a general metabolic stress response in cells (Wellen and Thompson 2010). Another reason for a stressed hepatocyte phenotype might be the complete absence of insulin in the “control” condition, which also showed the highest secretion of succinate. *In vivo*, even under fasting condition, still a basal level of the hormone is sustained which lies in humans between 30 and 60 pM insulin (Zierler 1999). The combination of these two factors can explain the stress response, which is amongst others characterized by the decoupled TCA cycle during cultivation, and why insulin can, at least to some extent, decrease it.

Alanine and glutamine were strongly taken up by the cells in both culture conditions and represented the major carbon sources of the cells except for glucose (Figure 5-6, 5-7, 5-13, 5-14). Although glutamine showed a constant net uptake in all culture conditions, it could be shown that it was at the same time synthesized in PMH under both, fasting and postprandial conditions, which was still increased if insulin was present. This could be proved by the constant decrease of the labeled fraction when [U-¹³C]-glutamine was used as a tracer (Figure 5-21). If 25 mM glucose were used for cultivation even glucose served as a precursor for glutamine synthesis (Figure 5-18). Nicolae et al. could show as well that the glutamine synthesis pathway was active in CHO-K1 cells even at high glutamine consumption rates (Nicolae et al. 2014). The synthesis of glutamine from glucose as a precursor also indicates that not only glycolysis but also the TCA cycle must be an active pathway in PMH. In PHH no labeling from glucose could be found in glutamine. However, a small increase of 3% in the non-labeled fraction could be found if [U-¹³C]-glutamine was used as a tracer (Supplementary Figure 11). This does not directly hint at an active TCA cycle in PHH using other carbon sources as pyruvate, since the increase in the non-labeled fraction of glutamine could also result from a direct interconversion of glutamate and glutamine *via* glutamine synthase or glutamate dehydrogenase. It should also not be forgotten, that extracellular glutaminolysis and thereby the conversion to glutamate slightly falsifies the absolute uptake rates, which were determined. In 24 h 0.84 μM unlabeled glutamine were produced. Niklas et al. computed the rate constant k_G for glutamine/glutamate hydrolysis to be 0.00198 h^{-1} (Niklas et al. 2011). If calculated, 0.32 μM unlabeled glutamine are produced from glutamate hydrolysis accounting for 37% of the unlabeled fraction. Therefore, the remaining

63% have to result from actual production of the cells. In the special case of hepatocytes one always has to keep in mind that *in vivo* the detoxification of ammonia takes place *via* two distinct pathways, namely the urea cycle and the synthesis of glutamine. Thereby, detoxification *via* the synthesis of glutamine *in vivo* plays a minor role compared to urea synthesis since only about two layers of hepatocytes around the central vein of each liver lobule are glutamine synthetase positive (Gebhardt 1992). However, one has to keep in mind that after isolation a mixture of periportal and perivenous hepatocytes is obtained. It is not completely understood, how or if periportal or perivenous phenotype is sustained *in vitro* under conventional culture conditions, since the gradients of certain factors, as pO₂, nutrients or hormones, along the acinus are no longer given (Kietzmann et al. 1999, Jungermann and Kietzmann 2000, Allen et al. 2005). Therefore, the exact contribution of hepatocytes with perivenous phenotype to the formation of glutamine could not be determined. Insulin led to an increase in the consumption not only of the shown amino acids alanine, glutamine and glycine but as a general trend of increased amino acid consumption could be observed (Figure 5-6, 5-7, 5-13, 5-14, Supplementary Table 3 to 10). The production of glutamic acid was significantly decreased in PHH to up to 30% the initial rate if insulin was added to the medium. This is in accordance with the effects of insulin *in vivo*. There, the hormone also leads to an enhanced amino acid transport into hepatocytes (Takenaka et al. 1989). Surprisingly, the general uptake of amino acids was completely independent of the extracellular glucose concentration. So even under fasting conditions, when amino acids like glutamine and alanine served as major carbon sources, the uptake rates were more or less identical compared to postprandial conditions. The basic uptake rate found for amino acids and their degradation seems to be sufficient to provide enough ATP and carbon to meet the cellular demand. The reason for the increased amino acid uptake

might be a combination of two factors. First of all, *in vivo* insulin leads to a higher protein production of hepatocytes, which could be confirmed *in vitro* and will be further discussed in Chapter 6 (Takenaka et al. 1989). At the same time, it was shown that insulin has an inhibitory effect on the proteasome activity (Duckworth et al. 1998a). This can lead to smaller intracellular pool sizes of freely available amino acids. The increased demand of amino acids through enhanced protein production coupled with decreased availability of amino acids from intracellular sources can explain the strongly increasing effect of insulin on amino acid consumption rates in general (Figure 5-6, 5-7, 5-13, 5-14, Supplementary Table 3 to 10). Ammonia from excessing amino acids is detoxified into urea, which is also increasingly produced if the cells are incubated with insulin (Chapter 6).

Glycine showed a strong increase in its m+1 labeled fraction of up to 80% in PMH independent of the labeled carbon source used (Figure 5-18, Figure 5-21). Usually one would expect an increase in the fully labeled fraction of glycine if it was directly produced from glucose. However, there are various resources for the production of glycine, labeled and unlabeled, resulting in a mixed glycine pool. Additionally, glycine is metabolized to CO₂ and NH₃ by the glycine cleavage system, thereby resulting in one molecule of N⁵-N¹⁰-

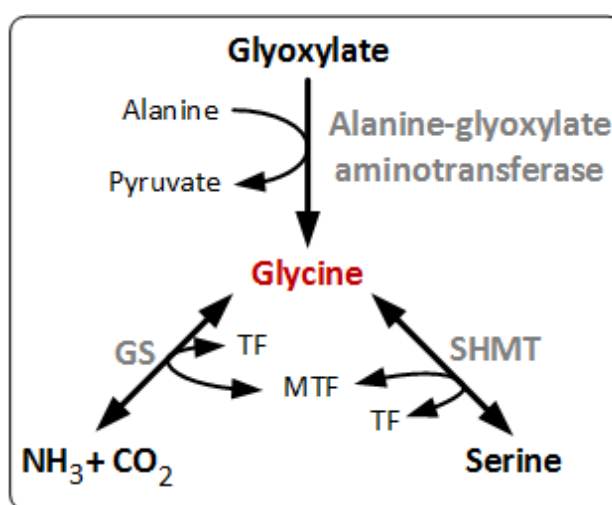


Figure 5-22 Glycine metabolism in mammalian cells. Glycine can be formed from glyoxylate and from serine. It can be degraded by the glycine cleavage system to CO₂ and NH₃. Thereby MTF is formed, which can be used again for the formation of serine. Abbreviations: GS Glycine cleavage system; MTF N⁵-N¹⁰-methylene tetrahydrofolate; SHMT Serine hydroxymethyltransferase; TF Tetrahydrofolate. Adapted from Wang et al. 2013.

methylene tetrahydrofolate, which again can be used for the synthesis of serine (Figure 5-22). Because of the strong exchange of C1-units between glycine and serine and the loss of a C-atom from glycine as CO₂ the m+1 fraction is finally accumulating. This also explains how more than 50% of labeling can be reached with labeled glucose as well as with glutamine as tracer.

In this study not only the effects of insulin and glucose on the metabolism of hepatocytes from two different species were analyzed, but also if the cultivation form has an influence on these effects. As already mentioned, the cells were only cultivated for 24 h to guarantee that

dedifferentiation has no significant influence on the metabolism. In general, the cells showed the same trends, if exposed to insulin, meaning a decrease in glucose production under fasting conditions, an increased consumption of glucose during postprandial conditions and a generally stronger consumption of amino acids. The absolute rates were slightly higher in the collagen ML cultures. However, regarding the carbon use determined by the labeling studies no differences between the used culture conditions could be found. PMH and PHH showed also similar behavior with respect to the uptake and production rates as function of insulin and glucose concentration. The same trends as already discussed above could be observed in both conditions, although for most metabolites the rates, which were calculated here, were slightly lower in human hepatocytes. This can be explained by the different sizes of the hepatocytes. PMH have a diameter of about 50 μm whereas PHH only have a diameter of about 20 μm . If the respective cellular volumes are regarded, PMH have a 15 times higher volume compared to PHH. Since the metabolic rates in this study are normalized to the living cell number and calculated per cell the cell size has an influence on the calculated metabolic rate. An often used reference is total protein content. However, determination of the living cell number was chosen as a reference, since the determination of the protein content in collagen SW and ML is disturbed by the ECM, which not only serves as a structural support for the cells but also as a reservoir for growth factors and other proteins. Additionally, the use of the actual living cell number is more exact, since dead cells are excluded and the protein content of cells is not constant in all situations (Priesnitz et al. 2014). However, this must be considered, if the uptake and consumption rates are compared. If the metabolic rates are calculated per cellular volume PHH show a considerable higher metabolic activity compared to PMH.

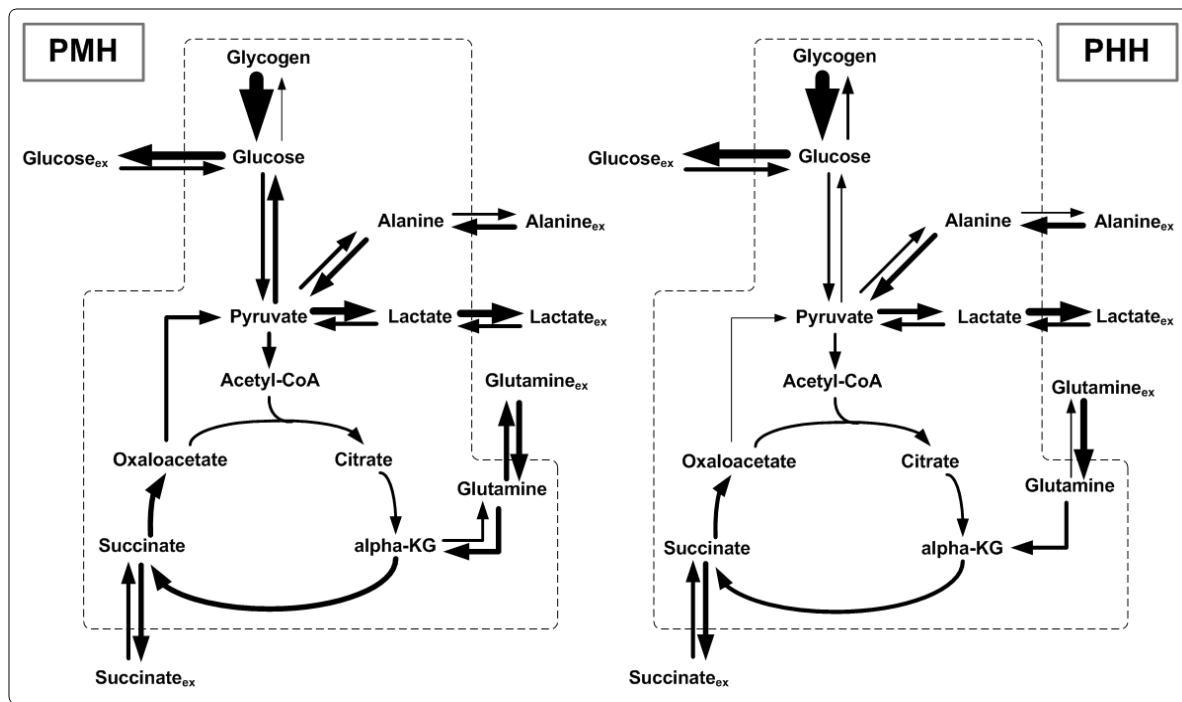


Figure 5-23 Activity of pathways in primary mouse and human hepatocytes under fasting conditions (7 mM extracellular glucose). Fluxes are estimated (not calculated) based on the uptake and consumption rates and on the labeling studies with glutamine and glucose. Width of arrows indicates activity of the respective pathway. The dashed line indicates the cell membrane. Abbreviations: alpha-KG – alpha-ketoglutarate; CoA – coenzyme A; ex – extracellular; PHH – primary human hepatocytes; PMH – Primary mouse hepatocytes.

Although a more or less identical reaction of the cells to insulin and glucose could be observed if only extracellular rates were compared, a rather different situation is presented when the intracellular carbon use was analyzed with the help of ^{13}C labeling. Figure 5-23 and Figure 5-24 show which pathways of the central carbon metabolism are active in PMH and PHH under fasting and under postprandial conditions. As already discussed above, PHH seem to use glucose, if available abundantly, solely for the refilling of glycogen stores and not for energy metabolism and biosynthesis. PMH, on the other hand, metabolize glucose, if postprandial conditions were applied, also *via* glycolysis for their own cellular energy demand.

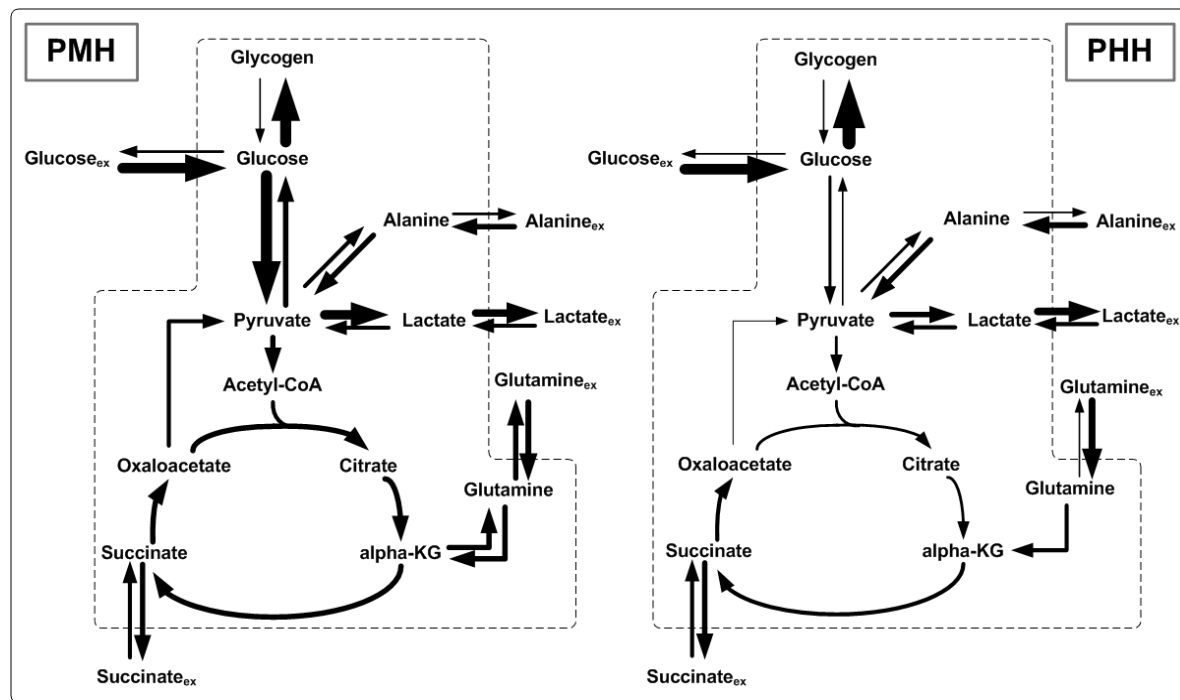


Figure 5-24 Activity of pathways in primary mouse and human hepatocytes under postprandial conditions (25 mM extracellular glucose). Fluxes are estimated (not calculated) based on the uptake and consumption rates and on the labeling studies with glutamine and glucose. Width of arrows indicates activity of the respective pathway. The dashed line indicates the cell membrane. Abbreviations: alpha-KG – alpha-ketoglutarate; CoA – coenzyme A; ex – extracellular; PHH – primary human hepatocytes; PMH – Primary mouse hepatocytes.

At the same time, gluconeogenesis is active in PMH during fasting as well as during high-glucose conditions as shown by the formation of labeled glycine if the cells are incubated with $[U^{13}C_5]$ -glutamine (Figure 5-21). *In vivo* various differences in metabolic activity and glucose metabolism are described (MacDonald et al. 2011, Bunner et al. 2014, Kowalski and Bruce 2014). The contribution of different tissues to blood glucose homeostasis and glucose use are different in these two species. In humans, skeletal muscle, an insulin sensitive tissue, plays a major role regarding the storage of glucose in form of glycogen. In mice only about 10% of the glucose available after a meal is taken up by skeletal muscle, whereas in humans this tissue is responsible for up to 25% of glucose clearance (Kowalski and Bruce 2014). However, in mice brown adipose tissue plays a major role in glucose clearance. Brown adipose tissue, which seems to be related to skeletal muscle tissue, does also exist in humans, but its role and its contribution to whole body glucose metabolism is mostly not understood (Nedergaard et al. 2007, Celi 2009). Furthermore, also the activation of pancreatic β -cells seems to be achieved by the use of different pathways in both species.

Metabolically mice tend to a rapid depletion of glycogen stores, which are completely emptied after about 16 h of fasting. Additionally, glycogen content, alone in liver, is also significantly lower compared to humans. Mice are therefore strongly dependent on the energetically expensive pathway of gluconeogenesis, which could be also confirmed *in vitro* by this study. This and the differential use of glucose by PMH compared to PHH confirms that hepatocytes, which are cultivated *in vitro* still sustain metabolic specificities derived from their original environment. This strongly hinders the use of PMH as a substitute for PHH to analyze carbon metabolism or insulin reactions. Bunner et al. reviewed diabetes mouse models and concluded that none of them can accurately represent the full spectrum of symptoms and complications of type II diabetes (Bunner et al. 2014). Taken together this leads to questioning the usefulness of murine *in vitro* cultures as well as mouse models in this special field of studying metabolism and metabolic disorders.

6. The influence of glucose and insulin on hepatic function

6.1 Introduction

The liver is a highly complex organ with numerous essential functions to guarantee physiological body function. It regulates glucose homeostasis, maintaining the blood glucose within the narrow range of 3.9 to 7.8 mM during fasting and after meals (American Diabetes Association, 1998, Klover and Mooney 2004). Furthermore, the liver is also the major producer of plasma proteins such as albumin (Pan et al. 2009). Albumin is the most abundant protein in human blood plasma accounting for about 50% of the total serum protein (Nicholson et al. 2000). Albumin transports hormones, e.g. thyroid hormones, fatty acids, and other compounds, buffers pH, and maintains oncotic pressure, among other functions. The production of albumin is known to react to physiological changes such as the concentration of insulin and can be impaired in diabetic subjects (Tessari et al. 2006). Another essential function of the liver is detoxification. In the course of amino acid metabolism ammonia is produced. Ammonia is a toxic metabolite leading to severe disorders if detoxification is impaired (Butterworth et al. 1987). In the liver ammonia is detoxified by the urea cycle, in which it is metabolized to urea which can be excreted *via* the urine. The metabolic activity of the urea cycle is also known to be influenced by hormonal regulation *in vivo*, e.g. by glucagon. The availability of glucose as a substrate also seems to play a role in regulation of urea production (Hamberg and Vilstrup 1994). In addition to the detoxification of endogenous compounds as ammonia, the liver is also the main site of xenobiotic metabolism (Hamilton et al. 2001). CYPs play a central role in the first phase of drug metabolism. Their main task is to introduce reactive and polar groups into their substrate, which enhances excretion or further conjugation reactions. This is achieved by hydroxylation, dealkylation or oxidation of the compound, but also ring-opening and reduction can be mediated by CYPs (Martignoni et al. 2006). The human CYP 3A is responsible for the biotransformation of 50% of oxidatively metabolized drugs (Williams et al. 2002, Zuber et al. 2002). Therefore, maintaining the activity of CYP 3A at a level close to the *in vivo* level is highly desirable. The activity of CYPs can be influenced by many factors, e.g. CYP 3A by grapefruit juice or drugs as phenytoin (Lynch and Price 2007). However, also endogenous factors as glucose can influence CYP activity. It has long been known that e.g. increased consumption of glucose can decrease metabolism of numerous

drugs (Buchholz et al. 1989). Normal CYP function can also be impaired in disease conditions related to metabolic changes, such as diabetes (Hasegawa et al. 2010). The clearance of insulin is an important feature of physiological body function and guarantees the maintenance of insulin sensitivity (Ader et al. 2014). The liver is the major site of insulin clearance. Approximately 80% of endogenous insulin is removed by the liver. The remaining 20% are cleared by the kidneys and muscles (Duckworth et al. 1998b). Insulin clearance is impaired in various metabolic disease conditions such as obesity and non-alcoholic fatty liver disease (NAFLD) and can subsequently lead to type II diabetes (TIID) (Meistas et al. 1983, Goto et al. 1995, Lee et al. 2013b). This indicates a strong effect of metabolic components on the activity of insulin clearance. In this study the influence of cultivation conditions on the hepatic functions of primary human and mouse hepatocytes described above was investigated. Therefore, the cells were cultivated in collagen SW and ML culture and were incubated with different concentrations of glucose and insulin. The aim of this study was to determine, if the *in vivo* changes induced by insulin and glucose are regulated in the same way in *in vitro* cultivation systems and to characterize inter species differences between mouse and human if existent.

6.2 Results

The experimental setup of this experiment largely resembles the one described in Chapter 5 to analyze the influence of glucose and insulin on the central carbon metabolism. PMH and PHH were cultivated with different insulin and glucose concentrations for 24 h to investigate the influence of both on the central carbon metabolism. The same concentrations, namely 7 and 25 mM glucose and 0-100 nM insulin, were chosen to analyze albumin and urea production and the metabolic clearance of insulin. The influence on CYP activity, namely CYP 3A, was only tested with 0 and 100 nM insulin. As described in Chapter 5, hepatocytes were not only cultivated in collagen ML but also collagen SW culture to examine if the cells react identically to insulin and glucose under both culture conditions.

6.2.1 Albumin production

Albumin is the main serum protein produced by the liver. The influence of insulin and glucose on the production of albumin was analyzed and the protein quantified after 4, 8 and 24 h. Then the production rates were calculated. Over time the production rate of albumin increased in all conditions. Thereby, the production of albumin in PMH was not significantly influenced by the applied glucose concentration neither in the SW nor in the ML culture (Figure 6-1). Insulin, on the other hand, led to a significant dose-dependent

increase in the production of albumin, which was most prominent after 24 h. In the ML culture incubated with 25 mM glucose the effect was, due to high differences in the absolute rates per mouse, not significant. However, a clear trend, in accordance with the other culture conditions, was evident.

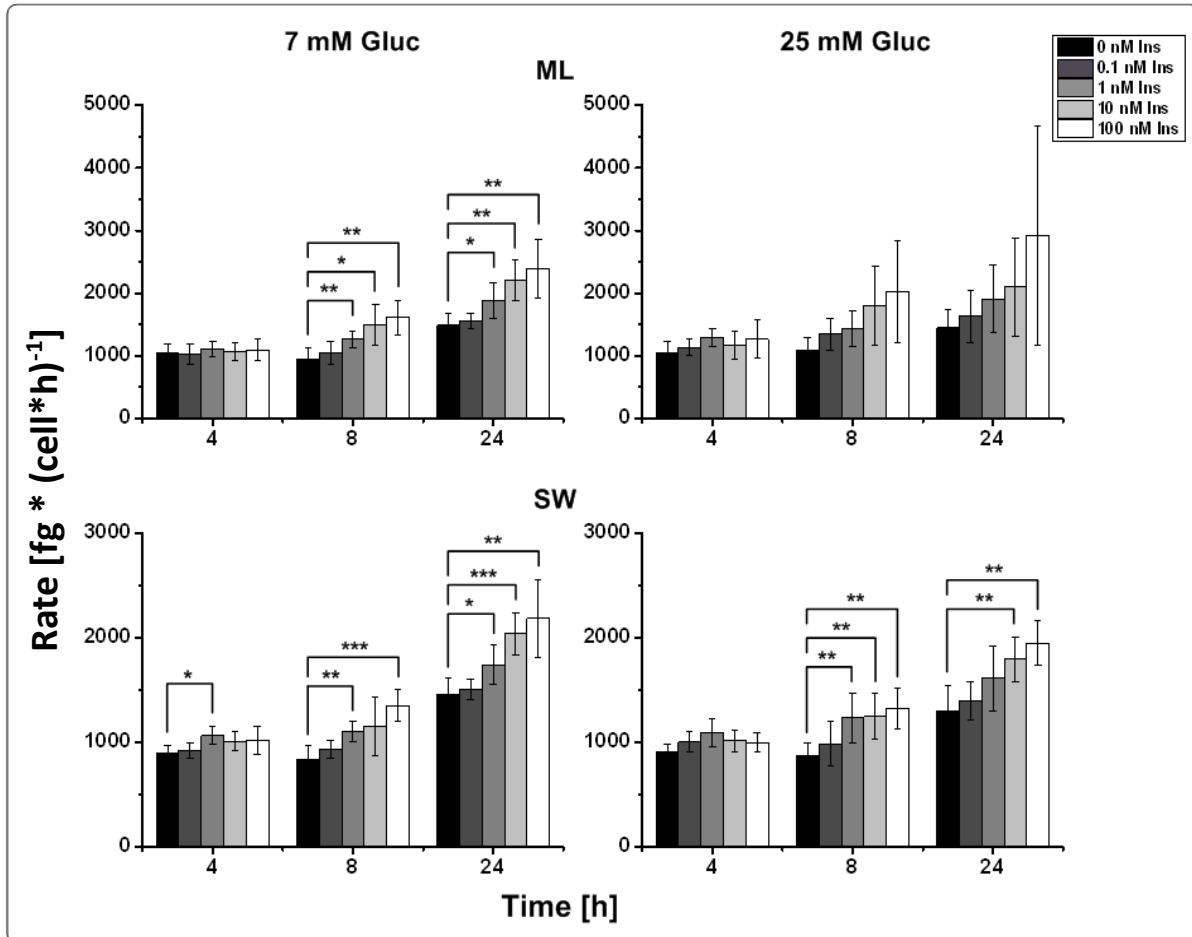


Figure 6-1 Albumin production rates in primary mouse hepatocytes in collagen sandwich (SW) and monolayer (ML) culture incubated with different combinations of insulin (Ins) (0-100 nM) and glucose (Gluc) (7 and 25 mM) for 24 h. Error bars indicate standard deviations (n = 3). * indicate significance (* p=0.05; ** p=0.005; *** p=0.001). Living cell number was determined after 24 h using calcein AM staining.

The production rate of albumin in PHH was overall slightly lower, if they were cultivated in the collagen SW culture (Figure 6-2). In contrast to PMH, the production of albumin decreased over time. As in PMH glucose concentration did not influence the production rate of serum albumin. In the ML culture incubation with insulin led to significantly increased production of albumin. In the SW culture this effect was not significant due to high standard deviation. This is mostly caused by differences in the absolute production rates of the donors. However, a trend towards increased production was still observable. Albumin production rates of single donors are depicted in Supplementary Figure 13 and 14.

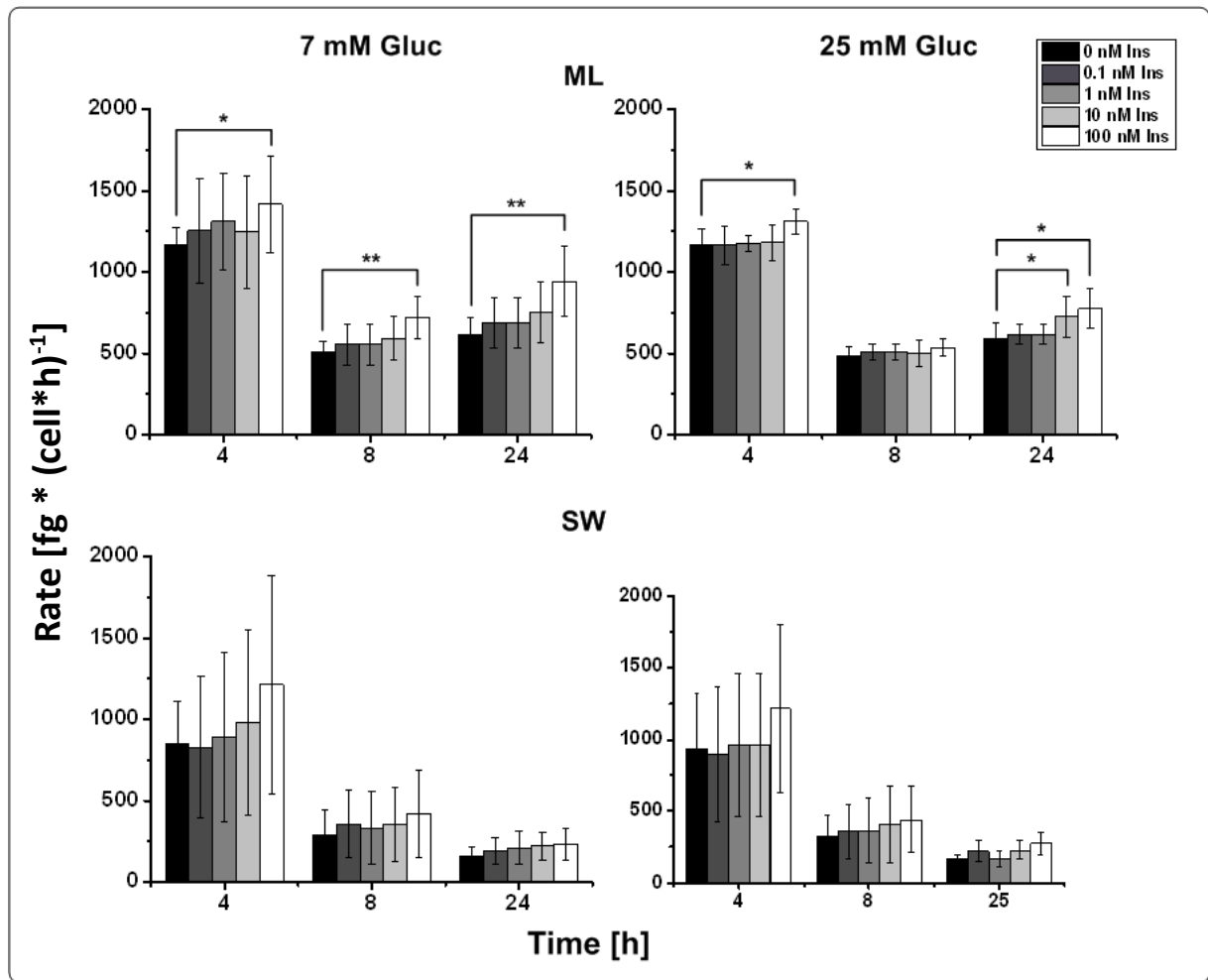


Figure 6-2 Albumin production rates in primary human hepatocytes in collagen sandwich (SW) and monolayer (ML) culture incubated with different combinations of insulin (Ins) (0-100 nM) and glucose (Gluc) (7 and 25 mM) for 24 h. Error bars indicate standard deviations (n = 3). * indicate significance (* p=0.05; ** p=0.005; *** p=0.001). Living cell number was determined after 24 h using calcein AM staining.

6.2.2 Urea Production

To determine if insulin and glucose have an influence on the activity of the urea cycle PMH and PHH were cultivated in collagen ML and SW culture with different concentrations of the hormone and glucose. The production of urea was determined after 4, 8 and 24 h and production rates were calculated. For PMH in the SW culture the inducing effect of glucose was slightly higher compared to the hepatocytes in ML culture (Figure 6-3). However, after 4 h of incubation a general decrease in production rates was observed and the metabolic rates adjusted on the same levels. Insulin had a very interesting effect. In the beginning insulin led to a dose-dependent decrease of urea production. In the later course of cultivation, most prominently in the ML culture, insulin, however, increased the production of urea.

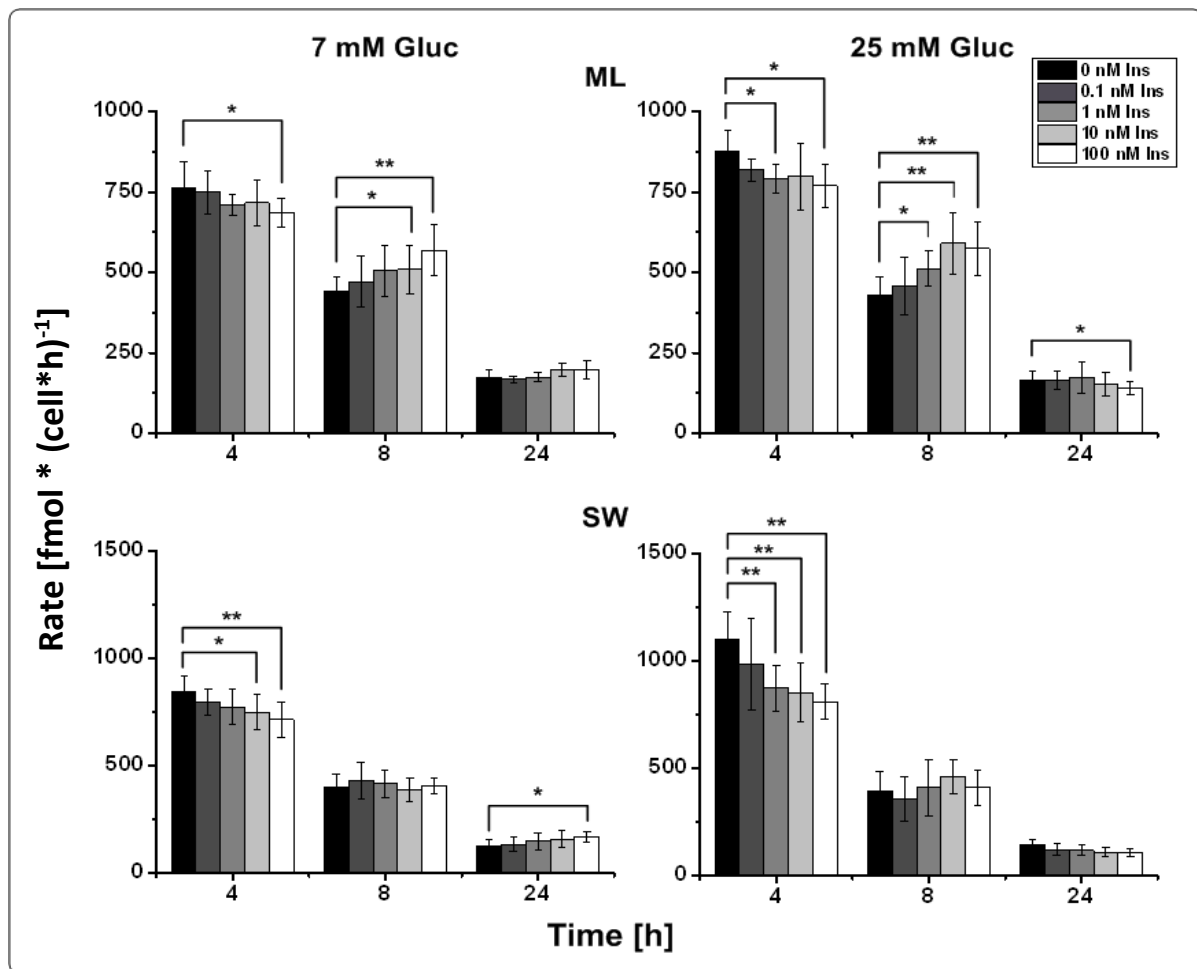


Figure 6-3 Urea production rates in primary mouse hepatocytes in collagen sandwich (SW) and monolayer (ML) culture incubated with different combinations of insulin (Ins) (0-100 nM) and glucose (Gluc) (7 and 25 mM) for 24 h. Error bars indicate standard deviations (n = 3). * indicate significance (* p=0.05; ** p=0.005; *** p=0.001). Living cell number was determined after 24 h using calcein AM staining.

For PHH the cultivation condition in respect of the collagen setup had the greatest influence on the production of urea (Figure 6-4). In the ML culture the rate of urea production was two times higher than for PHH in the collagen SW culture. As in PMH the production rate of urea constantly decreased within 24 h. Glucose had no influence on the activity of the urea cycle. Overall, insulin had an increasing effect on the production rate of urea in both culture conditions. If PMH are compared with PHH, the production rate of urea was significantly lower in the PHH. However, if the uptake rates are not calculated on the absolute cell number but on the cellular volume, the rates are comparable. The influence of glucose and insulin was differential in both cell types and in the case of insulin, more ambivalent.

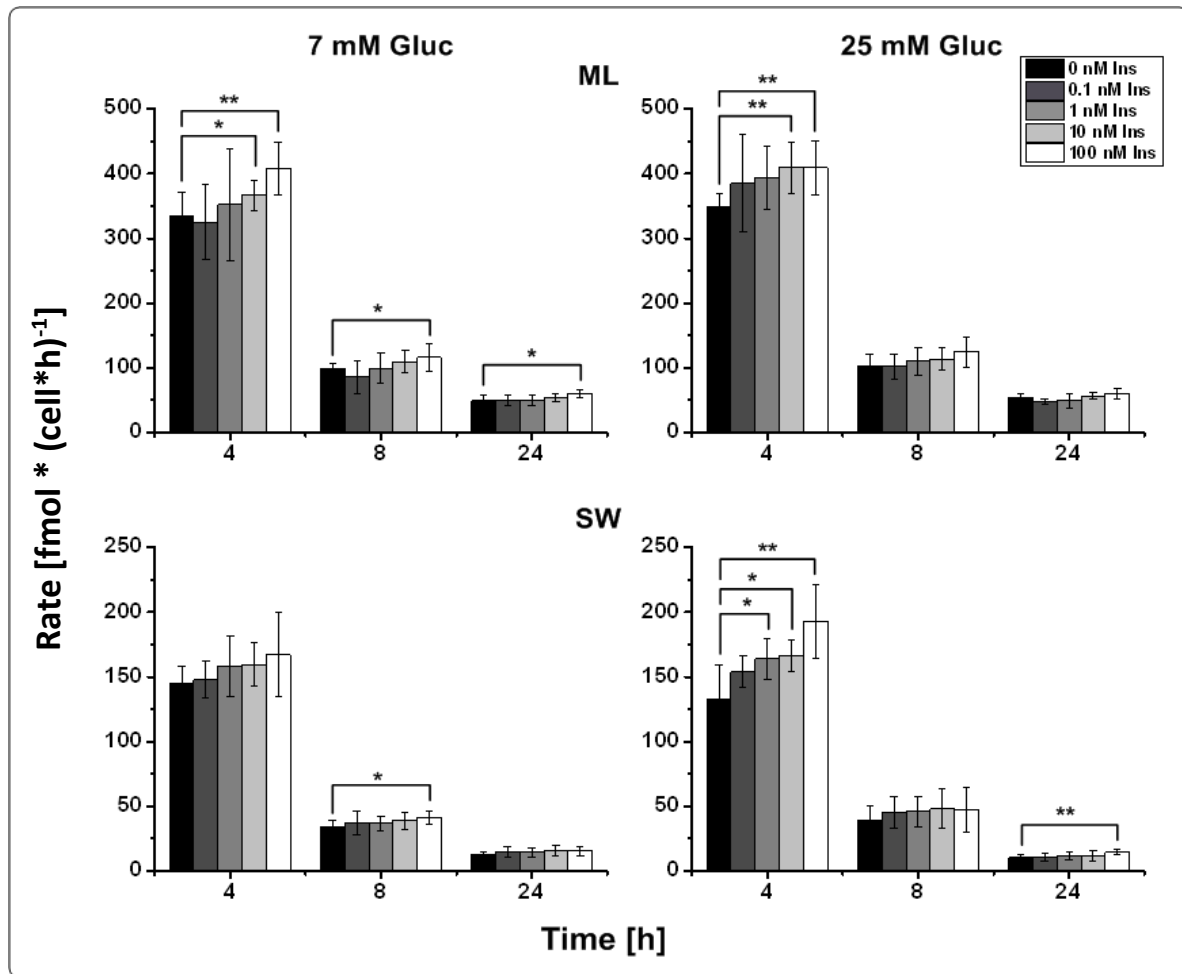


Figure 6-4 Urea production rates in primary human hepatocytes in collagen sandwich (SW) and monolayer (ML) culture incubated with different combinations of insulin (Ins) (0-100 nM) and glucose (Gluc) (7 and 25 mM) for 24 h. Error bars indicate standard deviations (n = 3). * indicate significance (* p=0.05; ** p=0.005; *** p=0.001). Living cell number was determined after 24 h using calcein AM staining.

6.2.3 CYP 3A activity

The activity of the phase I metabolism enzyme CYP 3A was determined after 24 h of incubation with the respective combination of insulin and glucose. The results for PMH and PHH are depicted in Figure 6-5 and Figure 6-6, respectively. In both culture conditions the CYP 3A activity was lower after 24 h of incubation compared to the initial activity. The glucose concentration had no significant influence on the activity of the phase I metabolism enzyme. Insulin, however, significantly increased the activity of CYP 3A in the ML culture. In the SW culture, the effect was rather opposite. If no insulin was present in the medium, CYP 3A activity was significantly higher than if insulin was present, although the initial activity was not reached.

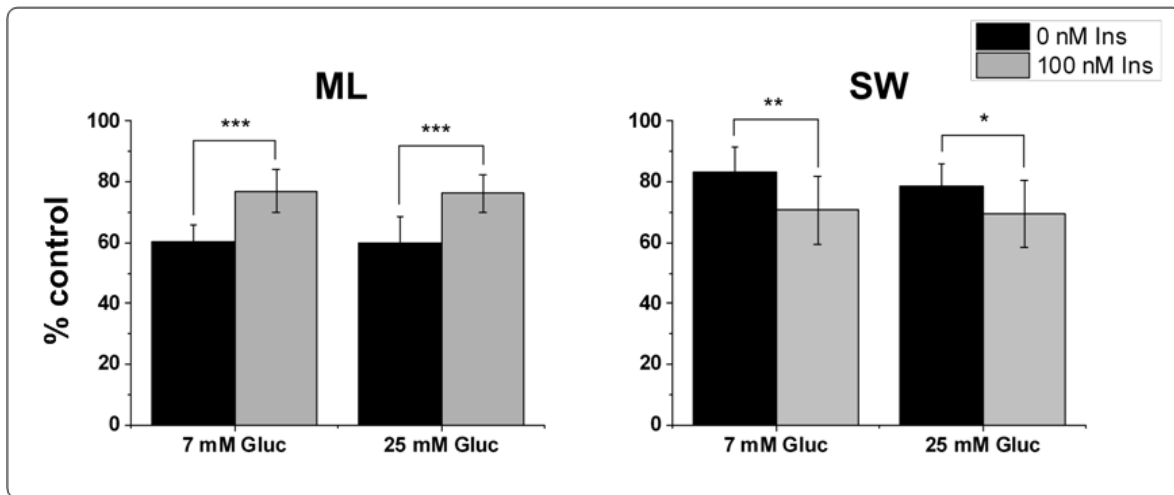


Figure 6-5 Relative activity of CYP 3A in primary mouse hepatocytes incubated with insulin (ins) (0 or 100 nM) and glucose (gluc) (7 and 25 mM) for 24 h. The cells were cultivated in collagen sandwich (SW) and monolayer (ML) culture. Activity was normalized to the activity at start of the experiment [% control] (timepoint 0 h). Error bars indicate standard deviations (N=3; n = 9). * indicate significance (* at p=0.05; **at p=0.005; *** at p=0.001).

In PHH the situation was a rather different one. As for PMH the activity of CYP 3A in the ML culture was around 75% when incubated with 100 nM insulin compared to the initial activity. Without insulin the activity was significantly higher, further enhanced by the low glucose concentration. The cultivation of the cells in the collagen SW culture itself had an inducing effect on CYP 3A activity. Insulin and glucose concentrations only had a minor impact on the activity of the enzyme, with the high insulin and glucose concentration leading to a slight increase in activity.

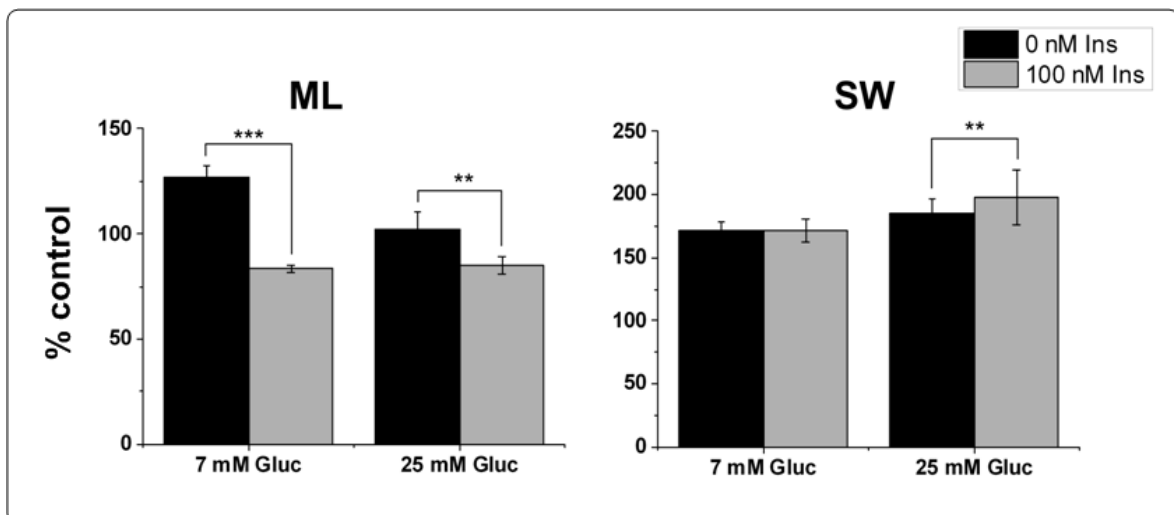


Figure 6-6 Activity of CYP 3A in primary human hepatocytes incubated with insulin (Ins) (0 or 100 nM) and glucose (Gluc) (7 and 25 mM) for 24 h. The cells were cultivated in collagen sandwich (SW) and monolayer (ML) culture. Activity was normalized in % to the activity at start of the experiment [% control] (timepoint 0 h). Error bars indicate standard deviations (N=3; n = 9). * indicate significance (**at p=0.005; *** at p=0.001).

6.2.4 Metabolic clearance of insulin

The hepatic clearance of insulin was determined after 4, 8 and 24 h of incubation with insulin and glucose. The remaining amount of insulin after 4 h of incubation is depicted in Figure 6-7. In none of the tested conditions insulin was cleared completely, so a basal level of insulin was always present. Thereby the rate of clearance strongly depended on the insulin concentration. The higher the administered concentration, the higher the overall clearance rate was. However, after the initial 4 h insulin was, independent of the remaining amount, almost not further decreased (Supplementary Figure 15 and 16). Glucose, on the other hand, had no significant influence on insulin clearance in the tested cell culture setup. If PMH and PHH were compared, insulin clearance was overall higher in PMH. However, PHH were more susceptible to the cultivation method used. With the lowest insulin concentration the clearance rate was significantly higher in the ML culture, whereas with the

highest concentration it was exactly the other way around.

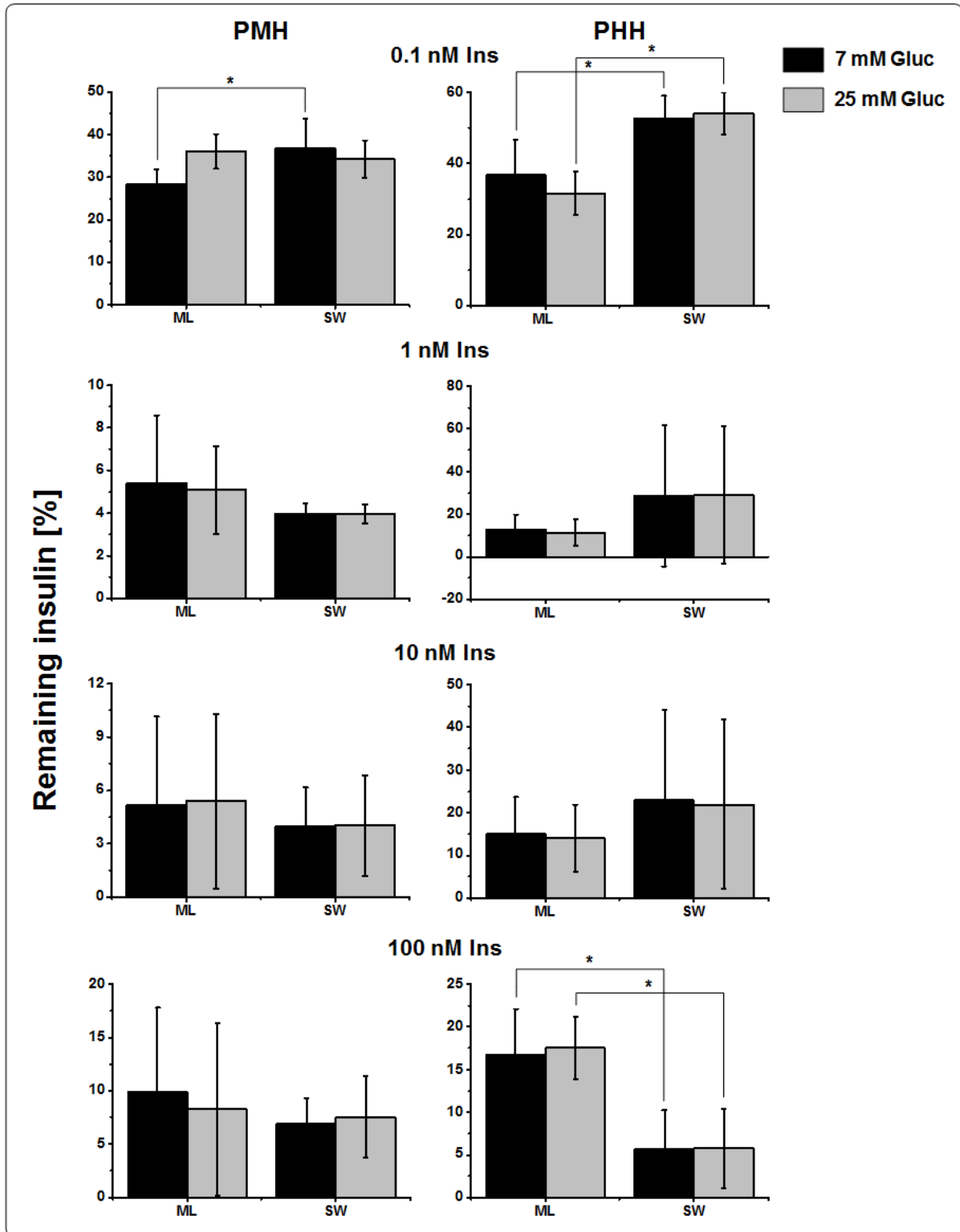


Figure 6-7 Remaining amount of insulin after 4 h of incubation. Primary mouse hepatocytes (PMH) and primary human hepatocytes (PHH) were cultivated in collagen sandwich (SW) and monolayer (ML) culture with different insulin (ins) (0-100 nM) and glucose (Gluc) concentrations (7 and 25 mM). The amount of insulin was normalized in % to the respective initially administered amount of insulin at start of the experiment [%]. Error bars indicate standard deviations (N=3; n = 6). * indicate significance (*at p=0.05).

6.3 Discussion

Hepatic function *in vivo* is influenced by numerous factors such as genetic predisposition, nutrition, disease state or drug intake (Hamberg and Vilstrup 1994, Zhou et al. 2009, Agustanti et al. 2014, Elcombe et al. 2014). Also under *in vitro* conditions hepatic functionality is susceptible to different cultivation conditions. The most prominent and most studied example is the loss of hepatic function, regarding albumin and urea synthesis as well as CYP activity, in collagen ML within a few days of cultivation (Iredale and Arthur 1994, Lu et al. 2012, Alépée et al. 2014). Thereby, this effect is mostly caused by dedifferentiation of hepatocytes, called epithelial to mesenchymal transition (Godoy et al. 2010). To abate this dedifferentiation effect in the here presented study, all experiments were conducted within the first 48 h of cultivation. Four major hepatic functions, namely albumin and urea production, CYP 3A activity and insulin clearance, have been chosen to investigate the influence of insulin, glucose and the cultivation condition *in vitro*. Due to the use of primary mouse and human hepatocytes species differences could also be addressed.

In PMH insulin led to a significant increase in albumin production, which was observable after 8 h of insulin treatment (Figure 6-1). The production rates were about twice as high with the highest insulin concentration administered, compared to control conditions (no insulin). Neither glucose nor the cultivation setup had an influence on the production of albumin. In PHH the overall albumin production rate decreased over time to about 50% the initial rate in the ML culture and even 25% in the SW culture. This was in contrast to PMH, which showed a constant production of the serum protein (Figure 6-2). The effect of insulin was not as prominent as in PMH, however a significant increase of up to 30% could still be observed. Among other things, this might be caused by the higher variance between the single donors and the larger differences regarding absolute production rates. The single donor profiles of albumin production can be found in Supplementary Figure 13 and 14. If the overall amount of taken up amino acids was concerned, only a minor part of the amino acids (1.3-2.2% in PMH and 1.2-3.8% in PHH) were used to form albumin (Supplementary Figure 17 and 18). In both PMH and PHH, the percentage of amino acids used for albumin production was constant, regardless of the applied insulin concentration. However, in PHH cultivated in ML culture the percentage was about twice as high compared to the SW culture, which is in accordance with the higher decrease of the albumin production rate in the SW culture. The *in vivo* described influence of insulin on albumin production could be confirmed for both culture conditions and for hepatocytes of both origins (Jeschke et al. 2005, Tessari et al. 2006). This is also in accordance with the increased amino acid uptake

caused by insulin, which was described in Chapter 5 (Figure 5-6, 5-7, 5-13, 5-14). Dahn et al. showed that under tumor necrosis factor α (TNF α) mediated inflammatory conditions, albumin production is also susceptible to the intra- (glycogen content) and extracellular glucose concentration (Dahn et al. 1994). However, under non-inflammatory conditions used in our experimental setup, this could not be confirmed for any of the tested conditions.

In PMH neither glucose nor the cultivation setup seemed to influence the production rate of urea (Figure 6-3). Insulin, however, in the beginning of cultivation led to concentration dependent decrease in urea production of up to 30%, which was most prominent in the SW culture. During the further course of cultivation, cells switched to an increase of the production rate, which was, with an increase of about 50% of the initial rate, most prominent in the ML culture. PHH were also not influenced by glucose regarding the production of urea (Figure 6-4). However, in the ML culture the production rates were about twice as high compared to the SW culture. This cannot be explained by differential amino acid uptake, since the uptake rates for amino acids were not lower in the SW culture (Chapter 5.2, 5-13, 5-14). However, also for PMH a lower initial urea cycle activity has been observed (Figure 3-1). Since urea cycle activity is mostly regulated by transcriptional control, this delay might be caused by an elongated adaption phase of primary hepatocytes in SW culture, in which an *in vivo* like structure of hepatocytes is regained (Morris 2002). In contrast to PMH, urea production in PHH was immediately increased due to the exposure to insulin (Figure 6-4). Exton et al. also found a reduction of urea and ketone bodies caused by insulin in perfused rat livers (Exton et al. 1971). This is in accordance with our initial findings for PMH (Figure 3-5). Due to the increased amino acid uptake the increase in urea production can be explained since the major part of consumed amino acids was degraded into urea (Supplementary Figure 17 and 18). In PMH the percentage of formed urea was between 100 and 68% in the ML culture, whereas in the SW culture it even was between 133 and 81%. PMH cultivated in the SW culture produced even more urea than they took up amino acids. However, this can also originate from protein degradation, which is known to be inhibited by insulin (Duckworth et al. 1998a). In both conditions the percentage of formed urea from the taken up amino acids decreased with increasing insulin concentration. The increasing effect of insulin on amino acid consumption is stronger than on the urea production (Figure 5-6, Figure 5-7). In human hepatocytes this increasing effect of insulin was directly observable (Figure 6-4). The percentage of urea formed from consumed amino acids was 131-87% in the ML culture and 37-26% in the SW culture. The above described effects of insulin were also observed in PHH. The most striking difference, however, was the three

times lower percentage of produced urea in the SW culture. The production rate of urea in the SW culture was 50% lower compared to the ML culture. Still, there must be a large amount of other proteins, which must be formed by PHH cultivated in SW culture as well. *In vivo* no influence of insulin on urea production was detected in humans (Hamberg and Vilstrup 1994). Glucagon via cAMP and the availability of nutrients seemed to be the major regulators of urea cycle activity (Hamberg and Vilstrup 1994, Morris 2002). This could not be tested with the setup used here, since only insulin and glucose were used as nutritional and hormonal variables. In addition, also other factors, as the pO₂ seem to play a role in the transcriptional control of urea cycle enzymes, since also the detoxification of ammonia is zoned along the acinus, with urea cycle enzymes expressed periportally and the detoxification via glutamine synthesis pericentrally. Mimicking this highly complex situation *in vivo* is probably only possible with a perfused cultivation system.

The activity of CYP 3A was significantly influenced by insulin but not by glucose in PMH (Figure 6-5). However, depending on the cultivation condition, insulin treatment resulted in an increased activity of up to 30% in the ML culture whereas it led to a decrease of activity of about 35% if the cells were incubated in collagen SW culture. In PHH the effect was exactly the other way around (Figure 6-6). Additionally, also glucose influenced the enzyme activity. Although CYPs are a highly conserved protein family, there are certain CYP subfamilies, such as CYP 1A, 2C, 2D and 3A, which show significant interspecies differences regarding their catalytic activity and substrate specificity (Whalen et al. 1999, Martignoni et al. 2006). Perloff et al., e.g. could show, that even structurally highly similar substances as midazolam and triazolam are differentially metabolized in humans and mice (Perloff et al. 2000). From the six CYP 3A isoforms, in contrast to the four isoforms in humans, murine CYP 3A11 is the isoform most similar to human CYP 3A4, having 76% amino acid homology (Yanagimoto et al. 1992). This however must not necessarily mean, that the test substance used in this assay is metabolized by this isoenzyme in mice. Numerous factors influencing the activity of CYPs have been identified. *In vivo*, a certain decrease of drug metabolism mediated by certain CYPs has been observed in mice, rats and humans with a high consumption of glucose (Stewart and Strother 1999). However, this was also no general effect, but different CYPs were differentially regulated due to glucose exposure. The authors further hypothesize, that not glucose directly is responsible for the regulatory events, but the changed lipid environment induced by the availability of glucose. Diseases, such as diabetes, seem to influence CYP activity as well. Hasegawa et al. found an enhanced CYP 3A activity in a rat model of diabetes and that insulin treatment was able to

decreased this enhanced activity in the diabetic group (Hasegawa et al. 2010). These findings are in accordance with our *in vitro* rodent model in the collagen SW culture, however, not the findings in the human cell culture model. This might indicate that the two CYP 3A isoforms are regulated differentially in mice and humans or that two different CYP subfamilies are responsible for the turn-over of luciferin-IPA to luciferin. Further characterization of rodent CYP isoforms compared to human isoforms, which has been mostly neglected over the last few years, is necessary to answer this question (Martignoni et al. 2006). Overall, we could show, that for PMH as well as for PHH, the cultivation condition does not only significantly influence the general activity of CYPs, but also how these enzymes react to regulatory factors.

The clearance of insulin represents an important physiological function, which also regulates the cellular response to insulin due to reducing its availability (Duckworth et al. 1997). Overall, the standard deviation of the results depicted in Figure 6-7 was rather high independent of the used cell type. The reason for this can be seen in the relatively low insulin concentrations used in this approach. In this case, also relatively small differences in the clearance activity of the different donors and mice can lead to a high standard deviation. Also the sensitivity of the insulin ELISA assay might be a problem. However, still general trends could be observed. In the used cell cultures the clearance of insulin was slightly higher in PMH compared to PHH (Figure 6-7). Glucose had no influence on the clearance rates. However, the more insulin was administered to the cells the more insulin was degraded. After the first 4 h of incubation almost no more changes in the amount of insulin was detectable (Supplementary Figure 15 and 16). It is known, that the insulin degrading enzyme (IDE) is down-regulated after a prolonged insulin exposure (Duckworth et al. 1998b). This regulatory mechanism seems to be independent of the still present extracellular insulin concentration. Duckworth et al. also describe an influence on insulin clearance dependent on the nutrient intake (Duckworth et al. 1998b). However, they also make clear, that to achieve that, certain signaling by the gut is necessary and altered glucose concentration in the liver alone is not enough. This is also the case in both of our characterized cultivation setups. Also Lee et al. describe a dependence of the insulin clearance rate on the fasting glucose concentration, as well as on other factors as high density lipoprotein or cholesterol (Lee et al. 2013b). However, also these findings are based on *in vivo* data, including whole system signaling. The greatest difference regarding the clearance of insulin was observed between PHH cultivated in collagen SW and ML culture. Insulin clearance was 30% lower in the SW culture, if a low amount of insulin was present

(Figure 6-7). The highest used insulin concentration, however, lead to a 15% increase in the insulin clearance rate. In this case the applied concentration of insulin does play a role. This is another example that the cultivation condition cannot only influence the enzyme activity, but also how it is regulated.

Overall, hepatic function is susceptible to multiple factors. In literature it is discussed, that insulin leads to gene expression related to pericentral hepatocytes (Jungermann and Kietzmann 1996). Although this might be the case regarding the expression of certain enzymes of glucose metabolism, a conversion of hepatocytes in general to a more pericentral phenotype in this direction is not observed in our study. In all conditions insulin lead to a significant increase in albumin production. However, *in vivo* albumin is produced by all hepatocytes but to a higher extent by the ones located periportally (Racine et al. 1995). The findings related to urea could also not support this theory, since under both cultivation conditions and in both cell types urea production was initially increased and also urea is a typical parameter related to periportal hepatocytes. Both urea and albumin production are strongly related to the uptake and metabolism of amino acids. An increased amino acid consumption was described in Chapter 5.2 (Figure 5-6, 5-7, 5-13, 5-14) due to insulin exposure, which might be partly used for albumin synthesis and partly be degraded leading to the production of urea. Thereby the major part of consumed amino acids was used for urea production and only a very small percentage of taken up amino acids (up to 3%) is used for albumin synthesis (Supplementary Figure 17 and 18). These hepatic functions might therefore depend on the amount of available substrate, which is initially altered by insulin. The numerous effects of insulin on hepatocytes make differentiation between single pathways very difficult. In addition, hepatic function can also be altered by other cultivation factors as glucose or the *in vitro* culture setup used. Thereby these factors can also influence each other, as seen for the activity of CYP 3A (Figure 6-5, Figure 6-6) or the insulin clearance in PHH (Figure 6-7). This has to be kept in mind when choosing the culture conditions for future experiments, but also if results from different studies are compared, since even a small change in the concentration of a certain factor can have a significant influence on the cells.

7. Discussion and Outlook

Due to increasing concerns with drug induced liver injury in drug development, liver toxicity induced by many chemicals and increasing incidence of metabolic diseases such as TIID or NAFLD, an in-depth understanding of liver physiology is more important than ever (Rombouts & Marra 2010, Mattes *et al.* 2014). It is therefore a substantial need in industry and science to develop valid and reliable *in vitro* test systems for the liver. There are different *in vitro* cultivation techniques available, ranging from conventional ML culture, over the more *in vivo* like collagen SW culture, liver spheroids up to complex bioreactor systems (Koebe *et al.* 1994, Mueller *et al.* 2011b, Mueller *et al.* 2012). Each of these cultivation setups has advantages and disadvantages, which are described in detail in the general introduction. In the thesis presented here the influence of collagen ML and SW cultivation on primary hepatocytes was analyzed.

In first part of the thesis (Chapter 3 and 4) PMH were characterized functionally, metabolically and proteomically. Many effects of cultivation on hepatocyte function have been known for years already. In ML culture hepatocytes lose hepatic function, such as urea and albumin production or CYP activity, within a few days of cultivation, whereas in the SW culture hepatic function can be maintained over weeks (Hengstler *et al.* 2009). Going along with this, hepatocytes in collagen SW culture show a morphology resembling the *in vivo* situation, regaining polarization with functional bile canaliculi and an *in vivo* like distribution of actin right below cell-cell-contacts (LeCluyse *et al.* 2000). Our findings were in accordance with these and can therefore serve as a quality marker for functional SW cultivation (Figure 3-1). Because of these substantial differences induced by the cultivation setups, it suggested itself, that also on the metabolic and proteomic level of organization major differences could be expected. However, metabolically this could not be confirmed. The focus was set on two phases of the cultivation period. First, the adaption phase in which polarization is regained and second the first 5 days of cultivation, in which epithelial-mesenchymal transition takes place in hepatocytes in ML culture (Figure 3-2 and Figure 3-3). In the first phase only a change to glucose production in collagen ML at the end of the cultivation period was found as well as a constantly higher production of acetate and lactate. Since glucose was only produced at the last sampling timepoint, a general trend could not be identified and the production of glucose could also be due to shortage of other substrates in the medium. Acetate itself is a degradation product of ketogenesis. Both elevated acetate and lactate production indicate a stressed phenotype during the adaption phase in ML culture. During the epithelial-

mesenchymal transition phase also only glucose metabolism was susceptible to the cultivation condition. However, surprisingly PMH in the SW culture started to use glucose after 96 h, whereas glucose consumption remained stable in the ML culture. The interpretation of these findings is unclear, however, it showed us that glucose metabolism itself is most susceptible to the used cultivation condition.

On the proteomic level, the loss of hepatic function could be confirmed. Albumin itself and certain enzymes of the urea cycle were down-regulated in the ML culture during the first 5 days of cultivation (Table 4-2). Also in the SW culture hepatic function was affected to a certain extent (Table 4-3). Extracellularly, the production of albumin decreased to almost zero after five days of ML cultivation. In the SW culture, however, the albumin production remained unaffected (Figure 3-5), which might indicate that albumin excretion is the critical step. Also the morphological changes induced by ML cultivation, which were observed in Chapter 3 through fluorescence staining, could be confirmed by proteomics (Figure 3-1). Actin was significantly up-regulated in the ML culture in the course of cultivation. However, in the comparison of the SW and ML culture at day 5 of cultivation, actin was not identified as a significantly changed protein and the finding was therefore not fully conclusive. The most prominent differentially expressed proteins in SW and ML culture were related to oxidative stress. ROS are constantly produced by aerobic metabolic processes such as respiration and can harm proteins, DNA or other cellular structures. In the ML culture proteins involved in oxidative stress defense were constantly down-regulated, whereas in the SW proteins related to oxidative stress were up-regulated. The down-regulation in defense mechanisms might substantially increase the vulnerability of PMH in ML culture to oxidative stress. This could be one of the reasons driving the cells into epithelial-mesenchymal transition and finally into cell death.

Overall, metabolomics and proteomics in combination with traditional functional characterization revealed a detailed picture of hepatocytes in cultivation. Although substantial morphological and functional changes occur in PMH in ML culture, the central carbon metabolism proved to be surprisingly robust towards extreme outer influences. The changes in glucose metabolism could be further analyzed determining the activity of glucose utilizing enzymes or by using ^{13}C tracers to track the metabolism of glucose. Quantification of intracellular glycogen would have been most useful, however, we were not able to quantify it due to insufficient analytical sensitivity. However, with more sensitive MS-based methods this could be achieved. On the proteomic level we could identify a snapshot of differentially

expressed proteins. However, with DIGE only a qualitative comparison between two conditions is possible and identification of differentially expressed proteins is additionally complicated by gel-to-gel-differences. Because of this, it is difficult to identify proteins with less prominent differences. DIGE itself is a very sensitive method with a detection limit of up to 125 pg (manufacturer's data, GE Lifesciences). However, in this approach the limiting factor is the protein quantification with Coomassie Brilliant Blue. The detection limit of this method lies at a range of 36-47 ng (manufacturer's data, Bio-Rad Laboratories). Therefore, no conclusions on proteins below this range can be drawn. With a more targeted approach, as described in the general introduction, the here identified pathways could be analyzed in more detail to confirm these findings. Additionally, further experiments with a focus on the handling of oxidative stress in the two cultivation setups would be most interesting. Thereby, the influence of e.g. anti-oxidative substances such as ascorbic acid, on the epithelial-mesenchymal transition would be most interesting. It could be shown, that a characterization not only focusing on a certain level of organization can provide complementary information on cellular aspects and is able to reveal findings, which were not yet detectable by classical approaches, such as the effects on hepatic function in PMH cultivated in collagen SW culture. Of course, also the integration of transcriptomic data would have been desirable in this study.

The metabolic characterization of PMH identified glucose metabolism to be most susceptible to the cultivation condition. This special issue was addressed in the second part of the thesis, in Chapter 5 and 6. Glucose metabolism is strictly controlled by hormones, such as insulin and glucagon amongst other factors, but also glucose itself is able to stimulate its own uptake. Therefore, it was analyzed how insulin and glucose treatment influence the central carbon metabolism and hepatic function in collagen SW and ML culture. Since there are substantial differences in glucose metabolism and regulation of mice and humans, these species-specific aspects were addressed as well by analyzing primary human and murine hepatocytes in both cultivation setups (Kowalski & Bruce, 2014). Only the first 24 h after over night adaption to the cultivation condition were considered to reduce the influence of epithelial-mesenchymal transition. The chosen insulin (0-100 nM) and glucose concentrations (7 and 25 mM) are in the range of physiological levels found in the liver. Thereby, PHH cultivated in collagen SW showed a generally higher standard deviation compared to PMH and PHH in the ML culture. PHH are generally more variable due to donor to donor differences, caused by different genetic background und individual lifestyle. However, in the SW culture this effect was even more prominent. An explanation for this might be an elongated adaption phase to the cultivation conditions and re-establishing of polarity.

PMH showed higher consumption and production rates than PHH, if the rates were normalized to the absolute cell numbers. However, PMH have a 15 times higher volume than PHH. If the rates are normalized to the overall available cellular mass, metabolic activity of PHH is comparable and in some cases, such as glucose, glutamine and alanine, even considerably higher than for PMH. Insulin had an increasing effect on amino acid consumption in all tested setups (Figure 5-6, 5-7, 5-13, 5-14). Thereby, the applied glucose concentration did not influence amino acid consumption in any way. The metabolism of glucose and amino acids seems to be independent from each other in hepatocytes. The increased uptake of amino acids was going along with an increased production of albumin and also urea. The amino acids taken up are only used to a very low percentage of maximally 3% for albumin synthesis and are mostly degraded to urea (Supplementary Figure 17 and 18). These trends were observed for primary mouse and human hepatocytes, independent of the cultivation setup. The uptake of glucose by the cells was impacted by insulin as expected with a dose dependent increase (Figure 5-4, 5-5, 5-11, 5-12). However, if glucose was produced or consumed, was mostly dependent on the extracellular glucose concentration, at least at the beginning of cultivation. Although the general trends were identical in PMH and PHH already, on this level certain differences could be observed. Whereas in PMH lactate production was dependent on the amount of consumed glucose, this was not the case for PHH. If human hepatocytes were cultivated, lactate production was independent of the glucose concentration. This indicates a certain difference in the use of glucose by the two cell types. To elucidate that in more detail, hepatocytes were also cultivated using fully labeled ^{13}C glucose and glutamine as substrates. The labeling patterns revealed that in PHH glucose was almost completely used for synthesis of glycogen. In contrast to that, PMH used glucose also for glycolysis and TCA cycle (Figure 5-23 and Figure 5-24). Glutamine was an important carbon source in both cases, however, gluconeogenesis is only active in PMH. This might partly reflect the smaller glycogen stores in mouse liver *in vivo*. It would have been most interesting to determine the amount of stored glycogen, which was however not possible due to the above mentioned reasons. Calculation of the intracellular metabolic fluxes used in metabolic network models, which are however only estimated in Chapter 5, would be able to shed light on the activity of metabolic pathways in a quantitative way. In this case a calculation of the metabolic fluxes was not possible due to the unknown amount of nutrients stored in the collagen reservoir. The differential use of glucose by PMH compared to PHH confirms that hepatocytes, which are cultivated *in vitro* still sustain metabolic specificities derived from their original environment.

Especially in the field of drug metabolizing enzymes such as CYPs, a lot has to be learned about human and murine homologues (Whalen *et al.*, 1999). Also small changes in the amino acid sequence can lead to different substrate specificity, which implicates that even if a certain enzyme in mouse shows a high correlation to a human CYP in regard of the amino acid sequence, it does not necessarily metabolize the same substrates (Perloff *et al.*, 2000). Since most assays are based on the specific turnover of a certain substrate by a certain human CYP, translation to rodents is challenging. In addition, single CYPs can also be regulated differentially by certain factors such as the cultivation conditions, which further complicates comparability. The clearance of insulin represents another hepatic function, which is regulated by a combination of certain factors, in this case SW or ML culture as well as insulin and glucose concentration (Figure 6-7). Also in this case the regulatory effect was dependent on the origin of hepatocytes.

Urea and albumin production were also susceptible to the applied insulin concentration, which can be partly explained by the increased amino acid uptake. Thereby, the major part of consumed amino acids was degraded into urea with only a small percentage of maximally 3% going into albumin production (Supplementary Figure 17 and 18). In PMH the percentage of formed urea was between 100 and 68% in the ML culture, whereas in the SW culture it even was between 133 and 81%. PMH cultivated in the SW culture produced even more urea than they took up amino acids. However, this can also originate from protein degradation, which is known to be inhibited by insulin (Duckworth *et al.* 1998a). In both conditions the percentage of formed urea from the taken up amino acids decreased with increasing insulin concentration, indicating that the increasing effect of insulin on amino acid consumption is stronger than on the urea production (Figure 5-6, Figure 5-7). In PHH the percentage of urea formed from consumed amino acids was 131-87% in the ML culture and 37-26% in the SW culture. The above described effects of insulin were also observed in PHH. The most striking difference, however, was the three times lower percentage of produced urea in the SW culture. The production rate of urea in the SW culture was 50% lower compared to the ML culture. Still, there must be a large amount of other proteins, which must be formed by PHH cultivated in SW culture as well.

Many of the here analyzed metabolic pathways and hepatic functions are zoned. Glycolysis is primarily active in the pericentral regions, whereas gluconeogenesis is mostly active in the periportal region of the liver lobule. Ammonia detoxification, which is achieved by two different processes is zoned as well. Urea formation is a typical periportal pathway with

glutamine synthesis being active in only the two innermost cell layers. In addition, also the detoxification of xenobiotics is settled in the pericentral region of the liver lobules (Brauning et al. 2006, LeCluyse et al. 2012). It has long been discussed how cultivation conditions, such as presence of insulin or glucagon or the configuration of ECM, influence the phenotype of hepatocytes in culture. Already in 1982 Probst et al. reported a pericentral hepatocyte phenotype, if insulin was present in culture, whereas glucagon induced a periportal phenotype (Probst et al. 1982). Also in our studies, we could observe how these factors can influence the cells. The cells were shown to handle ammonia stress rather differently depending on the cultivation setup, indicating a more pericentral phenotype in the ML culture (Figure 3-7). Also the lactate production rates were higher in the ML culture speaking for a higher activity of glycolysis (Figure 3-3, 5-4 and 5-5). However, the activity of CYP 3A does not fit to the pericentral phenotype, since it was considerable lower compared to the SW culture even after 24 h (Figure 6-5). Also on the proteomic level no changes were detected supporting this theory. Insulin did induce some pericentral features such as increased lactate production and glucose consumption (Figure 5-4 and 5-5). However, insulin influence on hepatic functions, e.g. urea production and CYP 3A activity, was contrary to these findings (Figure 6-3, 6-4, 6-5 and 6-6). Therefore, also in the case of insulin a shift to a certain hepatic phenotype in culture could not be confirmed. A more targeted proteomic approach directly addressing the enzymes involved in these pathways could give more insight on this topic.

The strong susceptibility of hepatic function to numerous factors such as cultivation condition, insulin concentration, nutrient availability or disease states, just to name a few, makes planning of *in vitro* liver studies challenging. Also comparability between different studies in literature becomes an issue, since *in vitro* cultivation protocols are not standardized in any way. The species-specific differences of CYP 3A activity also showed that especially in regard of drug metabolizing enzymes, it cannot directly be translated from humans to rodents or the other way around. In addition, the physiological differences of energy metabolism between mice and humans, which was shown to be reflected in *in vitro* culture, strongly hinders the use of PMH as a substitute for PHH to analyze carbon metabolism or insulin reactions. It is already known that rodent models of metabolic diseases such as THID cannot accurately represent the full spectrum of symptoms and complications (Bunner *et al.*, 2014). Taken together this leads to questioning the usefulness of murine *in vitro* cultures as well as mouse models in this special field of metabolism and metabolic disorders. Of course, *in vitro* cultures in general are always highly simplified and only represent an approximation of the actual *in vivo* physiology. Therefore, a reasonable compromise must always been made

between *in vivo* relevance (primary animal cells or cell lines), the complexity of the cultivation setup and feasibility of the planned studies.

8. Abbreviations

3-HPA	3-hydroxypicolinic acid
6PFK2/FBP2	6-phosphofructo-2-kinase/fructose-2,6-bisphosphatase
ACP	Acetyl carrier protein
AMP	Adenosine monophosphate
ANOVA	Analysis of variance
APS	Ammonium persulfate
AST	Aspartate aminotransferase
ATP	Adenosine triphosphate
BALs	Bioartificial livers
BSA	Bovine serum albumin
BSTFA	N,O-Bis(trimethylsilyl)trifluoroacetamide
cAMP	Cyclic AMP
CCA	4-chloro- α -cyanocinnamic acid
CHAPS	3-[(3-cholamidopropyl)dimethylammonio]-1-propanesulfonate hydrate
CHO	Chinese hamster ovary
CID	Collision-induced dissociation
CMFDA	5-chloromethylfluorescein diacetate
CMF	5-chloromethylfluorescein
CoA	Coenzyme A
CYP	Cytochrome P450
DAPI	4',6-diamidino-2-phenylindole
DHB	2,5-Dihydrobenzoic acid
DIGE	Difference gel electrophoresis
DMF	N,N-dimethylformamide

DNA	Deoxyribonucleic acid
DTT	Dithiothreitol
ECM	Extracellular matrix
EDTA	Ethylene diamine tetraacetic acid
EGF	Epidermal growth factor
ELISA	Enzyme-Linked Immunosorbent Assay
ER	Endoplasmatic reticulum
ESI	Electrospray ionization
F1P	Fructose 1-phosphate
F1,6BP	Fructose 1,6-bisphosphate
F1,6BPase	Fructose 1,6-bisphosphatase
F2,6BP	Fructose-2,6-bisphosphate
F6P	Fructose 6-phosphate
FA	Fatty acids
FAD/FADH ₂	Flavin adenine dinucleotide
FCS	Fetal calf serum
FFA	Free fatty acids
FT-ICR	Fourier transform ion cyclotron resonance
G1P	Glucose 1-phosphate
G6P	Glucose 6-phosphate
G6Pase	Glucose 6-phosphatase
GC	Gas chromatography
GDP	Guanosine diphosphate
GK	Glucokinase
Glut2/4	Glucose transporter 2/4
GPK	Glycogen phosphorylase kianse
GSK-3	Glycogen synthase kinase-3
GTP	Guanosine triphosphate

HCCA	α -cyano-4-hydroxycinamic acid
hESC	Human embryonal stem cells
HGF	Hepatocyte growth factor
HILIC	Hydrophilic interaction chromatography
HPLC	High performance liquid chromatography
HSC	Hepatic stellate cells
IAA	Indoleacetic acid
ICAT	Isotope-coded affinity tags
IEF	Isoelectric focusing
IPG	Immobilized pH gradient
iPSC	Induced pluripotent stem cells
ITS	Insulin/transferrine/selenium
KC	Kupffer cells
LC	Liquid chromatography
m/z	Mass to charge ratio
MALDI	Matrix-assisted laser desorption/ionization
MBDSTFA	N-(tert-Butyldimethylsilyl)-N-methyl-trifluoroacetamide
ML	Monolayer
mRNA	Messenger RNA
MS	Mass spectrometry
mTor	Mechanistic target of rapamycin
NAD ⁺ /NADH	Nicotinamide adenine dinucleotide
NADP ⁺ /NADPH	Nicotinamide adenine dinucleotide phosphate
NAFLD	Non-alcoholic fatty liver disease
NASH	non-alcoholic steatohepatitis
NMR	Nuclear magnetic resonance
PAGE	Polyacrylamide gel electrophoresis

PBS	Phosphate-buffered saline
PCA	Principle component analysis
pI	Isoelectric point
PI(3)K	Phosphatidylinositol-3 kinase
PKA	Protein kinase A
PEP	Phosphoenol pyruvate
PEPCK	Phosphoenol pyruvate carboxykinase
PFK-1	Phosphofructokinase-1
PHH	Primary human hepatocytes
PKA	Protein kinase A
PMH	Primary mouse hepatocytes
PPP	Pentose phosphate pathway
PRH	Primary rat hepatocytes
R5P	Ribose 5-phosphate
RNA	Ribonucleic acid
ROS	Reactive oxygen species
RP	Reversed phase
RT	Room temperature
SA	Sinapinic acid
SDS	Sodium dodecyl sulfate
SILAC	Stable isotope labeling by amino acids in cell culture
SREBP-1c	Sterol regulatory element binding protein-1c
SV40LT	Simian virus 40 large T antigen
SW	Sandwich
TIID	Type II diabetes
TCA	Tricarboxylic acid
TCAA	Trichloroacetic acid

TEMED	<i>N,N,N',N'</i> -tetramethylethylenediamine
TFA	Trifluoro acetic acid
TGF	Transforming growth factor
TNF α	Tumor necrosis factor α
ToF	Time of flight
TRIS	Tris(hydroxymethyl)aminomethane
UDP	Uridine-5'-diphosphate
UPLC	Ultra high performance liquid chromatography
UTP	Uridine-5'-triphosphate
UV	Ultraviolet
w/v	weight per volume
WME	William's medium E

9. References

- Achilli T-M, Meyer J, Morgan JR. Advances in the formation, use and understanding of multi-cellular spheroids. *Expert Opin. Biol. Ther.* 2012 Oct;12(10):1347–60.
- Ader M, Stefanovski D, Kim SP, Richey JM, Ionut V, Catalano KJ, et al. Hepatic insulin clearance is the primary determinant of insulin sensitivity in the normal dog. *Obes. Silver Spring Md.* 2014 May;22(5):1238–45.
- Agustanti N, Djumhana A, Abdurachman SA, Nmn S. Correlation between Serum Albumin and Fasting Blood Glucose Level in Patients with Liver Cirrhosis. *Indones. J. Gastroenterol. Hepatol. Dig. Endosc.* 2014 Dec 1;15(3):143–6.
- Alépée N, Bahinski A, Daneshian M, De Wever B, Fritsche E, Goldberg A, et al. State-of-the-art of 3D cultures (organs-on-a-chip) in safety testing and pathophysiology. *ALTEX.* 2014;31(4):441–77.
- Allen JW, Khetani SR, Bhatia SN. In Vitro Zonation and Toxicity in a Hepatocyte Bioreactor. *Toxicol. Sci.* 2005 Jan 3;84(1):110–9.
- Allen SW, Mueller L, Williams SN, Quattrochi LC, Raucy J. The use of a high-volume screening procedure to assess the effects of dietary flavonoids on human cyp1a1 expression. *Drug Metab. Dispos. Biol. Fate Chem.* 2001 Aug;29(8):1074–9.
- Altelaar AFM, Munoz J, Heck AJR. Next-generation proteomics: towards an integrative view of proteome dynamics. *Nat. Rev. Genet.* 2013 Jan;14(1):35–48.
- American Diabetes Association. Screening for Type 2 Diabetes. *Diabetes Care.* 1998 Jan 1;21(Supplement 1):S20–2.
- Ananthanarayanan A, Narmada BC, Mo X, McMillian M, Yu H. Purpose-driven biomaterials research in liver-tissue engineering. *Trends Biotechnol.* 2011;29(3):110–8.
- Aninat C, Piton A, Glaise D, Charpentier TL, Langouët S, Morel F, et al. Expression of Cytochromes P450, Conjugating Enzymes and Nuclear Receptors in Human Hepatoma HepaRG Cells. *Drug Metab. Dispos.* 2006 Jan 1;34(1):75–83.
- Apel K, Hirt H. Reactive oxygen species: metabolism, oxidative stress, and signal transduction. *Annu. Rev. Plant Biol.* 2004;55:373–99.

- Athersuch T. Metabolome analyses in exposome studies: Profiling methods for a vast chemical space. *Arch. Biochem. Biophys.* 2016 Jan 1;589:177–86.
- Azimifar SB, Nagaraj N, Cox J, Mann M. Cell-type-resolved quantitative proteomics of murine liver. *Cell Metab.* 2014 Dec 2;20(6):1076–87.
- Badylak SF. The extracellular matrix as a scaffold for tissue reconstruction. *Semin. Cell Dev. Biol.* 2002 Oct;13(5):377–83.
- Bantscheff M, Lemeer S, Savitski MM, Kuster B. Quantitative mass spectrometry in proteomics: critical review update from 2007 to the present. *Anal. Bioanal. Chem.* 2012 Sep;404(4):939–65.
- Bechmann LP, Hannivoort RA, Gerken G, Hotamisligil GS, Trauner M, Canbay A. The interaction of hepatic lipid and glucose metabolism in liver diseases. *J. Hepatol.* 2012 Apr;56(4):952–64.
- Beger RD, Sun J, Schnackenberg LK. Metabolomics approaches for discovering biomarkers of drug-induced hepatotoxicity and nephrotoxicity. *Toxicol. Appl. Pharmacol.* 2010 Mar 1;243(2):154–66.
- Beigel J, Fella K, Kramer P-J, Kroeger M, Hewitt P. Genomics and proteomics analysis of cultured primary rat hepatocytes. *Toxicol. Vitro Int. J. Publ. Assoc. BIBRA.* 2008 Feb;22(1):171–81.
- Bell EL, Guarente L. The SirT3 divining rod points to oxidative stress. *Mol. Cell.* 2011 Jun 10;42(5):561–8.
- Bensimon A, Heck AJR, Aebersold R. Mass spectrometry-based proteomics and network biology. *Annu. Rev. Biochem.* 2012;81:379–405.
- Berthiaume F, Moghe PV, Toner M, Yarmush ML. Effect of extracellular matrix topology on cell structure, function, and physiological responsiveness: hepatocytes cultured in a sandwich configuration. *Faseb J.* 1996;10(13):1471–84.
- Bhala N, Angulo P, van der Poorten D, Lee E, Hui JM, Saracco G, et al. The natural history of nonalcoholic fatty liver disease with advanced fibrosis or cirrhosis: An international collaborative study. *Hepatology.* 2011 Oct 1;54(4):1208–16.

- Bhatia SN, Ingber DE. Microfluidic organs-on-chips. *Nat. Biotechnol.* 2014 Aug;32(8):760–72.
- Birkenstock T, Liebeke M, Winstel V, Krismer B, Gekeler C, Niemiec MJ, et al. Exometabolome Analysis Identifies Pyruvate Dehydrogenase as a Target for the Antibiotic Triphenylbismuthdichloride in Multiresistant Bacterial Pathogens. *J. Biol. Chem.* 2012 Jan 20;287(4):2887–95.
- Blank LM, Kuepfer L, Sauer U. Large-scale ¹³C-flux analysis reveals mechanistic principles of metabolic network robustness to null mutations in yeast. *Genome Biol.* 2005;6(6):R49.
- Boccard J, Veuthey J-L, Rudaz S. Knowledge discovery in metabolomics: An overview of MS data handling. *J. Sep. Sci.* 2009;33(3):290–304.
- Bollard ME, Keun HC, Beckonert O, Ebbels TMD, Antti H, Nicholls AW, et al. Comparative metabolomics of differential hydrazine toxicity in the rat and mouse. *Toxicol. Appl. Pharmacol.* 2005 Apr 15;204(2):135–51.
- Bradford MM. A rapid and sensitive method for the quantitation of microgram quantities of protein utilizing the principle of protein-dye binding. *Anal. Biochem.* 1976 May 7;72(1–2):248–54.
- Braeuning A, Ittrich C, Köhle C, Hailfinger S, Bonin M, Buchmann A, et al. Differential gene expression in periportal and perivenous mouse hepatocytes. *FEBS J.* 2006 Nov 1;273(22):5051–61.
- Brown LA, Arterburn LM, Miller AP, Cowger NL, Hartley SM, Andrews A, et al. Maintenance of liver functions in rat hepatocytes cultured as spheroids in a rotating wall vessel. *In Vitro Cell. Dev. Biol. Anim.* 2003 Feb;39(1–2):13–20.
- Brulport M, Schormann W, Bauer A, Hermes M, Elsner C, Hammersen FJ, et al. Fate of extrahepatic human stem and precursor cells after transplantation into mouse livers. *Hepatology.* 2007 Sep;46(3):861–70.
- Bryant DM, Mostov KE. From cells to organs: building polarized tissue. *Nat Rev Mol Cell Biol.* 2008;9(11):887–901.
- Buchholz J, Strother A, Fraser IM. Effect of Glucose Administration on Various Rat Hepatic Constituents and on the Spectral Binding of Hexobarbital and Methadone to Rat Hepatic Cytochrome P450. *Pharmacology.* 1989;38(2):129–36.

- Bunner AE, Chandrasekera PC, Barnard ND. Knockout mouse models of insulin signaling: Relevance past and future. *World J. Diabetes.* 2014 Apr 15;5(2):146–59.
- Butterworth RF, Giguère J-F, Michaud J, Lavoie J, Layrargues GP. Ammonia: Key factor in the pathogenesis of hepatic encephalopathy. *Neurochem. Pathol.* 1987 Feb;6(1–2):1–12.
- Cantz T, Nies AT, Brom M, Hofmann AF, Keppler D. MRP2, a human conjugate export pump, is present and transports fluo 3 into apical vacuoles of Hep G2 cells. *Am J Physiol Gastrointest Liver Physiol.* 2000;278(4):G522–31.
- Carpentier B, Gautier A, Legallais C. Artificial and bioartificial liver devices: present and future. *Gut.* 2009 Jan 12;58(12):1690–702.
- Celi FS. Brown Adipose Tissue — When It Pays to Be Inefficient. *N. Engl. J. Med.* 2009 Apr 9;360(15):1553–6.
- Chan C, Berthiaume F, Lee K, Yarmush ML. Metabolic flux analysis of hepatocyte function in hormone- and amino acid-supplemented plasma. *Metab. Eng.* 2003 Jan;5(1):1–15.
- Cheatham B, Kahn CR. Insulin action and the insulin signaling network. *Endocr. Rev.* 1995 Apr;16(2):117–42.
- Cherrington AD. Banting Lecture 1997. Control of glucose uptake and release by the liver in vivo. *Diabetes.* 1999 May;48(5):1198–214.
- Clark S, Francis PS, Conlan XA, Barnett NW. Determination of urea using high-performance liquid chromatography with fluorescence detection after automated derivatisation with xanthidrol. *J Chromatogr A.* 2007;1161(1–2):207–13.
- Corkey BE, Glennon MC, Chen KS, Deeney JT, Matschinsky FM, Prentki M. A role for malonyl-CoA in glucose-stimulated insulin secretion from clonal pancreatic beta-cells. *J. Biol. Chem.* 1989 Dec 25;264(36):21608–12.
- Cox DG, Oh J, Keasling A, Colson KL, Hamann MT. The utility of metabolomics in natural product and biomarker characterization. *Biochim. Biophys. Acta.* 2014 Dec;1840(12):3460–74.
- Dahn MS, Hsu CJ, Lange MP, Jefferson LS. Effects of tumor necrosis factor-alpha on glucose and albumin production in primary cultures of rat hepatocytes. *Metabolism.* 1994 Apr;43(4):476–80.

- Dall TM, Zhang Y, Chen YJ, Quick WW, Yang WG, Fogli J. The Economic Burden Of Diabetes. *Health Aff. (Millwood)*. 2010 Jan 2;29(2):297–303.
- Damm G, Pfeiffer E, Burkhardt B, Vermehren J, Nüssler AK, Weiss TS. Human parenchymal and non-parenchymal liver cell isolation, culture and characterization. *Hepatol. Int.* 2013 Oct 1;7(4):951–8.
- Davis GL, Roberts WL. The Healthcare Burden Imposed by Liver Disease in Aging Baby Boomers. *Curr. Gastroenterol. Rep.* 2010 Feb 1;12(1):1–6.
- De Waziers I, Garlatti M, Bouguet J, Beaune PH, Barouki R. Insulin down-regulates cytochrome P450 2B and 2E expression at the post-transcriptional level in the rat hepatoma cell line. *Mol. Pharmacol.* 1995 Mar;47(3):474–9.
- Decaens C, Durand M, Grosse B, Cassio D. Which in vitro models could be best used to study hepatocyte polarity? *Biol Cell.* 2008;100(7):387–98.
- Dersch LM, Beckers V, Wittmann C. Green pathways: Metabolic network analysis of plant systems. *Metab. Eng.* 2016 Mar;34:1–24.
- Diamond DL, Prohl SC, Jacobs JM, Chan EY, Camp DG, Smith RD, et al. HepatoProteomics: applying proteomic technologies to the study of liver function and disease. *Hepatol. Baltim. Md.* 2006 Aug;44(2):299–308.
- Dooley S, Delvoux B, Lahme B, Mangasser-Stephan K, Gressner AM. Modulation of transforming growth factor beta response and signaling during transdifferentiation of rat hepatic stellate cells to myofibroblasts. *Hepatol. Baltim. Md.* 2000 May;31(5):1094–106.
- Dooley S, Hamzavi J, Breitkopf K, Wiercinska E, Said HM, Lorenzen J, et al. Smad7 prevents activation of hepatic stellate cells and liver fibrosis in rats. *Gastroenterology.* 2003;125(1):178–91.
- Draznin B. Insulin signaling network -- waiting for Copernicus. *Endocrinology.* 1996 Jul;137(7):2647–8.
- Duckworth WC, Bennett RG, Hamel FG. The significance of intracellular insulin to insulin action. *J. Investig. Med. Off. Publ. Am. Fed. Clin. Res.* 1997 Feb;45(2):20–7.
- Duckworth WC, Bennett RG, Hamel FG. Insulin Acts Intracellularly on Proteasomes through Insulin-Degrading Enzyme. *Biochem. Biophys. Res. Commun.* 1998a Mar 17;244(2):390–4.

- Duckworth WC, Bennett RG, Hamel FG. Insulin degradation: progress and potential. *Endocr. Rev.* 1998b Oct;19(5):608–24.
- Duckworth WC, Hamel FG, Peavy DE. Hepatic metabolism of insulin. *Am. J. Med.* 1988 Nov 28;85(5A):71–6.
- Dunn JC, Tompkins RG, Yarmush ML. Long-term in vitro function of adult hepatocytes in a collagen sandwich configuration. *Biotechnol Prog.* 1991;7(3):237–45.
- Dunn JC, Tompkins RG, Yarmush ML. Hepatocytes in collagen sandwich: evidence for transcriptional and translational regulation. *J. Cell Biol.* 1992 Feb;116(4):1043–53.
- Elcombe CR, Peffer RC, Wolf DC, Bailey J, Bars R, Bell D, et al. Mode of action and human relevance analysis for nuclear receptor-mediated liver toxicity: A case study with phenobarbital as a model constitutive androstane receptor (CAR) activator. *Crit. Rev. Toxicol.* 2014 Jan 1;44(1):64–82.
- Ellis DI, Dunn WB, Griffin JL, Allwood JW, Goodacre R. Metabolic fingerprinting as a diagnostic tool. *Pharmacogenomics.* 2007 Sep;8(9):1243–66.
- Espina V, Edmiston KH, Heiby M, Pierobon M, Sciro M, Merritt B, et al. A portrait of tissue phosphoprotein stability in the clinical tissue procurement process. *Mol. Cell. Proteomics MCP.* 2008 Oct;7(10):1998–2018.
- Europa AF, Gambhir A, Fu P-C, Hu W-S. Multiple steady states with distinct cellular metabolism in continuous culture of mammalian cells. *Biotechnol. Bioeng.* 2000 Jan 5;67(1):25–34.
- Exton JH, Lewis SB, Ho RJ, Robison GA, Park CR. The Role of Cyclic Amp in the Interaction of Glucagon and Insulin in the Control of Liver Metabolism*. *Ann. N. Y. Acad. Sci.* 1971 Dec 1;185(1):85–100.
- Ezzell RM, Toner M, Hendricks K, Dunn JC, Tompkins RG, Yarmush ML. Effect of collagen gel configuration on the cytoskeleton in cultured rat hepatocytes. *Exp Cell Res.* 1993;208(2):442–52.
- Farkas D, Bhat VB, Mandapati S, Wishnok JS, Tannenbaum SR. Characterization of the secreted proteome of rat hepatocytes cultured in collagen sandwiches. *Chem. Res. Toxicol.* 2005 Jul;18(7):1132–9.

- Feidt DM, Klein K, Hofmann U, Riedmaier S, Knobloch D, Thasler WE, et al. Profiling induction of cytochrome p450 enzyme activity by statins using a new liquid chromatography-tandem mass spectrometry cocktail assay in human hepatocytes. *Drug Metab. Dispos. Biol. Fate Chem.* 2010 Sep;38(9):1589–97.
- Feierman DE, Melnikov Z, Zhang J. The paradoxical effect of acetaminophen on CYP3A4 activity and content in transfected HepG2 cells. *Arch. Biochem. Biophys.* 2002 Feb 1;398(1):109–17.
- Fenn JB, Mann M, Meng CK, Wong SF, Whitehouse CM. Electrospray ionization for mass spectrometry of large biomolecules. *Science.* 1989 Oct 6;246(4926):64–71.
- Fiehn O, Kopka J, Dörmann P, Altmann T, Trethewey RN, Willmitzer L. Metabolite profiling for plant functional genomics. *Nat. Biotechnol.* 2000 Nov;18(11):1157–61.
- Friedman SL. Hepatic stellate cells: protean, multifunctional, and enigmatic cells of the liver. *Physiol Rev.* 2008;88(1):125–72.
- Friedrich N. Metabolomics in diabetes research. *J. Endocrinol.* 2012 Jan 10;215(1):29–42.
- Garfin DE. Two-dimensional gel electrophoresis: an overview. *TrAC Trends Anal. Chem.* 2003 May;22(5):263–72.
- Gebhardt R. Metabolic zonation of the liver: regulation and implications for liver function. *Pharmacol Ther.* 1992;53(3):275–354.
- Gebhardt R, Matz-Soja M. Liver zonation: Novel aspects of its regulation and its impact on homeostasis. *World J. Gastroenterol. WJG.* 2014 Jul 14;20(26):8491–504.
- Gerber SA, Rush J, Stemman O, Kirschner MW, Gygi SP. Absolute quantification of proteins and phosphoproteins from cell lysates by tandem MS. *Proc. Natl. Acad. Sci. U. S. A.* 2003 Jun 10;100(12):6940–5.
- Gerets HHJ, Tilmant K, Gerin B, Chanteux H, Depelchin BO, Dhalluin S, et al. Characterization of primary human hepatocytes, HepG2 cells, and HepaRG cells at the mRNA level and CYP activity in response to inducers and their predictivity for the detection of human hepatotoxins. *Cell Biol. Toxicol.* 2012 Apr;28(2):69–87.

- Ghafoory S, Breitkopf-Heinlein K, Li Q, Scholl C, Dooley S, Wöfl S. Zonation of Nitrogen and Glucose Metabolism Gene Expression upon Acute Liver Damage in Mouse. *PLoS ONE*. 2013 Oct 17;8(10):e78262.
- Gharbi S, Gaffney P, Yang A, Zvelebil MJ, Cramer R, Waterfield MD, et al. Evaluation of two-dimensional differential gel electrophoresis for proteomic expression analysis of a model breast cancer cell system. *Mol. Cell. Proteomics MCP*. 2002 Feb;1(2):91–8.
- Gille C, Bolling C, Hoppe A, Bulik S, Hoffmann S, Hubner K, et al. HepatoNet1: a comprehensive metabolic reconstruction of the human hepatocyte for the analysis of liver physiology. *Mol Syst Biol*. 2010;6:411.
- Godoy P, Hengstler JG, Ilkavets I, Meyer C, Bachmann A, Muller A, et al. Extracellular matrix modulates sensitivity of hepatocytes to fibroblastoid dedifferentiation and transforming growth factor beta-induced apoptosis. *Hepatology*. 2009;49(6):2031–43.
- Godoy P, Lakkapamu S, Schug M, Bauer A, Stewart JD, Bedawi E, et al. Dexamethasone-dependent versus -independent markers of epithelial to mesenchymal transition in primary hepatocytes. *Biol. Chem*. 2010 Jan;391(1):73–83.
- Gonnet F, Lemaître G, Waksman G, Tortajada J. MALDI/MS peptide mass fingerprinting for proteome analysis: identification of hydrophobic proteins attached to eucaryote keratinocyte cytoplasmic membrane using different matrices in concert. *Proteome Sci*. 2003 May 6;1(1):2.
- Goto T, Onuma T, Takebe K, Kral JG. The influence of fatty liver on insulin clearance and insulin resistance in non-diabetic Japanese subjects. *Int. J. Obes. Relat. Metab. Disord. J. Int. Assoc. Study Obes*. 1995 Dec;19(12):841–5.
- Gowda GN, Zhang S, Gu H, Asiago V, Shanaiah N, Raftery D. Metabolomics-based methods for early disease diagnostics. *Expert Rev. Mol. Diagn*. 2008 Sep 1;8(5):617–33.
- Gozal D, Jortani S, Snow AB, Kheirandish-Gozal L, Bhattacharjee R, Kim J, et al. Two-dimensional differential in-gel electrophoresis proteomic approaches reveal urine candidate biomarkers in pediatric obstructive sleep apnea. *Am. J. Respir. Crit. Care Med*. 2009 Dec 15;180(12):1253–61.
- Griffiths WJ, Koal T, Wang Y, Kohl M, Enot DP, Deigner H-P. Targeted Metabolomics for Biomarker Discovery. *Angew. Chem. Int. Ed*. 2010 Jul 26;49(32):5426–45.

- Guguen-Guillouzo C, Corlu A, Guillouzo A. Stem cell-derived hepatocytes and their use in toxicology. *Toxicology*. 2010 Mar 30;270(1):3–9.
- Guillarme D, Ruta J, Rudaz S, Veuthey J-L. New trends in fast and high-resolution liquid chromatography: a critical comparison of existing approaches. *Anal. Bioanal. Chem.* 2010 Jun;397(3):1069–82.
- Haas S, Jahnke H-G, Moerbt N, von Bergen M, Aharinejad S, Andrukhova O, et al. DIGE proteome analysis reveals suitability of ischemic cardiac in vitro model for studying cellular response to acute ischemia and regeneration. *PloS One*. 2012;7(2):e31669.
- Halliwell B. Reactive oxygen species in living systems: Source, biochemistry, and role in human disease. *Am. J. Med.* 1991 Sep 30;91(3, Supplement 3):S14–22.
- Hamberg O, Vilstrup H. Effects of insulin and glucose on urea synthesis in normal man, independent of pancreatic hormone secretion. *J. Hepatol.* 1994 Sep;21(3):381–7.
- Hamilton GA, Jolley SL, Gilbert D, Coon DJ, Barros S, LeCluyse EL. Regulation of cell morphology and cytochrome P450 expression in human hepatocytes by extracellular matrix and cell-cell interactions. *Cell Tissue Res.* 2001;306(1):85–99.
- Hasegawa Y, Kishimoto S, Shibatani N, Inotsume N, Takeuchi Y, Fukushima S. Effects of insulin on CYP3A activity and nifedipine disposition in streptozotocin-induced diabetic rats. *J. Pharm. Pharmacol.* 2010 Jul;62(7):883–9.
- Hengstler JG, Godoy P, Bolt HM. The dilemma of cultivated hepatocytes. *Arch Toxicol.* 2009;83(2):101–3.
- Henningson R, Lundquist I. Arginine-induced insulin release is decreased and glucagon increased in parallel with islet NO production. *Am. J. Physiol. - Endocrinol. Metab.* 1998 Sep 1;275(3):E500–6.
- Hers HG, De Wulf H, Stalmans W. The control of glycogen metabolism in the liver. *FEBS Lett.* 1970 Dec 28;12(2):73–82.
- Heslop JA, Rowe C, Walsh J, Sison-Young R, Jenkins R, Kamalian L, et al. Mechanistic evaluation of primary human hepatocyte culture using global proteomic analysis reveals a selective dedifferentiation profile. *Arch. Toxicol.* 2016 Apr 2;

- Hewitt NJ, Hewitt P. Phase I and II enzyme characterization of two sources of HepG2 cell lines. *Xenobiotica*. 2004 Mar 1;34(3):243–56.
- Höhme S, Hengstler JG, Brulport M, Schäfer M, Bauer A, Gebhardt R, et al. Mathematical modelling of liver regeneration after intoxication with CCl₄. *Chem. Biol. Interact.* 2007 May 20;168(1):74–93.
- Hollywood K, Brison DR, Goodacre R. Metabolomics: current technologies and future trends. *Proteomics*. 2006 Sep;6(17):4716–23.
- Holmes AM, Creton S, Chapman K. Working in partnership to advance the 3Rs in toxicity testing. *Toxicology*. 2010 Jan 12;267(1–3):14–9.
- Hynes RO. The Extracellular Matrix: Not Just Pretty Fibrils. *Science*. 2009 Nov 27;326(5957):1216–9.
- Iredale JP, Arthur MJ. Hepatocyte-matrix interactions. *Gut*. 1994;35(6):729–32.
- Jasmund I, Schwientek S, Acikgöz A, Langsch A, Machens HG, Bader A. The influence of medium composition and matrix on long-term cultivation of primary porcine and human hepatocytes. *Biomol. Eng.* 2007 Feb;24(1):59–69.
- Jeschke MG, Rensing H, Klein D, Schubert T, Mautes AEM, Bolder U, et al. Insulin prevents liver damage and preserves liver function in lipopolysaccharide-induced endotoxemic rats. *J. Hepatol.* 2005 Jun;42(6):870–9.
- Jitrapakdee S. Transcription factors and coactivators controlling nutrient and hormonal regulation of hepatic gluconeogenesis. *Int. J. Biochem. Cell Biol.* 2012 Jan;44(1):33–45.
- Johnson JD, Bernal-Mizrachi E, Alejandro EU, Han Z, Kalynyak TB, Li H, et al. Insulin protects islets from apoptosis via Pdx1 and specific changes in the human islet proteome. *Proc. Natl. Acad. Sci. U. S. A.* 2006 Dec 19;103(51):19575–80.
- Jossé R, Aninat C, Glaise D, Dumont J, Fessard V, Morel F, et al. Long-term functional stability of human HepaRG hepatocytes and use for chronic toxicity and genotoxicity studies. *Drug Metab. Dispos. Biol. Fate Chem.* 2008 Jun;36(6):1111–8.
- Jungermann K, Kietzmann T. Zonation of parenchymal and nonparenchymal metabolism in liver. *Annu Rev Nutr.* 1996;16:179–203.

- Jungermann K, Kietzmann T. Oxygen: Modulator of metabolic zonation and disease of the liver. *Hepatology*. 2000 Feb 1;31(2):255–60.
- Kamp H, Fabian E, Groeters S, Herold M, Krennrich G, Looser R, et al. Application of in vivo metabolomics to preclinical/toxicological studies: case study on phenytoin-induced systemic toxicity. *Bioanalysis*. 2012 Sep;4(18):2291–301.
- Kanebratt KP, Andersson TB. Evaluation of HepaRG Cells as an in Vitro Model for Human Drug Metabolism Studies. *Drug Metab. Dispos.* 2008 Jan 7;36(7):1444–52.
- Kanuri G, Bergheim I. In Vitro and in Vivo Models of Non-Alcoholic Fatty Liver Disease (NAFLD). *Int. J. Mol. Sci.* 2013;14(6):11963–80.
- Karas M, Krüger R. Ion Formation in MALDI: The Cluster Ionization Mechanism. *Chem. Rev.* 2003 Feb 1;103(2):427–40.
- Kasture VS, Musmade DS, B.Vakte M, Patil SBS and PP. Metabolomics: Current Technologies and Future Trends. *Int. J. Res. Dev. Pharm. Life Sci.* 2012
- Katz J, McGarry JD. The glucose paradox. Is glucose a substrate for liver metabolism? *J. Clin. Invest.* 1984 Dec;74(6):1901–9.
- Kern A, Bader A, Pichlmayr R, Sewing K-F. Drug metabolism in hepatocyte sandwich cultures of rats and humans. *Biochem. Pharmacol.* 1997 Oct 1;54(7):761–72.
- Kiang TKL, Teng XW, Surendradoss J, Karagiozov S, Abbott FS, Chang TKH. Glutathione depletion by valproic acid in sandwich-cultured rat hepatocytes: Role of biotransformation and temporal relationship with onset of toxicity. *Toxicol. Appl. Pharmacol.* 2011 May 1;252(3):318–24.
- Kienhuis AS, Wortelboer HM, Maas WJ, van Herwijnen M, Kleinjans JCS, van Delft JHM, et al. A sandwich-cultured rat hepatocyte system with increased metabolic competence evaluated by gene expression profiling. *Toxicol. Vitro Int. J. Publ. Assoc. BIBRA.* 2007 Aug;21(5):892–901.
- Kietzmann T, Dimova EY, Flugel D, Scharf JG. Oxygen: modulator of physiological and pathophysiological processes in the liver. *Z Gastroenterol.* 2006;44(1):67–76.
- Kietzmann T, Hirsch-Ernst KI, Kahl GF, Jungermann K. Mimicry in primary rat hepatocyte cultures of the in vivo perivenous induction by phenobarbital of cytochrome P-450 2B1

- mRNA: role of epidermal growth factor and perivenous oxygen tension. *Mol. Pharmacol.* 1999 Jul;56(1):46–53.
- Kietzmann T, Roth U, Freimann S, Jungermann K. Arterial oxygen partial pressures reduce the insulin-dependent induction of the perivenously located glucokinase in rat hepatocyte cultures: mimicry of arterial oxygen pressures by H₂O₂. *Biochem J.* 1997;321 (Pt 1):17–20.
- Kim J, Dang CV. Cancer's Molecular Sweet Tooth and the Warburg Effect. *Cancer Res.* 2006 Sep 15;66(18):8927–30.
- Kim K, Ohashi K, Utoh R, Kano K, Okano T. Preserved liver-specific functions of hepatocytes in 3D co-culture with endothelial cell sheets. *Biomaterials.* 2012 Feb;33(5):1406–13.
- Kim S-Y, Kim H, Kim T-H, Im S-S, Park S-K, Lee I-K, et al. SREBP-1c mediates the insulin-dependent hepatic glucokinase expression. *J. Biol. Chem.* 2004 Jul 16;279(29):30823–9.
- Kitano H. Biological robustness. *Nat. Rev. Genet.* 2004 Nov;5(11):826–37.
- Klein T, Heinzle E, Schneider K. Acetate-containing substrate mixtures improve recombinant protein secretion in *Schizosaccharomyces pombe*. *Eng. Life Sci.* 2015 May 1;15(4):437–42.
- Klein T, Lange S, Wilhelm N, Bureik M, Yang T-H, Heinzle E, et al. Overcoming the metabolic burden of protein secretion in *Schizosaccharomyces pombe*--a quantitative approach using ¹³C-based metabolic flux analysis. *Metab. Eng.* 2014 Jan;21:34–45.
- Klingmüller U, Bauer A, Bohl S, Nickel PJ, Breitkopf K, Dooley S, et al. Primary mouse hepatocytes for systems biology approaches: a standardized in vitro system for modelling of signal transduction pathways. *Syst Biol Stevenage.* 2006;153(6):433–47.
- Klover PJ, Mooney RA. Hepatocytes: critical for glucose homeostasis. *Int. J. Biochem. Cell Biol.* 2004 May;36(5):753–8.
- Koebe HG, Pahernik S, Eyer P, Schildberg FW. Collagen gel immobilization: a useful cell culture technique for long-term metabolic studies on human hepatocytes. *Xenobiotica.* 1994;24(2):95–107.

- Kohlstedt M, Becker J, Wittmann C. Metabolic fluxes and beyond-systems biology understanding and engineering of microbial metabolism. *Appl. Microbiol. Biotechnol.* 2010 Nov;88(5):1065–75.
- König M, Bulik S, Holzhütter H-G. Quantifying the Contribution of the Liver to Glucose Homeostasis: A Detailed Kinetic Model of Human Hepatic Glucose Metabolism. *PLoS Comput Biol.* 2012 Jun 21;8(6):e1002577.
- König M, Holzhütter H-G. Kinetic modeling of human hepatic glucose metabolism in type 2 diabetes mellitus predicts higher risk of hypoglycemic events in rigorous insulin therapy. *J. Biol. Chem.* 2012 Oct 26;287(44):36978–89.
- Kopka J. Current challenges and developments in GC-MS based metabolite profiling technology. *J Biotechnol.* 2006;124(1):312–22.
- Kostadinova R, Boess F, Applegate D, Suter L, Weiser T, Singer T, et al. A long-term three dimensional liver co-culture system for improved prediction of clinically relevant drug-induced hepatotoxicity. *Toxicol. Appl. Pharmacol.* 2013 Apr 1;268(1):1–16.
- Kowalski GM, Bruce CR. The regulation of glucose metabolism: implications and considerations for the assessment of glucose homeostasis in rodents. *Am. J. Physiol. Endocrinol. Metab.* 2014 Nov 15;307(10):E859-871.
- Krause P, Saghatolislam F, Koenig S, Unthan-Fechner K, Probst I. Maintaining hepatocyte differentiation in vitro through co-culture with hepatic stellate cells. *Vitro Cell. Dev. Biol. - Anim.* 2009 Jan 28;45(5–6):205–12.
- Krewski D, Acosta D, Andersen M, Anderson H, Bailar JC, Boekelheide K, et al. Toxicity Testing in the 21st Century: A Vision and a Strategy. *J. Toxicol. Environ. Health B Crit. Rev.* 2010 Feb;13(0):51–138.
- Kuepfer L. Towards whole-body systems physiology. *Mol Syst Biol.* 2010;6:409.
- Lambert CB, Spire C, Claude N, Guillouzo A. Dose- and time-dependent effects of phenobarbital on gene expression profiling in human hepatoma HepaRG cells. *Toxicol. Appl. Pharmacol.* 2009 Feb 1;234(3):345–60.
- Latta M, Künstle G, Leist M, Wendel A. Metabolic Depletion of Atp by Fructose Inversely Controls Cd95- and Tumor Necrosis Factor Receptor 1–Mediated Hepatic Apoptosis. *J. Exp. Med.* 2000 May 6;191(11):1975–86.

- LeCluyse EL, Audus KL, Hochman JH. Formation of extensive canalicular networks by rat hepatocytes cultured in collagen-sandwich configuration. *Am J Physiol.* 1994;266(6 Pt 1):C1764-74.
- LeCluyse EL, Fix JA, Audus KL, Hochman JH. Regeneration and maintenance of bile canalicular networks in collagen-sandwiched hepatocytes. *Toxicol Vitro.* 2000;14(2):117–32.
- LeCluyse EL, Witek RP, Andersen ME, Powers MJ. Organotypic liver culture models: Meeting current challenges in toxicity testing. *Crit. Rev. Toxicol.* 2012 Jul;42(6):501–48.
- Lee CC, Haffner SM, Wagenknecht LE, Lorenzo C, Norris JM, Bergman RN, et al. Insulin Clearance and the Incidence of Type 2 Diabetes in Hispanics and African Americans The IRAS Family Study. *Diabetes Care.* 2013a Jan 4;36(4):901–7.
- Lee CC, Haffner SM, Wagenknecht LE, Lorenzo C, Norris JM, Bergman RN, et al. Insulin Clearance and the Incidence of Type 2 Diabetes in Hispanics and African Americans The IRAS Family Study. *Diabetes Care.* 2013b Jan 4;36(4):901–7.
- Lei Z, Huhman DV, Sumner LW. Mass spectrometry strategies in metabolomics. *J. Biol. Chem.* 2011 Jul 22;286(29):25435–42.
- Lilienblum W, Dekant W, Foth H, Gebel T, Hengstler JG, Kahl R, et al. Alternative methods to safety studies in experimental animals: role in the risk assessment of chemicals under the new European Chemicals Legislation (REACH). *Arch. Toxicol.* 2008 Apr;82(4):211–36.
- Lilley KS, Friedman DB. All about DIGE: quantification technology for differential-display 2D-gel proteomics. *Expert Rev. Proteomics.* 2004 Dec;1(4):401–9.
- Lindon JC, Holmes E, Nicholson JK. Metabonomics Techniques and Applications to Pharmaceutical Research & Development. *Pharm. Res.* 2006 Jun 1;23(6):1075–88.
- Lu Y, Zhang G, Shen C, Uygun K, Yarmush ML, Meng Q. A novel 3D liver organoid system for elucidation of hepatic glucose metabolism. *Biotechnol. Bioeng.* 2012 Feb;109(2):595–604.
- Lynch T, Price A. The effect of cytochrome P450 metabolism on drug response, interactions, and adverse effects. *Am. Fam. Physician.* 2007 Aug 1;76(3):391–6.
- MacDonald MJ, Longacre MJ, Stoker SW, Kendrick M, Thonpho A, Brown LJ, et al. Differences between human and rodent pancreatic islets: low pyruvate carboxylase, atp citrate

- lyase, and pyruvate carboxylation and high glucose-stimulated acetoacetate in human pancreatic islets. *J. Biol. Chem.* 2011 May 27;286(21):18383–96.
- Maher JJ, Friedman SL. Parenchymal and nonparenchymal cell interactions in the liver. *Semin Liver Dis.* 1993;13(1):13–20.
- Maier K, Hofmann U, Reuss M, Mauch K. Dynamics and Control of the Central Carbon Metabolism in Hepatoma Cells. *BMC Syst. Biol.* 2010 Apr 28;4(1):54.
- Malaisse WJ, Sener A, Herchuelz A, Hutton JC. Insulin release: The fuel hypothesis. *Metabolism.* 1979 Apr;28(4):373–86.
- Mandenius C-F, Andersson TB, Alves PM, Batzl-Hartmann C, Björquist P, Carrondo MJT, et al. Toward preclinical predictive drug testing for metabolism and hepatotoxicity by using in vitro models derived from human embryonic stem cells and human cell lines - a report on the Vitrocellomics EU-project. *Altern. Lab. Anim. ATLA.* 2011 May;39(2):147–71.
- Martignoni M, Groothuis GMM, Kanter R de. Species differences between mouse, rat, dog, monkey and human CYP-mediated drug metabolism, inhibition and induction. *Expert Opin. Drug Metab. Toxicol.* 2006 Dec 1;2(6):875–94.
- Martínez Sánchez J, Ehnert S, Nüssler A, Yan X, Schyschka L. Entrapment of primary human hepatocytes in extracellular matrix gels for long term toxicity studies. *Z. Für Gastroenterol.* [Internet]. 2012 Jan 9 [cited 2012 Dec 10];50(1). Available from: <https://www.thieme-connect.com/ejournals/abstract/10.1055/s-0031-1295862>
- Mattes W, Davis K, Fabian E, Greenhaw J, Herold M, Looser R, et al. Detection of hepatotoxicity potential with metabolite profiling (metabolomics) of rat plasma. *Toxicol. Lett.* 2014 Nov 4;230(3):467–78.
- Mattes WB, Kamp HG, Fabian E, Herold M, Krennrich G, Looser R, et al. Prediction of Clinically Relevant Safety Signals of Nephrotoxicity through Plasma Metabolite Profiling, Prediction of Clinically Relevant Safety Signals of Nephrotoxicity through Plasma Metabolite Profiling. *BioMed Res. Int. BioMed Res. Int.* 2013 May 21;2013, 2013:e202497.
- McGarry JD, Foster DW. Regulation of hepatic fatty acid oxidation and ketone body production. *Annu. Rev. Biochem.* 1980;49:395–420.
- Meistas MT, Margolis S, Kowarski AA. Hyperinsulinemia of obesity is due to decreased clearance of insulin. *Am. J. Physiol.* 1983 Aug;245(2):E155-159.

- Messner S, Agarkova I, Moritz W, Kelm JM. Multi-cell type human liver microtissues for hepatotoxicity testing. *Arch. Toxicol.* 2012;1–5.
- van Midwoud PM, Verpoorte E, Groothuis GMM. Microfluidic devices for in vitro studies on liver drug metabolism and toxicity. *Integr. Biol. Quant. Biosci. Nano Macro.* 2011 May;3(5):509–21.
- Milburn MV, Lawton KA. Application of metabolomics to diagnosis of insulin resistance. *Annu. Rev. Med.* 2013;64:291–305.
- Monteiro MS, Carvalho M, Bastos ML, Guedes de Pinho P. Metabolomics Analysis for Biomarker Discovery: Advances and Challenges. *Curr. Med. Chem.* 2013 Jan 1;20(2):257–71.
- Moreira RK. Hepatic Stellate Cells and Liver Fibrosis. *Arch. Pathol. Lab. Med.* 2007 Nov 1;131(11):1728–34.
- Morris SM. Regulation of Enzymes of the Urea Cycle and Arginine Metabolism. *Annu. Rev. Nutr.* 2002;22(1):87–105.
- Mueckler M, Thorens B. The SLC2 (GLUT) family of membrane transporters. *Mol. Aspects Med.* 2013 Jun;34(2–3):121–38.
- Mueller D, Heinzle E, Noor F. 3D Hepatic In Vitro Models as Tools for Toxicity Studies. *Curr. Tissue Eng.* 2013a Feb 1;2(1):78–89.
- Mueller D, Koetemann A, Noor F. Organotypic Cultures of Hepg2 Cells for In Vitro Toxicity Studies. *J. Bioeng. Biomed. Sci.* . 2011a
- Mueller D, Krämer L, Hoffmann E, Klein S, Noor F. 3D organotypic HepaRG cultures as in vitro model for acute and repeated dose toxicity studies. *Toxicol. Vitro Int. J. Publ. Assoc. BIBRA.* 2014 Feb;28(1):104–12.
- Mueller D, Müller-Vieira U, Biemel KM, Tascher G, Nüssler AK, Noor F. Biotransformation of diclofenac and effects on the metabolome of primary human hepatocytes upon repeated dose exposure. *Eur. J. Pharm. Sci.* 2012 Apr 11;45(5):716–24.
- Mueller D, Tascher G, Damm G, Nüssler AK, Heinzle E, Noor F. Real-time in situ viability assessment in a 3D bioreactor with liver cells using resazurin assay. *Cytotechnology.* 2013b Mar;65(2):297–305.

- Mueller D, Tascher G, Müller-Vieira U, Knobloch D, Nuessler AK, Zeilinger K, et al. In-depth physiological characterization of primary human hepatocytes in a 3D hollow-fiber bioreactor. *J. Tissue Eng. Regen. Med.* 2011b Aug 1;5(8):e207–18.
- Nakagawa T, Lomb DJ, Haigis MC, Guarente L. SIRT5 Deacetylates carbamoyl phosphate synthetase 1 and regulates the urea cycle. *Cell.* 2009 May 1;137(3):560–70.
- Nakahigashi K, Toya Y, Ishii N, Soga T, Hasegawa M, Watanabe H, et al. Systematic phenome analysis of *Escherichia coli* multiple-knockout mutants reveals hidden reactions in central carbon metabolism. *Mol. Syst. Biol.* 2009 Sep 15
- Natarajan SS, Krishnan HB, Lakshman S, Garrett WM. An efficient extraction method to enhance analysis of low abundant proteins from soybean seed. *Anal. Biochem.* 2009 Nov 15;394(2):259–68.
- Nauck M, Wolfle D, Katz N, Jungermann K. Modulation of the glucagon-dependent induction of phosphoenolpyruvate carboxykinase and tyrosine aminotransferase by arterial and venous oxygen concentrations in hepatocyte cultures. *Eur J Biochem.* 1981;119(3):657–61.
- Nedergaard J, Bengtsson T, Cannon B. Unexpected evidence for active brown adipose tissue in adult humans. *Am. J. Physiol. - Endocrinol. Metab.* 2007 Aug 1;293(2):E444–52.
- Neuschwander-Tetri BA. Nonalcoholic steatohepatitis and the metabolic syndrome. *Am. J. Med. Sci.* 2005 Dec;330(6):326–35.
- Nicholson JK, Lindon JC, Holmes E. “Metabonomics”: understanding the metabolic responses of living systems to pathophysiological stimuli via multivariate statistical analysis of biological NMR spectroscopic data. *Xenobiotica Fate Foreign Compd. Biol. Syst.* 1999 Nov;29(11):1181–9.
- Nicholson JP, Wolmarans MR, Park GR. The role of albumin in critical illness. *Br. J. Anaesth.* 2000 Jan 10;85(4):599–610.
- Nicolae A, Wahrheit J, Bahnemann J, Zeng A-P, Heinzle E. Non-stationary ¹³C metabolic flux analysis of Chinese hamster ovary cells in batch culture using extracellular labeling highlights metabolic reversibility and compartmentation. *BMC Syst. Biol.* 2014;8:50.

- Nicolae A, Wahrheit J, Nonnenmacher Y, Weyler C, Heinzle E. Identification of active elementary flux modes in mitochondria using selectively permeabilized CHO cells. *Metab. Eng.* 2015 Nov;32:95–105.
- Niklas J, Schröder E, Sandig V, Noll T, Heinzle E. Quantitative characterization of metabolism and metabolic shifts during growth of the new human cell line AGE1.HN using time resolved metabolic flux analysis. *Bioprocess Biosyst. Eng.* 2011 Jun;34(5):533–45.
- Nüssler A, König S, Ott M, Sokal E, Christ B, Thasler W, et al. Present status and perspectives of cell-based therapies for liver diseases. *J. Hepatol.* 2006 Jul;45(1):144–59.
- Nuttall FQ, Ngo A, Gannon MC. Regulation of hepatic glucose production and the role of gluconeogenesis in humans: is the rate of gluconeogenesis constant? *Diabetes Metab. Res. Rev.* 2008 Sep;24(6):438–58.
- O'Farrell PH. High resolution two-dimensional electrophoresis of proteins. *J. Biol. Chem.* 1975 May 25;250(10):4007–21.
- Okar DA, Wu C, Lange AJ. Regulation of the regulatory enzyme, 6-phosphofructo-2-kinase/fructose-2,6-bisphosphatase. *Adv. Enzyme Regul.* 2004;44:123–54.
- Oldiges M, Lutz S, Pflug S, Schroer K, Stein N, Wiendahl C. Metabolomics: current state and evolving methodologies and tools. *Appl Microbiol Biotechnol.* 2007;76(3):495–511.
- Olson H, Betton G, Robinson D, Thomas K, Monroe A, Kolaja G, et al. Concordance of the toxicity of pharmaceuticals in humans and in animals. *Regul. Toxicol. Pharmacol. RTP.* 2000 Aug;32(1):56–67.
- Ong JP, Younossi ZM. Epidemiology and natural history of NAFLD and NASH. *Clin. Liver Dis.* 2007 Feb;11(1):1–16, vii.
- Ong S-E, Mann M. Mass spectrometry-based proteomics turns quantitative. *Nat. Chem. Biol.* 2005 Oct;1(5):252–62.
- O'Sullivan A, Willoughby RE, Mishchuk D, Alcarraz B, Cabezas-Sanchez C, Condori RE, et al. Metabolomics of Cerebrospinal Fluid from Humans Treated for Rabies. *J. Proteome Res.* 2013 Jan 4;12(1):481–90.

- den Ouden H, Pellis L, Rutten GEHM, Geerars-van Vonderen IK, Rubingh CM, van Ommen B, et al. Metabolomic biomarkers for personalised glucose lowering drugs treatment in type 2 diabetes. *Metabolomics Off. J. Metabolomic Soc.* 2016;12:27.
- Pan C, Kumar C, Bohl S, Klingmueller U, Mann M. Comparative proteomic phenotyping of cell lines and primary cells to assess preservation of cell type-specific functions. *Mol. Cell. Proteomics MCP.* 2009 Mar;8(3):443–50.
- Pan X, Li J, Du W, Yu X, Zhu C, Yu C, et al. Establishment and characterization of immortalized human hepatocyte cell line for applications in bioartificial livers. *Biotechnol. Lett.* 2012 Dec 1;34(12):2183–90.
- Patton WF, Schulenberg B, Steinberg TH. Two-dimensional gel electrophoresis; better than a poke in the ICAT? *Curr. Opin. Biotechnol.* 2002 Aug;13(4):321–8.
- Pearson K. On lines and planes of closest fit to systems of points in space. *Philos. Mag.* 1901;2(6):559–72.
- Peifer S, Barduhn T, Zimmet S, Volmer DA, Heinzle E, Schneider K. Metabolic engineering of the purine biosynthetic pathway in *Corynebacterium glutamicum* results in increased intracellular pool sizes of IMP and hypoxanthine. *Microb. Cell Factories.* 2012 Oct 24;11(1):138.
- Perkins DN, Pappin DJ, Creasy DM, Cottrell JS. Probability-based protein identification by searching sequence databases using mass spectrometry data. *Electrophoresis.* 1999 Dec;20(18):3551–67.
- Perloff MD, Moltke LL von, Court MH, Kotegawa T, Shader RI, Greenblatt DJ. Midazolam and Triazolam Biotransformation in Mouse and Human Liver Microsomes: Relative Contribution of CYP3A and CYP2C Isoforms. *J. Pharmacol. Exp. Ther.* 2000 Jan 2;292(2):618–28.
- Peters SJAC, Vanhaecke T, Papeleu P, Rogiers V, Haagsman HP, van Norren K. Co-culture of primary rat hepatocytes with rat liver epithelial cells enhances interleukin-6-induced acute-phase protein response. *Cell Tissue Res.* 2010;340(3):451–7.
- Peters SJ, Vanhaecke T, Papeleu P, Rogiers V, Haagsman HP, van Norren K. Co-culture of primary rat hepatocytes with rat liver epithelial cells enhances interleukin-6-induced acute-phase protein response. *Cell Tissue Res.* 2009;340(3):451–7.

- Pfeiffer E, Kegel V, Zeilinger K, Hengstler JG, Nüssler AK, Seehofer D, et al. Featured Article: Isolation, characterization, and cultivation of human hepatocytes and non-parenchymal liver cells. *Exp. Biol. Med.* Maywood NJ. 2015 May;240(5):645–56.
- Prabakaran S, Wengenroth M, Lockstone HE, Lilley K, Leweke FM, Bahn S. 2-D DIGE analysis of liver and red blood cells provides further evidence for oxidative stress in schizophrenia. *J. Proteome Res.* 2007 Jan;6(1):141–9.
- Priesnitz C, Sperber S, Garg R, Orsini M, Noor F. Fluorescence based cell counting in collagen monolayer cultures of primary hepatocytes. *Cytotechnology.* 2014 Nov 26;
- Probst I, Schwartz P, Jungermann K. Induction in Primary Culture of “Gluconeogenic” and “Glycolytic” Hepatocytes Resembling Periportal and Perivenous Cells. *Eur. J. Biochem.* 1982 Aug 1;126(2):271–8.
- Racine L, Scoazec JY, Moreau A, Chassagne P, Bernuau D, Feldmann G. Distribution of albumin, alpha 1-inhibitor 3 and their respective mRNAs in periportal and perivenous rat hepatocytes isolated by the digitonin-collagenase technique. *Biochem. J.* 1995 Jan 1;305 (Pt 1):263–8.
- van Ravenzwaay B, Herold M, Kamp H, Kapp MD, Fabian E, Looser R, et al. Metabolomics: a tool for early detection of toxicological effects and an opportunity for biology based grouping of chemicals—from QSAR to QBAR. *Mutat. Res.* 2012 Aug 15;746(2):144–50.
- Raz I, Riddle MC, Rosenstock J, Buse JB, Inzucchi SE, Home PD, et al. Personalized management of hyperglycemia in type 2 diabetes: reflections from a Diabetes Care Editors’ Expert Forum. *Diabetes Care.* 2013 Jun;36(6):1779–88.
- Reif R, Karlsson J, Günther G, Beattie L, Wrangborg D, Hammad S, et al. Bile canalicular dynamics in hepatocyte sandwich cultures. *Arch. Toxicol.* 2015 Aug 18;1–10.
- Righetti PG, Bossi A. Isoelectric focusing of proteins and peptides in gel slabs and in capillaries. *Anal. Chim. Acta.* 1998 Oct 19;372(1–2):1–19.
- Rochfort S. Metabolomics reviewed: a new “omics” platform technology for systems biology and implications for natural products research. *J. Nat. Prod.* 2005 Dec;68(12):1813–20.
- Roden M, Bernroider E. Hepatic glucose metabolism in humans—its role in health and disease. *Best Pract. Res. Clin. Endocrinol. Metab.* 2003 Sep;17(3):365–83.

- Rodriguez-Suarez E, Mato JM, Elortza F. Proteomics analysis of human nonalcoholic fatty liver. *Methods Mol. Biol.* Clifton NJ. 2012;909:241–58.
- Rombouts K, Marra F. Molecular mechanisms of hepatic fibrosis in non-alcoholic steatohepatitis. *Dig Dis.* 2010;28(1):229–35.
- Rowe C, Gerrard DT, Jenkins R, Berry A, Durkin K, Sundstrom L, et al. Proteome-wide analyses of human hepatocytes during differentiation and dedifferentiation. *Hepatology*. Baltimore, Md. 2013 Aug;58(2):799–809.
- Rowe C, Goldring CEP, Kitteringham NR, Jenkins RE, Lane BS, Sanderson C, et al. Network analysis of primary hepatocyte dedifferentiation using a shotgun proteomics approach. *J. Proteome Res.* 2010 May 7;9(5):2658–68.
- Rui L. Energy metabolism in the liver. *Compr. Physiol.* 2014 Jan;4(1):177–97.
- Ryan D, Robards K. Metabolomics: The Greatest Omics of Them All? *Anal. Chem.* 2006 Dec 1;78(23):7954–8.
- Saghatelian A, Cravatt BF. Discovery metabolite profiling — forging functional connections between the proteome and metabolome. *Life Sci.* 2005 Aug 19;77(14):1759–66.
- S J Pilkis, Granner and DK. Molecular Physiology of the Regulation of Hepatic Gluconeogenesis and Glycolysis. *Annu. Rev. Physiol.* 1992;54(1):885–909.
- Sakai J, Ishikawa H, Kojima S, Satoh H, Yamamoto S, Kanaoka M. Proteomic analysis of rat heart in ischemia and ischemia-reperfusion using fluorescence two-dimensional difference gel electrophoresis. *Proteomics.* 2003 Jul;3(7):1318–24.
- Saltiel AR, Kahn CR. Insulin signalling and the regulation of glucose and lipid metabolism. *Nature.* 2001 Dec 13;414(6865):799–806.
- Schug M, Heise T, Bauer A, Storm D, Blaszkewicz M, Bedawy E, et al. Primary rat hepatocytes as in vitro system for gene expression studies: comparison of sandwich, Matrigel and 2D cultures. *Arch. Toxicol.* 2008 Dec;82(12):923–31.
- Seglen PO. Preparation of rat liver cells: I. Effect of Ca²⁺ on enzymatic dispersion of isolated, perfused liver. *Exp. Cell Res.* 1972 Oct;74(2):450–4.

- Sener A, Malaisse-Lagae F, Malaisse WJ. Stimulation of pancreatic islet metabolism and insulin release by a nonmetabolizable amino acid. *Proc. Natl. Acad. Sci.* 1981 Jan 9;78(9):5460–4.
- Shambaugh GE. Urea biosynthesis I. The urea cycle and relationships to the citric acid cycle. *Am. J. Clin. Nutr.* 1977 Dec;30(12):2083–7.
- Shtrichman R, Germanguz I, Eldor JI-. Induced Pluripotent Stem Cells (iPSCs) Derived from Different Cell Sources and their Potential for Regenerative and Personalized Medicine. *Curr. Mol. Med.* 2013 May 1;13(5):792–805.
- Si-Tayeb K, Lemaigre FP, Duncan SA. Organogenesis and development of the liver. *Dev Cell.* 2010;18(2):175–89.
- Sivertsson L, Synnergren J, Jensen J, Björquist P, Ingelman-Sundberg M. Hepatic Differentiation and Maturation of Human Embryonic Stem Cells Cultured in a Perfused Three-Dimensional Bioreactor. *Stem Cells Dev.* 2012 Sep 12;22(4):581–94.
- Skytner HA, Rosahl TW, Knowles MR, Salim K, Reid L, Cothliff R, et al. Alterations of stress related proteins in genetically altered mice revealed by two-dimensional differential in-gel electrophoresis analysis. *PROTEOMICS.* 2002 Aug 1;2(8):1018–25.
- Slany A, Haudek VJ, Zwickl H, Gundacker NC, Grusch M, Weiss TS, et al. Cell Characterization by Proteome Profiling Applied to Primary Hepatocytes and Hepatocyte Cell Lines Hep-G2 and Hep-3B. *J. Proteome Res.* 2010 Jan 4;9(1):6–21.
- Smet KD, Brüning T, Blaszkewicz M, Bolt HM, Vercruyse A, Rogiers V. Biotransformation of trichloroethylene in collagen gel sandwich cultures of rat hepatocytes. *Arch. Toxicol.* 2000 Dec 1;74(10):587–92.
- Smilde AK, van der Werf MJ, Bijlsma S, van der Werff-van der Vat BJ, Jellema RH. Fusion of mass spectrometry-based metabolomics data. *Anal Chem.* 2005;77(20):6729–36.
- Soldatow VY, Lecluyse EL, Griffith LG, Rusyn I. In vitro models for liver toxicity testing. *Toxicol. Res.* 2013 Jan 1;2(1):23–39.
- Spielbauer G, Margl L, Hannah LC, Römisch W, Ettenhuber C, Bacher A, et al. Robustness of central carbohydrate metabolism in developing maize kernels. *Phytochemistry.* 2006 Jul;67(14):1460–75.

- Srivastava AK, Pandey SK. Potential mechanism(s) involved in the regulation of glycogen synthesis by insulin. *Mol. Cell. Biochem.* 1998 May;182(1–2):135–41.
- Stanley S, Pinto S, Segal J, Pérez CA, Viale A, DeFalco J, et al. Identification of neuronal subpopulations that project from hypothalamus to both liver and adipose tissue polysynaptically. *Proc. Natl. Acad. Sci. U. S. A.* 2010 Apr 13;107(15):7024–9.
- Stewart CC, Strother A. Glucose consumption by rats decreases cytochrome P450 enzyme activity by altering hepatic lipids. *Life Sci.* 1999 Apr 30;64(23):2163–72.
- Stewart S, Jones D, Day CP. Alcoholic liver disease: new insights into mechanisms and preventative strategies. *Trends Mol Med.* 2001;7(9):408–13.
- Strain AJ, Neuberger JM. A Bioartificial Liver--State of the Art. *Science.* 2002 Aug 2;295(5557):1005–9.
- Strigun A, Wahrheit J, Beckers S, Heinzle E, Noor F. Metabolic profiling using HPLC allows classification of drugs according to their mechanisms of action in HL-1 cardiomyocytes. *Toxicol Appl Pharmacol.* 2011;252(2):183–91.
- Swift B, Brouwer KL. Influence of seeding density and extracellular matrix on bile Acid transport and mrp4 expression in sandwich-cultured mouse hepatocytes. *Mol Pharm.* 2010;7(2):491–500.
- Takayama K, Kawabata K, Nagamoto Y, Kishimoto K, Tashiro K, Sakurai F, et al. 3D spheroid culture of hESC/hiPSC-derived hepatocyte-like cells for drug toxicity testing. *Biomaterials.* 2013 Feb;34(7):1781–9.
- Takenaka A, Ohishi Y, Noguchi T, Naito H. Effect of some essential amino acid deficiency in the medium on the action of insulin on primary cultured hepatocytes of rats. Hepatocytes do not respond to insulin in some essential amino acid-deficient medium. *Int. J. Biochem.* 1989;21(11):1255–63.
- Tanaka K. The Origin of Macromolecule Ionization by Laser Irradiation (Nobel Lecture). *Angew. Chem. Int. Ed.* 2003 Aug 25;42(33):3860–70.
- Temelkova-Kurktschiev T, Stefanov T. Lifestyle and Genetics in Obesity and type 2 Diabetes. *Exp. Clin. Endocrinol. Amp Diabetes.* 2012 Jan;120(1):1–6.

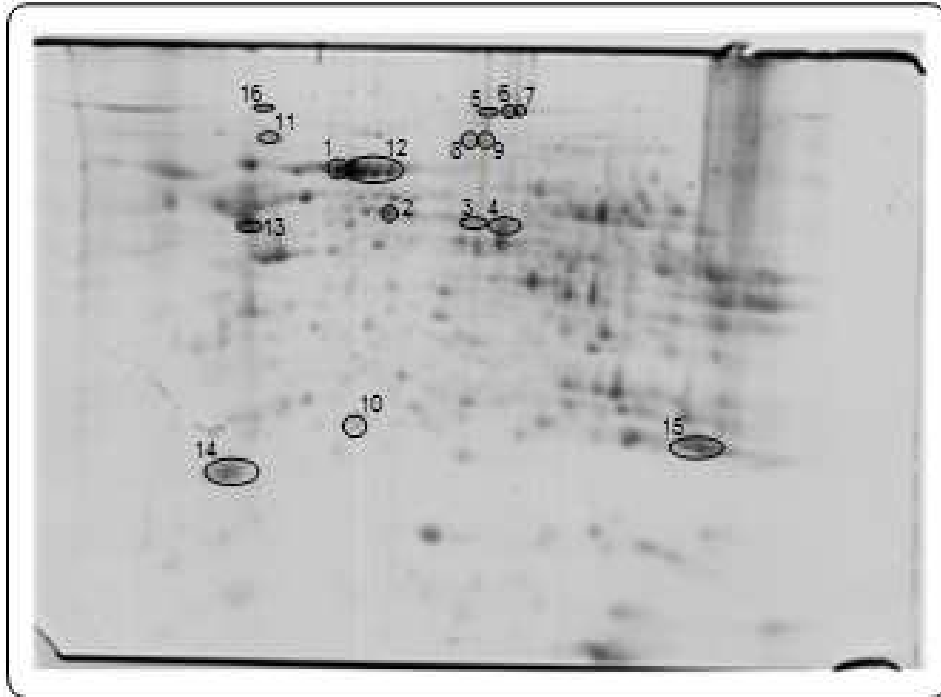
- Tessari P, Kiwanuka E, Million R, Vettore M, Puricelli L, Zanetti M, et al. Albumin and fibrinogen synthesis and insulin effect in type 2 diabetic patients with normoalbuminuria. *Diabetes Care*. 2006 Feb;29(2):323–8.
- Tonelli J, Kishore P, Lee D-E, Hawkins M. The regulation of glucose effectiveness: how glucose modulates its own production. *Curr. Opin. Clin. Nutr. Metab. Care*. 2005 Jul;8(4):450–6.
- Tostões RM, Leite SB, Miranda JP, Sousa M, Wang DIC, Carrondo MJT, et al. Perfusion of 3D encapsulated hepatocytes--a synergistic effect enhancing long-term functionality in bioreactors. *Biotechnol. Bioeng*. 2011 Jan;108(1):41–9.
- Turpeinen M, Tolonen A, Chesne C, Guillouzo A, Uusitalo J, Pelkonen O. Functional expression, inhibition and induction of CYP enzymes in HepaRG cells. *Toxicol. Vitro Int. J. Publ. Assoc. BIBRA*. 2009 Jun;23(4):748–53.
- Tuschl G, Hrach J, Walter Y, Hewitt PG, Mueller SO. Serum-free collagen sandwich cultures of adult rat hepatocytes maintain liver-like properties long term: a valuable model for in vitro toxicity and drug-drug interaction studies. *Chem. Biol. Interact*. 2009 Sep 14;181(1):124–37.
- Tuschl G, Mueller SO. Effects of cell culture conditions on primary rat hepatocytes-cell morphology and differential gene expression. *Toxicology*. 2006;218(2–3):205–15.
- Unlü M, Morgan ME, Minden JS. Difference gel electrophoresis: a single gel method for detecting changes in protein extracts. *Electrophoresis*. 1997 Oct;18(11):2071–7.
- Usynin IF, Panin LE. Mechanisms determining phenotypic heterogeneity of hepatocytes. *Biochem. Mosc*. 2008;73(4):367–80.
- Uto H, Kanmura S, Takami Y, Tsubouchi H. Clinical proteomics for liver disease: a promising approach for discovery of novel biomarkers. *Proteome Sci*. 2010 Dec 31;8:70.
- Vassallo JD, Hicks SM, Daston GP, Lehman-McKeeman LD. Metabolic detoxification determines species differences in coumarin-induced hepatotoxicity. *Toxicol. Sci. Off. J. Soc. Toxicol*. 2004 Aug;80(2):249–57.
- Vinken M, Papeleu P, Snykers S, De Rop E, Henkens T, Chipman JK, et al. Involvement of cell junctions in hepatocyte culture functionality. *Crit Rev Toxicol*. 2006;36(4):299–318.

- Wahrheit J, Nicolae A, Heinzle E. Investigation of glutamine metabolism in CHO cells by dynamic metabolic flux analysis. *BMC Proc.* 2013 Dec 4;7(S6):1–2.
- Wahrheit J, Niklas J, Heinzle E. Metabolic control at the cytosol-mitochondria interface in different growth phases of CHO cells. *Metab. Eng.* 2014 May;23:9–21.
- Walker JN, Ramracheya R, Zhang Q, Johnson PRV, Braun M, Rorsman P. Regulation of glucagon secretion by glucose: paracrine, intrinsic or both? *Diabetes Obes. Metab.* 2011 Oct 1;13:95–105.
- Wang J, Reijmers T, Chen L, Van Der Heijden R, Wang M, Peng S, et al. Systems toxicology study of doxorubicin on rats using ultra performance liquid chromatography coupled with mass spectrometry based metabolomics. *Metabolomics.* 2009 Dec;5(4):407–18.
- Wang W, Wu Z, Dai Z, Yang Y, Wang J, Wu G. Glycine metabolism in animals and humans: implications for nutrition and health. *Amino Acids.* 2013 Apr 25;45(3):463–77.
- Wang Y, Liu S, Hu Y, Li P, Wan J-B. Current state of the art of mass spectrometry-based metabolomics studies – a review focusing on wide coverage, high throughput and easy identification. *RSC Adv.* 2015 Sep 15;5(96):78728–37.
- Weiss RH, Kim K. Metabolomics in the study of kidney diseases. *Nat. Rev. Nephrol.* 2012 Jan;8(1):22–33.
- Wellen KE, Thompson CB. Cellular metabolic stress: considering how cells respond to nutrient excess. *Mol. Cell.* 2010 Oct 22;40(2):323–32.
- Wen X, Donepudi AC, Thomas PE, Slitt AL, King RS, Aleksunes LM. Regulation of hepatic phase II metabolism in pregnant mice. *J. Pharmacol. Exp. Ther.* 2013 Jan;344(1):244–52.
- van der Werf MJ, Jellema RH, Hankemeier T. Microbial metabolomics: replacing trial-and-error by the unbiased selection and ranking of targets. *J Ind Microbiol Biotechnol.* 2005;32(6):234–52.
- Whalen RD, Tata PN, Burckart GJ, Venkataramanan R. Species differences in the hepatic and intestinal metabolism of cyclosporine. *Xenobiotica Fate Foreign Compd. Biol. Syst.* 1999 Jan;29(1):3–9.

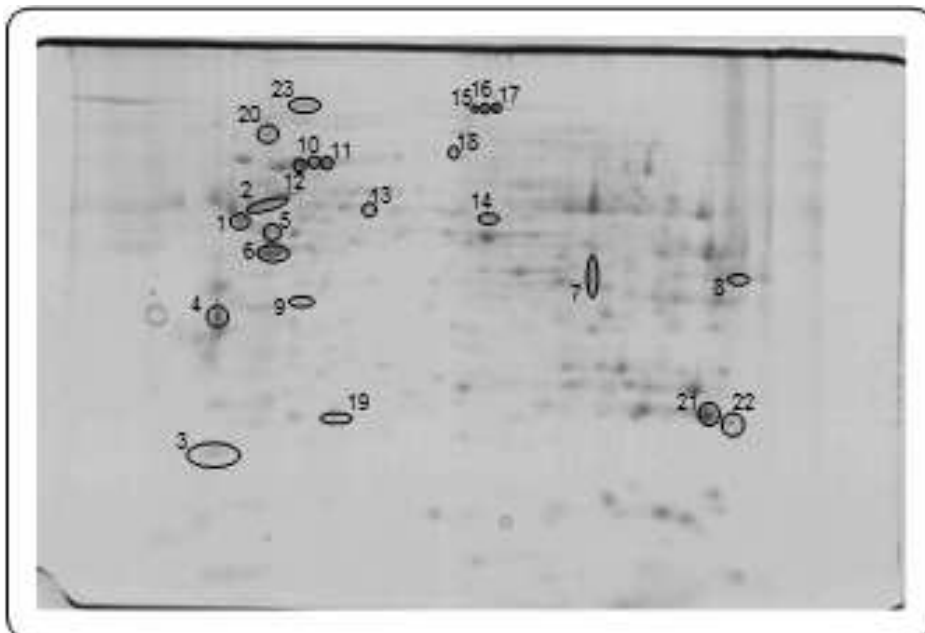
- Williams JA, Ring BJ, Cantrell VE, Jones DR, Eckstein J, Ruterbories K, et al. Comparative Metabolic Capabilities of CYP3A4, CYP3A5, and CYP3A7. *Drug Metab. Dispos.* 2002 Jan 8;30(8):883–91.
- Wilson JE. Isozymes of mammalian hexokinase: structure, subcellular localization and metabolic function. *J. Exp. Biol.* 2003 Jun;206(Pt 12):2049–57.
- Woodcroft KJ, Novak RF. Insulin differentially affects xenobiotic-enhanced, cytochrome P-450 (CYP)2E1, CYP2B, CYP3A, and CYP4A expression in primary cultured rat hepatocytes. *J. Pharmacol. Exp. Ther.* 1999 May;289(2):1121–7.
- Wright PC, Noirel J, Ow S-Y, Fazeli A. A review of current proteomics technologies with a survey on their widespread use in reproductive biology investigations. *Theriogenology.* 2012 Mar 1;77(4):738–765.e52.
- Wu C, Khan SA, Peng L-J, Lange AJ. Roles for fructose-2,6-bisphosphate in the control of fuel metabolism: beyond its allosteric effects on glycolytic and gluconeogenic enzymes. *Adv. Enzyme Regul.* 2006;46:72–88.
- Wu M-H, Huang S-B, Lee G-B. Microfluidic cell culture systems for drug research. *Lab. Chip.* 2010 Apr 1;10(8):939–56.
- Yanagimoto T, Itoh S, Muller-Enoch D, Kamataki T. Mouse liver cytochrome P-450 (P-450IIIAM1): its cDNA cloning and inducibility by dexamethasone. *Biochim. Biophys. Acta.* 1992 Apr 6;1130(3):329–32.
- Yanes O, Tautenhahn R, Patti GJ, Siuzdak G. Expanding Coverage of the Metabolome for Global Metabolite Profiling. *Anal. Chem.* 2011 Mar 15;83(6):2152–61.
- Yaney GC, Corkey BE. Fatty acid metabolism and insulin secretion in pancreatic beta cells. *Diabetologia.* 2003 Oct;46(10):1297–312.
- Yang TH, Bolten CJ, Coppi MV, Sun J, Heinzle E. Numerical bias estimation for mass spectrometric mass isotopomer analysis. *Anal. Biochem.* 2009 May 15;388(2):192–203.
- Yates JR, Ruse CI, Nakorchevsky A. Proteomics by mass spectrometry: approaches, advances, and applications. *Annu. Rev. Biomed. Eng.* 2009;11:49–79.
- Yu C-B, Pan X-P, Li L-J. Progress in bioreactors of bioartificial livers. *Hepatobiliary Pancreat. Dis. Int. HBPD INT.* 2009 Apr;8(2):134–40.

- Zeilinger K, Holland G, Sauer IM, Efimova E, Kardassis D, Obermayer N, et al. Time course of primary liver cell reorganization in three-dimensional high-density bioreactors for extracorporeal liver support: an immunohistochemical and ultrastructural study. *Tissue Eng.* 2004 Aug;10(7-8):1113-24.
- Zellmer S, Schmidt-Heck W, Godoy P, Weng H, Meyer C, Lehmann T, et al. Transcription factors ETF, E2F, and SP-1 are involved in cytokine-independent proliferation of murine hepatocytes. *Hepatol. Baltim. Md.* 2010 Dec;52(6):2127-36.
- Zhou S-F, Liu J-P, Chowbay B. Polymorphism of human cytochrome P450 enzymes and its clinical impact. *Drug Metab. Rev.* 2009;41(2):89-295.
- Zierler K. Whole body glucose metabolism. *Am. J. Physiol.* 1999 Mar;276(3 Pt 1):E409-426.
- Zuber R, Anzenbacherová E, Anzenbacher P. Cytochromes P450 and experimental models of drug metabolism. *J. Cell. Mol. Med.* 2002 Jun;6(2):189-98.

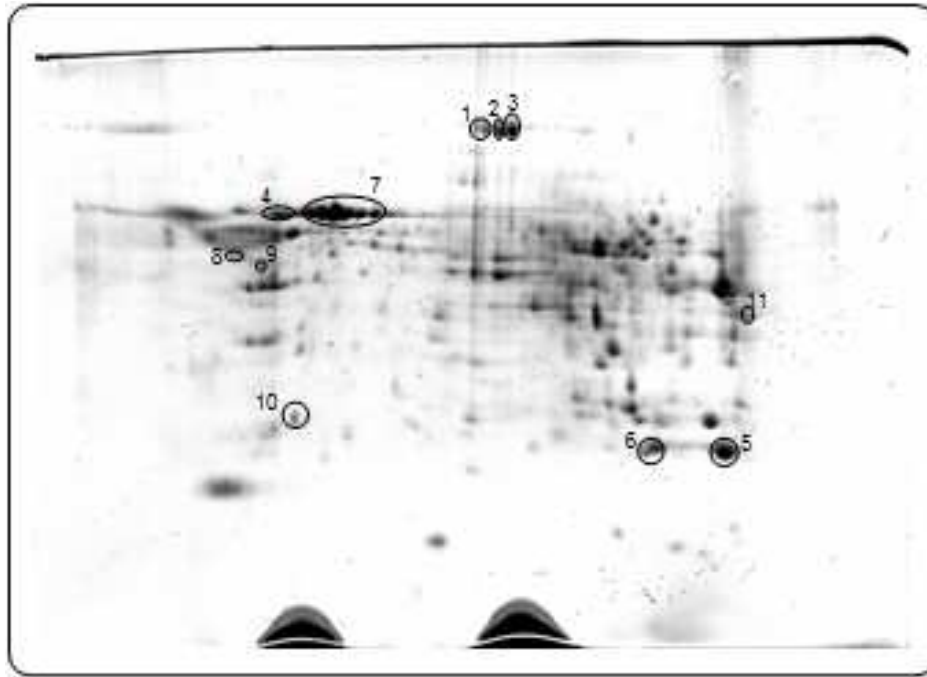
10. Supplementary material



Supplementary Figure 1 2D gel electrophoresis of the intracellular proteome of PMH in ML culture at day 1 of cultivation. 1) 75 kDa glucose regulated protein 2) Selenium-binding protein 3 and 4) Aldehyde dehydrogenase 5, 6 and 7) Carbamoyl-phosphate synthase 8 and 9) Sarcosine dehydrogenase 10) Ferritin 11) Transitional ER ATPase 12) serum albumin 13) ATP synthase 14) Major urinary protein 16) Argininosuccinate synthase.



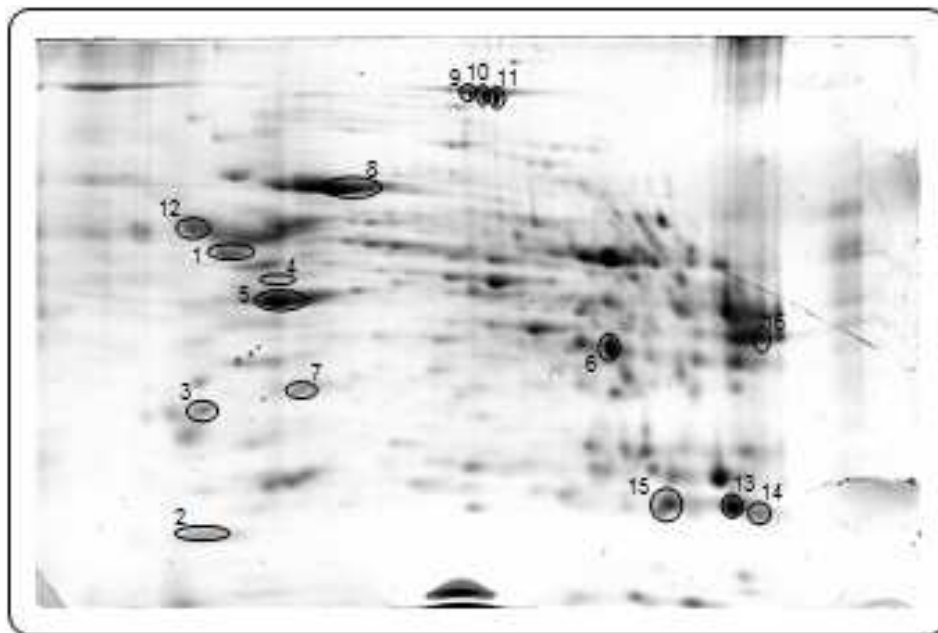
Supplementary Figure 2 2D gel electrophoresis of the intracellular proteome of PMH in ML culture at day 5 of cultivation. 1 and 2) ATP synthase 3) Major urinary protein 4) Regucalcin 5 and 6) Actin 7) Ornithine carbamoyltransferase 8) Fructose-bisphosphate aldolase 9) Apolipoprotein E 10 and 11) Serum albumin 12) 75 kDa glucose regulated protein 13) Selenium binding protein 14) Aldehyde dehydrogenase 15, 16 and 17) Carbamoyl-phosphate synthase 18) Sarcosine dehydrogenase 19) Ferritin 20) Transitional ER ATPase 21 and 22) Glutathion-S transferase.



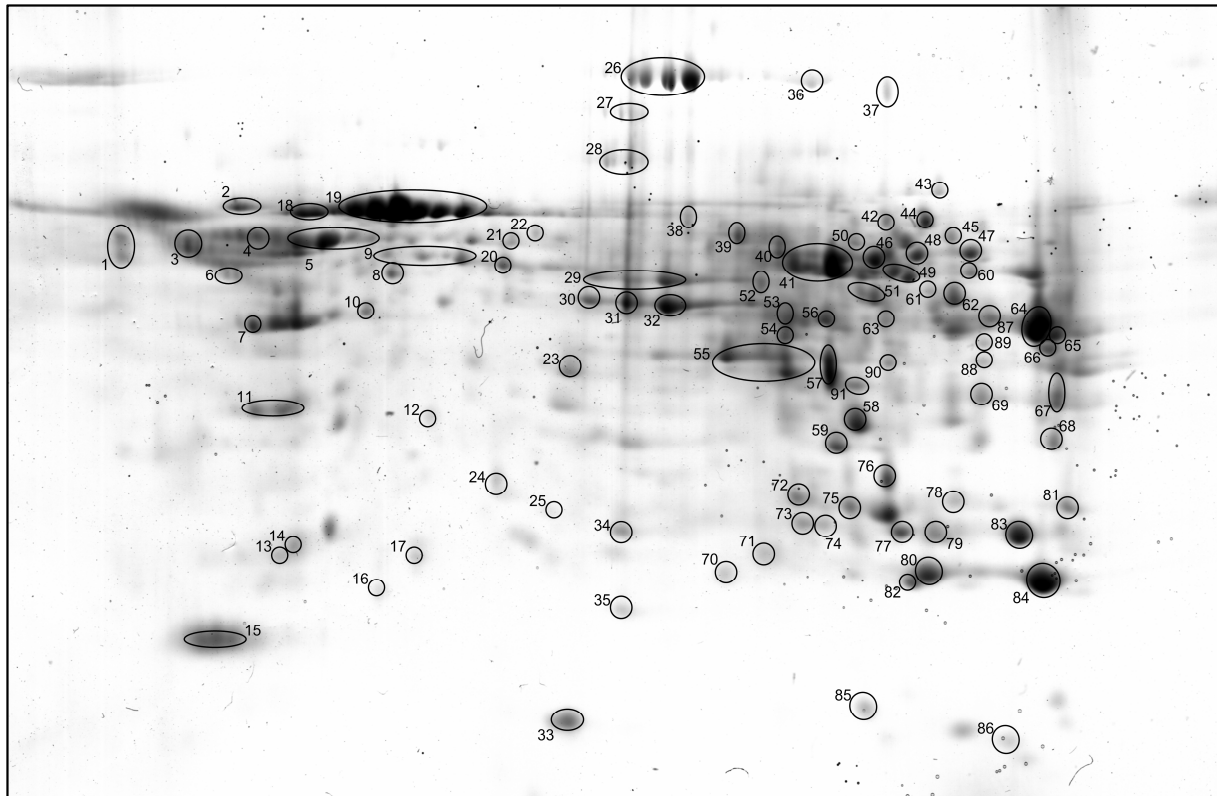
S
u
p
p
l
e
m
e
n
t
a
r
y

F
i

Figure 3 2D gel electrophoresis of the intracellular proteome of PMH in SW culture at day 1 of cultivation. 1, 2 and 3) Carbamoyl phosphate synthase 4) Protein disulfate isomerase 5) Glutathion S transferase 6) Superoxid dismutase 7) Serum albumin 8 and 9) ATP synthase 10) Regucalcin 11) Fructose-bisphosphate aldolase.



Supplementary Figure 4 2D gel electrophoresis of the intracellular proteome of PMH in SW culture at day 5 of cultivation. 1) ATP synthase 2) Major urinary protein 3) Regucalcin 4 and 5) Actin 6) Ornithin carbamoyltransferase 7) Apolipoprotein E 8) 9, 10 and 11) Carbamoylphosphate synthase 12) Protein disulfate isomerase 13 and 14) Glutathion S transferase 15) Superoxid dismutase 16) Fructose-bisphosphate aldolase.



Supplementary Figure 5 2D gel electrophoresis of the intracellular proteome of PMH. In total 91 proteins and protein isoforms could be identified with MALDI ToF MS/MS. Each spot is assigned to a protein in Supplementary Table 1.

Supplementary Table 1 List of all intracellular proteins of primary mouse hepatocytes identified with MALDI ToF MS/MS. Spot numbers correlate to Supplementary Figure 5.

Spot no.	Protein
1	Calreticulin
2	78 kDa glucose-regulated protein
3	Protein disulfide-isomerase
4	Obscurin-like protein 1
5	60 kDa heat shock protein, mitochondrial
6	ATP synthase subunit beta, mitochondrial
7	Apolipoprotein A-IV
8	S-adenosylmethionine synthase isoform type-1
9	Selenium-binding protein 2
10	Adenosine kinase

Spot no.	Protein
11	Regucalcin
12	Ketohexokinase
13	Lactoylglutathione lyase
14	Apolipoprotein A-I
15	Major urinary proteins
16	Ferritin light chain 1
17	Ferritin heavy chain
18	Heat shock cognate 71 kDa protein
19	Serum albumin
20	Selenium-binding protein 1
21	Bifunctional epoxide hydrolase 2
22	Carboxylesterase 3A
23	Fructose-1,6-bisphosphatase 1
24	Indolethylamine N-methyltransferase
25	Peroxiredoxin-4
26	Carbamoyl-phosphate synthase [ammonia],
27	Pyruvate carboxylase, mitochondrial
28	Sarcosine dehydrogenase, mitochondrial
29	Aldehyde dehydrogenase, mitochondrial
30	Alpha-enolase
31	Adenosylhomocysteinase
32	Alpha-enolase
33	Superoxide dismutase [Cu-Zn]
34	Peroxiredoxin-6
35	Retinol-binding protein 4

Spot no.	Protein
36	Keratin, type II cytoskeletal 73
37	Carbonic anhydrase 3
38	FAST kinase domain-containing protein 2
39	Triokinase/FMN cyclase
40	Pyruvate kinase PKLR
41	Glutamate dehydrogenase 1, mitochondrial
42	Transketolase
43	Aconitate hydratase, mitochondrial
44	Transketolase
45	Non-specific lipid-transfer protein
46	Catalase
47	Catalase
48	Delta-1-pyrroline-5-carboxylate dehydrogenase,
49	UTP--glucose-1-phosphate uridylyltransferase
50	Delta-1-pyrroline-5-carboxylate dehydrogenase,
51	Hydroxymethylglutaryl-CoA synthase, mitochondrial
52	Argininosuccinate lyase
53	Long-chain specific acyl-CoA dehydrogenase,
54	Fumarylacetoacetase
55	Arginase-1
56	Isocitrate dehydrogenase [NADP] cytoplasmic
57	Ornithine carbamoyltransferase, mitochondrial
58	Glycine N-methyltransferase
59	Electron transfer flavoprotein subunit alpha,
60	Retinal dehydrogenase 1

Spot no.	Protein
61	4-aminobutyrate aminotransferase, mitochondrial
62	Hydroxymethylglutaryl-CoA synthase, mitochondrial
63	Argininosuccinate synthase
64	Betaine--homocysteine S-methyltransferase 1
65	3-ketoacyl-CoA thiolase, mitochondrial
66	Acetyl-CoA acetyltransferase, mitochondrial
67	Glyceraldehyde-3-phosphate dehydrogenase
68	Hydroxyacyl-coenzyme A dehydrogenase,
69	Glyceraldehyde-3-phosphate dehydrogenase
70	Glutathione peroxidase 1
71	Glutathione S-transferase P 1
72	Phosphoglycerate mutase 1
73	Triosephosphate isomerase
74	Glutathione S-transferase Mu 1
75	Carbonic anhydrase 3
76	Carbonic anhydrase 3
77	Triosephosphate isomerase
78	Electron transfer flavoprotein subunit beta
79	Glutathione S-transferase Mu 1
80	Glutathione S-transferase
81	Electron transfer flavoprotein subunit beta
82	Superoxide dismutase [Mn], mitochondrial
83	Glutathione S-transferase Mu 1
84	Glutathione S-transferase P 1
85	Nucleoside diphosphate kinase B

Spot no.	Protein
86	Peptidyl-prolyl cis-trans isomerase A
87	Betaine--homocysteine S-methyltransferase 1
88	Fructose-bisphosphate aldolase B
89	Glutaryl-CoA dehydrogenase, mitochondrial
90	Ornithine carbamoyltransferase, mitochondrial
91	Alcohol dehydrogenase [NADP(+)]

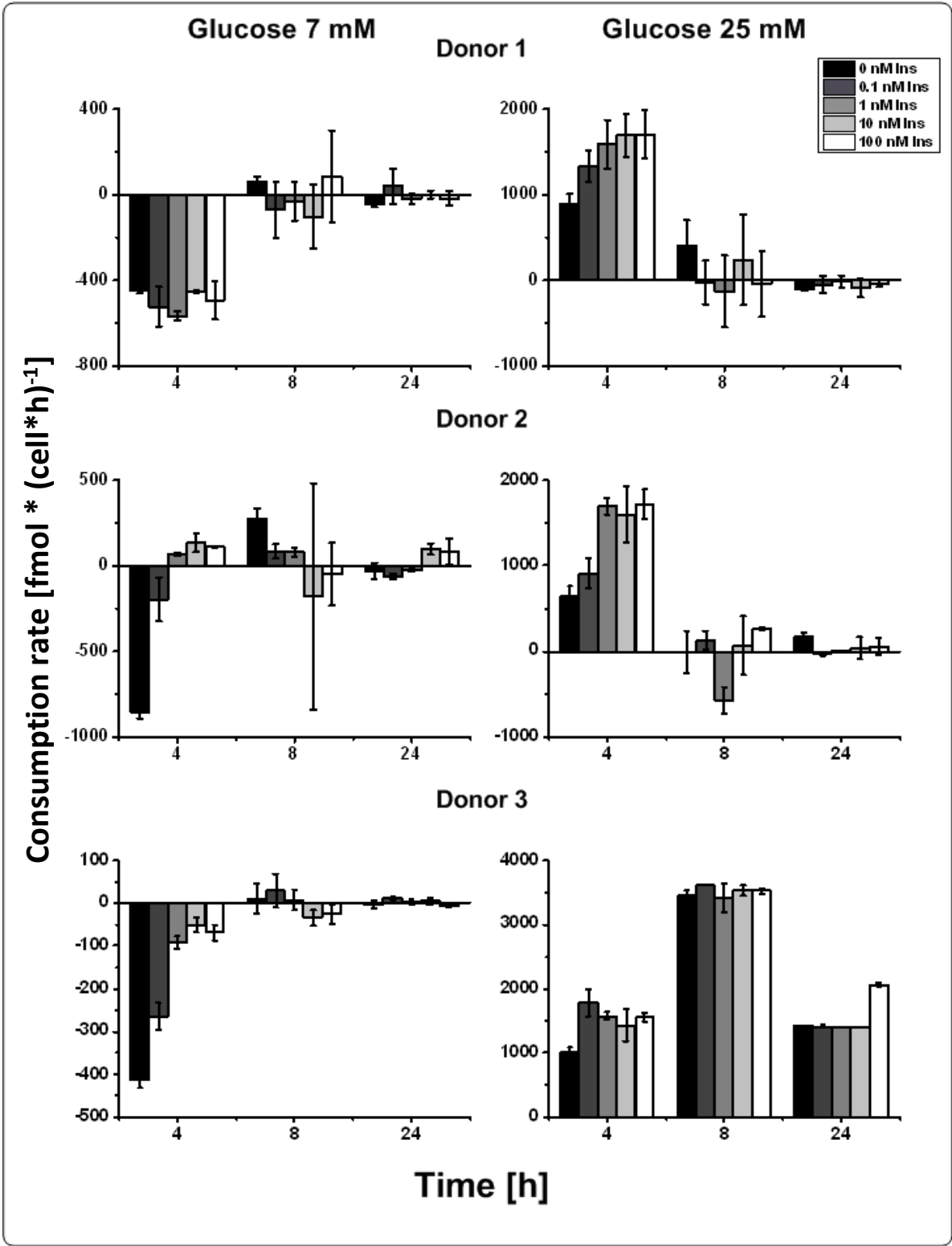
Supplementary Table 2 Identified proteins, which were not significantly different in PMH cultivated in collagen ML culture and SW culture after 1 or 5 days of cultivation. DIGE analysis showed mean fold changes between – 1.5 and + 1.5. Spot numbers correlate to Supplementary Figure 5.

Spot no.	Accession no.	Protein	Protein function
1	P14211	Calreticulin	response to hormones, cell cycle arrest
2	P20029	78 kDa glucose-regulated protein	protein folding, stress response
3	P09103	Protein disulfide-isomerase	oxidative stress response
4	D3YYU8	Obscurin-like protein 1	regulation of mitotic nuclear division
5	P63038	60 kDa heat shock protein	protein folding, stress response
7	P06728	Apolipoprotein A-IV	oxidative stress response
8	Q91X83	S-adenosylmethionine synthase	S-adenosylmethionine biosynthesis
10	P55264	Adenosine kinase	AMP synthesis from adenosine
12	P97328	Ketohexokinase	fructose catabolic process
13	Q9CPU0	Lactoylglutathione lyase	glutathione metabolic process
14	Q00623	Apolipoprotein A-I	lipid transport
16	P63017	Heat shock cognate 71 kDa protein	protein folding, inflammatory response
21	P34914	Bifunctional epoxide hydrolase 2	xenobiotic metabolism, lipid

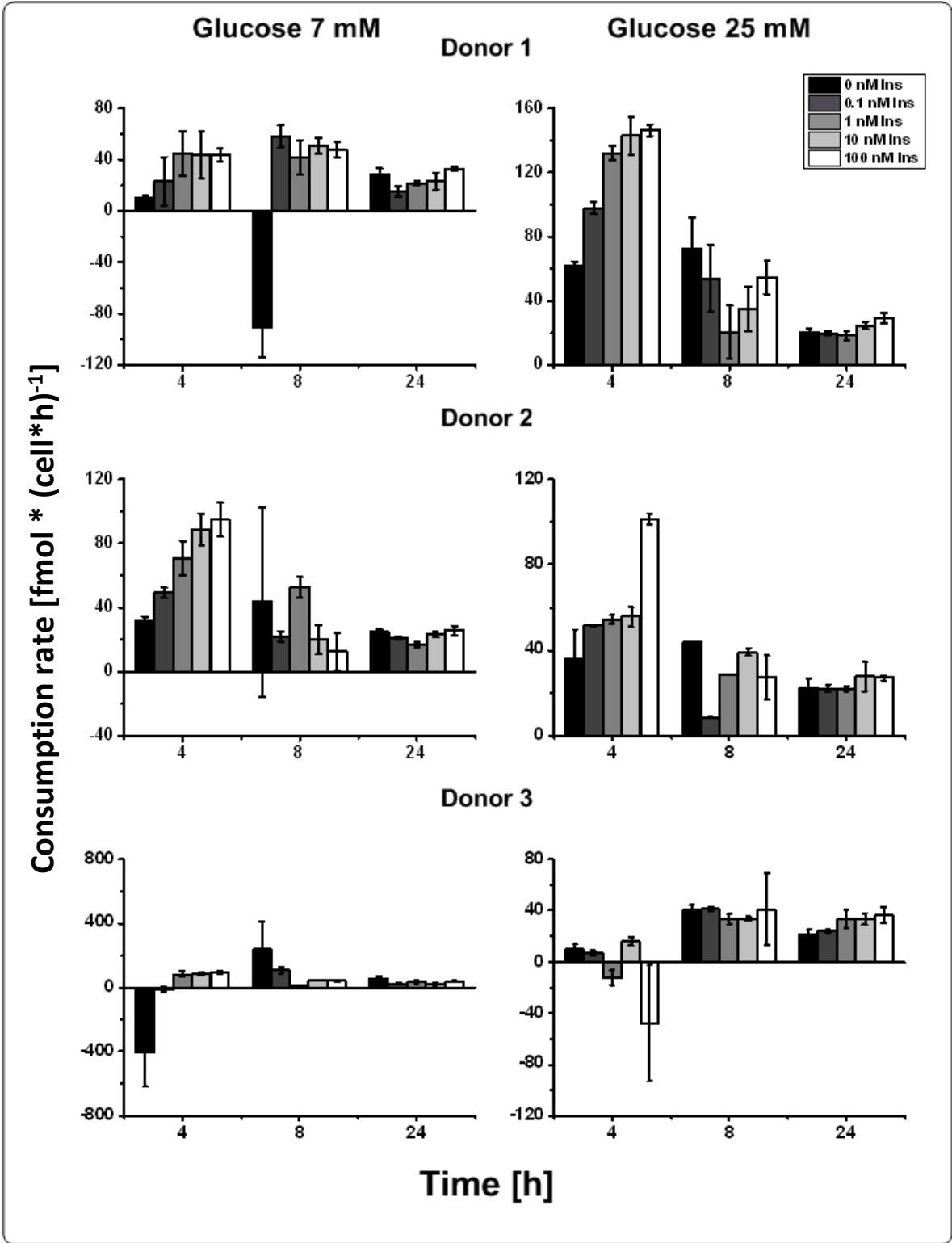
Spot no.	Accession no.	Protein	Protein function
			phosphatase activity
22	Q63880	Carboxylesterase 3A	xenobiotic metabolism
23	Q9QXD6	Fructose-1,6-bisphosphatase	gluconeogenesis
24	P40936	Indolethylamine N-methyltransferase	response to toxic substances
25	O08807	Peroxiredoxin-4	oxidative stress response
27	Q05920	Pyruvate carboxylase	gluconeogenesis
30	P17182	Alpha-enolase	glycolytic process
31	P50247	Adenosylhomocysteinase	amino-acid biosynthesis
34	O08709	Peroxiredoxin-6	oxidative stress response
35	Q00724	Retinol-binding protein 4	response to insulin
37/75/76	P16015	Carbonic anhydrase 3	oxidative stress response
38	Q922E6	FAST kinase domain-containing protein 2	assembly of the mitochondrial large ribosomal subunit
39	Q8VC30	Triokinase/FMN cyclase	cellular carbohydrate metabolic process
40	P53657	Pyruvate kinase PKLR	glycolysis
41	P26443	Glutamate dehydrogenase 1, mitochondrial	TCA cycle
42	P40142	Transketolase	binds cofactors and metal ions
43	Q99KI0	Aconitate hydratase	TCA cycle
45	P32020	Non-specific lipid-transfer protein	steroid biosynthetic process
46/47	P24270	Catalase	oxidative stress response
48/50	Q9Z110	Delta-1-pyrroline-5-carboxylate dehydrogenase	cellular amino acid biosynthetic process
49	Q91ZJ5	UTP-glucose-1-phosphate uridylyltransferase	glucosyl donor in cellular metabolic pathways

Spot no.	Accession no.	Protein	Protein function
52	Q91YI0	Argininosuccinate lyase	L- arginine biosynthesis, urea cycle
53	P51174	Long-chain specific acyl-CoA dehydrogenase	mitochondrial fatty acid beta-oxidation
54	P35505	Fumarylacetoacetase	amino- acid degradation
55	Q61176	Arginase-1	urea cycle
56	O88844	Isocitrate dehydrogenase [NADP] cytoplasmic	TCA cycle
58	Q9QXF8	Glycine N-methyltransferase	gluconeogenesis
59	Q99LC5	Electron transfer flavoprotein subunit alpha	fatty acid beta-oxidation
60	P24549	Retinal dehydrogenase 1	retinol metabolic process
61	P61922	4-aminobutyrate aminotransferase, mitochondrial	response to ethanol and hypoxia
52/62	P54869	Hydroxymethylglutaryl-CoA synthase, mitochondrial	response to various stress stimuli
63	P16460	Argininosuccinate synthase	urea cycle
64/87	O35490	Betaine-homocysteine S-methyltransferase 1	amino- acid biosynthesis
65	Q921H8	3-ketoacyl-CoA thiolase, mitochondrial	lipid metabolism
66	Q8QZT1	Acetyl-CoA acetyltransferase, mitochondrial	response to hormones and starvation
67/69	P16858	Glyceraldehyde-3-phosphate dehydrogenase	glycolysis
68	Q61425	Hydroxyacyl-coenzyme A dehydrogenase	lipid metabolism
70	P11352	Glutathione peroxidase 1	response to oxidative stress
72	Q9DBJ1	Phosphoglycerate mutase 1	glycolysis regulation

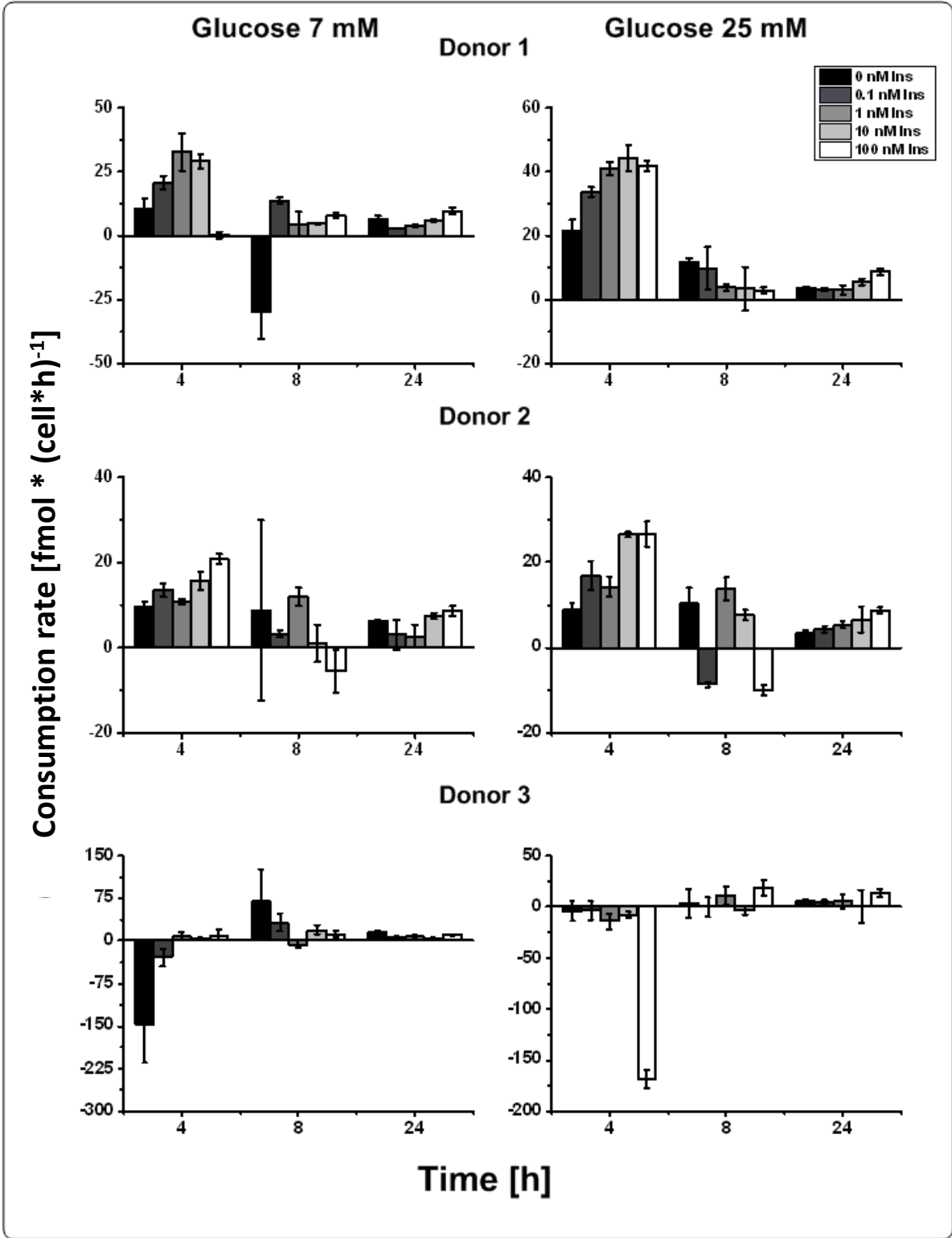
Spot no.	Accession no.	Protein	Protein function
73/77	P17751	Triosephosphate isomerase	glycolysis
78/81	Q9DCW4	Electron transfer flavoprotein subunit beta	fatty acid beta-oxidation
85	Q01768	Nucleoside diphosphate kinase B	Nucleotide metabolism
86	P30416	Peptidyl-prolyl cis-trans isomerase A	response to mitochondrial oxidative stress
89	Q60759	Glutaryl-CoA dehydrogenase, mitochondrial	amino- acid metabolism
91	Q9JII6	Alcohol dehydrogenase [NADP(+)]	response to xenobiotics and drugs



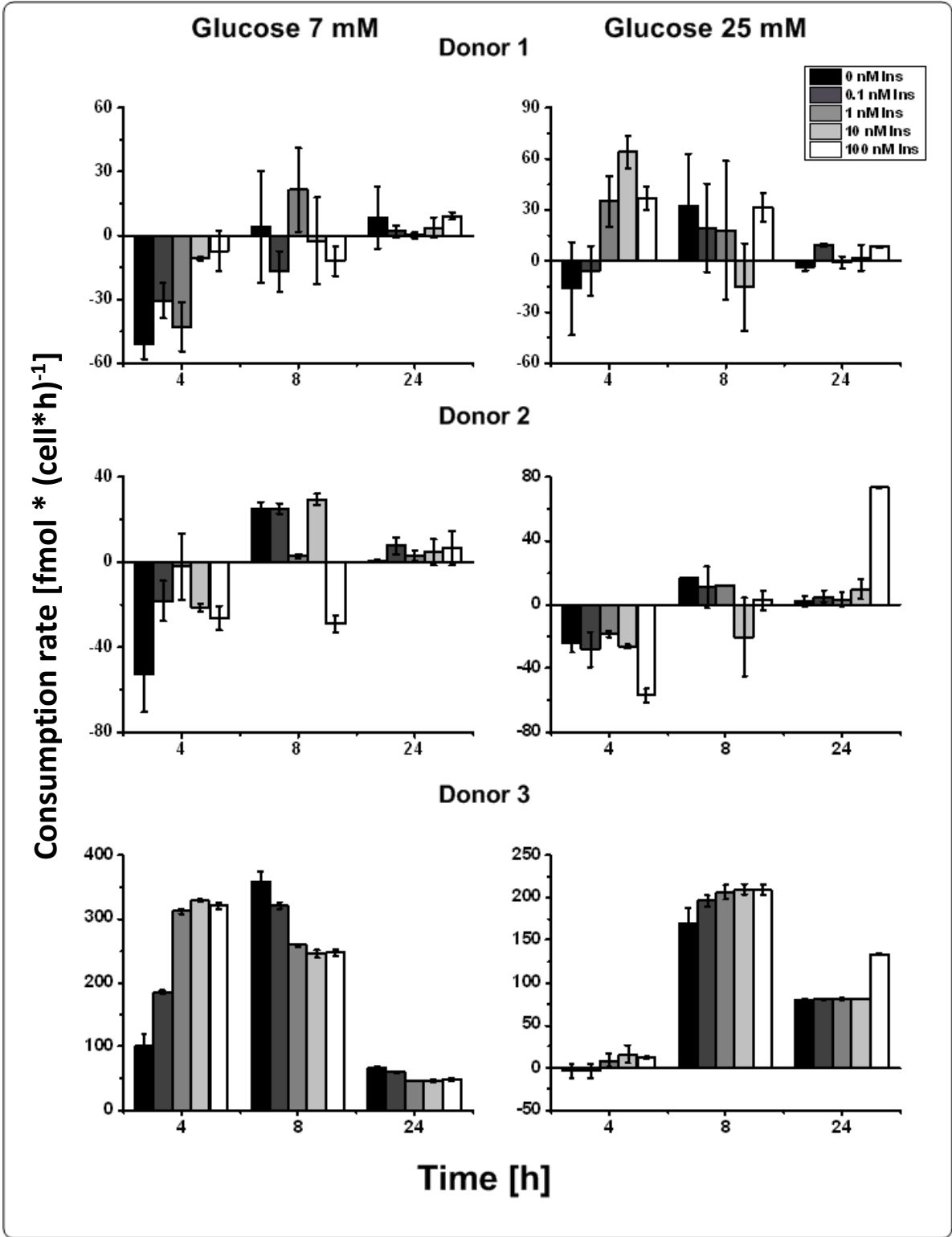
Supplementary Figure 6 Conversion rates of glucose of the three single donors of primary human hepatocytes cultivated in collagen sandwich culture under the influence of different insulin (0-100 nM) and glucose (7 and 25 mM) concentrations. Positive values indicate uptake, negative values production. Error bars indicate standard deviation (n=3). Living cell number was determined after 24 h of cultivation using calcein AM staining. Abbreviations: Ins Insulin.



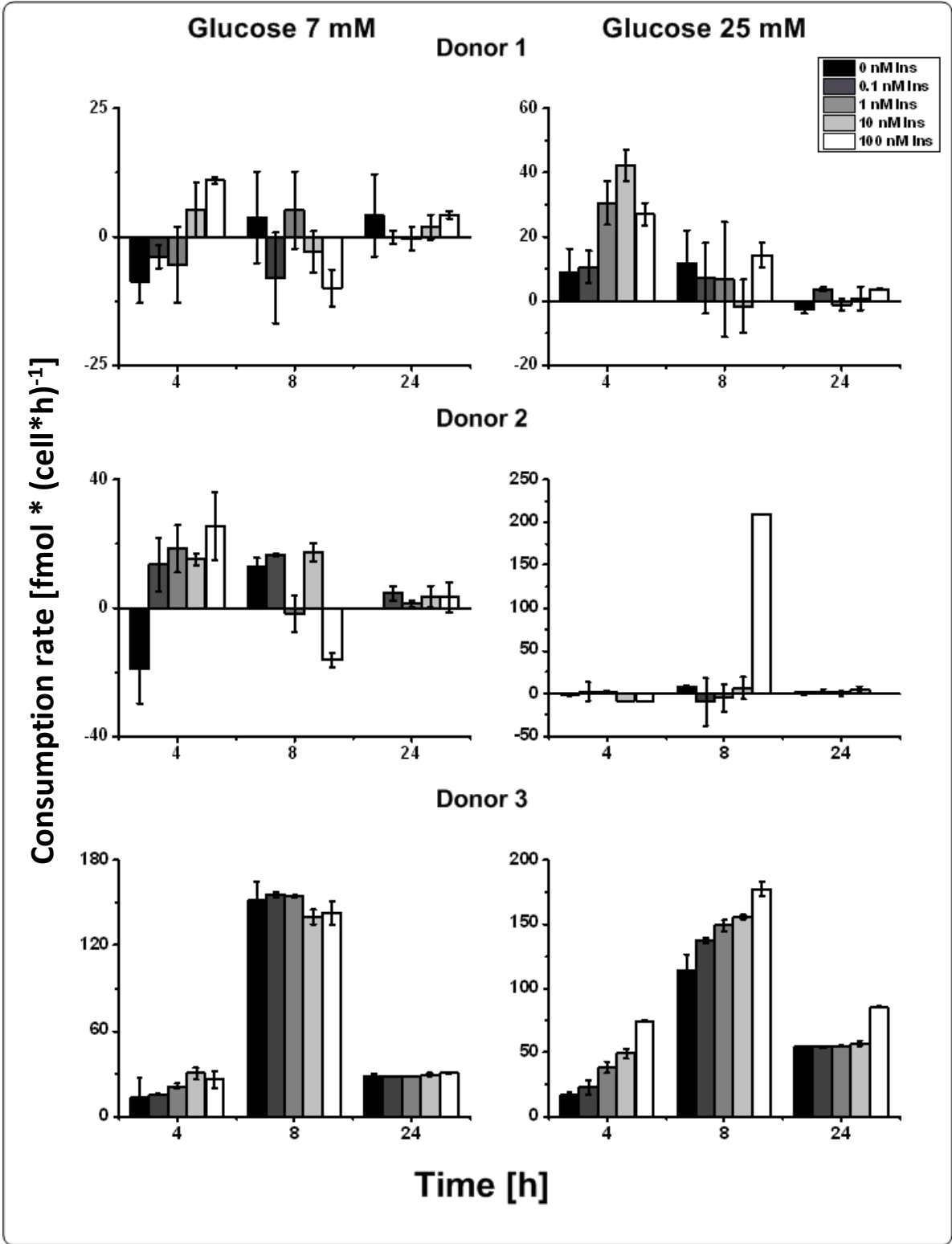
Supplementary Figure 7 Conversion rates of glutamine of the three single donors of primary human hepatocytes cultivated in collagen monolayer culture under the influence of different insulin (0-100 nM) and glucose (7 and 25 mM) concentrations. Positive values indicate uptake, negative values production. Error bars indicate standard deviation (n=3). Living cell number was determined after 24 h of cultivation using calcein AM staining. Abbreviations: Ins Insulin.



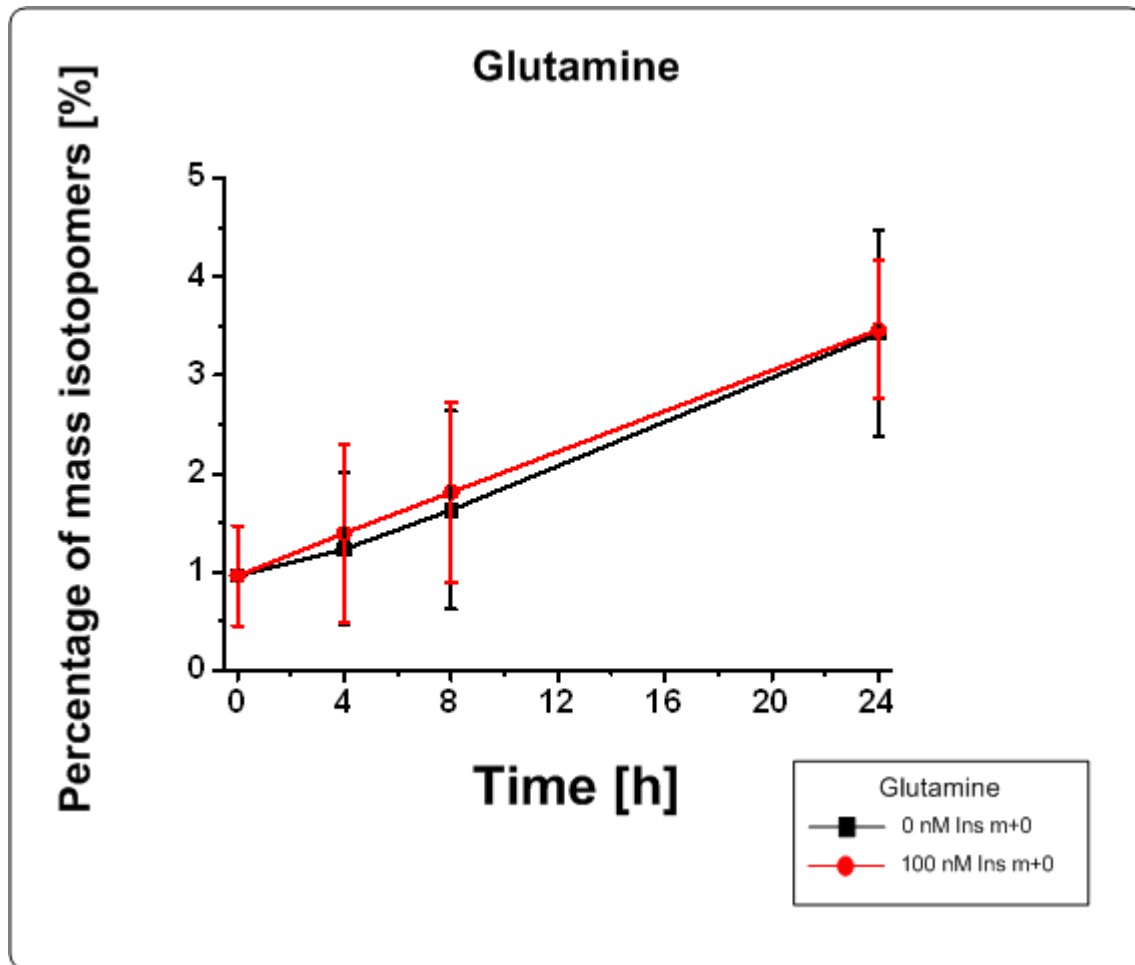
Supplementary Figure 8 Conversion rates of glycine of the three single donors of primary human hepatocytes cultivated in collagen monolayer culture under the influence of different insulin (0-100 nM) and glucose (7 and 25 mM) concentrations. Positive values indicate uptake, negative values production. Error bars indicate standard deviation (n=3). Living cell number was determined after 24 h of cultivation using calcein AM staining. Abbreviations: Ins Insulin.



Supplementary Figure 9 Conversion rates of glutamine of the three single donors of primary human hepatocytes cultivated in collagen sandwich culture under the influence of different insulin (0-100 nM) and glucose (7 and 25 mM) concentrations. Positive values indicate uptake, negative values production. Error bars indicate standard deviation (n=3). Living cell number was determined after 24 h of cultivation using calcein AM staining. Abbreviations: Ins Insulin.



Supplementary Figure 10 Conversion rates of glycine of the three single donors of primary human hepatocytes cultivated in collagen sandwich culture under the influence of different insulin (0-100 nM) and glucose (7 and 25 mM) concentrations. Positive values indicate uptake, negative values production. Error bars indicate standard deviation (n=3). Living cell number was determined after 24 h of cultivation using calcein AM staining. Abbreviations: Ins Insulin.



Supplementary Figure 11 Percentages of unlabeled glutamine of PHH cultivated in collagen ML culture with [U-¹³C₅] glutamine and 7 mM glucose. Black indicates incubation without insulin, red indicates incubation with 100 nM insulin, m+0 pointing to the number of labeled carbons. Error bars indicate standard deviation (N=2; n=6). Values were corrected for background contamination. Abbreviations: Ins Insulin.

Supplementary Table 3 Uptake rates of amino acids and organic acids, which are not depicted in Chapter 3, of primary mouse hepatocytes cultivated in collagen monolayer culture under the influence of different insulin concentrations (0-100 nM) and 7 mM glucose (n=3). Positive values indicate uptake, negative values production in [fmol*(cell*h)⁻¹]. Amino acids are abbreviated by the official three letter codes, FUM fumarate, PYR pyruvate.

Ins conc	Time		ARG	ASN	ASP	FUM	HIS	ILE	LEU	LYS	MET	PHE	PYR	SER	THR	TRP	TYR	VAL
0 nM	4 h	mean	182.56	36.87	4.56	-0.60	7.97	16.68	16.08	35.66	11.34	5.43	40.87	24.59	24.61	0.69	5.30	1.06
		SD	49.21	13.74	12.19	0.41	5.16	32.34	37.20	35.64	6.55	8.62	36.96	11.62	18.13	3.10	13.27	25.31
	8 h	mean	18.73	10.50	3.08	-0.45	3.60	-14.36	-18.04	8.90	0.46	-0.45	-1.65	7.04	2.70	1.13	3.25	-6.72
		SD	23.02	5.77	12.33	0.09	5.06	25.20	40.64	30.00	12.86	10.33	3.85	5.52	18.65	3.30	13.63	32.41
	24 h	mean	3.11	6.58	7.98	-0.46	3.31	-2.91	-0.33	21.34	3.78	7.52	-2.70	4.55	10.55	2.25	14.79	-3.56
		SD	4.43	2.75	3.96	0.12	1.74	5.22	7.99	10.48	4.28	3.82	3.37	2.85	6.04	0.92	9.00	5.77
0.1 nM	4 h	mean	188.81	36.60	3.57	-0.52	21.91	16.03	11.72	43.21	13.26	7.57	39.06	36.60	67.41	0.15	8.56	2.26
		SD	49.31	14.97	7.04	0.37	15.05	27.26	30.67	36.42	7.81	5.17	37.28	4.87	59.94	1.10	6.39	11.33
	8 h	mean	15.46	13.27	6.21	-0.38	-1.78	-2.63	-2.69	20.45	4.84	2.66	-1.45	1.44	-9.04	2.92	6.60	1.20
		SD	21.65	4.45	3.68	0.09	13.65	11.85	15.34	14.98	8.80	3.04	3.88	18.01	45.80	1.55	3.92	10.32
	24 h	mean	2.56	6.27	8.21	-0.43	1.02	-4.29	-1.80	18.24	2.09	6.39	-2.97	3.49	5.10	1.70	12.77	-2.73
		SD	4.07	2.26	4.32	0.11	3.95	2.90	3.71	8.68	5.20	2.68	3.75	3.79	14.13	0.62	7.19	5.52
1 nM	4 h	mean	195.04	36.98	2.09	-0.43	8.51	17.26	12.61	42.70	13.78	8.66	37.61	26.31	24.20	0.27	10.20	7.50
		SD	65.70	14.80	5.94	0.32	5.29	20.54	21.77	34.66	5.14	3.57	38.60	13.00	14.96	1.04	4.69	7.11
	8 h	mean	13.97	16.96	4.05	-0.24	4.66	1.05	4.14	12.98	8.49	5.99	-0.67	12.63	13.08	3.51	7.55	3.41
		SD	19.15	7.10	3.05	0.04	3.30	6.25	9.29	10.90	5.92	3.81	2.66	6.29	9.10	1.50	5.03	6.15
	24 h	mean	1.76	6.89	8.82	-0.40	2.14	-4.73	-1.13	16.91	2.62	4.95	-3.22	4.62	11.56	1.30	11.63	-3.22
		SD	2.42	2.84	4.91	0.11	1.03	2.38	3.79	8.49	5.68	2.08	3.72	2.86	6.77	0.46	7.90	4.92
10 nM	4 h	mean	195.49	44.66	3.50	-0.50	11.33	29.50	25.76	56.06	21.61	11.75	39.99	32.48	34.75	1.44	16.03	13.56
		SD	59.73	20.98	14.18	0.38	6.59	44.15	55.42	60.07	22.12	10.66	37.48	19.00	20.56	3.11	14.01	15.63
	8 h	mean	17.47	19.07	3.34	-0.19	5.13	4.78	9.70	15.06	11.27	6.34	-1.89	15.40	17.18	3.06	7.25	5.18
		SD	23.43	6.17	4.15	0.08	2.23	6.46	8.90	10.18	3.09	3.32	1.26	5.79	8.24	1.53	4.24	6.47
	24 h	mean	2.49	7.63	9.47	-0.39	2.96	-3.64	1.63	18.31	4.49	5.45	-2.63	5.68	14.75	1.58	14.52	-1.43
		SD	3.73	3.16	4.00	0.11	1.18	1.65	2.85	5.91	4.79	2.50	3.69	2.81	6.82	0.28	8.68	4.13

Ins conc	Time		ARG	ASN	ASP	FUM	HIS	ILE	LEU	LYS	MET	PHE	PYR	SER	THR	TRP	TYR	VAL
100 nM	4 h	mean	201.79	43.35	-16.62	-0.48	9.66	10.21	0.61	40.09	12.75	6.67	38.25	31.10	25.61	0.17	6.74	7.63
		SD	48.27	16.94	12.63	0.35	5.00	27.09	35.24	43.16	12.98	7.77	36.22	14.31	19.82	2.05	11.55	17.64
	8 h	mean	15.16	22.44	6.26	-0.23	7.53	9.40	17.83	19.04	13.95	9.02	-2.53	17.49	22.57	2.90	8.84	9.73
		SD	17.54	8.64	9.27	0.03	3.70	24.01	32.30	23.38	15.01	7.21	3.05	7.64	13.57	3.15	9.24	11.80
	24 h	mean	1.77	7.37	10.62	-0.33	3.42	-2.09	4.22	18.81	5.16	6.41	-1.94	6.01	17.65	1.74	16.56	-0.01
		SD	2.56	2.58	3.36	0.06	0.80	1.67	3.16	5.66	4.52	2.68	3.65	2.30	6.74	0.44	7.58	3.45

Supplementary Table 4 Uptake rates of amino acids and organic acids, which are not depicted in Chapter 3, of primary mouse hepatocytes cultivated in collagen monolayer culture under the influence of different insulin concentrations (0-100 nM) and 25 mM glucose (n=3). Positive values indicate uptake, negative values production in [fmol*(cell*h)⁻¹]. Amino acids are abbreviated by the official three letter codes, FUM fumarate, PYR pyruvate.

Ins conc	Time		ARG	ASN	ASP	FUM	HIS	ILE	LEU	LYS	MET	PHE	PYR	SER	THR	TRP	TYR	VAL
0 nM	4 h	mean	184.79	33.68	3.38	-0.57	7.12	7.01	10.72	32.88	5.89	4.61	0.86	22.11	19.72	0.53	4.75	0.30
		SD	46.42	10.95	5.22	0.39	4.46	14.73	13.24	20.32	11.58	4.48	18.29	9.73	13.47	1.69	6.97	9.75
	8 h	mean	17.25	11.28	7.68	-0.43	3.56	-7.30	-6.29	16.60	0.57	2.42	1.54	7.98	5.63	2.33	5.22	1.13
		SD	22.69	4.92	8.08	0.13	3.80	16.22	21.47	26.21	14.24	5.39	17.02	4.55	13.54	2.64	8.36	11.19
	24 h	mean	2.45	5.10	8.80	-0.46	2.01	-4.01	0.02	16.86	2.66	6.35	-0.35	3.79	8.80	1.69	11.84	-4.09
		SD	3.48	1.76	2.25	0.11	0.64	4.63	6.98	7.40	3.77	1.94	22.81	2.22	2.87	0.50	5.40	6.61
0.1 nM	4 h	mean	186.42	33.27	7.07	-0.49	7.77	10.85	17.63	43.28	7.92	7.86	-7.07	21.97	21.09	1.88	8.76	1.73
		SD	49.15	11.52	3.76	0.33	4.53	14.64	8.58	17.67	9.18	2.17	24.25	10.67	12.33	1.01	4.34	5.62
	8 h	mean	13.66	11.85	6.32	-0.39	2.97	-6.57	-5.43	13.60	2.76	2.48	1.83	8.94	5.84	2.22	5.96	-1.19
		SD	18.04	4.17	4.09	0.11	2.75	12.17	13.41	20.09	10.84	2.65	19.95	4.31	7.77	1.99	3.81	7.96
	24 h	mean	2.58	4.63	8.17	-0.42	1.93	-3.36	0.21	15.61	2.07	5.99	1.18	2.96	7.72	1.28	10.38	-2.07
		SD	3.67	1.19	5.76	0.11	1.15	4.17	4.97	6.14	4.51	1.79	23.35	1.37	5.58	0.50	5.09	5.86

Ins conc	Time		ARG	ASN	ASP	FUM	HIS	ILE	LEU	LYS	MET	PHE	PYR	SER	THR	TRP	TYR	VAL
1 nM	4 h	mean	186.73	28.57	-4.43	-0.41	9.94	23.35	31.98	51.29	10.01	12.92	4.74	15.30	37.23	2.68	13.05	11.74
		SD	53.32	15.29	33.43	0.28	8.01	19.62	28.28	28.96	7.36	5.72	10.77	13.82	55.61	2.60	5.55	4.49
	8 h	mean	20.12	27.13	32.29	-0.28	7.14	25.03	21.21	85.73	33.64	11.72	1.82	23.64	19.70	4.20	16.65	8.51
		SD	27.98	31.07	53.19	0.09	10.36	137.20	181.26	161.40	81.87	27.77	20.32	29.70	78.42	8.32	38.19	16.69
	24 h	mean	1.49	4.56	8.75	-0.41	0.60	-5.68	-7.22	2.84	0.28	3.14	-0.41	3.12	9.25	0.75	6.68	-3.44
		SD	2.68	5.26	8.77	0.09	2.14	26.15	36.87	28.51	17.07	6.19	20.82	4.58	10.42	1.72	9.91	5.12
10 nM	4 h	mean	191.10	34.17	14.26	-0.44	13.02	48.98	29.43	104.47	33.21	17.75	6.88	23.55	49.96	4.27	12.19	21.51
		SD	54.21	18.04	19.23	0.36	8.64	63.53	48.88	110.69	30.24	12.32	17.82	14.89	24.88	5.02	9.66	13.42
	8 h	mean	11.88	15.59	4.19	-0.28	-0.03	-41.83	-41.46	-39.94	-22.12	-4.51	-3.08	11.75	-0.74	-0.97	-4.22	-4.15
		SD	35.38	45.30	36.80	0.12	12.51	105.58	173.60	110.87	70.51	28.10	16.85	36.43	39.59	7.78	49.41	10.57
	24 h	mean	0.09	5.13	4.52	-0.48	1.52	-5.56	3.62	8.23	2.90	3.16	0.66	3.71	7.67	0.96	10.08	-1.86
		SD	6.44	7.37	12.48	0.16	1.50	9.33	4.11	13.65	7.86	3.33	23.17	6.16	13.67	0.94	10.21	1.93
100 nM	4 h	mean	198.08	40.69	-24.41	-0.41	12.50	15.99	20.49	52.36	10.21	11.90	5.42	27.14	23.08	2.00	11.28	90.36
		SD	57.89	13.48	48.84	0.40	7.28	13.51	12.38	29.56	8.81	5.27	17.15	10.41	17.58	2.56	4.16	150.85
	8 h	mean	13.59	24.89	23.06	-0.27	5.37	2.79	19.14	21.22	11.25	9.45	3.16	20.64	22.30	3.55	10.17	-71.14
		SD	14.76	13.09	35.11	0.05	3.44	12.73	13.50	21.68	8.42	4.39	21.58	9.95	21.48	1.52	9.08	154.94
	24 h	mean	1.04	6.21	14.09	-0.45	2.84	9.77	17.62	22.25	11.08	6.23	2.86	5.37	17.15	1.83	14.27	1.71
		SD	1.93	2.33	4.12	0.11	1.30	27.96	27.21	16.25	15.04	3.38	22.71	2.34	6.62	0.94	7.59	2.27

Supplementary Table 5 Uptake rates of amino acids and organic acids, which are not depicted in Chapter 3, of primary mouse hepatocytes cultivated in collagen sandwich culture under the influence of different insulin concentrations (0-100 nM) and 7 mM glucose (n=3). Positive values indicate uptake, negative values production in [fmol*(cell*h)⁻¹]. Amino acids are abbreviated by the official three letter codes, FUM fumarate, PYR pyruvate.

Ins conc	Time		ARG	ASN	ASP	FUM	HIS	ILE	LEU	LYS	MET	PHE	PYR	SER	THR	TRP	TYR	VAL
0 nM	4 h	mean	90.47	19.92	0.55	-0.71	3.45	-12.94	-13.74	-1.70	6.00	-2.92	45.44	11.52	6.80	-0.01	-5.33	-16.43
		SD	11.09	3.94	10.50	0.57	3.43	13.74	31.82	20.90	3.91	6.66	14.54	4.99	12.87	2.15	8.61	14.79
	8 h	mean	18.69	5.57	1.14	-0.42	2.22	-5.08	-6.27	7.75	4.47	0.64	0.08	3.96	5.41	0.38	3.57	-5.48
		SD	6.64	4.54	7.38	0.16	3.03	15.11	23.82	17.35	3.77	5.90	0.73	3.46	12.16	2.05	7.57	17.31
	24 h	mean	3.32	2.20	2.76	-0.47	1.25	-4.91	-6.10	13.77	2.68	2.85	-0.65	1.63	3.74	2.06	8.92	-6.70
		SD	2.48	0.66	1.85	0.15	0.67	3.51	5.16	3.21	0.72	2.02	0.88	0.53	2.21	0.48	3.93	3.85
0.1 nM	4 h	mean	87.83	18.65	-3.27	-0.69	2.73	-11.14	-22.19	-6.19	4.72	-5.77	44.94	10.24	0.84	-1.08	-9.31	-24.53
		SD	11.11	2.71	8.28	0.56	2.11	18.38	23.81	15.08	2.30	5.08	14.61	4.04	9.37	1.66	6.40	11.42
	8 h	mean	21.07	4.34	-7.38	-0.42	1.05	2.93	5.28	18.40	5.73	3.41	0.54	2.77	-0.87	1.40	6.39	1.28
		SD	6.69	6.71	21.34	0.16	5.73	15.52	23.23	18.47	3.97	6.32	0.53	5.50	21.70	1.86	7.22	17.69
	24 h	mean	3.56	2.72	4.15	-0.52	1.43	-5.77	-4.74	13.54	2.79	2.81	-0.78	2.14	5.39	1.93	8.70	-5.36
		SD	2.56	0.84	2.58	0.18	0.80	3.92	4.61	4.96	0.52	2.64	1.11	0.99	2.78	0.78	5.17	3.42
1 nM	4 h	mean	91.87	19.48	-5.58	-0.65	3.50	-11.93	-14.86	0.21	5.53	-3.31	45.06	11.28	3.52	-0.78	-6.44	-19.44
		SD	9.89	3.36	10.66	0.51	2.44	15.43	28.57	17.62	2.81	5.79	14.43	4.67	9.88	1.98	7.46	12.48
	8 h	mean	20.25	6.99	2.98	-0.32	2.68	-4.77	-2.71	5.26	4.85	1.69	0.44	5.07	8.87	0.57	3.52	-2.94
		SD	6.95	2.07	6.94	0.13	1.00	12.38	10.86	9.63	1.48	3.16	0.72	1.37	5.32	0.92	4.31	7.89
	24 h	mean	3.00	2.65	4.12	-0.44	1.47	-3.24	-2.73	13.29	3.27	2.95	-1.04	2.05	5.21	1.67	8.19	-4.34
		SD	1.81	0.62	1.85	0.14	0.60	1.64	2.48	1.49	0.85	1.31	0.84	0.39	1.65	0.32	2.90	2.06
10 nM	4 h	mean	101.59	22.84	-0.15	-0.70	6.34	-7.56	-4.14	9.09	7.62	-0.35	45.13	13.77	11.44	-0.29	-2.09	-11.97
		SD	17.24	4.94	9.10	0.56	2.82	12.13	26.86	15.81	2.38	5.33	14.84	5.04	11.94	1.87	7.42	12.70
	8 h	mean	16.67	7.14	-3.83	-0.30	2.15	-0.99	-4.04	-0.24	4.39	1.05	0.13	5.66	5.30	-0.30	0.54	-4.76
		SD	7.45	1.58	5.89	0.17	1.62	12.43	12.49	10.59	1.44	3.72	0.69	1.12	6.11	1.25	5.75	9.46
	24 h	mean	2.17	3.70	3.80	-0.30	1.41	-1.87	-0.91	7.81	4.43	2.80	-0.40	2.58	6.70	0.92	5.95	-2.48
		SD	1.78	0.36	1.10	0.11	0.43	2.83	2.81	3.03	0.67	1.51	0.64	0.40	1.85	0.44	2.47	2.26

Ins conc	Time		ARG	ASN	ASP	FUM	HIS	ILE	LEU	LYS	MET	PHE	PYR	SER	THR	TRP	TYR	VAL
100 nM	4 h	mean	107.77	26.58	-1.51	-0.75	7.40	-3.37	-5.29	8.47	8.29	1.21	44.96	15.87	12.50	2.26	-3.30	-10.77
		SD	17.42	5.34	13.05	0.49	3.48	16.45	32.86	20.37	2.68	6.07	14.84	5.27	12.89	1.86	10.94	15.57
	8 h	mean	14.88	9.70	-0.43	-0.31	3.20	-4.47	-1.21	2.73	8.86	3.56	0.22	7.69	12.62	0.83	3.90	-2.03
		SD	6.73	4.82	12.20	0.17	2.87	7.14	12.23	16.23	8.85	5.01	0.66	3.50	15.06	1.98	9.51	7.37
	24 h	mean	-1.13	2.78	3.86	-0.25	1.33	0.00	3.12	8.39	3.91	2.89	-0.12	2.34	7.49	0.60	6.67	0.08
		SD	8.91	5.06	2.76	0.10	1.68	2.17	2.64	5.21	4.80	2.05	0.34	3.45	7.79	0.76	4.07	2.39

Supplementary Table 6 Uptake rates of amino acids and organic acids, which are not depicted in Chapter 3, of primary mouse hepatocytes cultivated in collagen sandwich culture under the influence of different insulin concentrations (0-100 nM) and 25 mM glucose (n=3). Positive values indicate uptake, negative values production in [fmol*(cell*h)⁻¹]. Amino acids are abbreviated by the official three letter codes, FUM fumarate, PYR pyruvate.

Ins conc	Time		ARG	ASN	ASP	FUM	HIS	ILE	LEU	LYS	MET	PHE	PYR	SER	THR	TRP	TYR	VAL
0 nM	4 h	mean	116.62	29.83	17.90	-0.64	11.48	9.99	22.19	28.67	15.54	10.62	46.00	18.10	30.28	5.28	10.55	13.15
		SD	64.18	18.74	21.82	0.56	10.87	37.98	45.74	53.50	13.93	18.33	17.30	10.60	34.19	7.28	20.80	43.53
	8 h	mean	23.80	7.73	2.70	-0.36	2.68	-0.42	2.63	14.72	4.89	-0.55	0.29	5.75	7.89	0.81	3.98	-3.01
		SD	8.78	4.27	4.67	0.27	1.71	13.39	18.58	16.39	2.77	6.14	0.76	3.05	7.48	1.17	5.27	9.95
	24 h	mean	3.42	2.29	4.03	-0.51	1.44	-3.12	-4.25	14.19	2.95	2.80	-1.16	1.80	4.52	1.97	7.86	-5.53
		SD	2.55	1.08	2.55	0.23	0.80	2.18	3.70	3.01	1.38	2.38	1.57	0.47	2.40	0.37	2.97	2.64
0.1 nM	4 h	mean	120.65	33.15	23.60	-0.62	13.96	21.61	32.43	50.36	18.65	13.32	45.10	21.02	35.79	7.21	20.07	14.74
		SD	58.37	18.61	25.60	0.57	11.00	38.52	53.13	51.39	15.55	18.62	17.45	10.75	38.11	8.10	26.17	55.81
	8 h	mean	13.43	5.05	2.77	-0.34	2.44	5.04	6.96	7.98	3.58	-0.26	0.18	3.46	6.19	0.05	-0.43	5.25
		SD	27.03	7.58	8.35	0.26	3.83	14.52	20.48	31.52	7.22	7.85	1.18	6.26	14.34	4.66	20.62	18.03
	24 h	mean	3.81	1.97	3.18	-0.46	1.01	-5.53	-5.09	10.80	2.58	2.08	-1.18	1.49	3.53	1.41	5.84	-6.13
		SD	1.90	0.89	2.19	0.18	0.67	3.32	4.16	4.16	1.27	2.31	1.75	0.47	2.29	0.82	4.08	3.49

Ins conc	Time		ARG	ASN	ASP	FUM	HIS	ILE	LEU	LYS	MET	PHE	PYR	SER	THR	TRP	TYR	VAL
1 nM	4 h	mean	119.47	34.16	26.22	-0.59	16.29	32.83	51.12	56.09	19.72	8.50	45.24	22.15	39.95	7.21	20.20	29.40
		SD	60.10	22.13	33.72	0.59	14.89	49.35	69.26	72.35	19.20	17.46	16.75	13.80	49.68	10.31	31.08	65.23
	8 h	mean	20.20	4.80	-3.41	-0.24	0.47	-10.82	-14.94	-2.11	3.04	7.67	0.84	3.53	0.29	-0.48	-1.49	-12.52
		SD	4.45	1.22	8.37	0.22	2.59	14.59	20.98	18.20	1.34	15.34	1.99	1.11	7.56	2.00	8.41	15.41
	24 h	mean	3.55	2.37	4.82	-0.43	1.19	-3.50	-1.65	12.56	3.23	2.87	-2.15	1.72	5.46	1.60	7.36	-3.95
		SD	1.57	1.09	3.51	0.24	0.94	3.01	4.57	6.15	1.57	0.93	1.24	0.67	3.58	0.67	2.91	3.10
10 nM	4 h	mean	131.22	34.98	24.94	-0.61	17.65	33.63	51.14	59.25	19.77	1.91	44.08	22.15	41.04	6.33	20.89	29.96
		SD	64.71	21.77	33.47	0.63	15.45	49.26	68.23	74.89	19.04	2.34	17.32	13.05	48.69	10.22	31.93	64.34
	8 h	mean	16.47	5.86	-5.94	-0.29	0.91	-10.06	-12.18	-5.07	3.14	10.92	-0.35	4.65	-0.04	-0.48	-2.74	-11.87
		SD	8.26	2.83	9.90	0.22	2.53	17.52	22.01	16.88	2.63	19.91	0.84	2.80	11.12	2.44	8.58	16.85
	24 h	mean	2.43	3.50	5.74	-0.28	1.37	-0.87	3.37	9.62	4.33	3.44	0.22	2.51	7.73	1.19	5.27	0.56
		SD	1.96	1.05	3.03	0.14	0.64	4.25	5.30	3.46	1.55	4.15	1.03	0.97	2.94	0.78	1.79	4.11
100 nM	4 h	mean	128.81	37.49	24.78	-0.59	17.73	33.81	54.55	57.44	21.00	20.08	45.37	24.69	41.88	9.08	22.43	33.09
		SD	57.79	21.63	35.48	0.56	14.72	53.05	72.66	74.03	20.23	27.29	16.89	12.25	50.91	10.72	33.31	66.84
	8 h	mean	19.03	8.05	-3.12	-0.29	2.22	-3.05	-1.77	0.53	5.46	2.37	-1.18	6.72	6.68	0.46	1.37	-3.18
		SD	4.10	2.14	8.15	0.22	1.89	10.74	17.47	14.34	2.36	3.78	0.85	1.87	7.16	2.04	6.64	12.17
	24 h	mean	2.73	3.87	5.41	-0.26	2.82	8.97	16.01	16.97	5.33	6.01	-1.08	3.75	14.61	1.72	8.88	10.54
		SD	1.83	0.47	1.92	0.12	2.36	18.52	25.42	16.52	1.42	5.35	1.72	2.05	10.39	1.53	7.59	19.98

Supplementary Table 7 Uptake rates of amino acids and organic acids, which are not depicted in Chapter 3, of primary human hepatocytes cultivated in collagen monolayer culture under the influence of different insulin concentrations (0-100 nM) and 7 mM glucose (n=3). Positive values indicate uptake, negative values production in [fmol*(cell*h)⁻¹]. Amino acids are abbreviated by the official three letter codes, FUM fumarate, PYR pyruvate.

Ins conc	Time		ARG	ASN	ASP	FUM	HIS	ILE	LEU	LYS	MET	PHE	PYR	SER	THR	TRP	TYR	VAL
0 nM	4 h	mean	40.98	-13.44	-18.98	-0.55	-13.49	-45.98	-69.55	-54.22	-8.23	-18.50	10.08	-11.24	-45.39	-4.33	-26.92	-51.59
		SD	18.87	12.75	33.55	0.24	10.13	41.79	77.73	50.55	10.87	18.28	5.17	11.46	35.21	4.52	29.53	45.41
	8 h	mean	18.77	2.70	1.40	0.05	1.89	7.46	9.34	10.33	4.78	5.41	1.23	3.24	6.80	1.90	7.74	8.26
		SD	16.36	9.40	20.99	0.35	7.40	29.97	45.40	34.59	6.93	12.24	0.91	7.08	28.74	3.75	20.07	35.46
	24 h	mean	5.82	1.62	1.89	-0.05	1.29	3.56	8.00	7.27	3.11	3.47	0.02	1.64	3.52	1.16	4.27	3.92
		SD	3.16	0.66	3.59	0.05	0.52	2.91	8.00	2.97	0.96	1.45	0.14	0.65	2.38	0.35	2.34	2.99
0.1 nM	4 h	mean	54.25	-5.28	-13.51	-0.33	-6.80	-18.48	-29.12	-22.85	-2.08	-7.40	9.77	-4.04	-19.49	-1.21	-8.68	-20.57
		SD	17.26	3.15	5.99	0.15	3.43	10.40	28.30	16.54	3.01	4.95	5.06	3.64	9.60	1.34	7.13	10.33
	8 h	mean	17.13	3.15	5.83	-0.06	3.17	9.22	12.88	15.16	4.62	5.96	1.63	2.93	7.86	1.94	8.44	9.30
		SD	8.96	2.51	4.81	0.08	2.52	8.49	13.62	11.76	2.55	4.05	1.26	2.19	8.32	1.42	6.98	9.65
	24 h	mean	3.88	0.59	0.99	-0.06	0.53	0.40	3.08	3.38	2.29	1.99	0.00	0.82	0.36	0.68	2.06	0.07
		SD	2.43	0.39	1.04	0.01	0.31	1.49	5.35	1.45	0.46	0.91	0.13	0.37	1.31	0.15	1.17	1.54
1 nM	4 h	mean	57.14	-2.25	-7.04	-0.36	-2.56	-9.37	-14.44	-7.80	0.78	-2.52	9.62	-1.62	-9.28	-0.12	-0.80	-10.27
		SD	16.07	1.37	8.18	0.31	2.12	4.92	10.70	5.18	0.63	2.23	4.70	1.27	11.78	1.72	3.23	8.72
	8 h	mean	14.08	-0.05	-0.94	-0.01	0.03	-1.98	-4.30	-0.47	2.35	1.29	2.02	0.41	-0.21	0.62	1.23	-2.11
		SD	5.62	2.37	6.63	0.23	1.97	7.83	12.29	8.38	1.25	3.54	0.64	1.67	8.04	1.14	4.73	9.92
	24 h	mean	4.10	0.83	1.63	-0.05	0.58	1.31	4.46	3.71	2.42	2.28	-0.10	1.16	1.32	0.88	2.29	1.37
		SD	2.56	0.59	2.12	0.03	0.50	2.69	6.43	1.90	0.55	1.31	0.24	0.50	2.34	0.23	1.33	2.96
10 nM	4 h	mean	60.48	-1.76	-5.63	-0.32	-2.43	-8.14	-13.80	-9.16	1.19	-2.30	9.99	-1.04	-5.05	-0.09	-0.01	-7.49
		SD	16.38	1.52	8.48	0.16	1.80	4.80	13.82	5.78	0.64	2.59	4.63	1.45	10.86	1.89	2.07	9.75
	8 h	mean	13.94	1.40	1.31	-0.05	1.11	2.62	3.20	5.99	3.36	2.93	1.54	1.82	3.06	1.09	3.56	2.55
		SD	4.14	1.17	3.59	0.07	0.87	3.77	5.63	3.92	1.23	2.27	0.86	1.17	3.80	0.79	2.39	4.50
	24 h	mean	3.50	0.91	1.12	-0.07	0.61	1.35	4.65	3.96	2.51	2.27	-0.23	1.40	0.89	0.88	2.23	1.02
		SD	1.90	0.47	1.02	0.01	0.32	1.15	3.67	1.41	0.35	0.66	0.31	0.46	0.95	0.18	0.98	1.38

Ins conc	Time		ARG	ASN	ASP	FUM	HIS	ILE	LEU	LYS	MET	PHE	PYR	SER	THR	TRP	TYR	VAL
100 nM	4 h	mean	49.12	16.73	-0.54	-1.11	-0.24	-1.76	-30.21	-5.01	1.63	1.00	5.19	1.73	-7.07	-0.12	0.19	0.96
		SD	38.74	24.75	4.75	1.28	0.96	2.82	29.17	5.59	1.51	0.97	11.97	1.49	14.15	2.72	3.09	4.71
	8 h	mean	13.49	1.47	0.24	-0.05	1.21	0.38	-0.04	4.61	3.76	2.96	1.18	2.32	0.01	1.89	2.85	-0.23
		SD	5.80	1.88	5.83	0.07	1.31	5.42	7.18	5.82	1.88	3.31	1.64	2.04	4.71	2.72	2.64	7.78
	24 h	mean	2.94	1.62	1.64	-0.08	0.96	2.41	6.83	5.31	3.06	3.00	-0.08	1.89	2.21	1.13	3.19	2.45
		SD	1.69	0.16	0.85	0.03	0.17	0.69	4.25	0.88	0.52	0.77	0.50	0.63	0.52	0.23	0.54	0.63

Supplementary Table 8 Uptake rates of amino acids and organic acids, which are not depicted in Chapter 3, of primary human hepatocytes cultivated in collagen monolayer culture under the influence of different insulin concentrations (0-100 nM) and 25 mM glucose (n=3). Positive values indicate uptake, negative values production in [fmol*(cell*h)⁻¹]. Amino acids are abbreviated by the official three letter codes, FUM fumarate, PYR pyruvate.

Ins conc	Time		ARG	ASN	ASP	FUM	HIS	ILE	LEU	LYS	MET	PHE	PYR	SER	THR	TRP	TYR	VAL
0 nM	4 h	mean	66.68	-1.86	-6.57	-0.57	-1.53	-12.34	-19.77	-19.99	0.01	-1.81	7.99	-1.61	-3.63	1.93	-3.61	-3.76
		SD	15.29	2.81	8.83	0.32	1.45	12.47	15.04	14.04	1.30	2.08	6.09	2.84	4.63	1.27	4.45	14.65
	8 h	mean	13.49	1.51	3.28	-0.18	1.01	4.00	10.74	6.11	3.28	3.64	1.07	1.59	4.07	1.46	4.84	4.29
		SD	7.41	2.09	5.13	0.20	1.58	6.95	16.56	7.59	1.51	3.49	1.70	1.52	6.14	1.05	4.12	8.17
	24 h	mean	2.90	0.74	1.30	-0.07	0.55	1.14	3.21	3.98	2.29	2.17	0.00	0.96	1.07	0.78	2.48	1.15
		SD	1.94	0.33	0.99	0.02	0.25	1.04	2.85	1.13	0.28	0.76	0.15	0.23	0.91	0.12	0.75	1.18
0.1 nM	4 h	mean	70.39	0.06	-2.60	-0.62	-0.76	-6.28	-10.98	-14.92	1.16	0.75	7.61	-0.20	2.11	2.54	0.62	3.52
		SD	19.65	1.91	6.83	0.36	0.80	8.74	16.02	9.93	1.73	1.39	5.76	2.55	2.86	1.07	2.00	10.65
	8 h	mean	10.49	0.75	2.70	-0.07	0.97	2.76	7.67	4.91	2.72	2.59	1.69	1.01	2.77	1.45	3.62	2.27
		SD	7.58	1.63	5.46	0.07	0.81	5.51	17.66	6.04	1.09	2.79	0.79	0.91	4.87	1.12	2.58	6.61
	24 h	mean	2.79	0.60	1.04	-0.07	0.49	0.80	3.90	3.64	2.27	2.03	-0.12	0.89	0.65	0.75	2.21	0.56
		SD	2.09	0.32	1.33	0.02	0.24	0.93	3.92	0.93	0.23	0.74	0.28	0.13	1.03	0.11	0.52	1.27

Ins conc	Time		ARG	ASN	ASP	FUM	HIS	ILE	LEU	LYS	MET	PHE	PYR	SER	THR	TRP	TYR	VAL
1 nM	4 h	mean	68.90	1.12	-1.01	-0.59	0.24	-1.60	-5.53	-9.03	1.70	1.45	7.69	0.55	4.87	2.75	2.44	5.59
		SD	15.08	2.30	3.99	0.29	1.09	7.23	18.90	10.34	2.62	3.32	5.56	3.26	5.00	0.47	2.31	4.54
	8 h	mean	13.19	0.24	-0.93	-0.01	0.49	-0.93	-1.10	4.33	2.48	1.69	1.31	0.95	-1.50	1.00	1.77	-2.17
		SD	6.84	0.97	3.55	0.08	0.83	2.99	4.74	4.79	0.64	1.40	1.35	0.90	3.49	0.84	1.97	4.37
	24 h	mean	2.63	0.67	1.28	-0.06	0.46	1.06	8.88	3.43	2.43	2.20	-0.02	1.04	0.77	0.83	2.21	0.84
		SD	1.83	0.34	0.81	0.02	0.33	0.63	14.22	1.42	0.52	0.69	0.22	0.41	0.64	0.13	0.80	0.56
10 nM	4 h	mean	76.55	1.08	-2.30	-0.58	0.20	-3.68	-9.56	-10.81	1.26	0.55	7.32	0.30	8.07	1.96	1.17	3.95
		SD	13.66	1.56	6.73	0.34	1.59	3.58	17.64	5.13	3.19	4.47	5.07	1.94	6.37	1.63	5.62	10.35
	8 h	mean	10.02	0.38	-0.97	-0.04	0.52	-0.75	2.58	4.05	2.77	1.08	1.57	0.98	-1.43	1.13	2.34	-1.59
		SD	5.76	0.93	2.42	0.10	0.86	2.45	11.37	4.28	0.63	1.54	1.26	0.65	3.19	0.98	1.93	2.74
	24 h	mean	1.74	1.01	1.38	-0.05	0.39	2.09	5.99	5.55	2.76	2.50	-0.28	1.43	1.55	0.87	2.79	1.56
		SD	1.39	0.41	1.46	0.02	1.09	1.39	4.23	1.36	0.51	0.61	0.48	0.38	1.11	0.27	0.98	1.65
100 nM	4 h	mean	65.81	-1.13	19.82	0.11	43.60	15.03	-6.27	-19.10	2.24	-3.24	8.57	10.32	6.31	-7.68	4.42	4.92
		SD	21.41	1.95	30.24	1.44	74.36	21.65	14.58	33.35	3.90	2.66	3.52	18.61	7.07	13.28	6.63	11.66
	8 h	mean	12.86	1.32	6.88	-0.08	-0.81	4.88	1.74	5.19	2.48	4.05	1.64	0.80	3.35	1.33	3.51	5.28
		SD	9.40	1.38	6.08	0.10	6.59	5.76	4.47	8.10	1.27	2.95	1.06	4.16	4.80	3.20	1.73	4.27
	24 h	mean	2.20	1.36	1.30	-0.08	1.13	1.92	3.98	5.13	3.01	2.66	-0.22	1.74	1.39	1.09	3.13	1.72
		SD	1.83	0.34	1.63	0.02	0.28	1.00	1.32	1.10	0.64	0.80	0.34	0.89	0.67	0.41	0.58	1.25

Supplementary Table 9 Uptake rates of amino acids and organic acids, which are not depicted in Chapter 3, of primary human hepatocytes cultivated in collagen sandwich culture under the influence of different insulin concentrations (0-100 nM) and 7 mM glucose (n=3). Positive values indicate uptake, negative values production in [fmol*(cell*h)⁻¹]. Amino acids are abbreviated by the official three letter codes, FUM fumarate, PYR pyruvate.

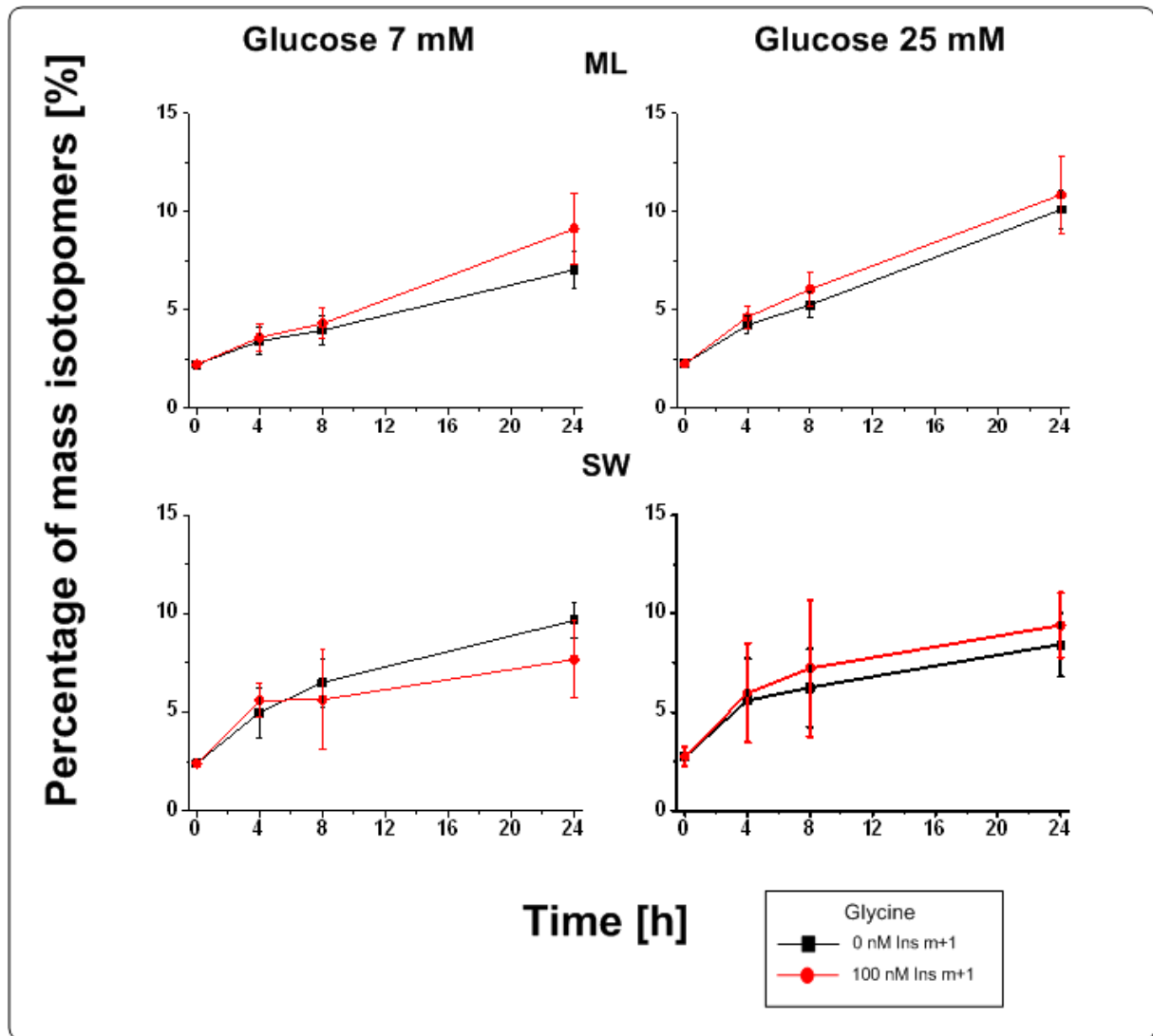
Ins conc	Time		ARG	ASN	ASP	FUM	HIS	ILE	LEU	LYS	MET	PHE	PYR	SER	THR	TRP	TYR	VAL
0 nM	4 h	mean	54.28	2.61	-5.56	-442.31	-2.39	-7.51	-9.35	-10.87	-1.09	-3.09	47.46	-4.19	-6.41	0.38	-2.21	-8.69
		SD	13.80	3.50	17.93	89.34	2.99	6.17	10.28	7.39	1.99	3.42	35.69	2.07	7.19	1.28	4.32	7.62
	8 h	mean	18.74	11.35	18.11	58.96	8.49	35.04	50.72	42.70	9.49	16.09	5.63	10.16	30.35	4.56	21.57	40.85
		SD	16.28	15.08	23.74	77.97	9.43	37.92	53.23	42.09	9.44	17.26	4.70	11.23	34.50	4.87	23.49	44.90
	24 h	mean	4.73	2.31	2.25	-26.60	1.57	5.68	8.33	7.41	2.13	2.88	0.11	1.88	5.12	0.94	3.84	6.57
		SD	3.57	2.57	2.26	30.94	1.84	7.38	10.47	8.18	1.67	3.31	0.17	2.10	6.72	0.94	4.58	8.74
0.1 nM	4 h	mean	52.74	4.19	3.47	-340.72	-0.52	-5.24	-3.17	-2.42	-0.34	-2.18	49.13	-3.97	-4.26	1.12	-0.61	-6.59
		SD	13.32	1.82	2.39	116.19	2.40	6.24	8.40	7.55	2.20	3.53	37.04	3.28	8.48	0.88	4.27	8.26
	8 h	mean	19.81	9.92	7.98	37.71	6.61	27.56	39.57	31.60	7.79	13.12	3.91	8.16	23.38	3.80	17.33	32.49
		SD	17.33	15.40	11.94	46.83	11.25	42.97	61.05	48.61	10.41	19.49	3.11	12.25	39.73	6.03	26.52	50.92
	24 h	mean	4.80	2.16	2.13	6.28	1.55	5.82	8.21	6.68	2.19	3.03	0.18	1.98	5.26	0.94	4.04	6.78
		SD	3.26	2.53	1.61	58.79	1.74	6.93	9.95	8.16	1.59	3.13	0.20	1.95	6.26	0.99	4.51	8.21
1 nM	4 h	mean	53.16	2.68	-9.86	-208.48	-1.55	-3.46	-2.11	-1.41	-0.11	-0.97	49.03	-2.29	-4.52	0.59	0.48	-5.37
		SD	10.80	1.30	25.86	275.92	2.40	5.84	9.43	8.74	2.31	2.38	36.88	2.21	6.12	0.72	2.81	6.76
	8 h	mean	20.86	10.89	14.98	10.80	8.41	29.54	41.43	32.69	8.04	13.75	4.26	8.40	28.66	4.23	18.82	35.13
		SD	16.36	15.21	31.03	68.04	11.04	43.80	61.73	49.31	10.59	20.00	3.34	12.23	38.78	5.68	27.07	52.41
	24 h	mean	3.96	2.08	3.76	-0.64	1.31	5.06	7.08	5.86	1.96	2.64	0.09	1.67	4.47	0.92	3.53	5.93
		SD	2.86	2.80	6.14	41.25	2.15	7.92	11.08	8.74	1.82	3.58	0.16	2.22	7.22	1.06	5.02	9.39
10 nM	4 h	mean	57.43	3.58	-4.07	-158.60	-0.39	-3.28	-2.27	-0.94	-0.13	-1.36	49.90	-2.45	-2.03	0.38	0.85	-4.97
		SD	9.66	3.16	18.80	258.15	2.94	6.81	10.17	7.41	2.54	3.39	37.83	3.16	7.30	0.94	4.08	7.50
	8 h	mean	20.39	12.85	8.39	-103.28	7.87	29.00	39.91	29.90	8.17	14.08	3.19	8.28	24.16	5.31	18.40	35.10
		SD	16.64	18.76	20.07	87.03	11.81	43.24	59.65	42.29	10.74	20.26	3.77	12.08	36.16	7.80	27.13	52.66
	24 h	mean	3.51	1.69	3.19	13.28	1.25	5.18	7.84	7.07	2.04	2.78	0.16	1.82	4.78	0.84	3.79	5.91
		SD	2.40	1.78	3.59	57.98	1.71	7.06	10.41	8.63	1.54	3.18	0.22	1.88	6.90	0.77	4.39	8.20

Ins conc	Time		ARG	ASN	ASP	FUM	HIS	ILE	LEU	LYS	MET	PHE	PYR	SER	THR	TRP	TYR	VAL
100 nM	4 h	mean	67.16	10.54	-8.28	-31.93	2.15	1.32	2.66	2.87	2.75	2.69	49.57	-0.18	-2.05	3.25	5.00	1.87
		SD	11.70	10.37	19.94	123.60	3.49	6.64	8.30	6.03	3.88	4.37	37.13	3.97	3.04	3.05	4.46	9.73
	8 h	mean	11.33	5.38	12.15	-8.80	4.61	21.73	30.58	23.47	5.57	9.50	3.45	5.99	20.94	2.18	13.64	25.38
		SD	18.51	11.31	23.64	87.41	10.68	43.09	61.72	49.39	10.24	19.04	3.06	11.34	42.23	4.79	26.13	50.46
	24 h	mean	3.69	2.59	4.46	-0.07	1.52	5.79	8.63	7.33	2.13	2.96	0.10	1.86	5.73	0.90	4.10	6.60
		SD	2.42	2.53	4.05	0.00	1.56	6.79	10.07	8.58	1.56	3.07	0.17	1.89	6.38	0.75	4.28	7.82

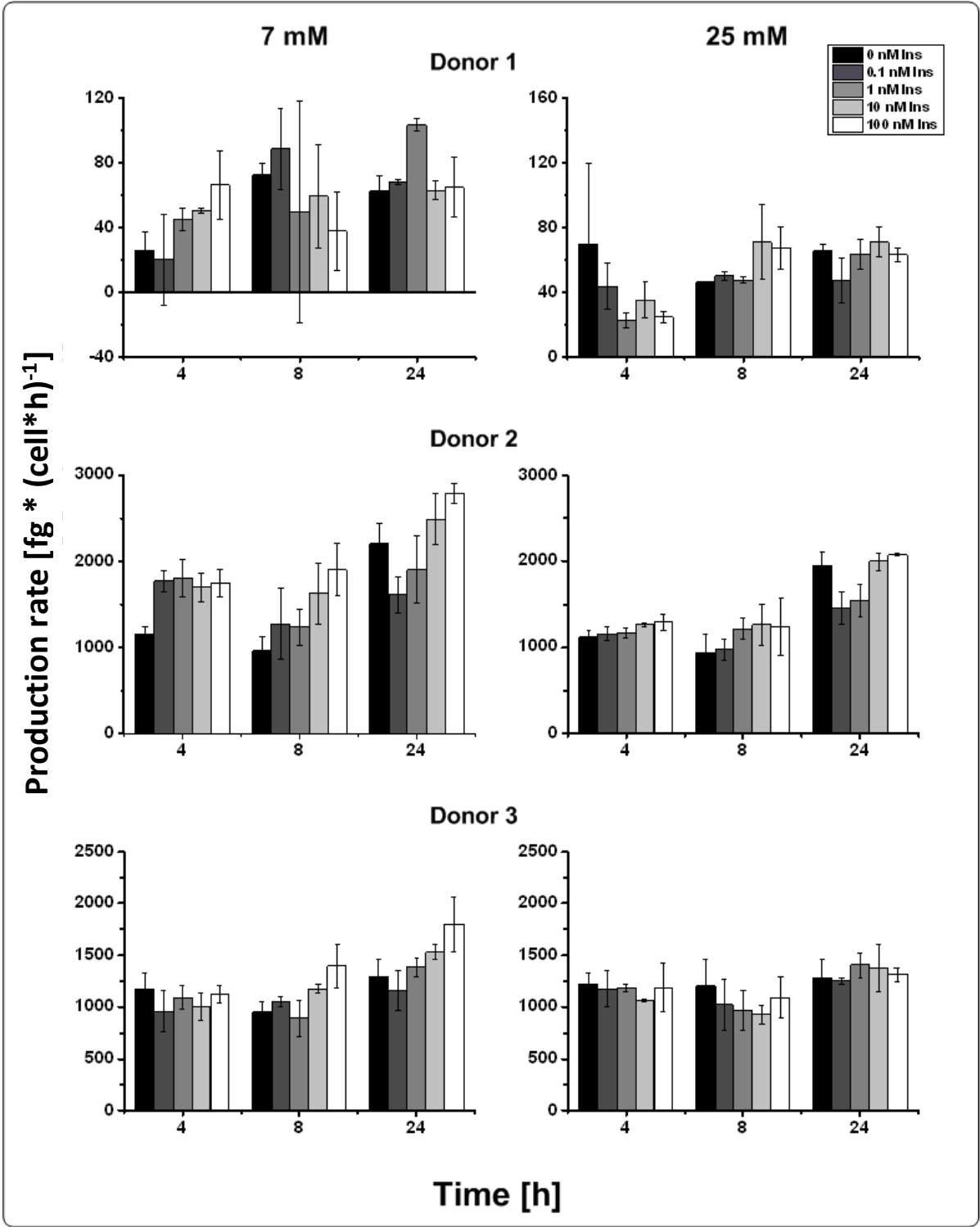
Supplementary Table 10 Uptake rates of amino acids and organic acids, which are not depicted in Chapter 3, of primary human hepatocytes cultivated in collagen sandwich culture under the influence of different insulin concentrations (0-100 nM) and 25 mM glucose (n=3). Positive values indicate uptake, negative values production in [fmol*(cell*h)⁻¹]. Amino acids are abbreviated by the official three letter codes, FUM fumarate, PYR pyruvate.

Ins conc	Time		ARG	ASN	ASP	FUM	HIS	ILE	LEU	LYS	MET	PHE	PYR	SER	THR	TRP	TYR	VAL
0 nM	4 h	mean	51.27	2.91	3.86	-0.20	-1.56	-7.63	-6.88	-6.77	-0.88	-3.02	47.23	-4.57	-6.27	1.16	-2.25	-8.85
		SD	21.28	2.63	2.79	0.03	0.88	3.72	9.35	6.18	0.77	1.16	34.80	0.74	3.16	0.55	1.72	3.32
	8 h	mean	34.92	6.67	12.54	-0.25	4.66	16.58	21.45	18.93	6.18	8.43	5.39	4.04	16.17	3.08	12.66	20.30
		SD	36.36	7.41	14.83	0.09	5.72	18.79	23.37	22.35	6.38	9.61	3.64	4.06	18.72	3.48	14.28	23.80
	24 h	mean	8.35	2.45	4.83	-0.01	1.74	6.93	9.56	7.84	2.34	3.40	0.23	1.85	6.19	1.10	4.73	8.44
		SD	8.70	3.81	7.18	0.00	2.87	11.90	16.31	13.02	2.32	5.06	0.17	2.73	10.99	1.47	7.32	14.59
0.1 nM	4 h	mean	56.40	3.90	4.50	-0.12	-0.84	-6.51	-5.18	-0.77	-0.05	-2.26	47.81	-4.13	-6.13	1.64	-1.15	-8.23
		SD	18.16	2.70	3.41	-0.21	1.45	4.85	10.87	7.45	1.78	2.74	35.24	1.93	4.78	0.87	2.95	5.05
	8 h	mean	36.97	6.88	11.15	-0.29	4.69	14.88	18.74	20.18	6.83	8.76	4.84	4.56	14.07	3.61	13.23	17.51
		SD	39.64	10.82	18.66	0.01	7.00	26.77	35.76	31.47	9.43	14.31	3.60	7.73	25.40	5.59	20.45	32.39
	24 h	mean	8.93	3.08	6.01	-0.01	2.14	8.68	11.90	10.45	2.70	4.08	0.22	2.34	7.80	1.27	5.73	10.37
		SD	8.59	3.37	7.30	0.00	2.62	10.85	14.63	11.54	2.06	4.59	0.12	2.39	10.07	1.34	6.63	13.37

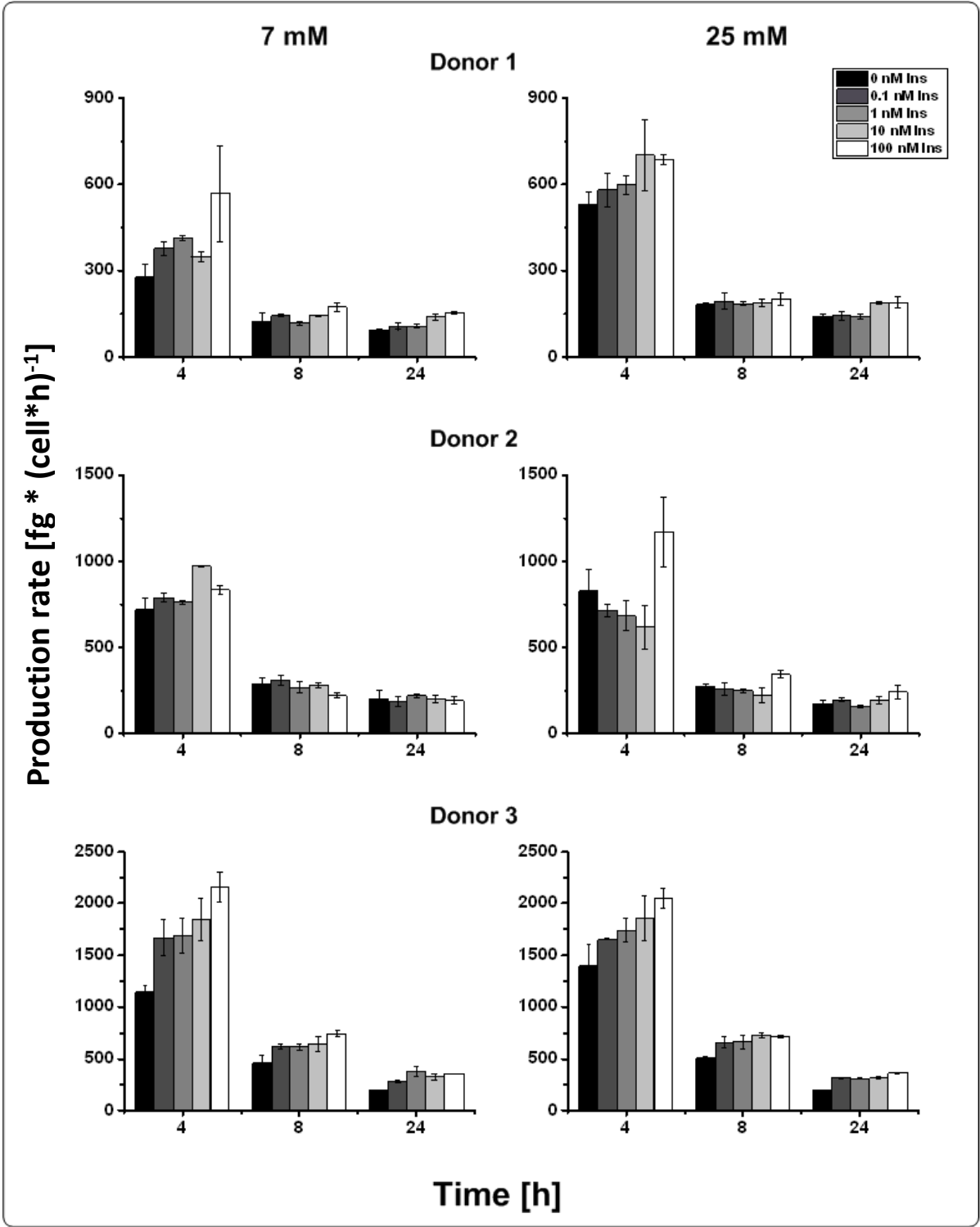
Ins conc	Time		ARG	ASN	ASP	FUM	HIS	ILE	LEU	LYS	MET	PHE	PYR	SER	THR	TRP	TYR	VAL
1 nM	4 h	mean	62.23	4.84	5.79	-0.21	0.72	-0.16	2.06	7.83	1.23	0.27	48.49	-1.69	0.35	1.89	2.96	-2.26
		SD	15.05	4.67	6.33	0.02	2.37	14.38	22.69	21.42	2.73	4.52	35.74	3.41	9.41	1.31	6.97	13.31
	8 h	mean	36.52	7.30	12.39	-0.36	4.57	16.59	21.64	21.25	7.20	9.49	3.93	4.98	16.60	3.85	14.36	19.42
		SD	41.91	10.57	17.55	0.04	7.02	25.04	33.66	31.69	9.40	13.72	2.68	7.48	23.51	5.33	20.09	29.53
	24 h	mean	8.47	2.58	5.08	-0.02	1.87	7.44	10.04	8.52	2.40	3.53	0.28	1.92	6.90	1.17	4.99	8.95
		SD	9.38	3.73	7.04	0	2.84	11.71	16.04	13.05	2.33	5.01	0.20	2.69	10.78	1.42	7.23	14.22
10 nM	4 h	mean	66.25	5.37	7.03	-0.23	1.39	2.07	3.94	11.33	1.75	0.97	48.63	-1.19	4.24	2.20	4.59	-0.19
		SD	11.16	6.54	9.15	0.03	3.08	19.73	30.42	25.95	4.21	6.88	35.85	5.09	12.08	1.67	10.14	19.46
	8 h	mean	35.11	6.66	10.61	-0.34	5.03	14.86	19.51	20.93	6.94	8.84	4.10	4.41	16.87	2.98	12.96	17.25
		SD	44.82	10.98	18.22	0.02	7.15	25.71	33.88	32.25	9.80	14.31	2.94	7.76	24.04	5.79	20.93	30.00
	24 h	mean	8.87	2.94	5.69	-0.02	2.13	8.37	11.51	10.07	2.67	4.03	0.23	2.23	7.67	1.33	5.56	10.04
		SD	8.93	3.51	6.68	0	2.67	11.11	15.04	12.13	2.17	4.66	0.15	2.48	10.19	1.35	6.86	13.50
100 nM	4 h	mean	63.92	4.64	5.33	-0.24	1.82	-0.23	-0.72	9.17	1.26	-0.01	49.50	-2.60	22.55	2.23	3.07	-2.03
		SD	8.79	3.94	5.37	0.02	1.78	13.67	23.75	19.15	3.37	4.98	36.54	3.45	36.80	1.91	6.95	11.94
	8 h	mean	39.68	8.51	13.13	-0.36	5.19	17.73	24.35	24.67	8.36	10.76	3.34	5.86	25.54	4.41	16.05	20.85
		SD	41.28	10.31	16.90	0.02	6.76	21.94	28.12	29.48	9.53	13.42	2.15	7.00	26.76	5.98	19.37	26.74
	24 h	mean	10.58	6.03	11.37	0	4.26	18.97	27.01	21.24	4.81	8.62	0.14	5.09	12.38	2.48	11.80	22.84
		SD	11.68	5.42	10.40	0	4.18	18.16	25.20	19.40	3.67	7.72	0.11	4.35	17.29	2.09	10.95	22.10



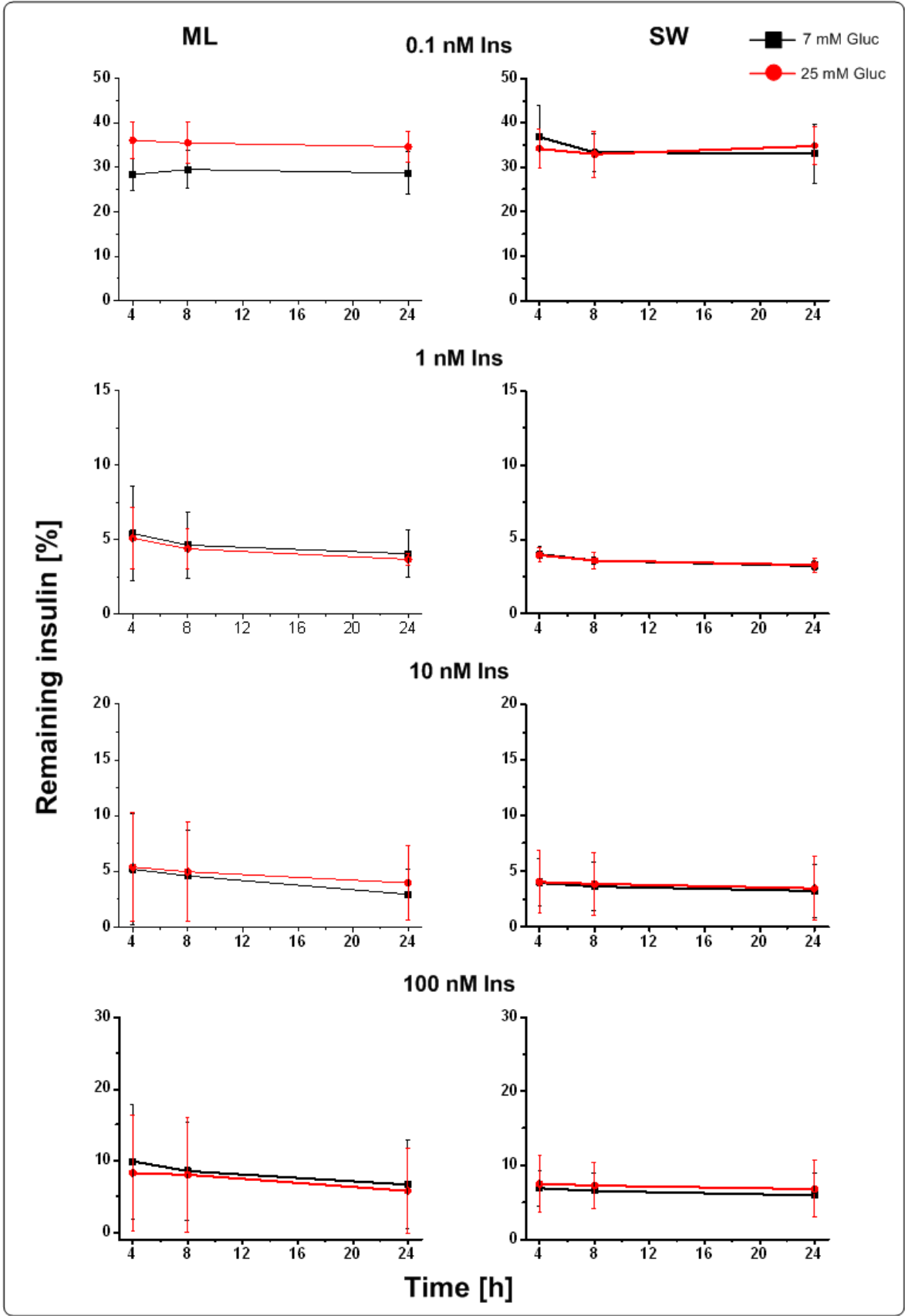
Supplementary Figure 12 Percentages of glycine with the mass m+1 of PMH cultivated in collagen ML and SW culture with [U-¹³C₅] glutamine. Black indicates incubation without insulin, red indicates incubation with 100 nM insulin, m+1 pointing to the number of labeled carbons. Error bars indicate standard deviation (N=2; n=6). Abbreviations: Ins Insulin.



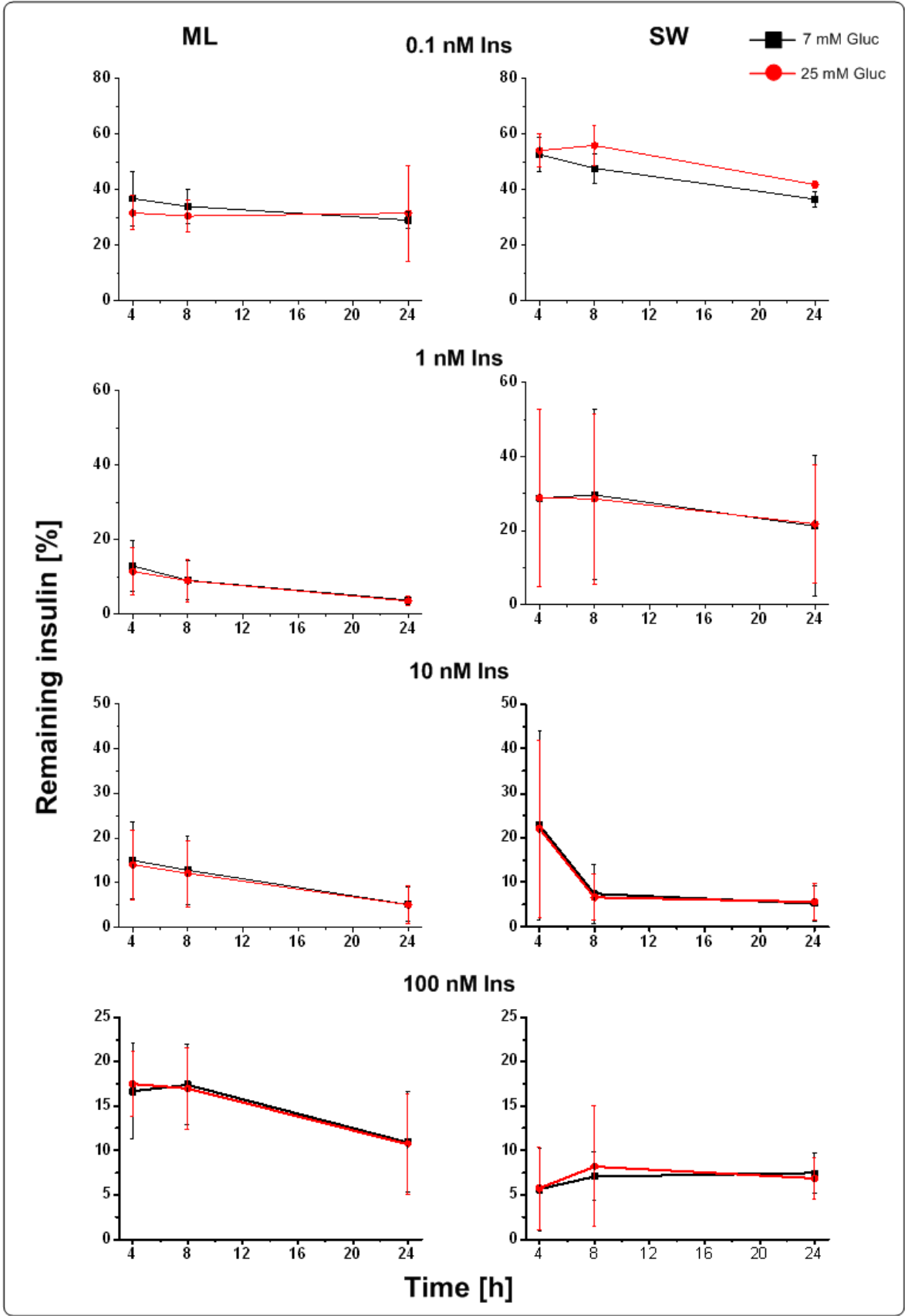
Supplementary Figure 13 Separate albumin production rates of the three single human donors cultivated in collagen monolayer culture 7 or 25 mM glucose and different concentrations of insulin (ins) (0-100 nM). Error bars indicate standard deviations (n=3).



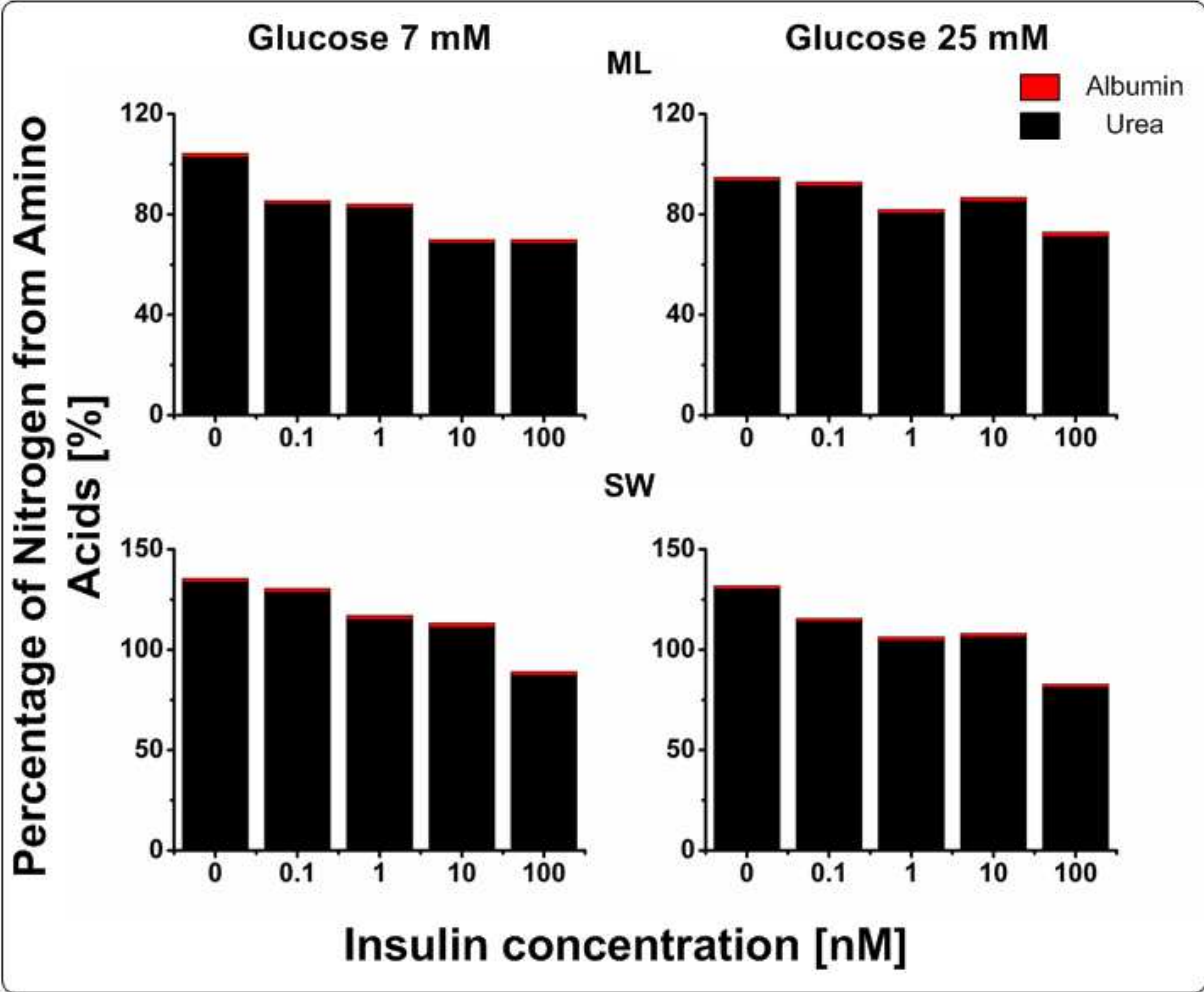
Supplementary Figure 14 Separate albumin production rates of the three single human donors cultivated in collagen sandwich culture 7 or 25 mM glucose and different concentrations of insulin (ins) (0-100 nM). Error bars indicate standard deviations (n=3).



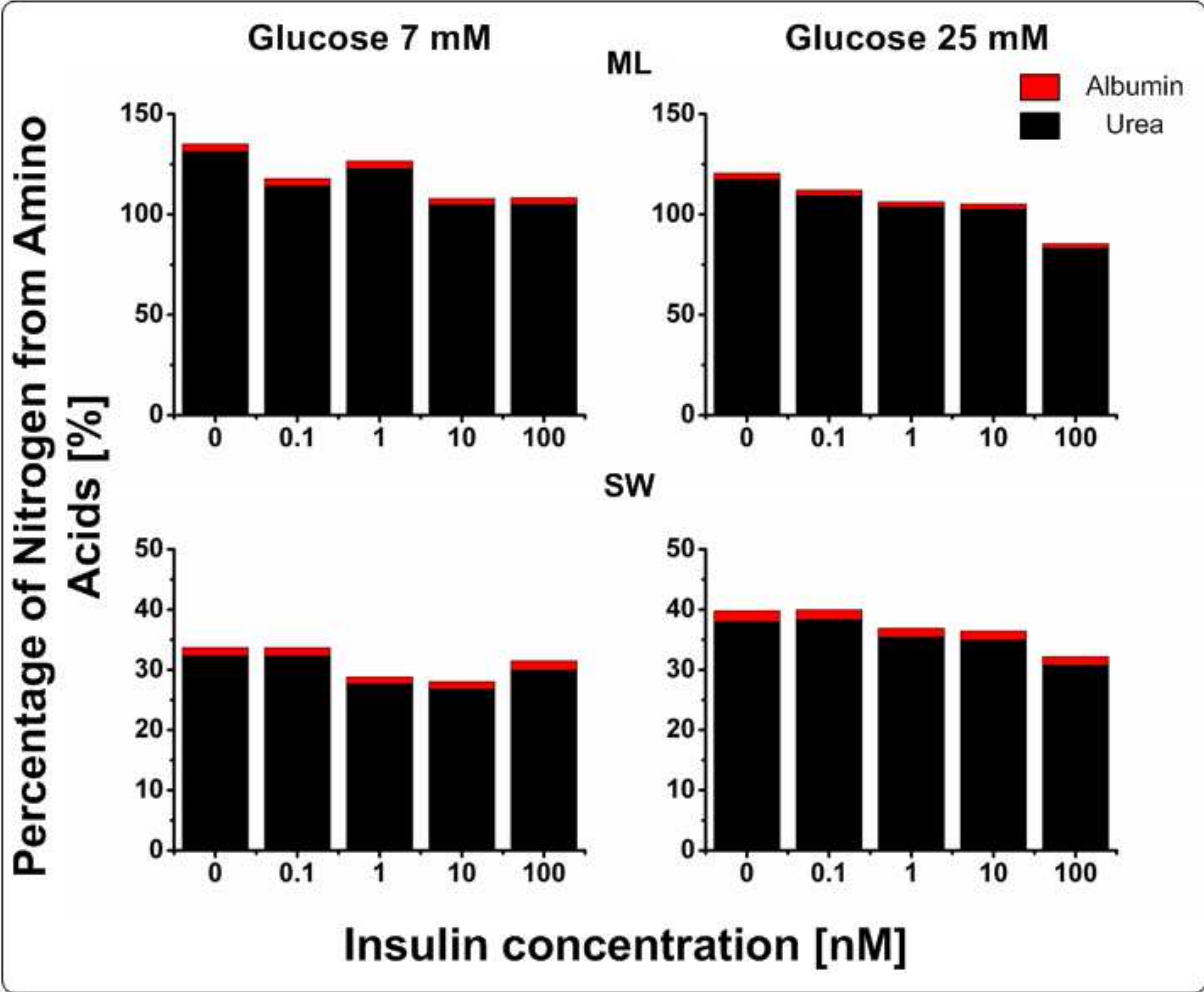
Supplementary Figure 15 Degradation of insulin by primary mouse hepatocytes cultivated in collagen monolayer (ML) and sandwich (SW) culture. The cells were cultivated with 7 and 25 mM glucose (gluc) und different concentrations of insulin (ins) (0-100 nM). The remaining amounts of insulin [%] are depicted. Error bars indicate standard deviations (n=3).



Supplementary Figure 16 Degradation of insulin by primary human hepatocytes cultivated in collagen monolayer (ML) and sandwich (SW) culture. The cells were cultivated with 7 and 25 mM glucose (gluc) and different concentrations of insulin (ins) (0-100 nM). The remaining amounts of insulin [%] are depicted. Error bars indicate standard deviations (n=3).



Supplementary Figure 17 Nitrogenbalance of PMH. Percentage of nitrogen from taken up amino acids found in produced urea and albumin over 24 h.



Supplementary Figure 18 Nitrogenbalance of PHH. Percentage of nitrogen from taken up amino acids found in produced urea and albumin over 24 h.

Danksagung

Prof. Dr. Elmar Heinzle möchte ich herzlich für die Bereitstellung dieses interessanten Themas, seine Betreuung und die kritischen Diskussionen über die letzten 5 Jahre danken.

Prof. Dr. Christoph Wittmann möchte ich herzlich für die Übernahme der Zweitkorrektur meiner Arbeit danken.

Dr. Fozia Noor möchte ich sehr gerne für ihre Betreuung und die vielen lebhaften Diskussionen danken.

Ein besonderer Dank gilt Malina Orsini. Zusammen mit ihr erfolgte die komplette Arbeit bezüglich des Proteoms primärer Maushepatozyten. Vielen Dank für die tolle Zusammenarbeit! Ebenfalls ein großes Dankeschön gebührt Esther Hoffmann, die ebenfalls einen großen Beitrag zu dieser Arbeit geleistet hat. Vielen Dank euch beiden!

Bei allen Leuten des BMBF-Projekts Virtual Liver möchte ich mich ganz herzlich für die gute Zusammenarbeit und die hierbei gemachten Erfahrungen bedanken. Ganz besonders möchte ich hierbei Adriano Henney, Johannes Bausch, Patricio Godoy, Agata Widera, Georg Damm und die Leute aus dem Organisations-Team des Student and PostDoc Retreats hervorheben.

Bei meinem neuen Arbeitgeber möchte ich vor allem Prof. Dr. Bennard van Ravenzwaay und Dr. Henicke Kamp für ihr Verständnis danken und dass sie mir die nötige Zeit eingeräumt haben meine Arbeit auch parallel zu meinen neuen Aufgaben fertig zu stellen.

Michel Fritz möchte ich sehr gerne für seine Unterstützung in allen die Analytik betreffenden Fragen und Probleme und seine unfassbare Geduld bezüglich dessen danken.

Dr. Susanne Kohring möchte ich herzlichst für ihre Unterstützung in allen organisatorischen Dingen danken.

Veronique Beckers und Xiaoqi Jiang danke ich sehr für ihre Hilfe bei allen mathematischen und statistischen Fragen.

Der gesamten Arbeitsgruppe der Technischen Biochemie möchte ich für das gute Arbeitsklima über die letzten 5 Jahre, die gegenseitige Hilfe, die man sich untereinander hat zukommen lassen, die vielen Kaffeemaschinen-Gespräche, Balkon-Mittagspausen und Feierabendbiere danken.

Ein besonderer Dank gebührt meinen Freunden Judith Wahrheit, Stephanie Saul, Christian Priesnitz, Malina Orsini, Vassilis Delis, Tobi Klein, Esther Hoffmann und Mirjam Selzer für die vielen guten Gespräche, die ganzen lustigen Zeiten, von denen man besser nicht so viel erzählen sollte, die guten Ratschläge und die viele nerdigen Diskussionen (manchmal muss man sich eben auch mal reinsteigern). Mit euch hat die Arbeit wirklich richtig Spaß gemacht! Judith, Stephanie und Christian möchte ich hier dann auch nochmal extra danken für das kritische Korrekturlesen meiner Arbeit und für die vielen Anregungen, die sie mir mitgegeben haben.

Der meiste Dank gebührt meinem Ehemann, Sascha Sperber, der mich die ganze Zeit unterstützt und an mich geglaubt hat und dass, obwohl er alle meine Launen aushalten musste, wenn es im Labor mal wieder nicht so lief wie erhofft und auch bei allen anderen Rückschlägen. Vielen Dank, dass du immer für mich da bist!

Curriculum Vitae

Name: Saskia Sperber,
née Müller

Address: Trippstadter Straße 97
67663 Kaiserslautern
Germany
saskia.sperber@gmx.de
 +49 176 / 64329656

Date of birth: 25.10.1985

Place of birth: Homburg (Saar), Germany

Family status: married

Sept. 2015-now Specialist Metabolomics, Experimental Toxicology, BASF SE

2010-now PhD Thesis in the framework of the German BMBF project “Virtual liver” with focus on the metabolic and proteomic characterization of different cultivation systems with primary mouse hepatocytes and the metabolic changes involved during activation of primary mouse hepatic stellate cells. The work is being prepared in the group of Prof. Elmar Heinzle at the Saarland University (Saarbrücken, Germany)

April–Sept. 2013 Study of economic sciences at Fernuniversität Hagen (Hagen, Germany)

Aug.-Sept. 2008 Trainee at the University of Oxford (Oxford, United Kingdom) at the Department of Physiology, Anatomy and Genetics;

Analysis of acidification process in osteoclasts as well as investigation of a possible selective ion channel which leads to lysis of sickle cells

- 2005-2010** Study of biology at the Saarland University (Saarbrücken, Germany) with main focus on Human- and Molecular biology;
- Diploma Thesis: “3D cell cultivation techniques for the analysis of drug toxicity” in the framework of the BMBF project “HepaTox” Major subjects: Biochemistry, Biophysics, Virology
- (Final Grade: 1.3)
- 1996-2005** High school “Helmholtz-Gymnasium” in Zweibrücken, Germany finished with the German university-entrance diploma
- (Final Grade: 1.2).

Publications

Malina Orsini^{1*}, **Saskia Sperber^{1*}**, Esther Hoffmann¹ and Elmar Heinzle^{1**}. Proteomic characterization of primary mouse hepatocytes in collagen monolayer and sandwich culture.

In preparation

van Ravenzwaay, B., **Sperber, S.**, Lemke, O., Fabian, E., Faulhammer, F., Kamp, H., Mellert, W., Strauss, V., Strigun, A., Peter, E., Spitzer, M., Walk, T., 2016. Metabolomics as read-across tool: A case study with phenoxy herbicides. Regul. Toxicol. Pharmacol. RTP 81, 288–304.

Priesnitz C, **Sperber S**, Garg R, Orsini M & Noor F (2014). Fluorescence based cell counting in collagen monolayer cultures of primary hepatocytes. *Cytotechnology*; DOI: 10.1007/s10616-014-9821-1.